

**Automated High-throughput Approaches for the
Development and Investigation of Novel Oxidative
Biocatalytic Processes**

A Thesis Submitted to University College London for the degree of

DOCTOR OF PHILOSOPHY

Jasmin Zerlina Baboo

Department of Biochemical Engineering
University College London

2012

Declaration

I, Jasmin Baboo, confirm that the work presented in this thesis is my own. Where information has been derived from other sources, I confirm that this has been indicated in the thesis.

Signature: _____ Date: _____

Acknowledgements

I would like to firstly thank my principal supervisor Dr Martina Micheletti for her guidance and encouragement throughout this project and continual confidence in me. In addition I wish to thank Professor Gary Lye for his support, and willingness to provide help and advice whenever needed. Thanks must also go to Professor John Ward and Professor Helen Hailes for their input and expertise in the areas of biochemistry and chemistry where their comments and critical insights have been an immense help. I would also like to acknowledge Dr Suzanne Farid for encouraging me to pursue a doctorate and for her ongoing support since my undergraduate studies.

I am particularly grateful to many departmental colleagues who have provided help and assistance in various aspects of my project including Dhushy Stainslaus for laboratory support and her always welcoming nature along with Alan Craig and Graeme Smith both whom provided technical expertise for the construction and maintenance of a variety of devices, which proved pivotal in many experimental studies.

I would like to acknowledge those friendships I have made prior to and during my doctoral studies which have been a source of happiness, laughter and motivation. In particular thanks goes to Candy Ng, Kara Cox, Dr Paul Mondragon-Teran and Krisztina Kovacs-Schreiner who I have known since my undergraduate studies, Gemma Ordidge and Dr Shahina Ahmad who have made my PhD experience more enjoyable and Dr James Galman who in addition to expert guidance in chemical characterisation has provided ongoing advice.

Finally, it goes without saying that my parents and my sister Salina, have been a great support throughout my life and special thanks goes to them for their continued encouragement, motivation and confidence during these studies.

Abstract

Oxidative biocatalysts have a vast industrial and biotechnological potential in areas such as fine chemical and antibiotic synthesis. They offer an environmentally compatible and sustainable route to catalysis, often simpler and more specific than chemical alternatives. However, the routine use of biocatalysts in biopharmaceutical manufacture has been hindered by biocatalyst complexity and the experimental burden necessary for implementation. This thesis aims to investigate, using automated microscale technologies, how oxidative biocatalytic bioprocesses can be designed and developed at a reduced cost and timeframe compared to conventional laboratory scale experimentation.

A robotic platform was used with 96-Deep square well microtiter plates to develop an effective bioprocess for investigating cyclohexanone monooxygenase (CHMO). *E. coli* cultivations for CHMO production, bioconversion, liquid-liquid metabolite extraction and analytic techniques were conducted using the developed microscale automated approach. Each step allowed rapid and reproducible collection of quantitative kinetic data over multiples runs achieving 'walk away operation'. Whole bioprocess evaluation was achieved, whereby linking multiple unit operations enabled rapid assessment of process interactions. Factors influencing CHMO activity and bioconversion yields were investigated along with alternative bioconversion substrates. From identified limitations of the CHMO system an optimised process was developed where the processing time was almost halved and CHMO activity increased 5-fold.

Two novel self-sufficient cytochrome P450 systems, P450SU1 and P450SU2 were investigated using an automated approach where factors limiting bioconversion were identified. Implementation of the required improvements resulted in a 5-fold improvement in enzymatic expression and 5-fold and 1.5-fold increase in product formation from cytochrome P450SU1 and P450SU2, respectively.

A matched oxygen transfer coefficient approach was used for predictive scale-up. The optimised microscale CHMO and P450 processes were scaled to 75 L and 7.5 L bioreactor scale, respectively. Growth and bioconversion kinetics were found to be identical between scales for the CHMO system whereas differences were observed for the P450 systems.

Results described in this thesis have demonstrated the benefits of microscale automated methodologies for the creation, investigation and predictive scale-up of oxidative biocatalytic bioprocesses. The established strategies evaluated in this work contribute to meeting the current demand to decrease developmental costs and timelines.

Contents

Abstract	4
Nomenclature	12
List of Figures	15
List of Tables	31
1 Introduction	32
1.1 The Context of the Research	32
1.2 Literature Survey	33
1.2.1 Microscale Bioprocessing	33
1.2.1.1 Overview of Technology	33
1.2.1.2 Miniature Stirred Systems	34
1.2.1.3 Miniature Shaken Systems	37
1.2.1.3.1 Bioprocess Applications of Microwells.....	41
1.2.1.3.2 Bioprocess Applications of Whole Process Approach.....	46
1.2.2 Process Automation	48
1.2.2.1 Overview of Automation Technology	48
1.2.2.2 Automated Robotic Platforms	49
1.2.2.2.1 Application for Microscale Process Development.....	50
1.2.3 Bioconversions	52
1.2.3.1 Oxidative Bioconversions	53
1.2.3.1.1 Baeyer-Villiger Monooxygenases.....	54
1.2.3.1.1.1 Cyclohexanone Monooxygenase.....	56
1.2.3.1.2 Cytochrome P450s.....	60
1.2.3.1.2.1 The Cytochrome P450 Reaction Repertoire.....	60
1.2.3.1.2.2 Classification of Cytochrome P450s.....	62
1.2.3.1.2.2.1 Class I.....	63
1.2.3.1.2.2.2 Class II.....	64
1.2.3.1.2.2.3 Class III.....	65
1.2.3.1.2.2.4 Novel Class IV.....	66

1.2.3.1.2.2.4.1	Cytochrome P450 SU1 and P450SU2.....	68
1.2.3.1.2.3	Application of High-throughput Approaches.....	70
1.3	Conclusions of the Literature Survey.....	71
1.4	The Present Contribution.....	73
1.5	Outline of the Thesis.....	74
2	Materials and Methods.....	76
2.1	Materials.....	76
2.1.1	Chemicals.....	76
2.1.2	Microorganisms.....	77
2.2	General Methods.....	77
2.2.1	<i>E. coli</i> TOP10 [pQR210].....	77
2.2.1.1	Seed Stock Preparation.....	77
2.2.1.2	Sequencing Analysis.....	78
2.2.1.3	Inoculum Preparation.....	78
2.2.1.4	Shake Flask Cultivations and Bioconversions.....	79
2.2.2	<i>E. coli</i> [pQR367] and <i>E. coli</i> [pQR368].....	79
2.2.2.1	Production of <i>E. coli</i> [pQR367] and <i>E. coli</i> [pQR368].....	79
2.2.2.2	Seed Stock Preparation.....	80
2.2.2.3	Sequencing Analysis.....	80
2.2.2.4	Inoculum Preparation.....	81
2.2.2.5	Shake Flask Cultivations and Bioconversions.....	81
2.3	Microscale Process Sequences.....	82
2.3.1	<i>E. coli</i> TOP10 [pQR210].....	82
2.3.1.1	Manual Operations.....	82
2.3.1.1.1	Microwell Based Temperature Study.....	82
2.3.1.2	Automated Microscale Linked Process Sequence.....	82
2.3.1.3	Bioprocess Evaluation using Automated	

	Sequence.....	84
2.3.2	<i>E. coli</i> [pQR367] and <i>E. coli</i> [pQR368].....	84
2.3.2.1	Manual Operations.....	84
2.3.2.1.1	Microwell Based Temperature Study.....	84
2.3.2.1.2	Microwell Based Evaporation Study.....	85
2.3.2.2	Automated Microscale Linked Process Sequence.....	85
2.3.2.3	Automated Screening Approach.....	86
2.4	Parallel Process Sequences at Matched K_{La}	87
2.4.1	<i>E. coli</i> TOP10 [pQR210].....	87
2.4.1.1	75 L Operation.....	87
2.4.1.2	Microwell Linked Process Sequence.....	87
2.4.2	<i>E. coli</i> [pQR367] and <i>E. coli</i> [pQR368].....	88
2.4.2.1	7.5 L Operation.....	88
2.4.2.2	Microwell Linked Process Sequence.....	89
2.5	Substrate Solubility Studies.....	89
2.6	Analytical Techniques.....	89
2.6.1	Optical Density Measurements.....	89
2.6.2	Dry Cell Weight Measurements.....	90
2.6.3	Automated Robotics.....	90
2.6.4	Gas Chromatography (GC).....	91
2.6.4.1	Sample Preparation for GC.....	91
2.6.4.2	GC Operation and Quantification.....	92
2.6.5	High Pressure Liquid Chromatography (HPLC).....	93
2.6.5.1	Sample Preparation for HPLC.....	93
2.6.5.2	HPLC Operation and Quantification.....	93
2.6.6	Thin Layer Chromatography (TLC).....	94
2.6.7	Product Identification.....	95
2.6.7.1	Oxocan-2-one.....	95
2.6.7.2	2-Oxa-bicyclo[3.2.1]octan-3-one.....	96
2.6.8	NADPH Consumption Microscale Assay.....	96
2.6.8.1	Sample Preparation.....	96
2.6.8.2	NADPH Consumption Assay.....	97
2.6.9	Carbon Monoxide (CO) Assay.....	98

2.6.9.1	Sample Preparation.....	98
2.6.9.2	CO Assay.....	98
2.6.10	Bradford Assay.....	99
2.6.11	K_La Measurement.....	100
2.6.11.1	Microscale Measurements.....	100
2.6.11.2	Laboratory Scale Measurements.....	103
2.6.11.3	Pilot Plant Scale Measurements.....	105
2.6.12	Enzyme Units.....	105
3	Design and Development of a Automated Microscale Platform for Investigation of Whole Cell Oxidative Biocatalytic Processes.....	106
3.1	Introduction.....	106
3.2	Results and Discussion.....	108
3.2.1	Production of Cyclohexanone Monooxygenase.....	108
3.2.2	A Robotic Platform for Microscale Process Development.....	112
3.2.3	Automated Microwell Cultivation.....	117
3.2.4	Automated Microwell Bioconversion.....	122
3.2.5	Automated Liquid-liquid Extraction.....	124
3.2.6	Automated Linked Process of Cultivation, Bioconversion and Liquid-liquid Extraction.....	127
3.3	Concluding Remarks.....	130
4	Whole Bioprocess Evaluation Using an Automated Microscale Platform.....	132
4.1	Introduction.....	132
4.2	Results and Discussion.....	134
4.2.1	Automated Investigation of CHMO Specific Activity.....	134
4.2.1.1	Impact of Oxygen Transfer Rate on Bioprocess Performance.....	134
4.2.1.2	Impact of Biomass Concentration on Biocatalyst Activity.....	141

4.2.1.3 Evaluation of Media Composition.....	146
4.2.2 Automated Investigation of Alternative CHMO Reactions.....	151
4.2.2.1 The Impact of Substrate Concentration.....	151
4.2.2.2 High-throughput Screening of Baeyer-Villiger Substrates.....	155
4.2.3 Automated Process Optimisation.....	165
4.3 Concluding Remarks.....	174
5 Microscale Process Development of Novel Cytochrome P450 Biocatalysts.....	176
5.1 Introduction.....	176
5.2 Results and Discussion.....	178
5.2.1 Production of Cytochrome P450SU1 and P450SU2.....	178
5.2.2 Automated Microscale Production of Cytochrome P450s.....	186
5.2.2.1 The Effect of Temperature During Expression.....	186
5.2.2.2 The Effect of Agitation Speed.....	189
5.2.2.3 The Influence of Microwell Fill Volume.....	192
5.2.2.4 The Effect of Microwell Evaporation.....	195
5.2.2.5 Automated Data Collection on Cytochrome P450s.....	197
5.2.3 Applying the Automated Approach for Bioconversion Improvement.....	209
5.2.3.1 The Effect of δ -aminolevulinic Acid (ALA).....	215
5.2.3.2 The Effect of Glycerol.....	221
5.2.3.3 The Effect of 7-ethoxycoumarin Concentration.....	227
5.2.3.4 Improved Bioconversion of 7-ethoxycoumarin.....	231
5.3 Concluding Remarks.....	235
6 Establishing the Scalability of Oxidative Biocatalytic Microscale Processes.....	237
6.1 Introduction.....	237
6.2 Results and Discussion.....	241

6.2.1 Scale Translation at Matched K_{La} – Application to CHMO.....	241
6.2.2 Scale Translation at Matched K_{La} – Optimised Production of CHMO.....	245
6.2.2.1 K_{La} Measurement Using Dynamic Gassing Out.....	245
6.2.2.2 Scale Comparison at Matched K_{La}	251
6.2.3 Scale Translation at Matched K_{La} – Application to Cytochrome P450SU1 and P450SU2.....	254
6.2.3.1 K_{La} Measurement Using Dynamic Gassing Out.....	254
6.2.3.2 Scale Comparison at Matched K_{La}	257
6.2.4 Alternative Scale-Up Strategies.....	264
6.2.4.1 The Dynamic Measurement of K_{La}	264
6.2.4.2 Volumetric Power Consumption.....	265
6.3 Concluding Remarks.....	266
7 Conclusions and Future Work.....	269
7.1 Concluding Remarks.....	269
7.2 Future Work.....	272
8 References.....	275
9 Appendices.....	308
9.1 Appendix A – Calibration Curves.....	308
9.2 Appendix B – Sample Chromtograms.....	317
9.3 Appendix C – Assays.....	335
9.4 Appendix D – NMR, MS and IR Data.....	340

Nomenclature

Upper Case

D = Oxygen diffusion coefficient, m^2s^{-1}

H_V = Vessel height, m

$K_{L,a}$ = Gas liquid mass transfer coefficient, s^{-1}

N = Shaking frequency, s^{-1}

W = Wetting tension, Nm^{-1}

X = Biomass concentration, $\text{g}_{\text{DCW}}\text{L}^{-1}$

DOT = Dissolved oxygen tension, %

OD = Optical density, dimensionless

P_g = Gassed power, W

V = Volume, m^3

OTR = Oxygen transfer rate, $\text{mmolL}^{-1}\text{h}^{-1}$

CER = Carbon evolution rate, $\text{mmolL}^{-1}\text{h}^{-1}$

CV = Coefficient of variance, %

C_L = Dissolved oxygen concentration in the bulk liquid, mmolL^{-1}

C_L^* = Dissolved oxygen concentration in liquid phase which is in equilibrium with the gas phase, mmolL^{-1}

E = Biological enhancement, dimensionless

U = Units, μmolmin^{-1}

Lower Case

a_i = Initial specific surface area, m^{-1}

d_V = Vessel diameter, m

d_i = Impeller diameter, m

dt = Shaking amplitude, m

g = Gravitational acceleration, m s^{-2}

x = Geometry dependent coefficient, constant in Eq. (4.1), dimensionless

y = Geometry dependent coefficient, constant in Eq. (4.1), dimensionless

C_p = unsaturated oxygen fraction at time t, dimensionless

Greek

μ = Specific growth rate, s^{-1}

ρ = Density, kgm^{-1}

τ_p = probe response time, s

Dimensionless Groups (μ ($kgm^{-1}s^{-1}$) refers to viscosity below)

Bo = Bond number, ($= (\rho v^2 g)/W$), dimensionless

Fr = Froude number, ($= dt*(2*\pi*N)^2/2 * g$), dimensionless

Re = Reynolds number, ($= \rho N d v^2 / \mu$), dimensionless

Sc = Schmidt number, ($= \mu/\rho D$), dimensionless

Abbreviations

96-DSW = 96-Deep square well

96-SRW = 96 standard round well

CHMO = Cyclohexanone monooxygenase

BVMO = Baeyer-Villiger monooxygenase

E. coli [pQR367] = *E. coli* BL21 Star (DE3)pLysS [pQR367]

E. coli [pQR368] = *E. coli* BL21 Star (DE3)pLysS [pQR368]

CHO = Chinese hamster ovary

DO = Dissolved Oxygen

DMSO = Dimethyl sulfoxide

IPTG = Isopropylthiogalactoside

CO = Carbon monoxide

CYP = Cytochrome

FAD = Flavin adenine dinucleotide

FMN = Flavin mononucleotide

ALA = Alpha-aminolevulinic acid

FeCl₃ = Ferric chloride

DTT = Dithiothreitol

EDTA = Ethylenediaminetetraacetic acid

PPG = Polypropylene glycol
BSA = Bovine serum albumin
PMSF = Phenylmethylsulfonyl fluoride
LB = Luria Bertani
TB = Terrific Broth
SOC = Super optimal broth with catabolite repression
UV = Ultra violet
HPLC = High pressure liquid chromatography
GC = Gas chromatography
TLC = Thin layer chromatography
IPA = Isopropyl alcohol
DMF = Dimethyl formamide
RO = Reverse osmosis
DNA = Deoxyribonucleic acid
cDNA = Complementary deoxyribonucleic acid
SDS PAGE = Sodium dodecyl sulphate polyacrylamide gel electrophoresis
POF = Polymer optical fibre
LED = Light emitting diode
LiHa = Liquid handling arm
RoMa = Robotic movement arm
MS = Mass spectroscopy
NMR = Nuclear magnetic resonance
IR = Infrared spectroscopy
CFD = Computational fluid dynamics
rpm = Revolutions per minute

List of Figures

Figure	Page
Figure 1.1 Representation of a three-component P450 system. Reproduced from Roberts et al. (2002).	63
Figure 1.2 Representation of a two-component P450 system. Reproduced from Roberts et al. (2002).	64
Figure 1.3 Representation of a one-component P450 system. Reproduced from Roberts et al. (2002).	65
Figure 1.4 Representation of a class four P450 system. Reproduced from Roberts et al. (2002).	66
Figure 2.1 (A) Front view of a single well with oxygen sensing spot and (B) cross-sectional view of a single well with oxygen sensing spot and adjacent miniature polymer optical fibre for fluorescent signal transmission.	102
Figure 3.1 Growth (A) and bioconversion kinetics (B) of <i>E. coli</i> TOP10 [pQR210] biocatalyst catalysing bicyclo[3.2.0]hept-2-en-6-one (filled symbols) to lactone product (unfilled symbols) collected during a typical shake flask culture. Error bars indicate the range of measured values about the mean.	110
Figure 3.2 Chromatograms displaying the conversion of 1 gL ⁻¹ bicyclo[3.2.0]hept-2-en-6-one (retention time: 6.7 min) to (-)-(1 <i>S</i> ,5 <i>R</i>)-2-oxabicyclo[3.3.0]oct-6-en-3-one and (-)-(1 <i>R</i> ,5 <i>S</i>)-3-oxabicyclo[3.3.0]oct-6-en-2-one (retention times: 13.7 min and 13.8 min) at (A) 0 minutes, (B) 15 minutes and (C) 60 minutes of bioconversion. Peak present at 11 minutes corresponds to naphthalene which was used as an internal standard and added to all samples.	111
Figure 3.3 Tecan Genesis automated platform. (A) Front view of enclosed platform within Bioneat Biosafety Cabinet with (a) HPLC. (B) Internal view of robotic platform with ancillaries including (a) pipette waste station (b) plate carrier and plates, (c) disposable tip racks, (d) reagent reservoirs, (e) eppendorf and vial carriers, (f) microplate reader, (g) access hole for centrifuge. (C) LiHa. (D) RoMa. (E) Thermomixer. (F) Centrifuge.	113
Figure 3.4 P1000 single dispense accuracy (A) and precision (B) . Accuracy	115

and precision calculated over three separate dispenses. Tip 1 (◆), tip 2 (■), tip 3 (▲), tip 4 (×), tip 5 (*), tip 6 (●), tip 7 (+) and tip 8 (-). The dashed line displays 5 % coefficient of variance for precise and accurate liquid handling.

Figure 3.5 P200 single dispense accuracy (A) and precision (B). Accuracy and precision calculated over three separate dispenses. Tip 1 (◆), tip 2 (■), tip 3 (▲), tip 4 (×), tip 5 (*), tip 6 (●), tip 7 (+) and tip 8 (-). The dashed line displays 5 % coefficient of variance for precise and accurate liquid handling. For 20 µL and 10 µL a wash was used between each dispense. 116

Figure 3.6 The effect of well position on well temperature. Top left (dark blue), top right (pink), bottom left (light blue), bottom right (purple), middle (green). Error bars indicate the range of measured values about the mean. 118

Figure 3.7 Reproducibility of growth kinetics of *E. coli* TOP10 [pQR210] across a 96-DSW plate collected during an automated culture. Columns 1-2 (◆), columns 3-4 (■), columns 5-6 (×), columns 7-8 (●), columns 9-10 (*), columns 11-12 (▲). Error bars indicate the range of measured values about the mean. 118

Figure 3.8 Growth kinetics of *E. coli* TOP10 [pQR210] biocatalyst collected using the automated process sequence from three separate runs (run 1 (square), run 2 (circle) and run 3 (triangle)). Error bars indicate the range of measured values about the mean. 121

Figure 3.9 Bioconversion kinetics of *E. coli* TOP10 [pQR210] biocatalyst catalysing bicyclo[3.2.0]hept-2-en-6-one (filled symbols) to lactone product (unfilled symbols) collected using the automated process sequence from three separate runs (run 1 (square), run 2 (circle) and run 3 (triangle)). Error bars indicate the range of measured values about the mean. 123

Figure 3.10 The effect of agitation time on the concentration of ketone (A) and lactone (B) extracted into ethyl acetate using a vortex mixer (■) and a Eppendorf thermomixer (●). For each data point the same sample was extracted with both devices. Error bars indicate the range of values about the mean of duplicate well measurements for the thermomixer results and duplicate samples for the vortex mixer results. 126

Figure 3.11 Schematic representation of the fully automated linked process 129

sequence using *E. coli* TOP10 [pQR210] expressing cyclohexanone monooxygenase. Coloured wells represent filled wells as an example (yellow: media and culture, blue: RO water).

Figure 4.1 (A) Growth kinetics of *E. coli* TOP10 [pQR210] at varying fill volumes of 400 μL (■), 500 μL (○), 600 μL (▲), 800 μL (□) and 1000 μL (◆) for 6 hours of growth and **(B)** bioconversion kinetics at each of the volumes tested with 1 gL^{-1} bicyclo[3.2.0]hept-2-en-6-one (filled symbols) to lactone product (unfilled symbols). All well volumes changed to 500 μL at 6 h time point except for 400 μL volume where well transfer was not carried out due to insufficient volume. Error bars indicate the range of measured values about the mean. 137

Figure 4.2 (A) Bioconversion kinetics of *E. coli* TOP10 [pQR210] with 1 gL^{-1} bicyclo[3.2.0]hept-2-en-6-one using a well fill volume of 200 μL (×), 400 μL (*), 500 μL (○), 600 μL (△), 800 μL (□) and 1000 μL (◇). Error bars indicate the range of measured values about the mean. **(B)** Effect of bioconversion fill volume on specific activity (◆) and % mass balance (●) at different fill volumes after a 1 hour bioconversion defined as $[(\text{mass of ketone in well} + \text{mass of lactone in well}) / (\text{total ketone added to well})] * 100$. 140

Figure 4.3 (A) Growth kinetics of *E. coli* TOP10 [pQR210] grown for a period of 1 hour (◆), 2 hours (*), 3 hours (■), 4 hours (▲), 5 hours (×) and 6 hours (●) to a biomass concentration of 0.60 $\text{g}_{\text{DCW}}\text{L}^{-1}$, 1.04 $\text{g}_{\text{DCW}}\text{L}^{-1}$, 1.85 $\text{g}_{\text{DCW}}\text{L}^{-1}$, 2.55 $\text{g}_{\text{DCW}}\text{L}^{-1}$, 3.06 $\text{g}_{\text{DCW}}\text{L}^{-1}$, and 3.50 $\text{g}_{\text{DCW}}\text{L}^{-1}$ respectively. **(B)** Bioconversion kinetics of bicyclo[3.2.0]hept-2-en-6-one (filled symbols) to lactone product (unfilled symbols) collected using cells from each culture. 143

Figure 4.3 (C) Specific activity at each biomass concentration tested. Error bars indicate the range of measured values about the mean. 144

Figure 4.4 (A) The change in absorbance due to NADPH consumption by isolated CHMO samples incubated with cyclohexanone prepared as described in section 2.6.8.1 from cultures grown for 1 hour (◆), 2 hours (*), 3 hours (■), 4 hours (▲), 5 hours (×) and 6 hours (●) to a biomass concentration of 0.46 $\text{g}_{\text{DCW}}\text{L}^{-1}$, 0.88 $\text{g}_{\text{DCW}}\text{L}^{-1}$, 1.57 $\text{g}_{\text{DCW}}\text{L}^{-1}$, 2.42 $\text{g}_{\text{DCW}}\text{L}^{-1}$, 2.98 $\text{g}_{\text{DCW}}\text{L}^{-1}$, and 3.52 $\text{g}_{\text{DCW}}\text{L}^{-1}$ respectively. **(B)** Specific activity at each 145

biomass concentration tested. Error bars indicate the range of measured values about the mean.

Figure 4.5 (A) Growth kinetics and **(B)** bioconversion kinetics of *E. coli* TOP10 [pQR210] grown in soyabean peptone (*), broadbean peptone (●), bacteriological peptone (◆), peptone (□), peptone from casein pancreatic digest (▲), peptone from casein tryptic digest (■), tryptone pancreatic digest from casein (△) and tryptone enzymatic digest from casein (◇) as the amino acid source. Error bars indicate the range of measured values about the mean. 148

Figure 4.5 (C) Specific activities achieved using cells grown in the eight media formulations tested. 149

Figure 4.6 Specific activities achieved using cells grown to a similar biomass concentration in the eight media formulations tested. 149

Figure 4.7 (A) Growth and **(B)** Bioconversion kinetics of *E. coli* TOP10 [pQR210] at varying substrate (bicyclo[3.2.0]hept-2-en-6-one) concentrations of 0.2 gL⁻¹ (×), 0.4 gL⁻¹ (■), 0.5 gL⁻¹ (▲), 2 gL⁻¹ (◆), 4 gL⁻¹ (*), and 6 gL⁻¹ (●). Substrate addition was at the 6.25 h time point. Error bars indicate the range of measured values about the mean. 153

Figure 4.7 (C) The effect of substrate concentration on specific activity. 154

Figure 4.8 (A) Growth and **(B)** bioconversion kinetics of *E. coli* TOP10 [pQR210] with substrates (1*R*)-camphor (+), (1*R*)-fenchone (▲), (+)-dihydrocarvone (×), cyclooctanone (*), norcamphor (■) to 2-oxabicyclo[3.2.1]octan-3-one (□), cycloheptanone (●) to oxocan-2-one (○) and cyclohexanone (◆) to ε-caprolactone (◇). The results of cyclohexanone presented here were collected in a separate automated run to that of the other six substrates. Substrate addition was at the 6.25 h time point. Error bars indicate the range of measured values about the mean. 159

Figure 4.9 GC chromatogram of mixed chemically synthesised and biologically produced oxocan-2-one (retention time: 10.04 minutes) from cycloheptanone (retention time: 8.12 minutes). Naphthalene was used as an internal standard (retention time: 11.23 minutes). 162

Figure 4.10 Growth **(A)** and bioconversion kinetics **(B)** of *E. coli* TOP10 [pQR210] biocatalyst catalysing bicyclo[3.2.0]hept-2-en-6-one (unfilled 166

symbols) to lactone product (filled symbols) collected from a optimised (●) and non-optimised run (■). Error bars indicate the range of measured values about the mean.

Figure 4.11 (A) Growth and (B) bioconversion kinetics of *E. coli* TOP10 [pQR210] with substrates (1*R*)-camphor (*), (1*R*)-fenchone (▲), (+)-dihydrocarvone (×), cyclooctanone (◆), norcamphor (■) to 2-oxabicyclo[3.2.1]octan-3-one (□) and cycloheptanone (●) to oxocan-2-one (○). Substrate addition was at the 3 h time point. Error bars indicate the range of measured values about the mean. 168

Figure 4.12 GC chromatogram of (1*R*)-camphor (retention time: 10.76 minutes) bioconversion after (A) 0 hours and (B) 4 hours. Peak at a retention time of 9.23 minutes is a potential camphor product and peak at 6.34 minutes is DMSO used to solubilise camphor during the bioconversion. 170

Figure 4.13 Percentage relative activity of CHMO in the presence of each substrate compared to the natural substrate cyclohexanone. 173

Figure 5.1 Growth kinetics of *E. coli* [pQR367] (●), *E. coli* [pQR368] (■) and *E. coli* BL21 Star (DE3)pLysS (control) (▲) during a induced (closed symbol) and non-induced (open symbol) shake flask culture catalysing 7-ethoxycoumarin to 7-hydroxycoumarin. Error bars indicate the range of measured values about the mean. 181

Figure 5.2 Representative CO difference spectra of (A) P450SU1 expressed in *E. coli* [pQR367] and (B) P450SU2 expressed in *E. coli* [pQR368]. Samples were from cultures where no 7-ethoxycoumarin was added. 182

Figure 5.3 TLC analysis showing the bioconversion of 7-ethoxycoumarin to 7-hydroxycoumarin. (A) Shows compounds under UV light. Column S and P contain standards of 7-ethoxycoumarin and 7-hydroxycoumarin in ethyl acetate. (B) Shows compounds stained with permanganate and visualised under UV light. Columns 2, 4 and 5 are from induced cultures of *E. coli* [pQR368], *E. coli* [pQR367] and *E. coli* BL21 Star (DE3)pLysS (control). Columns 1 and 3 are from non-induced cultures of *E. coli* [pQR368] and *E. coli* [pQR367]. 184

Figure 5.4 7-hydroxycoumarin concentration after 30 hours of induced and non-induced culture of *E. coli* [pQR368], *E. coli* [pQR367] and induced 184

culture of *E. coli* BL21 Star (DE3)pLysS (control). Error bars indicate the range of measured values about the mean.

Figure 5.5 Cooling time required to achieve the correct induction temperature of 25 °C. 188

Figure 5.6 The effect of microwell agitation rate on growth of *E. coli* [pQR367] (●) and *E. coli* [pQR368] (■). 600 rpm (unfilled symbols), 800 rpm (grey filled symbols), 1000 rpm (black filled symbols). Error bars indicate the range of measured values about the mean. 191

Figure 5.7 The effect of microwell agitation rate on 7-hydroxycoumarin production from *E. coli* [pQR367] expressing P450SU1 (grey bars) and *E. coli* [pQR368] expressing P450SU2 (white bars). Error bars indicate the range of measured values about the mean. 191

Figure 5.8 The effect of microwell fill volume on growth *E. coli* [pQR367]. 1000 µL (▲), 800 µL (◆), 700 µL (■), 600 µL (×), 500 µL (*), 400 µL (●). Error bars indicate the range of measured values about the mean. 194

Figure 5.9 The effect of microwell fill volume on 7-hydroxycoumarin production from *E. coli* [pQR367] expressing P450SU1. Error bars indicate the range of measured values about the mean. 194

Figure 5.10 The effect of well position on the amount of liquid evaporated from a 96-DSW plate at 25 °C and 800 rpm. Plate locations: top left (◆), top right (■), middle left (▲), middle (×), middle right (+), bottom left (●), bottom right (*). Error bars indicate the range of measured values about the mean. 196

Figure 5.11 The effect of covering wells with a gas permeable membrane (open symbols) on the culture of *E. coli* [pQR367] (●) and *E. coli* [pQR368] (■) compared to uncovered wells (closed symbols). Error bars indicate the range of measured values about the mean. 196

Figure 5.12 7-hydroxycoumarin production from *E. coli* [pQR367] (grey bars) and *E. coli* [pQR368] (white bars). Substrate addition took place after 3 hours of culture. No product detected prior to 20 hours of culture. Error bars indicate the range of measured values about the mean. 199

Figure 5.13 The effect of substrate addition time on 7-hydroxycoumarin production from *E. coli* [pQR367] (grey bars) and *E. coli* [pQR368] (white 199

- bars). Error bars indicate the range of measured values about the mean.
- Figure 5.14** Schematic representation of the fully automated linked process sequence using *E. coli* [pQR367] and *E. coli* [pQR368] expressing cytochrome P450SU1 and P450SU2 respectively. Coloured wells represent filled wells as an example (orange: media and culture, blue: RO water). 201
- Figure 5.15** User prompt to initiate expression phase. 202
- Figure 5.16** Reproducibility of growth kinetic data collected from three separate runs on the culture of **(A)** *E. coli* [pQR367] in different areas of a 96-DSW plate (■) columns 3-4, (●) columns 7-8 and (▲) columns 11-12 and **(B)** of *E. coli* [pQR368] in different areas of a 96-DSW plate (□) columns 1-2, (○) columns 5-6 and (△) columns 9-10. Error bars indicate the range of measured values about the mean. 204
- Figure 5.17** Reproducibility of bioconversion kinetic data collected on the culture of *E. coli* [pQR367] in different areas of a 96-DSW plate (□) columns 3-4, (○) columns 7-8 and (△) columns 11-12 and the culture of *E. coli* [pQR368] (■) columns 1-2, (●) columns 5-6 and (▲) columns 9-10. Error bars indicate the range of measured values about the mean. 207
- Figure 5.18** Representative CO difference spectra of **(A)** P450SU1 expressed in *E. coli* [pQR367] and **(B)** P450SU2 expressed in *E. coli* [pQR368] during automated process sequence. Samples were from cultures where no 7-ethoxycoumarin was added. 208
- Figure 5.19** The effect of α -benzoflavone (α -B), β -benzoflavone (β -B), ALA, hemin, FeCl₃, thiamine, and trace elements on 7-hydroxycoumarin production from **(A)** *E. coli* [pQR367] expressing P450SU1 and **(B)** *E. coli* [pQR368] expressing P450SU2. Error bars indicate the range of measured values about the mean. 211
- Figure 5.20** The effect of the sugars D-fructose, D-glucose, maltose, L-arabinose, D-ribose and glycerol on 7-hydroxycoumarin production from **(A)** *E. coli* [pQR367] expressing P450SU1 and **(B)** *E. coli* [pQR368] expressing P450SU2. Error bars indicate the range of measured values about the mean. 212
- Figure 5.21** The effect of ALA concentration on the culture of **(A)** *E. coli* [pQR367] and **(B)** *E. coli* [pQR368]. 0 mM (▲), 1 mM (×), 2 mM (*), 3 216

mM (●), 4 mM (◆), 5 mM (■). Error bars indicate the range of measured values about the mean.

Figure 5.22 The effect of ALA concentration on 7-hydroxycoumarin production from (A) *E. coli* [pQR367] and (B) *E. coli* [pQR368]. 0 mM (▲), 1 mM (×), 2 mM (*), 3 mM (●), 4 mM (◆), 5 mM (■). Error bars indicate the range of measured values about the mean. 217

Figure 5.23 Representative CO difference spectra of (A) P450SU1 expressed in *E. coli* [pQR367] and (B) P450SU2 expressed in *E. coli* [pQR368] cultured at varying ALA concentrations. Samples were from cultures where no 7-ethoxycoumarin was added. 220

Figure 5.24 The effect of glycerol concentration on the culture of (A) *E. coli* [pQR367] and (B) *E. coli* [pQR368]. 2.5 gL⁻¹ (*), 5 gL⁻¹ (●), 10 gL⁻¹ (◆), 20 gL⁻¹ (■), fed 10 gL⁻¹ every 5 hours (▲). Error bars indicate the range of measured values about the mean. 222

Figure 5.25 The effect of glycerol concentration on 7-hydroxycoumarin production from (A) *E. coli* [pQR367] and (B) *E. coli* [pQR368]. 2.5 gL⁻¹ (*), 5 gL⁻¹ (●), 10 gL⁻¹ (◆), 20 gL⁻¹ (■), fed 10 gL⁻¹ every 5 hours (▲). Error bars indicate the range of measured values about the mean. 224

Figure 5.26 Representative CO difference spectra of P450SU2 expressed in *E. coli* [pQR368] cultured at varying glycerol concentrations. Samples were from cultures where no 7-ethoxycoumarin was added. 226

Figure 5.27 The effect of substrate concentration on 7-hydroxycoumarin production from (A) *E. coli* [pQR367] expressing P450SU1 and (B) *E. coli* [pQR368] expressing P450SU2. Experiments were conducted as described in section 2.3.2.3. Error bars indicate the range of measured values about the mean. 228

Figure 5.28 The effect of 7-ethoxycoumarin concentration on the culture of *E. coli* [pQR368]. 0.5 mM (■), 0.6 mM (◆), 0.7 mM (●), 0.8 mM (*), 1 mM (×). Error bars indicate the range of measured values about the mean. 230

Figure 5.29 The effect of substrate concentration on 7-hydroxycoumarin production from *E. coli* [pQR368]. 0.5 mM (■), 0.6 mM (◆), 0.7 mM (●), 0.8 mM (*), 1 mM (×). Error bars indicate the range of measured values about the mean. 230

- Figure 5.30** (A) Growth kinetics and (B) time course of 7-hydroxycoumarin production from *E. coli* [pQR367] (■) and *E. coli* [pQR368] (●) with 20 gL⁻¹ glycerol, 5 mM ALA and 1 mM 7-ethoxycoumarin (closed symbols) and no media supplementation with 1 mM 7-ethoxycoumarin (open symbols). Error bars indicate the range of measured values about the mean. 232
- Figure 5.31** CO difference spectra of (A) P450SU1 expressed in *E. coli* [pQR367] and (B) P450SU2 expressed in *E. coli* [pQR368] with (blue line) and without (green line) the addition of 5 mM ALA and 20 gL⁻¹ glycerol. Samples were from cultures where no 7-ethoxycoumarin was added. 234
- Figure 6.1** (A) Growth kinetics at a matched K_La of 115 h⁻¹ for *E. coli* TOP10 [pQR210] in a 75 L bioreactor (working volume 45 L) (■) and 96-DSW plate with a 500 μL fill volume (□) and corresponding 75 L DOT profile (----). Error bars indicate the standard deviation of triplicate optical density readings for the 75 L process and the range of measured values about the mean for the microwell process. (B) Bioconversion kinetics of CHMO with 0.5 gL⁻¹ bicyclo[3.2.0]hept-2-en-6-one (unfilled symbols) to lactone product (filled symbols) at a matched K_La of 115 h⁻¹ in a 75 L bioreactor (●) and 96-DSW plate (■). Error bars indicate the range of measured values about the mean. 243
- Figure 6.2** Relationship between 96-DSW plate fill volume and K_La. Values were measured using the gassing out approach in an adapted 96-DSW as described in section 2.6.11.1. These experiments were conducted at 37 °C, in LB glycerol medium with 0.2 mL⁻¹ PPG and at 1000 rpm. Errors bars indicate the standard deviation of triplicate measurements. 248
- Figure 6.3** Relationship between 75 L stirred bioreactor agitation speed and K_La. Values were measured using the gassing out approach as described in section 2.6.11.3. These experiments were conducted at 37 °C, in LB glycerol medium with 0.2 mL⁻¹ PPG, at a working volume of 45 L and an aeration rate of 1 vvm. Errors bars indicate the standard deviation of triplicate measurements. 249
- Figure 6.4** (A) Growth kinetics of *E. coli* TOP10 [pQR210] at a matched K_La of 228 h⁻¹ in a 75 L bioreactor (working volume 45 L) (■) and 96-DSW plate with a 500 μL fill volume (□) and corresponding 75 L DOT profile (-- 253

--). Error bars indicate the standard deviation of triplicate optical density readings for the 75 L process and microwell process. **(B)** Bioconversion kinetics of *E. coli* TOP10 [pQR210] biocatalyst with 0.5 gL⁻¹ bicyclo[3.2.0]hept-2-en-6-one (unfilled symbols) to lactone product (filled symbols) at a matched K_La of 228 h⁻¹ in a 75 L bioreactor (■) and 96-DSW plate (●). Error bars indicate the standard deviation of triplicate GC samples.

Figure 6.5 The effect of agitation speed and temperature (◆ 37 °C, ● 25 °C) on measured K_La values in a 7.5 L stirred bioreactor. Values were measured using the gassing out approach as described in section 2.6.11.2. These experiments were conducted in TB medium with 0.2 mL⁻¹ PPG, at a working volume of 5 L and an aeration rate of 1 vvm. Errors bars indicate the standard deviation of triplicate measurements. 256

Figure 6.6 (A) Growth kinetics of *E. coli* [pQR367] (■) and *E. coli* [pQR368] (●) at a matched K_La of 200 h⁻¹ in a 7.5 L bioreactor (working volume 5 L) and 96-DSW plate with a 1 mL fill volume (open symbols) for the first 3 hours of culture and then a matched K_La of 62 h⁻¹ for the remaining culture time and corresponding 7.5 L DOT profile for *E. coli* [pQR367] (light grey line) and *E. coli* [pQR368] (dark grey line) cultures. Error bars indicate the standard deviation of triplicate optical density readings for the 7.5 L process and the range of measured values about the mean for the microwell process. 259

Figure 6.6 (B) 7-hydroxycoumarin production from P450SU1 (■) and P450SU2 (●) at a matched K_La of 62 h⁻¹ in a 7.5 L bioreactor (closed symbol) and 96-DSW plate (open symbol). Error bars indicate the standard deviation of triplicate 7.5 L HPLC samples and the range of measured values about the mean for 96-DSW plate HPLC samples. 260

Figure A.1 Dry cell weight calibration curve for *E. coli* TOP10 [pQR210] cells. Error bars indicate the range about the mean of duplicate optical density readings (x) and duplicate biomass concentration measurements (y). Measurements were conducted as described in section 2.6.1 and 2.6.2. 308

Figure A.2 Dry cell weight calibration curve for *E. coli* [pQR367] cells. Error bars indicate the range about the mean of duplicate optical density 309

readings (x) and duplicate biomass concentration measurements (y).
Measurements were conducted as described in section 2.6.1 and 2.6.2.

Figure A.3 Dry cell weight calibration curve for *E. coli* [pQR368] cells. 309
Error bars indicate the range about the mean of duplicate optical density
readings (x) and duplicate biomass concentration measurements (y).
Measurements were conducted as described in section 2.6.1 and 2.6.2.

Figure A.4 Bicyclo[3.2.0]hept-2-en-6-one calibration curve. Error bars 310
indicate the standard deviation of triplicate stock preparations in ethyl
acetate. Experiments were conducted as described in section 2.6.4.2.

Figure A.5 (1*S*,5*R*)-2-oxabicyclo[3.3.0]oct-6-en-3-one calibration curve. 310
Error bars indicate the standard deviation of triplicate stock preparations in
ethyl acetate. Experiments were conducted as described in section 2.6.4.2.

Figure A.6 Cyclohexanone calibration curve. Error bars indicate the 311
standard deviation of triplicate stock preparations in ethyl acetate.
Experiments were conducted as described in section 2.6.4.2.

Figure A.7 ϵ -caprolactone calibration curve. Error bars indicate the standard 311
deviation of triplicate stock preparations in ethyl acetate. Experiments were
conducted as described in section 2.6.4.2.

Figure A.8 Norcamphor calibration curve. Error bars indicate the standard 312
deviation of triplicate stock preparations in ethyl acetate. Experiments were
conducted as described in section 2.6.4.2.

Figure A.9 2-oxabicyclo[3.2.1]octan-3-one calibration curve. Error bars 312
indicate the standard deviation of triplicate stock preparations in ethyl
acetate. Experiments were conducted as described in section 2.6.4.2.

Figure A.10 Cycloheptanone calibration curve. Error bars indicate the 313
standard deviation of triplicate stock preparations in ethyl acetate.
Experiments were conducted as described in section 2.6.4.2.

Figure A.11 Oxocan-2-one calibration curve. Error bars indicate the 313
standard deviation of triplicate stock preparations in ethyl acetate.
Experiments were conducted as described in section 2.6.4.2.

Figure A.12 (1*R*)-(-)-fenchone calibration curve. Error bars indicate the 314
standard deviation of triplicate stock preparations in ethyl acetate.
Experiments were conducted as described in section 2.6.4.2.

- Figure A.13** (+)-(3*R*,6*SR*)-Dihydrocarvone calibration curve. Error bars indicate the standard deviation of triplicate stock preparations in ethyl acetate. Experiments were conducted as described in section 2.6.4.2. 314
- Figure A.14** Cyclooctanone calibration curve. Error bars indicate the standard deviation of triplicate stock preparations in ethyl acetate. Experiments were conducted as described in section 2.6.4.2. 315
- Figure A.15** (1*R*)-(+)-camphor calibration curve. Error bars indicate the standard deviation of triplicate stock preparations in ethyl acetate. Experiments were conducted as described in section 2.6.4.2. 315
- Figure A.16** 7-ethoxycoumarin calibration curve. Error bars indicate the standard deviation of triplicate stock preparations in acetonitrile. Experiments were conducted as described in section 2.6.5.2. 316
- Figure A.17** 7-hydroxycoumarin calibration curve. Error bars indicate the standard deviation of triplicate stock preparations in acetonitrile. Experiments were conducted as described in section 2.6.5.2. 316
- Figure B.1** Chromatogram of 1 gL⁻¹ bicyclo[3.2.0]hept-2-en-6-one (retention time: 6.44 min) dissolved in ethyl acetate. Peak present at 11 minutes corresponds to naphthalene which was used as an internal standard and added to all samples. 317
- Figure B.2** Chromatogram of 1 gL⁻¹ (1*S*,5*R*)-2-oxabicyclo[3.3.0]oct-6-en-3-one (retention time: 13.53 min) dissolved in ethyl acetate. Peak present at 11 minutes corresponds to naphthalene which was used as an internal standard and added to all samples. 318
- Figure B.3** Chromatogram of 1 gL⁻¹ cyclohexanone (retention time: 5.65 min) dissolved in ethyl acetate. Peak present at 11 minutes corresponds to naphthalene which was used as an internal standard and added to all samples. 318
- Figure B.4** Chromatogram of 1 gL⁻¹ ε-caprolactone (retention time: 12.81 min) dissolved in ethyl acetate. 319
- Figure B.5** Chromatogram of 1 gL⁻¹ norcamphor (retention time: 7.39 min) dissolved in ethyl acetate. Peak present at 11 minutes corresponds to naphthalene which was used as an internal standard and added to all samples. 319

- Figure B.6** Chromatogram of 1 gL⁻¹ 2-oxabicyclo[3.2.1]octan-3-one (retention time: 14.83 min) dissolved in ethyl acetate. Peak present at 11 minutes corresponds to naphthalene which was used as an internal standard and added to all samples. 320
- Figure B.7** Chromatogram of 1 gL⁻¹ cycloheptanone (retention time: 8.25 min) dissolved in ethyl acetate. Peak present at 11 minutes corresponds to naphthalene which was used as an internal standard and added to all samples. 320
- Figure B.8** Chromatogram of 0.5 gL⁻¹ oxocan-2-one (retention time: 10.13 min) dissolved in ethyl acetate. Peak present at 11 minutes corresponds to naphthalene which was used as an internal standard and added to all samples. 321
- Figure B.9** Chromatogram of 1 gL⁻¹ (1R)-(-)-fenchone (retention time: 9.19 min) dissolved in ethyl acetate. Peak present at 11 minutes corresponds to naphthalene which was used as an internal standard and added to all samples. 321
- Figure B.10** Chromatogram of 1 gL⁻¹ (+)-(3R,6SR)-dihydrocarvone (isomer 1 retention time: 11.68 min, isomer 2 retention time: 11.86 min) dissolved in ethyl acetate. Peak present at 11 minutes corresponds to naphthalene which was used as an internal standard and added to all samples. 322
- Figure B.11** Chromatogram of 1 gL⁻¹ cyclooctanone (retention time: 10.42 min) dissolved in ethyl acetate. Peak present at 11 minutes corresponds to naphthalene which was used as an internal standard and added to all samples. 322
- Figure B.12** Chromatogram of 1 gL⁻¹ camphor (retention time: 10.81 min) dissolved in ethyl acetate. Peak present at 11 minutes corresponds to naphthalene which was used as an internal standard and added to all samples. 323
- Figure B.13** Chromatograms displaying the *E. coli* TOP10 [pQR210] bioconversion of 1 gL⁻¹ bicyclo[3.2.0]hept-2-en-6-one (retention time: 6.57 min) to (-)-(1S,5R)-2-oxabicyclo[3.3.0]oct-6-en-3-one and (-)-(1R,5S)-3-oxabicyclo[3.3.0]oct-6-en-2-one (retention times: 13.56 min and 13.67 min) at (A) 0 minutes and (B) 60 minutes. Peak present at 11 minutes corresponds 324

to naphthalene which was used as an internal standard and added to all samples. Results are from microwell based bioconversions.

Figure B.14 Chromatograms displaying the *E. coli* TOP10 [pQR210] 325
bioconversion of 1 gL⁻¹ cyclohexanone (retention time: 5.10 min) to ϵ -
caprolactone (retention time: 12.77 min) at **(A)** 0 minutes and **(B)** 60
minutes. Peak present at 11 minutes corresponds to naphthalene which was
used as an internal standard and added to all samples. Results are from
microwell based bioconversions.

Figure B.15 Chromatograms displaying the *E. coli* TOP10 [pQR210] 326
bioconversion of 1 gL⁻¹ norcamphor (retention time: 7.66 min) to 2-
oxabicyclo[3.2.1]octan-3-one (retention time: 14.79 min) at **(A)** 0 minutes
and **(B)** 60 minutes. Peak present at 11 minutes corresponds to naphthalene
which was used as an internal standard and added to all samples. Results are
from microwell based bioconversions.

Figure B.16 Chromatograms displaying the *E. coli* TOP10 [pQR210] 327
bioconversion of 1 gL⁻¹ cycloheptanone (retention time: 8.28 min) to
oxocan-2-one (retention time: 10.18 min) at **(A)** 0 minutes and **(B)** 60
minutes. Peak present at 11 minutes corresponds to naphthalene which was
used as an internal standard and added to all samples. Results are from
microwell based bioconversions.

Figure B.17 Chromatograms displaying the *E. coli* TOP10 [pQR210] 328
bioconversion of 1 gL⁻¹ (1R)-(-)-fenchone (retention time: 9.24 min) at **(A)** 0
minutes and **(B)** 60 minutes. Peak present at 6.34 minutes corresponds to
DMSO used to solubilise substrate. Peak present at 11 minutes corresponds
to naphthalene which was used as an internal standard and added to all
samples. Results are from microwell based bioconversions.

Figure B.18 Chromatograms displaying the *E. coli* TOP10 [pQR210] 329
bioconversion of 1 gL⁻¹ camphor (retention time: 10.82 min) at **(A)** 0
minutes and **(B)** 60 minutes. Peak present at 6.37 minutes corresponds to
DMSO used to solubilise substrate. Peak present at 11 minutes corresponds
to naphthalene which was used as an internal standard and added to all
samples. Results are from microwell based bioconversions.

Figure B.19 Chromatograms displaying the *E. coli* TOP10 [pQR210] 330

bioconversion of 1 gL⁻¹ cyclooctanone (retention time: 10.44 min) at (A) 0 minutes and (B) 60 minutes. Peak present at 11 minutes corresponds to naphthalene which was used as an internal standard and added to all samples. Results are from microwell based bioconversions.

Figure B.20 Chromatograms displaying the *E. coli* TOP10 [pQR210] bioconversion of 1 gL⁻¹ (+)-(3*R*,6*SR*)-dihydrocarvone (isomer 1 retention time: 11.83 min, isomer 2 retention time: 12.02 min) at (A) 0 minutes and (B) 60 minutes. Peak present at 6.40 minutes corresponds to DMSO used to solubilise substrate. Peak present at 11 minutes corresponds to naphthalene which was used as an internal standard and added to all samples. Results are from microwell based bioconversions. 331

Figure B.21 Chromatogram of 1 gL⁻¹ 7-ethoxycoumarin (retention time: 9.7 min) dissolved in acetonitrile. 332

Figure B.22 Chromatogram of 1 gL⁻¹ 7-hydroxycoumarin (retention time: 6.26 min) dissolved in acetonitrile. 332

Figure B.23 Chromatograms displaying *E. coli* [pQR367] bioconversion of 1 mM 7-ethoxycoumarin (retention time: 9.73 min) to 7-hydroxycoumarin (retention time: 6.26 min) at (A) 0 minutes and (B) 30 hours of bioconversion. Results are from induced shake flask based bioconversions. 333

Figure B.24 Chromatograms displaying *E. coli* [pQR368] bioconversion of 1 mM 7-ethoxycoumarin (retention time: 9.73 min) to 7-hydroxycoumarin (retention time: 6.26 min) at (A) 0 minutes and (B) 30 hours of bioconversion. Results are from induced shake flask based bioconversions. 334

Figure C.1 The background absorbance change with time and the absorbance change with time after addition of the cyclohexanone substrate for a typical spectrophotometric assay for CHMO activity. Assay performed as described in section 2.6.8. 336

Figure C.2 CO difference spectrums showing the effect of sample incubation time with carbon monoxide prior to wavelength scan. 337

Figure C.3 The effect of substrate addition on CO difference spectrum. 337

Figure C.4 Spectrums of sample reduced with sodium hydrosulphite and the same sample which has been bubbled with CO. 339

Figure C.5 CO difference spectrum. 339

Figure D.1 Representative Proton NMR of purified norcamphor products 2-oxabicyclo[3.2.1]octan-3-one and 3-oxabicyclo[3.2.1]octan-2-one.	340
Figure D.2 Representative C-13 NMR of purified norcamphor products 2-oxabicyclo[3.2.1]octan-3-one and 3-oxabicyclo[3.2.1]octan-2-one.	341
Figure D.3 Representative mass spectrum of purified norcamphor products 2-oxabicyclo[3.2.1]octan-3-one and 3-oxabicyclo[3.2.1]octan-2-one.	342
Figure D.4 Representative infra red spectrum of purified norcamphor products 2-oxabicyclo[3.2.1]octan-3-one and 3-oxabicyclo[3.2.1]octan-2-one. Trough at 1730.1 cm^{-1} indicates a carbonyl group (C=O) and a trough at 2949.5 cm^{-1} indicates a C-H group.	343
Figure D.5 Representative Proton NMR of chemically synthesised oxocan-2-one from cycloheptanone.	344
Figure D.6 Representative mass spectrum of chemically synthesised oxocan-2-one from cycloheptanone.	345
Figure D.7 Representative Proton NMR of purified oxocan-2-one from CHMO catalysed cycloheptanone.	346
Figure D.8 Representative C-13 NMR of purified oxocan-2-one from CHMO catalysed cycloheptanone.	347
Figure D.9 Representative mass spectrum of purified oxocan-2-one from CHMO catalysed cycloheptanone.	348
Figure D.10 Representative infra red spectrum of purified oxocan-2-one from CHMO catalysed cycloheptanone. Trough at 1724.9 cm^{-1} indicates a carbonyl group (C=O) and a trough at 2930.6 cm^{-1} indicates a C-H group.	349

List of Tables

Table	Page
Table 2.1 HPLC gradient programme	94
Table 3.1 Comparison of <i>E. coli</i> TOP10 [pQR210] culture to <i>E. coli</i> TOP10 [pQR239].	109
Table 4.1 Summary of calculated values for prediction of K_{La} at different well fill volumes.	138
Table 4.2 Amino acid sources tested using automated sequence.	146
Table 4.3 Selected ketone substrates catalysed by CHMO.	156
Table 4.4 Percentage evaporation of substrates tested.	164
Table 4.5 CHMO specific activity in the presence of substrates.	172
Table 5.1 Summary of P450 expression from shake flask cultures.	183
Table 5.2 Summary of the effect of carbon source on growth.	214
Table 5.3 P450 expression a varying ALA concentrations.	219
Table 5.4 P450 expression at varying glycerol concentrations.	225
Table 5.5 Comparison of P450 study with media additions.	233
Table 6.1 Comparison of microwell and bioreactor parameters.	242
Table 6.2 Summary of growth and bioconversion kinetics achieved at a matched K_{La} of 115 h^{-1} .	245
Table 6.3 Range of K_{La} values achievable in microwell formats compared to stirred bioreactors.	246
Table 6.4 Comparison of microwell and bioreactor parameters.	252
Table 6.5 Summary of growth and bioconversion kinetics achieved at a matched K_{La} of 228 h^{-1} .	254
Table 6.6 Comparison of microwell and bioreactor parameters.	257
Table 6.7 Summary of growth and bioconversion kinetics achieved at a matched K_{La} .	262

1 Introduction

1.1 The Context of the Research

There is a current trend to minimise the environmental impact of pharmaceutical manufacturing processes. It is well known that most of the organic chemistry forming the basis of such processes utilise multi-step synthetic methods with poor atom efficiency, where the by-product formation outweighs the final product recovery (Strukul, 1998). In particular, chemical oxidations are highlighted as being one of the least atom efficient and green of all industrial reactions (Lye et al., 2002). Biocatalytic alternatives hold many desirable traits such as the use of cleaner reagents and reactants, reduction in waste and simplification of synthetic procedures (Strukul, 1998), all of which are compatible with the concept of green chemistry. However, the design and implementation of a biocatalytic process can be challenging and has until now hindered the progression to full industrial exploitation. This is because biological processes involve multiple variables and individual process steps each requiring identification, characterisation and eventual optimisation. The experimental burden required to achieve optimised large-scale bioproduction will be labour intensive, time consuming and characterised by high investment in resources. The pharmaceutical industry is an ever competitive market with over 600 biologics under development each year (Bareither and Pollard, 2010), thus, in order to achieve a commercially viable product or process, methods need to be put in place to decrease costs and accelerate process development.

An approach is proposed where existing unit operations are miniaturised and linked to create small-scale process sequences within contained robotic platforms. The use of miniaturisation reduces resources and simplifies operation while automation increases consistency, speed and cuts down operator requirement. The integration of multiple operations is crucially important to streamline development and enable the interactions having an impact on product quality to be evaluated. Furthermore, key factors influencing biological parameters such as cellular growth and yield can be rapidly identified and further

optimised (Bareither and Pollard, 2010). In this way large-scale expensive trials can be minimised and conducted earlier using small-scale models. In addition if routine and repetitive tasks are conducted by robotic devices process performance can be improved by having a reduced downtime and operators assigned problem solving tasks. In order for scale down methods to be adopted such methods must demonstrate robustness and, more importantly, scalability to effectively mimic the performance of stirred tank systems for which a large-scale platform exists. The thesis will examine the hypothesis that high-throughput automated microscale approaches can be used for the development and investigation of novel oxidative biocatalytic processes. This is in line with one of the most challenging problems the pharmaceutical sector faces to establish financially viable and robust manufacturing processes (Chhatre and Titchener-Hooker, 2009).

1.2 Literature Survey

1.2.1 Microscale Bioprocessing Technology

1.2.1.1 Overview of Technology

There is continual pressure on the pharmaceutical and biotechnology industries to reduce developmental timelines and costs. Revenue reduction due to patent expiration, the requirement of reduced product costs from healthcare providers, and increased competition from generics on company pipeline portfolios are the main factors contributing to these pressures (Bareither and Pollard, 2010). One approach to tackle this issue is to invest in microscale bioprocessing technologies which refer to the microlitre study of individual bioprocess unit operations (Micheletti and Lye, 2006). Using microlitre volumes reduces the reagent requirements which can be significant when working with expensive media components, substrates or enzymatic cofactors (Bhambure et al., 2011). A wide range of process variables can be investigated enabling an increased knowledge of process constraints and limitations for fast identification of optimal conditions. Furthermore, such studies can be used as a rational basis for scale-up of the

systems evaluated (Fernandes and Cabral, 2006). Therefore microscale technologies have the potential to accelerate both upstream (Baboo et al., 2012) and downstream (Rayat et al., 2010) experimentation during early process design. This would ultimately lead to a reduction in the time it takes to progress from the initial discovery stages to delivering a usable product to the market. Thus microscale technologies aim at delivering quantitative bioprocess information early so that the translation from bioprocess design to manufacturing scale can be accelerated (Micheletti and Lye, 2006).

Two approaches currently being adopted are miniature stirred systems and miniature shaken systems. Miniaturisation is a common feature of both where the primary aim is to achieve higher throughput and the ultimate challenge is to accurately mimic large-scale processes whilst retaining the degree of functionality present in conventional bioreactors (Betts and Baganz, 2006). Miniature stirred systems and miniature shaken systems will be discussed in the following sections where the key features of each system will be highlighted and the most promising technologies will be discussed.

1.2.1.2 Miniature Stirred Systems

Currently there are two types of miniature stirred systems used for small-scale development. One approach is to use geometrically similar scaled down versions of conventional stirred tank reactors, with volumes ranging from 50 mL to 300 mL (Kumar et al., 2006). The second type have volumes of 10 mL and below and examples exist which utilise microtiter plates (Girard et al., 2001) or cuvettes (Kostov et al., 2001) containing stirrer bars or miniature agitation systems. Miniature stirred systems are used for early-stage process development and cell characterisation to speed up bioprocessing and reduce the labour requirement and material cost (Betts and Baganz, 2006). This is achieved through increased throughput and parallelization. Reducing the size of a bioreactor means that multiple units can be run in parallel to investigate a range of process variables. Gill et al. (2008) developed a novel miniature bioreactor system with the capacity to run 4 to 16 independently controlled fermentations. By using an

agitated microwell plate Girard et al. (2001) reported a small-scale bioreactor system where up to 12 experiments could be run simultaneously with the potential for parallelization of several hundred bioreactors if multiple plates were used within an automated platform. The highest throughput achievable in a stirred miniature system was reported by Puskeiler et al. (2005) who developed a “Bioreactor Block” with 48 individual bioreactors able to run simultaneously. The idea of multiplexing to achieve high-throughput processes has also been applied to microfluidic systems. Szita et al. (2005) reported a 150 μ L working volume microbioreactor system and demonstrated how 8 bioreactors could be run in parallel. While reproducible performance was obtained across all bioreactors, these systems still face the challenge of providing sufficient material for analytical and purification studies.

A disadvantage of reduced volumes can be a lack of monitoring and control. However, the scale at which miniature stirred systems operate means this has not been found to be an issue. While standard industrial probes are bulky and cannot be used in volumes below 2 mL, online monitoring and control of pH, temperature and dissolved oxygen tension (DOT) has been demonstrated using miniature probes (Gill et al., 2008), fibre optics (Lamping et al., 2003) and sensing patches (Puskeiler et al., 2005; Harms et al., 2006). A few years ago Fluorometrix developed Cellstation, a miniature bioreactor system with the capacity to monitor pH (Kermis et al., 2002), DOT and OD using online optical sensors during cultivations (Betts and Baganz, 2006). However, the addition of monitoring and control capacity to small-scale bioreactors increases costs (Kumar et al., 2004) as miniaturised probes are expensive or, in some cases, detrimental to the process in cases where oxygen is actually consumed by particular probes (Kostov et al., 2001). Therefore considering these drawbacks Kostov et al. (2001) reported a 2 mL low cost microbioreactor for high-throughput bioprocessing equipped with pH, oxygen and OD detection systems based on optical sensors for monitoring the culture environment.

Automation is a useful method to increase the productivity and robustness of a process. Presently, this is an area of much interest and continual research where the incorporation of automated technology with miniature stirred systems has

proved promising. Automation can be applied for the setup, preparation and monitoring of the culture. Medical Explorer is a 15 parallel unit fermentation system with automated sample collection and online OD measurement (Bareither and Pollard, 2010). Sterilisation, probe calibration, inoculation, sampling and harvesting have also been automated using Biospectra for mammalian cell culture (Bareither and Pollard, 2010). Gill et al. (2008) demonstrated fully integrated automated control of DOT and pH in each of 16 miniature reactors. Smaller systems can also be combined with sophisticated robotics for an increased level of process automation and will be discussed in section 1.2.2.

During bioreactor operation effective oxygen transfer to growing cells is a critical parameter. This needs to be maximised as in general higher oxygen transfer rates lead to higher cell densities and therefore increased product yield. The mechanical stirring utilised by miniature bioreactor systems provides both agitation of the cell suspension and the dispersion of the gas phase. This method of agitation has been found to achieve oxygen transfer capacities typically characterised by oxygen mass transfer coefficient (K_{La}) values similar to conventional lab-scale stirred tank reactors (Kumar et al., 2004; Betts and Baganz, 2006). In general, K_{La} values range from 100 – 300 h^{-1} in standard stirred-tank bioreactors of volumes varying from 30 to 50000 L (Trilli, 1986). A range of miniature bioreactors have been reported to achieve a K_{La} of 360 h^{-1} (Lamping et al., 2003), 480 h^{-1} (Betts et al., 2006), and even as high as 1600 h^{-1} (Puskeiler et al., 2005), the later values being close to the level achieved in industrial scale bioreactors. However, it has been reported that as these systems have only produced biomass concentrations below 10 $g_{DCW}L^{-1}$ they have yet to be truly challenged in maintaining high cell density cultures (Bareither and Pollard, 2010). Only the “Bioreactor Block” has shown promise in culturing cells of *Bacillus subtilis* up to 50 $g_{DCW}L^{-1}$ which was achieved using a intermittent feeding regime (Knorr et al., 2007).

It is important that small-scale systems can mimic conditions and productivity that would be expected at larger scales of operation (Gill et al., 2008). Due to the geometrical similarities matched performance to conventional bioreactors has been reported in 10 mL miniature bioreactors using a matched gassed power per

unit volume (Pg/V) approach (Betts et al., 2006) and in 100 mL (Gill et al., 2008) and 2 mL (Kostov et al., 2001) miniature bioreactors using a matched K_{La} . Therefore, modelling miniature bioreactors on lab scale systems is clearly an advantage in terms of providing scalable data. Furthermore, the importance of matching critical process parameters is also demonstrated where K_{La} is often the parameter of choice in aerobic systems.

Miniature stirred systems are currently being applied to areas of process optimisation, media and strain development and therapeutic drug development (Betts and Baganz, 2006). In particular the miniature bioreactor system reported by Betts et al. (2006) has been shown to effectively mimic conventional stirred tank reactor cell cultivations of varying rheology, shear-sensitivity and oxygen demand, demonstrating its versatility with a range of microorganisms. In general, miniature bioreactor systems at present have proved to be scalable, able to carry out parallel operations and can utilise sophisticated technology for the monitoring and control of critical parameters. However the degree of throughput cannot yet match that of microtiter plates. For example, while a variety of miniature stirred bioreactor systems do utilise the standard microplate format as yet there are limited reports of stirred bioreactor technologies being applied to more than 48 vessels limiting the progression of this technology to the ultra-high throughput level. The ability to increase the number of parameters which can be rapidly assessed is particularly important when developing a process for a new biological system especially if raw materials are rare and/or expensive. For this reason microtiter plates are potentially a more suitable method to achieving this goal.

1.2.1.3 Miniature Shaken Systems

In shaken systems fluid mixing, heat and mass transfer are achieved via shaking rather than using mechanical agitation. Shake flasks are one of the earliest forms of shaken systems and have been widely used due to their simple operation, inexpensiveness, lack of mechanical complications and reproducibility for a range of industrially relevant cell cultivations. In particular, they have been used

for bacterial (Losen et al., 2004), yeast (Guarna et al., 1997), fungi (Punt et al., 2002), animal (Micheletti et al., 2006), insect (Yamaji et al., 1999) and plant cell culture (Dörnenburg, 2010). Shake flask operation had remained unchanged for over fifty years with additions and sampling being carried out manually and no incorporation of online monitoring methods until quite recently (Weuster-Botz et al., 2001; Betts and Baganz, 2006). Despite such attempts to improve shake flasks this system has primarily remained as a screening and inoculum expansion tool (Bareither and Pollard, 2010). Major drawbacks include the difficulty in robotic handling, due to their shape and size, and limitations in miniaturisation and parallelisation (Duetz and Witholt, 2004). Furthermore, maintaining feed capability can be difficult which is of industrial relevance and the lack of similarity to stirred systems can make scale-up problematic (Bareither and Pollard, 2010). Sampling also requires removing the flask from optimum culture conditions where agitation and oxygen supply is interrupted. Such challenges have led to the development and use of alternative high-throughput microtiter plate formats.

Shaken microtiter plates were initially applied as analytical tools predominantly for screening in enzyme and gene assays (Persidis, 1998). They are already an established technology for high and ultra-high throughput (Major, 1998; Sundberg, 2000) processing and, more recently, this system has also been adopted for bioprocess studies. Plates come in a range of sizes from 6 up to 3456-well plates with volumes ranging from 3-3000 μL . This feature makes microtiter plates attractive in an effort to speed up bioprocess development particularly in the area of biocatalytic processes where there is a requirement to screen large libraries of biocatalysts before process optimisation can begin. In the case of the 3456-well plate format ultra-high throughput screening can process 10^5 compounds per assay per day (Sundberg, 2000).

Microtiter plates are available in different geometries and the application determines the most suitable one. The wells can be round, square and more recently flower petal designs have also been reported (Funke et al., 2009). While surface aeration can be a limiting factor to efficient oxygen transfer (Lamping et al., 2003), well geometry selection can help to override this issue. It has been

reported that the square geometry is particularly well suited for aerobic cultures as it aids mixing and oxygen transfer (Duetz and Witholt, 2001). The volumetric activity of oxidative enzymes has also been found to be higher in square well formats than in round wells (Doig et al., 2002). Higher turbulence levels due to the baffling effect of square edges promoting gas-liquid mass transfer have been suggested as a possible reason for the results observed (Doig et al., 2002; Betts and Baganz, 2006).

This effect becomes more pronounced as the number of edges in a well increases where the introduction of baffles into a circular microtiter plate has been found to double the oxygen transfer capacity (Funke et al., 2009). A range of thirty baffled microtiter plates have been designed by Funke et al. (2009) and these were tested to maximise the oxygen transfer whilst avoiding out-of-phase mixing conditions, maximise well fill volume and enable online-monitoring. From this study a 6-petal flower shaped well geometry which redirects the flow of the rotating liquid as baffles would, was found to fulfil all the above requirements producing K_{La} values above 500 h^{-1} and enhanced growth of microbial cultures. This value is nearly double that generally achievable in conventional microtiter plates (Duetz, 2007). It is important to note that Funke et al. (2009) measured K_{La} by using the sulphite oxidation method which has been claimed to overestimate mass transfer rates (Linek et al., 2004). However, the research clearly illustrates the benefits of baffled geometries and such improvements in oxygen transfer rates have clear implications for use with oxidative bioconversions. Microwell plates can also be of a standard geometry (300 μL) or a deep well format (2 mL) where an increased fill volume increases the culture capacity.

In addition to well geometry, the shaking diameter, intensity of orbital shaking and fill volume are also key variables in the gas-liquid mass transfer and mixing process (Duetz and Witholt, 2001; Lye et al., 2003; Duetz and Witholt 2004). Greater shaking diameters increase the surface area to volume ratio in the well, promoting vertical mixing and turbulent flow and contributing to improved oxygen transfer rates (Duetz and Witholt, 2001). Increasing the shaking intensity also promotes oxygen transfer and may also be required if a small shaking

diameter is used. Hermann et al. (2003) reported that a smaller critical shaking frequency is required at higher shaking diameters to increase the maximum oxygen transfer capacity. In-phase conditions have been defined as those where the bulk fluid moves in-phase with the shaking platform (Büchs et al., 2001; Duetz and Witholt, 2004). At high agitation rates, or when using baffled geometries, out-of-phase mixing can occur where the liquid does not circulate in phase with the orbital motion of the shaker resulting in splashing or spillage of the well contents (Duetz and Witholt, 2004; Betts and Baganz, 2006). Considering the size of microwell formats, fill volume is also noted to have an influence on air-liquid mass transfer (John et al., 2003; Kensy et al., 2005; Funke et al., 2009) where K_{La} has been reported to be inversely proportional to well fill volume (John et al., 2003). However, investigations on the effect of fill volume on K_{La} are limited and it would be worth investigating this parameter further to determine the extent to which this factor can control oxygen levels in microwells.

Some challenges are usually encountered when using microwell plate formats. Firstly, liquid evaporation can prevent their application for extended cultures. This issue can be tackled by using an appropriate plate cover. One such system designed by Duetz and Witholt (2001) has been shown to prevent well-to-well contamination, excessive evaporation, airborne contamination and maintain sufficient aeration rates. Alternatively, a sacrificial sampling method can ensure that the well content is not depleted excessively (Doig et al., 2002). Secondly, the use of small volumes can make the incorporation of monitoring and control devices quite challenging. Nevertheless, as covered in section 1.2.1.2, the miniaturisation of sensing equipment has been successfully developed and applied to small culture vessels. Sensing patches are probably the best option as they do not interfere with the culturing environment however fibre optics have also been successfully reported to work in well format (Islam et al., 2008; Ferreira, 2008).

The most impressive feature of microwells is the capacity to accommodate the need for multi-variable studies and as such it is important that such studies are conducted in a robust and timely manner. This can be achieved through automated processing whereby the microplate footprint and dimensions makes

them readily amenable to automation. This aspect will be discussed in detail in section 1.2.2. Features of microtiter plates have highlighted them as an attractive option for bioprocessing applications and have already been utilised in a number of areas.

1.2.1.3.1 Bioprocess Applications of Microwells

Several works in the published literature have demonstrated the use of microwells for individual unit operations including cell cultivation, bioconversion and downstream processing.

Microwell technology has been applied to the cultivation of a number of microorganisms including gram-negative bacteria, gram-positive bacteria and actinomycetes. Using a square well format Duetz et al. (2000) demonstrated the growth of 48 different *Pseudomonas* and *Rhodococcus* strains. A novel development in this work was a replication system capable of extracting volumes from frozen bacterial glycerol stocks without defrosting the whole stock. Using the same system Minas et al. (2000) cultured *Streptomyces* in 96-deep square well format where biomass concentrations and secondary metabolite production were found to be similar to both shake flask and bioreactor cultivations. Microwells have also been applied to the culture of *Saccharopolyspora erythraea* CA340 producing the polyketide antibiotic erythromycin (Elmahdi et al., 2003). In this work Elmahdi et al. (2003) demonstrated the importance of pH control at the microscale and reported enhanced maximum specific growth rates, biomass concentrations and product synthesis when pH control was used. In addition the results observed at the microscale were found to be similar to those obtained in a 7 L stirred tank reactor. One final example of microwell formats being used to culture a range of microorganisms is reported by Isett et al. (2007) who demonstrated that a 24-well plate miniature bioreactor system could be applied to *Saccharomyces cerevisiae*, *E. coli* and *Pichia pastoris* cultivations. When culturing *Pichia pastoris* with oxygen and pH control, ammonia and oxygen blending and a controlled glycerol feeding strategy, the miniature bioreactor was able to maintain biomass levels up to $278 \text{ g}_{\text{wcw}}\text{L}^{-1}$ (Isett et al.,

2007). Such studies confirm microwell techniques for screening libraries of microorganisms and evaluating physiological parameters that have an impact on growth and product synthesis.

Microtiter plates can be used for a variety of cell types including mammalian culture (Chen et al., 2009). For example, VPM8 hybridoma cells in suspension culture have been investigated for antibody production and shown reasonable similarity to stirred bioreactor cultures in terms of maximum cell densities (Micheletti et al., 2006). In addition, culture medium optimisation of Chinese hamster ovary cell (CHO) line cultures has been reported (Deshpande et al. 2004). In the area of bioprocessing there are also reports of microwell geometries being applied for the investigation of yeast (Hammonds et al., 1998; Weis et al., 2004), fungi (Bills et al., 2008) and algae (Skjelbred et al., 2012) culture.

Data collection on enzyme activity in bioconversions can also greatly benefit from the use of microtiter plates. A simple, efficient and timely method has been described by Stahl et al. (2000) who employed 24-well microtiter plates to effectively screen libraries of yeast and *rhodococci* for bioconversion activity. Among the 240 strains tested, 78 % were found to be positive when tested for the bioreduction of 6-bromo- β -tetralone to 6-bromo- β -tetralol (Stahl et al., 2000). This method proved to outperform the traditional screening methods as it reduced manual handling, screening initiation time and analytical operation time by utilising a robotic system capable of preparing assays directly from 24-well plate formats. Methods to determine kinetic parameters such as k_{cat} and k_m were also established. Parallel pH assays in 96-well formats were developed by John and Heinzle (2001) to screen for hydrolase activity. While the assay was developed using penicillin acylase to hydrolyse 4-nitrophenyl acetate, the method could be applied to different reactions where acids or bases are consumed or released (John and Heinzle, 2001). The Baeyer-Villiger oxidation is one such reaction which has been investigated using *E. coli* expressed CHMO (Doig et al., 2002; Ferreira-Torres et al., 2005). Marques et al. (2007, 2009) reported using microtiter plates for multistep biotransformation in two-liquid biphasic systems. The method would be suitable for systems using substrates

and/or products which are poorly water soluble or toxic to the cell. Similarly, Grant et al. (2012) developed a microwell based approach for the characterisation of two-liquid phase systems namely the bio-oxidation of alkanes. The high-throughput enzymatic performance and stability in microwell formats has also been demonstrated by Rachinskiy et al. (2009) where the effect of extreme conditions on enzymes over short time frames could be assessed.

Being able to predicatively evaluate growth and bioconversion conditions early on at the microscale have clear benefits in terms of reduced cost, however the impact of these upstream processes on downstream unit operations is also important. One particular area which has been focussed on for microscale studies is filtration (Chandler and Zydney, 2004; Vandezande et al., 2005). A system comprising both a commercial and custom-designed well filter plate integrated within a robotic platform has been shown to efficiently evaluate the impact of upstream processing conditions on microfiltration (Jackson et al., 2006). Cell type, buffer and media composition were all shown to affect the specific cake cell resistance during microscale normal flow filtration (Jackson et al., 2006). Following on from this work Rayat et al. (2010) investigated the effects of cell disruption on microscale microfiltration performance. In the area of purification an assay was developed to investigate purification adsorbents in 96-well plate format (Welch et al., 2002). Identified adsorbents could then be applied for impurity removal from process streams and Welch et al. (2002) demonstrated a quick and easy route to purification problems which is compatible with a range of separation types. In addition, bioconversion products have been recovered using microwell approaches (Lander, 2003). Lander (2003) used resins to bind CHMO bioconversion products in microwells where the resulting binding capacity was subsequently used to inform the design of in-situ product removal operations. This is a particularly useful approach where product inhibition occurs, a typical limitation of many biocatalytic processes. The ability to assess such methods at the microscale could also cut down the costs associated with selecting the best final product purification approach during initial developmental stages. In the area of chromatography there are some high-throughput chromatographic studies which have been reported based on ion exchange (Rege et al., 2004; Mazza et al., 2002) and the miniaturization of

protein purification (Rege et al., 2006). Additionally, microtiter filtration plates are available for nickel chelate affinity chromatography for protein purification (Holz et al., 2002). Filter plates are a common scale down separation technique and have been combined with automated dispensing to ensure rapid and reproducible transfer of resins and/or buffers (Coffman et al., 2008). Therefore such approaches are beneficial for chromatography development studies and have the capacity to screen multiple purification options simultaneously (Chhatre and Titchener-Hooker, 2009). The use of microscale techniques have the potential to enable the effective evaluation of interactions between unit operations in a complete bioprocess. In particular, due to the recent uptake of microwells for upstream process development, it is important to apply them more extensively to the downstream operations thus preventing these from becoming a processing bottleneck.

Due to the fact that microtiter plates are not mechanically agitated it is expected that these do not effectively mimic the behaviour of large-scale processes, occurring in aerated stirred tank systems. However, a number of studies have been published proving the reproducibility of data collected at the microscale to those achieved in lab scale systems. K_{La} values of 130 h^{-1} were estimated from measured dissolved oxygen concentrations during microbial culture in 96 round-bottomed microtiter plates and John et al. (2003) reported these values as being similar to a typical K_{La} achieved in moderately stirred bioreactor. Values up to 241 h^{-1} have also been reported in square deep well geometries due to the reported improved mixing and oxygen transfer capabilities (Duetz et al., 2000; Islam, 2007; Ferreira-Torres, 2008). K_{La} values up to 600 h^{-1} were achieved using a baffled 24-well microtiter plate (Funke et al., 2009). In the case of cellular cultivation the provision of oxygen unlimited conditions is desirable for effective study of growth and product formation. Previous works have indicated the potential for scale-up of microwell cultivations by matching the culture conditions at both scales. For example Isett et al. (2007) reported similar dextrose utilisation and oxygen uptake rate of *E. coli* BL21 cultures between microscale and a 20 L bioreactor even though differences in pH and dissolved oxygen levels were reported.

Traditionally successful scale-up is demonstrated when defined engineering conditions, such as K_{La} or P/V , are kept constant. A constant K_{La} has more been used where growth and/or bioconversion data from microwell plates have been reproduced in 1.4 L (Micheletti et al., 2006; Kensy et al., 2009), 2 L (Ferreira-Torres et al., 2002), 5 L (Marques et al., 2009) 7.5 L and 75 L (Islam et al., 2008) stirred bioreactors using microbial systems. Doig et al. (2002) also demonstrated that microwell systems could reasonably replicate substrate inhibition kinetics observed in a 2 L stirred tank reactor, confirming the use of microwells to successfully collect quantitative kinetic data. Protein formation has been effectively scaled up with microwell protein yields reproduced in 7.5 L and 75 L reactors (Islam et al., 2008) and 1.4 L stirred bioreactors (Kensy et al., 2009) at matched K_{La} conditions. By utilising a high-throughput microwell-based screen Marques et al. (2012) recently identified some enhanced siderophore producing strains. When the microtiter plate bioprocess was scaled up on the basis of a matched K_{La} approach the overall volumetric siderophore productivity was maintained in a 5 L stirred tank reactor (Marques et al., 2012).

In the case of mammalian systems power consumption has been tested as a scale-up parameter between microwell plates and a 5 L stirred bioreactor (Micheletti et al., 2006). The data achieved was not identical nevertheless there was similarity between growth profiles of VPM8 hybridoma cells providing a basis for scale translation studies. Chen et al. (2009) later reported the feasibility of using 24 well microplates as an effective scale down tool for CHO cell culture process development. It was established that cell growth, metabolite profiles, protein titre and quality from a microscale and 2 L stirred reactor CHO cell culture were within typical cell culture process variations however no specific scale-up criteria was followed. Both bioreactors were seeded at the same initial cell density, using the same cells and cultured with the same media which enabled comparable data to be obtained between both scales (Chen et al., 2009).

Finally, scale translation has also been observed in some of the microwell based downstream processing operations. Notably Jackson et al. (2006) found microscale results using filter plates to be comparable to a conventional laboratory scale membrane cell. Therefore by setting up consistent cultures

conditions or by maintaining crucial engineering parameters on scale-up microwell approaches have been shown to provide data which are similar to those achieved at lab scale.

The uptake of microtiter plates for bioprocess evaluation of a range of systems for both upstream and downstream operations has increased in the last ten years due to their high-throughput capabilities. In each of these areas multiple factors can be tested to achieve optimum processing performance and effective scale-up. In particular, the importance of investigating the interactions between changes occurring in upstream processing operations on subsequent downstream operations is crucial. Challenges are also faced in developing scale down downstream replicates in line with the advances achieved in upstream process development to prevent this from becoming the process bottleneck. In addition faster analytics are required to cope with the increase in data collection. From recent developments it is clear that microtiter plates are a promising technology platform for whole bioprocess development studies. While considerable work has been carried out on individual unit operations, limited effort has been directed to develop and integrate multiple microscale process steps.

1.2.1.3.2 Bioprocess Applications of Whole Process Approach

If the cost and time savings of performing a single unit operation at the microscale are desirable, the implications of being able to carry out a whole process from start to finish in microwell geometry would significantly enhance these benefits. In order to quantify the effects of changes made on individual stages in a bioprocess the development of linked process sequences is required. A good example concerns biocatalysts production for the synthesis of pharmaceutically active compounds. Genetic modifications to host cells can cause changes in substrate specificity (Raillard et al., 2001; Matsumura and Ellington et al., 2001), alterations in substrate uptake (Mirjalili et al., 1999) and unexpected by-product formation (Stassi et al., 1998). Combining a series of unit operations means such effects can be effectively evaluated. It was previously mentioned how Jackson et al. (2006) used differing feed streams to

determine the effects on microfiltration performance. Therefore upstream processing conditions can have effects on the choice of solid-liquid separation and this could be more rapidly evaluated if an appropriate microscale sequence was developed.

A microscale process for high-throughput expression of cDNAs in yeast was described by Holz et al. (2002). Clone selection, growth, protein expression and protein purification were each carried out at the microscale. However, this process was focussed on microwell based screens for protein production and eventual gene characterisation rather than on bioprocess optimisation or on informing large-scale protein expression. A clear motivation for mimicking process sequences at the microscale is to predict the performance in larger scale pilot plant trials therefore conditions used at the microscale can ultimately be used to design larger scale reactor conditions (Hibbert et al., 2005). This can be critical for evolving enzymes where microscale studies have identified the desired ideal properties and characteristics. For example, if a microscale screen shows an enzyme to remain active under extreme temperatures, this should also hold true in a bioreactor environment where enzyme deactivation or denaturation can occur due to oxidation (Mozhaev and Martinek, 1982) and hydrolysis (Srinivas and Panda, 1999).

An initial demonstration of automated process sequences was addressed by Ferreira-Torres et al. (2005) which involved linked growth, induction and bioconversion steps carried out using a Packard Multiprobe II robot. The system was able to evaluate recombinant whole cell biocatalysts libraries for the synthesis of chiral lactones. A similar approach was employed for an *E. coli* biocatalyst expressing Transketolase enzyme using a Tecan robot (Micheletti et al., 2006). In both cases results obtained at the microscale demonstrated a quantitative agreement in terms of maximum specific growth rate and final biomass concentration to those measured in lab scale bioreactors. It is therefore of interest to apply this methodology to an increased number of biocatalytic systems in particular those which are newly identified or have yet to be characterised to allow for quick identification of efficient industrial biocatalysts. Such systems will be discussed in section 1.2.3.1.2. In the studies described by

Ferreira-Torres et al. (2005) and Micheletti et al. (2006) complete ‘walk away operation’ was not achieved and many steps still required manual intervention. Additionally the process sequences were only used for a limited number of studies as a proof of concept. They were not applied extensively for process sequence optimisation which is required if microwell based process sequences are to be accepted as low cost design and development platforms.

In bioprocessing the scalability of a microwell whole process sequence plays a crucial role for process development as the production of biopharmaceuticals will inevitably need to be developed and manufactured at scale. Whereby reliable and reproducible bioprocess data from every step in the development cycle can be made available from a miniaturised automated system early on, optimisation studies can follow and lead to shorter product release times. For this reason there are continual efforts to increase the range of unit operations which can be studied in microwell format and to apply the knowledge gained from established automated process sequences to the analysis of larger libraries of evolved biocatalysts (Ferreira-Torres et al., 2005; Micheletti et al., 2006). The standardization of microwell plates makes them readily available for the incorporation with automation platforms as already highlighted. The benefits and advances of automation will therefore be discussed in the following section.

1.2.2 Process Automation

1.2.2.1 Overview of Automation Technology

There is a current industrial need for bioprocess automation to ‘guarantee constant high quality standards,’ ‘with high levels of precision, and to gain independence from specific personnel’ which can be achieved through automated execution and analysis of bioprocessing steps (Sonnleitner, 1997). In currently available platforms there are two commonly used robotic arms, including one used for liquid handling operations and another capable of transferring plates and devices from different locations on the robotic deck. The use of automation can provide significant advantages. Firstly the labour requirement is reduced where

repetitive tasks, such as preparing culture plates and growth monitoring, can be automated. Depending on the level of automation the roles of a laboratory worker can change considerably whereby major responsibilities will move away for culture maintenance and towards data analysis, process improvement and other developmental activities. This ultimately can lead to facilities with increased productivity.

Problems in bioprocesses often originate from two sources, namely human error and a lack of process understanding, both resulting in unexpected outcomes. Automation can remove human error and increase processing consistency. If a robot is programmed correctly then it has the capability to run for 24 hours without any reduction in processing performance and with a high degree of consistency. There is therefore a considerable reduction in production downtime where batch processes could be run back-to-back and overnight with the requirement of a single operator for monitoring and control. Moreover, overnight sampling increases the understanding of rate kinetics and the process which can increase the success of process targets being achieved (Bareither and Pollard 2010). An automated system can also cope with a larger number of strains or target compounds enabling rapid identification of growth or expression conditions. This is clearly desirable in bioprocessing where the number of variables affecting a process is often considered a bottleneck.

1.2.2.2 Automated Robotic Platforms

There are a number of commercially available robotic platforms which have been specifically developed to meet the bioprocessing needs. These are supplied by a variety of manufacturers including Gilson, Perkin Elmer, Tecan and The Automation Partnership. Specific features, as already mentioned, include pipetting and movement arms along with barcode readers for tracking plates, shakers with heating and cooling capacity for cell cultivation, vacuum filtration for separation steps and automated washing systems. Many are also housed within biosafety cabinets to ensure aseptic operation. While the benefits of automation have been realised for some time (Sonnleitner, 1997), only recently

and with the availability of automated platforms has there been a greater interest in applying automation for process development.

1.2.2.2.1 Application for Microscale Process Development

Automation platforms have been applied in both miniature stirred and miniature shaken systems. In the case of miniature stirred systems Puskeiler et al. (2005), Weuster-Botz et al. (2005) and Knorr et al. (2007) reported the use of a Tecan automated robot for the robotic sampling, analytics and pH control integrated with for the “Bioreactor Block”. The high degree of automation and control makes the system well suited for the optimisation of bioconversion reaction conditions. One disadvantage of the “Bioreactor Block” was that, although DOT could be monitored, only 8 out of 48 reactors could be simultaneously monitored. More recently an impressive technology developed by The Automation Partnership called the ambrTM (automated microscale bioreactor) system has been developed (Bareither and Pollard, 2010). This comprises 24, 10 mL working volume disposable cell culture reactors on the deck of a liquid handling robot. Sampling, additions and intermittent feeding regimes can all be automated using sterile processing and the system has been developed for mammalian cell culture. DO and pH are also measured using sensor patches on the base of each reactor.

Automation and integration with associated equipment is easier when working with microwell geometries due to their standard footprint of 86 X 128 mm² and a typical height of 14 mm (Lye et al., 2003). They can be stacked or placed in racks allowing multiple plates to be used for higher throughput processing. A commercially available micro fermentation system has been developed by m2p-labs which allows real time monitoring of biomass, pH, DOT and fluorescent proteins. Huber et al. (2009) used this system with an automated liquid handling robot and described high-throughput cultivations along with recombinant protein expression. This system has not been linked with other microwell based operations however Huber et al. (2009) did report that continual work into combining this approach with small-scale downstream processing techniques and

analytical assays was underway. A microscale automated screening approach for optimisation of protein refolding has recently been described (Ordidge et al., 2012). In this study it was demonstrated how the automated approach was suitable to carry out refold screening of a large number of experimental conditions which is required to identify the best conditions to increase active protein yields. A combination of growth and bioconversion has already been mentioned where automated platforms including the Packard Multiprobe II robot (Ferreira-Torres et al., 2005) and a Tecan Genesis (Micheletti et al., 2006) robot were utilised to demonstrate the potential for process automation and the respective shortcomings discussed. A crucial advantage of automation is the ability to create linked process sequences all using the same microwell format enabling a better understanding of process interactions which will be investigated further in this thesis.

A field that can significantly benefit from the use of automated microscale techniques is biocatalysis. Chemical oxidations typically require quantities of toxic or highly reactive reagents resulting in waste treatment and disposal difficulties. Applying automated microscale approaches can enable identification of sustainable biocatalytic alternatives for industrial pharmaceutical synthesis. Biocatalytic systems have been criticised due to the relatively slow implementation time. This is because of the number of steps required in the development of a bioconversion process, which include biocatalysts screening steps and selection of suitable operational conditions for production and bioconversion (Fernandes, 2010). Advantages of automation include faster biocatalysts library evaluation and rapid identification of industrially relevant substrates which is particularly desirable especially when substrates and associated cofactors for enzymatic synthesis can be costly raw materials at scale. Ultimately this leads to accelerated translation from discovery to pilot plant production (Lye et al., 2003).

1.2.3 Bioconversions

There is a current need to establish more productive biocatalytic processes to enable a greater industrial uptake. Biocatalysts can either be in the form of whole cells or isolated enzymes. Typically hydrolytic or isomerisation reactions are conducted by isolated/purified enzymes as they do not require cofactor regeneration, however removal of enzymes from their natural environment can be detrimental. In the case of reactions requiring cofactor recycling or regeneration, whole cells are preferred as it is easier and less expensive to utilise the cells natural ability to regenerate cofactors (Schmid et al., 2001). Isolation and purification increases costs therefore, as long as other host cell enzymes do not have a negative influence on the reaction, it is usually more economical to use whole cells. Moreover, enzymes within their natural environment can be more stable where they are protected from shear forces with a resultant longer half-life in bioreactor systems (Duetz et al., 2001).

Bioconversions utilising biocatalysis over chemical synthesis have many advantages and thus have become an attractive option in the synthesis of pharmaceuticals and optically pure fine chemicals as well as for the production of food and detergents (Duetz et al., 2001; Lye et al., 2003). In particular, the high regio, stereo and enantioselectivity possessed by a biocatalyst often result in fewer by-products produced while blocking/de-blocking steps are not required (Schmid et al., 2001). In the case of high regioselectivity this increases the degree of certainty that a particular product will or will not be made due to the biocatalyst having a particular preference for the direction of bond making or bond breaking (Tramper, 1996). Biocatalysts also reduce the number of reaction steps required and can operate under mild conditions using cheap and clean reagents (Tramper, 1996; Strukul, 1998).

For these reasons there has been an increase in the number of industrial applications for biocatalytic processes (Tramper, 1996; Schmid et al., 2001). For example penicillin acylase from *E. coli* is used to produce 6-aminopenicillanic acid. This is a one step process whereas the chemical route would require three

reaction steps and would operate under extreme conditions (Tramper, 1996). Other successful industrial examples are the use of xylose isomerase for the production of high fructose corn syrup (Jensen and Rugh, 1987), the synthesis of phenolic resins using peroxidases and the hydration of acrylonitrile into acrylamide catalysed by nitrile hydratase (Nagasawa and Yamada, 1990). In line with these successes it is of interest to increase the number of biocatalytic systems which can be applied for industrial processes. Oxidative biocatalysts are a promising group which have yet to be fully exploited at this scale.

1.2.3.1 Oxidative Bioconversions

Oxidative bioconversions incorporate oxygen into the substrate. They are particularly useful in synthetic chemistry to carry out a range of reactions such as epoxidations to produce styrene oxide and ethylene oxide, sulfoxidations for the production of dimethyl sulfoxide (DMSO), hydroxylations for steroid hydroxylation and the Baeyer-Villiger oxidation for antibiotic synthesis (Leak et al., 2009). Due to the industrial application of many of these reactions there is currently a need for the widespread usage of these bioconversions. The limitations of chemical synthesis has already been discussed, moreover chemical oxidations present additional problems whereby the requirement of high energy oxidants and flammable solvents is a safety concern often limiting large-scale industrial production (Blaser and Federsel, 2011). Biocatalysis is identified as a potential route forward in achieving simpler, cleaner, cheaper and more specific processes. However, the use of oxygenases also pose limitations including the requirement of co-factors, they can consist of multiple components which are sometimes membrane-bound, they can be unstable and reactions often require biphasic systems due to products or substrates not being water soluble (Van Beilen et al., 2003). Reactions utilising molecular oxygen can cause the formation of reactive oxygen species or radicals which can be detrimental resulting in biocatalysts inactivation (Leak et al., 2009). Such drawbacks can cause significant bottlenecks preventing efficient biocatalytic oxygenation processes being developed due to poor operational stability (Duetz et al., 2001).

Using whole cells is a useful method to tackle such issues as they have the ability to naturally remove reactive oxygen species which may be generated and can naturally regenerate essential cofactors. By utilising in-situ resin-based substrate feeding and product removal Hilker et al. (2008) operated a kilogram scale whole cell Baeyer-Villiger oxidation. This allowed increased substrate concentrations to be processed thus developing an industrially suitable method for asymmetric synthesis. In the case of the isolated enzyme approach, using the same whole cell system Zambianchi et al. (2002) has shown the use of isolated cyclohexanone monooxygenase and a NADPH regeneration system can yield products with high optical purity. However, the high cost of using cofactor regeneration systems still makes isolated enzyme systems undesirable. Commercial examples include the use of oxygenases for steroid hydroxylation for the production of corticosterone (Van Beilen et al., 2003) and for the production of Pravastatin (Serizawa and Matsuoka, 1991) which is used to lower cholesterol. Additionally a number of biotechnology companies have previously used oxidative microbes for sterol side-chain degradation which can result in the formation of pharmacologically active steroids (Kieslich, 1991). Oxidative systems therefore have been commercially exploited and are of great interest to both pharmaceutical and agrochemical industries due to the production of enantiomerically pure compounds justifying the requirement for continual research in this area to overcome many of the limitations already mentioned. Two such oxidative systems are Baeyer-Villiger monooxygenases and cytochrome P450s which have been investigated in this work.

1.2.3.1.1 Baeyer-Villiger Monooxygenases

The Baeyer-Villiger oxidation involves the oxidation of a ketone to an ester in the presence of a peroxy acid which acts as the oxidising agent (Baeyer and Villiger, 1899; Kamerbeek et al., 2003). Reaction scheme 1.1 shows a schematic diagram of the steps in a Baeyer-Villiger oxidation. An intermediate step involves the formation of a Criegee adduct when the ketone is attacked by a nucleophilic peroxy acid, then the intermediate is transformed into an ester and carboxylic acid (Criegee, 1948; Kamerbeek et al., 2003).

Reaction Scheme 1.1 Scheme removed due to copyright issues.

The Baeyer-Villiger oxidation has a number of applications in organic chemistry including antibiotic, steroid synthesis and pheromone synthesis which are utilised in agrochemistry as well as synthesis of monomers for polymerization (Strukul, 1998). The main reason why this reaction has been successful lies in a number of key properties. Firstly, the presence of many functional groups does not restrict the reaction and oxidation of unsaturated ketones will generally proceed. Secondly, the reaction is generally stereoselective and thus the regiochemistry of a reaction can be controlled (Strukul, 1998). Finally, there are a number of peroxy acids which can participate in the reaction (Strukul, 1998).

The production of spent carboxylic acids from the Baeyer-Villiger reaction need to be separated and disposed of which is not really feasible during large-scale industrial operations (Strukul, 1998). Many of the oxidants used in this reaction can also be toxic and unstable (Alphand et al., 2003). A possible alternative is to use transition metal catalysts for Baeyer-Villiger oxidations, however these have not been extremely successful as the reaction mechanism is not completely defined (Strukul 1998). A clear solution is represented by biocatalysis which has a number of benefits over chemical synthesis as previously discussed.

Baeyer-Villiger monooxygenases (BVMOs) are enzymes which, by employing molecular oxygen, can catalyse the nucleophilic oxygenation of cyclic or linear

ketones and generate the corresponding esters (Willets, 1997). BVMOs have also been found capable of electrophilic oxygenation of heteroatoms, an example being where sulfoxides are formed from organosulfides (Secundo et al., 1993). In particular, they have the ability to catalyse a wide variety of oxidative reactions in a regio- and enantioselective manner which can be difficult and often impossible to conduct chemically (Kamerbeek et al., 2003). Furthermore, such reactions can be carried out under mild and aqueous conditions. In combination with their broad substrate scope, Blaser and Federsel, (2011) state that BVMOs are currently the most advantageous biocatalysts for asymmetric Baeyer-Villiger oxidations. While there are a number of BVMOs which can synthesise industrially useful compounds (Tressl et al., 1978; Levitt et al., 1990; Carnell et al., 1991) no industrial process has yet to incorporate a BVMO catalysed step. This is mainly due to low volumetric productivities, product and substrate inhibition and cofactor requirements which in general limit many oxidoreductase catalysed bioconversions (Schulze and Wubbolts, 1999). A number of BVMOs have been cloned and expressed including cyclopentanone monooxygenase (Iwaki et al., 2002), cyclododecanone monooxygenase (Kostichka et al., 2001), steroid monooxygenase (Morii et al., 1999) and 4-hydroxyacetophenone monooxygenase (Kamerbeek et al., 2001). The most studied BVMO in terms of biocatalytic properties is cyclohexanone monooxygenase (CHMO).

1.2.3.1.1.1 Cyclohexanone Monooxygenase

Cyclohexanone monooxygenase (CHMO) from *Acinetobacter calcoaceticus* NCIMB 9871 is, at present, the best characterised BVMO. It was first discovered in 1975 where the bacterium was able to grow on cyclohexanol as a sole carbon source (Donoghue and Trudgill, 1975). It is NADPH and oxygen-dependent and has a molecular mass of 59 kDa. DNA sequencing was initially conducted by Chen et al. (1988) where CHMO was found to contain 542 amino acids however a corrected sequence was later published by Iwaki et al. (1999). Its ability to catalyse the stereoselective Baeyer-Villiger oxidation of a wide range of ketones means there is potential for industrial application (Alphand et al., 2003). Different types of commercially interesting lactones could potentially

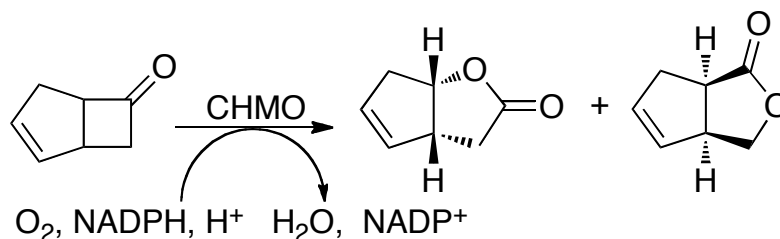
be produced via CHMO. For example, monocyclic lactones are used in the production of anti-tumour compounds and as intermediates in the synthesis of potent drugs for hypertension treatment, while hydroxylated lactones are components of immunosuppressant drugs (Alphand et al., 2003).

However, the use of the wild type strain has a number of undesirable features namely it being a class 2 pathogen, cyclohexanol is a toxic carbon required for enzyme induction (Trudgill, 1990) and it contains an active hydrolase which needs to either be removed or inhibited before biotransformation (Stewart et al., 1996). The purified enzyme presents an additional difficulty and would require an efficient cofactor recycling process as the enzyme is NADPH-dependant whereby the addition of stoichiometric amounts of NADPH during large-scale synthesis would be too expensive (Abril et al., 1989).

These implicit limitations have led to the development of a number of recombinant systems. One of the first was described by Chen et al. (1988) using *E. coli* to overexpress CHMO. A few years later Stewart et al. (1996) developed a recombinant yeast expressing CHMO, however as yeast contains an alcohol dehydrogenase, reduction of the starting ketone occurred and no improvement in usable substrate concentration was achieved (Stewart et al., 1996). Similarly, Chen et al. (1999) found that native yeast enzymes compromised the efficiency of CHMO oxidations while this was not found to be an issue with *E. coli* expression hosts which did not possess any competing oxidative enzymes. A study conducted by Doig et al. (2001) aimed at overcoming these limitations through the establishment of a recombinant *E. coli* expressing CHMO. This was developed through a series of plasmid constructs which began with cloning the CHMO gene from *Acinetobacter calcoaceticus* NCIMB 9871 to produce a construct pQR210 enabling CHMO induction from *E. coli* using isopropylthiogalactoside (IPTG). This system was improved further by replacing IPTG induction with L-arabinose to create the recombinant *E. coli* TOP10 [pQR239] which is non-pathogenic, easy to grow, it is lactose hydrolase (β -galactosidase) free and, as it is a whole cell biocatalyst, takes advantage of the intracellular recycling of NADPH (Doig et al., 2001). The use of an L-arabinose inducible promoter represents a cheaper alternative to IPTG and thus makes it

more attractive for large-scale production (Doig et al., 2001). A number of other recombinant bacterial strains have been developed to carry out Baeyer-Villiger type oxidations using the CHMO gene from *Acinetobacter calcoaceticus* NCIMB 9871 (Cheesman et al. 2001; Doo et al., 2009). Such studies have demonstrated that microbial strains can be genetically engineered to express CHMO which are a useful substitute to purified enzymes and can provide chemical and optical yields comparable to those obtained using traditional methods (Chen et al., 1999).

Once an appropriate recombinant system is available, in view of achieving improved biocatalytic systems for oxidative bioconversions, strategies are focussed on defining the best bioprocess steps for effective production at scale. This can involve optimising growth, expression and enzymatic activity. Progress has already been achieved with CHMO expressed from *E. coli* TOP10 [pQR239] and will be taken further in this thesis. Stemming from the initial characterisation studies in 2001, work has been done to demonstrate biocatalyst production at a range of scales from the microscale (Doig et al., 2002) up to 300 L stirred tank bioreactor scale (Doig et al., 2001). In particular, conditions impacting the CHMO specific activity have been evaluated including growth temperature and pH, inducer concentration and induction time, reductant type and reductant concentration. By increasing the level and activity of CHMO it can be used for efficient bioconversion processes where the majority of work has focused on the substrate bicyclo[3.2.0]hept-2-en-6-one. The use of this substrate has become the standard reaction when testing for asymmetric Baeyer-Villigerase oxidations (Doig et al., 2003). The CHMO catalysed Baeyer-Villiger oxidation of bicyclo[3.2.0]hept-2-en-6-one yields the regio-isomeric lactones (-)-(1*S*,5*R*)-2-oxabicyclo[3.3.0]oct-6-en-3-one and (-)-(1*R*,5*S*)-3-oxabicyclo[3.3.0]oct-6-en-2-one as shown in reaction scheme 1.2.



Reaction Scheme 1.2 CHMO catalysed oxidation of bicyclo[3.2.0]hept-2-en-6-one to (-)-(1*S*,5*R*)-2-oxabicyclo[3.3.0]oct-6-en-3-one and (-)-(1*R*,5*S*)-3-oxabicyclo[3.3.0]oct-6-en-2-one.

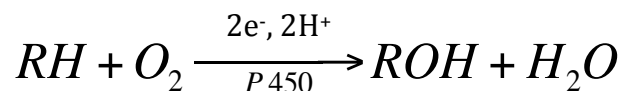
Shipston et al. (1992) found this enantioselectivity could not be achieved chemically using standard peracid and alkaline peroxide mediated oxidations making this an attractive biocatalyst. Bicyclo[3.2.0]hept-2-en-6-one and the related products have been found to be inhibitory to the whole cell biocatalysts (Shitu et al., 2009) and thus methods to overcome this issue have involved working below inhibitory limits or better still using reactant feeding and in-situ product removal approaches as described by Doig et al. (2002) and Hilker et al. (2008). In addition, CHMO expressed from *E. coli* TOP10 [pQR239] has been tested with a range of other substrates including cyclohexanone and cyclopentanone (Doig et al., 2003; Ferreira-Torres et al., 2005), racemic bicyclic diketones (Ottolina et al., 2005), 1,3-diathiane (Zambianchi et al., 2004) and α -substituted cyanocyclohexanones (Berezina et al., 2007). Therefore investigating multiple parameters and screening useful reactions is a demanding process and a move towards microscale approaches can offer a reliable solution as already discussed in section 1.2.1.1. Doig et al. (2002) initially demonstrated the successful application of microscale processing to quantify Baeyer-Villiger oxidation kinetics. This work was then extended by Ferreira-Torres et al. (2008) who demonstrated a microscale two-step part automated process sequence for evaluating whole cell CHMO libraries. Notably, the reproduction of growth and bioconversion kinetics collected from microwell studies in a 2 L stirred bioreactor confirmed the use of microwell technologies for process design and investigation (Ferreira-Torres et al., 2008).

1.2.3.1.2 Cytochrome P450s

Cytochrome P450 proteins have been studied since 1958 when they were first identified in the mammalian liver and found to be essential for drug metabolism (Klingenberg, 1958; Garfinkel, 1958). The P450 term originates from the absorption band exhibited at 450 nm when the protein is bound with carbon-monoxide which was first reported by Omura and Sato (1964) and is now used to identify the presence of active cytochrome P450s. Cytochrome P450s are enzymes belonging to a superfamily of haemoprotein monooxygenases found in both prokaryotes and eukaryotes (Degtyarenko and Archakov, 1993). Each cytochrome P450 is identified by a name all of which begin with the abbreviation CYP followed by a number representing the P450 family, a letter representing the subfamily and a number representing the individual gene such as CYP3A7 (Nebert and Nelson, 1991). The number can also be associated with the function of the enzyme where CYP21 is a steroid 21-hydroxylase however this is not always the case. This naming system only began in 1991 thus in some cases the original name may be used such as P450_{BM3} also known as CYP102.

1.2.3.1.2.1 The Cytochrome P450 Reaction Repertoire

Cytochrome P450s can carry out a range of oxidative reactions, however, hydroxylations are the most typical. Reaction scheme 1.3 shows the substrate is hydroxylated to form a hydroxylated metabolite and water.



Reaction Scheme 1.3 Cytochrome P450 mediated hydroxylation. RH represents the substrate.

The ability of P450s to carry out hydroxylations in a regiospecific and stereospecific manner highlights them as highly useful biocatalysts as such reactions are difficult to achieve using chemical methods (Speight et al., 2004). Depending on the host organism the function of P450 enzymes may vary. In the

case of prokaryotes, P450s are in a soluble form and used to detoxify xenobiotics, synthesise antibiotics and for fatty acid metabolism (Werck-Reichhart and Feyereisen, 2000). Plants use P450s for the synthesis of fatty acids and cutins (Bolwell et al., 1994). The synthesis of membrane sterols and mycotoxins is a common use in fungi (Werck-Reichhart and Feyereisen, 2000), whereas in bacteria they degrade numerous natural substrates (Celik et al., 2005 b). The function in animals can also be applied to the biosynthesis of steroids and hormones as well as having an important role in detoxification pathways (Werck-Reichhart and Feyereisen, 2000; Celik et al., 2005 b).

It is clear that the functions of cytochrome P450 enzymes are vast and the diversity of enzyme sources is considerable. For these reasons P450s have evolved to be able to catalyse a range of reactions such as isomerisations, dehydrogenations, dimerizations and carbon-carbon bond cleavage as well as many other pivotal reactions in drug metabolism. There is therefore a significant commercial interest in these enzymes. Ongoing research is being conducted using P450s to predict drug metabolism to prevent adverse side effects of drugs and to tailor enzymes to carry out specific functions by using methods such as site directed mutagenesis. It has been reported that the human liver enzyme CYP2D6 could be used to determine an individual's reaction to antipsychotics and antidepressants (Werck-Reichhart and Feyereisen, 2000). A recombinant *E. coli* system capable of carrying out the hydroxylation of α -ionone and β -ionone to mono-hydroxylated derivatives by over-expressing cytochrome P450SU1 (CYP105A1), P450SU2 (CYP105B1) and P450 soyC (CYP105D1) with high regioselectivity has also been investigated (Celik et al., 2005 a). Due to the fact that compounds such as ionones contain aroma elements from plant oils, the perfume and cosmetic industry are also showing interest in the utilisation of the reaction ability of P450s (Celik et al., 2005 a).

The synthetic potential of these biocatalysts is impressive, however, due their instability, complexity and in most cases low catalytic activity biotechnological use has been limited (Bernhardt, 2006). Presently, there are some commercial processes which utilise P450 catalysed steps. This includes steroid production such as hydrocortisone (Sonomoto et al., 1983; Szczebara et al., 2003) and

cortisone (Peterson et al., 1952) and statin production such as Pravastatin. The P450 gene CYP75A has also been used in creation of transgenic plants in particular production of blue roses (Holton et al., 1993) and creation of multicoloured carnations (Fukui et al., 2003). Considerable time is needed to generate adequate knowledge of the P450 system, as demonstrated by the aforementioned examples, in order to enable industrial process development (Bernhardt, 2006). It is therefore clear that establishing a platform for efficient P450 expression and bioconversion investigation has the potential to increase the industrial uptake of P450 catalysis and extend it to bioremediation, fine chemical synthesis and development of herbicide resistant plants (Celik et al., 2005 b).

1.2.3.1.2.2 Classification of Cytochrome P450s

Electrons from NAD(P)H are utilised by many P450s to activate molecular oxygen and initiate the regio and stereo oxidative attack of target substrates (Werck-Reichhart and Feyereisen, 2000). In P450-containing monooxygenase systems these electrons are delivered to the catalytic site by crucial protein components and thus are typically classified on the number they contain (Degtyarenko and Archakov, 1993). For this reason cytochrome P450s fall under the category of external monooxygenases due to their requirement of external electron donors (Bernhardt, 2006). Presently, there are three well-established classes along with a new class four, where the first example was reported in 2002 (Roberts et al., 2002). Since the 1980s a number of unusual electron transfer chains have been identified for a range of P450s taking the number of P450 classes up to ten and these have been reviewed by Hannemann et al. (2007).

1.2.3.1.2.2.1 Class I

Figure 1.1 Figure removed due to copyright issues.

Class one are three-component (or protein) systems consisting of a FAD-containing flavoprotein (NADPH or NADH-dependant reductase), an iron-sulfur protein (ferredoxin) and a P450 as shown in Figure 1.1. They are typically found in mammalian mitochondrial cells involved in steroid metabolism (Fulco, 1991) and bacterial systems which have a range of uses including xenobiotic metabolism (Taylor et al., 1999) and the production of secondary metabolites (Bernhardt, 2006). Mitochondrial P450s are membrane bound and the reductase is membrane associated, while the ferredoxin component is soluble (Fulco, 1991). This feature can make heterologous expression in *E. coli* difficult where functional activity is often low due to generation of insoluble precipitates (Arinc et al., 1999). Moreover, the lack of a P450 reductase means activity needs to be reconstituted by isolation and solubilisation of membranes along with the addition of an appropriate P450 reductase (Arinc et al., 1999). An example of a mammalian class P450 includes P450_{scc} (CYP11A1) from adrenal mitochondrial cells. This is involved in cholesterol side chain cleavage which results in the conversion of cholesterol to pregnenolone, a rate limiting step in steroid hormone biosynthesis (Hannemann, 2007). In general, the bacterial P450s and electron-transfer components are soluble. One of the best characterised class one cytochrome P450s is P450_{cam} (CYP101) from *Pseudomonas putida*. P450_{cam} has three fractions including a putidaredoxin reductase, an iron sulfur protein (putidaredoxin) and the cytochrome P450_{cam} (Katagiri et al., 1968). It is also the first cytochrome P450 to have its crystal

structure determined (Sevrioukova et al., 2004). It catalyses the regio and stereospecific hydroxylation of (1R)-(+)-camphor to 5-exo-hydroxy camphor (Katagiri et al., 1968) and is now established as the model bacterial cytochrome P450 for the study of other P450 monooxygenases (Celik et al., 2005 b).

1.2.3.1.2.2.2 Class II

Figure 1.2 Figure removed due to copyright issues.

Figure 1.2 shows a class two P450. Class two are two-component systems consisting of FAD/FMN-containing NADPH-dependant P450 reductase and a P450 and are commonly found in eukaryotic microsomal systems. The role of this class of P450 in mammals include oxidative metabolism of fatty acids, steroids and prostaglandins along with environmental toxins and carcinogens (Hasler et al., 1999). They can also be found in plants and are involved in cutin and lignin barrier synthesis as well as production of defence substances (Bolwell et al., 1994). While less common a prokaryotic two-component system was reported from *Streptomyces carbophilus* (Serizawa and Matsuoka, 1991). This prokaryotic P450, P450sca (CYP105A3) catalyses a hydroxylation reaction of mevastatin to pravastatin. Previous to this work all two-component systems reported were membrane bound and this was the first example of a prokaryotic system which was soluble with the potential to be more readily utilised for its reaction ability (Serizawa and Matsuoka, 1991).

1.2.3.1.2.2.3 Class III

Figure 1.3 Figure removed due to copyright issues.

Class three are one-component systems consisting of a single polypeptide as shown in Figure 1.3 and have been identified in various prokaryotes and eukaryotes. The first identified example was P450_{BM3} (CYP102A1) which has been intensively studied from *Bacillus megaterium* and has a haem and flavin domain (Nahri and Fulco, 1986) and is a soluble catalytically self-sufficient fatty acid monooxygenase. For this reason it is the most catalytically active of all P450s with a specific activity of greater than 4500 moles substrate oxygenated/mole of haem/minute (Fulco, 1991). It has been stated that the transfer of electrons to the P450 is often the rate-limiting step in catalysis (Bernhardt, 2006) and, as observed from P450_{BM3} this is not an issue when the electron transport functions and substrate oxygenation function are combined into one molecule. Due to the structural advantage of this system it is currently used as a model for mammalian hepatic P450 systems as the electron transfer system operates in a similar fashion (Warman et al., 2005). In this way isolation of the membrane-embedded hepatic P450 systems can be avoided.

Following the discovery of P450_{BM3} two other one-component systems from the same strain *Bacillus megaterium* were identified and expressed in *E. coli* and characterised using spectroscopic and enzymatic techniques (Gustafsson et al., 2004). This included CYP102A2 and CYP102A3 which had similarities in sequence and amino acid identities to P450_{BM3} but clear differences were observed in fatty acid binding preference and hydroxylation products demonstrating a difference in cellular roles within the source strain. A number

of class three P450s have now been identified with similar enzymatic traits to P450_{BM3} such as P450foxy (CYP505A1) isolated from the fungus *Fusarium oxysporum* which is self-sufficient has high catalytic turnover and similar molecular mass (Nakayama al., 1996). The hydroxylation of fatty acids also seems to be a common feature with many of the one-component systems.

The use of P450s can be limited especially eukaryotic systems which compared to bacterial have lower catalytic rates are typically insoluble and do not always express well in heterologous hosts (Bernhardt, 2006). Moreover, the complex electron transport systems limit the use. Self-sufficient P450s such as class three are more useful as they do not require the participation of additional proteins as they are already bound to the required protein components and this makes them good candidates for industrial applications (Liu et al., 2006). It is possible to clone the genes of these P450s into recombinant strains to gain a better understanding of how these systems work and increase the yield to enable the exploitation of the benefits of their catalytic ability. In view of the benefits of self-sufficient systems there is an interest in class four P450s which present a novel electron transport chain.

1.2.3.1.2.2.4 Novel Class IV

Figure 1.4 Figure removed due to copyright issues.

In 2002 a new class of cytochrome P450 enzymes was identified from *Rhodococcus sp.* strain NCIMB 9784 (Roberts et al., 2002) by using a polymerase chain reaction based methodology and shown in Figure 1.4. This strain of microorganism was of particular interest due to their role in the transformation of a range of xenobiotic compounds (Finnerty, 1992). The structure of this P450 differs from that of the classes already mentioned in that the C-terminal reductase is made up of a FMN-binding, NADH-binding and iron sulfur protein centre which closely resembles a dioxygenase reductase. Electrons are transferred through the FMN centre and the iron sulfur protein to the active site. This new P450, P450RHF (CYP116B2) does share a common feature with P450_{BM3} in that the activity of the enzyme is located at the N-terminal and it is another example of a self-sufficient single polypeptide system. Both the natural function and substrate specificity of this enzyme were unknown and due to the fused composition of this P450 to the required reductase it was cloned into an *E. coli* expression system whereby its ability to carry out the O-dealkylation of 7-ethoxycoumarin to 7-hydroxycoumarin was observed.

Liu et al. (2006) has reported the cloning, expression and characterisation of another P450 belonging to class 4, CYP116B3. It was identified in *Rhodococcus rubber* strain by using microbial strain screening and the protein sequence had a 93 % identity to P450RHF (Roberts et al., 2002). This P450 was found to hydroxylate a broad range of aromatics indicating the potential for bioremediation and synthesis applications. P450SMO which also has 73 % protein sequence identity to P450RHF has recently been expressed in *E. coli* and has been found to be an attractive biocatalyst for asymmetric synthesis or enantiopure sulfoxides (Zhang et al., 2010).

Hussain and Ward (2003 a, 2003 b) demonstrated the creation of three fused P450 systems. This includes P450SU1 and P450SU2 where *Streptomyces griseolus* is the source of P450 and ferredoxin and *Streptomyces coelicolor* is the source of the ferredoxin reductase (Hussain and Ward, 2003 b). In addition the fused system incorporating P450 soyC and ferredoxin from *Streptomyces griseus* and ferredoxin reductase from *Streptomyces coelicolor* is described (Hussain and Ward, 2003 a). In common with class three P450s and the novel class four they

are all self-sufficient single polypeptide systems receiving electrons from NADPH-cytochrome P450 reductase fused to the P450. Previous to these works a minimal number of prokaryotic P450 system ferredoxin reductases had been purified and characterised due to low expression compared to cytochrome P450s and unstable nature (Ramachandra et al., 1991). However, Hussain and Ward (2003 a, 2003 b) demonstrated that cloning the genes encoding the ferredoxin reductase downstream of the P450 and ferredoxins and coexpressing them stabilised the folded active form of the P450. This also resulted in greater whole cell biotransformation ability.

1.2.3.1.2.2.4.1 Cytochrome P450SU1 and P450SU2

Cytochrome P450SU1 and P450SU2 were found to be sulfonylurea herbicide metabolising enzymes in *Streptomyces griseolus* (O'Keefe et al., 1991). They were found to be enzymatically inactive alone, requiring an electron transport system. The activity could be reconstituted in the presence of the ferredoxins Fd-1 and Fd-2 from *Streptomyces griseolus* and an appropriate ferredoxin reductase (O'Keefe et al., 1991). This prompted the work conducted by Hussain and Ward (2003 b) to trial a 'mix and match' system combining components from two different strains. It was found that these systems could be expressed in *E. coli*, and high level expression of both P450SU1 and P450SU2 were found using *E. coli* BL21 Star (DE3)pLyS [pQR367] (referred to here on as *E. coli* [pQR367]) and *E. coli* BL21 Star (DE3)pLyS [pQR368] (referred to here on as *E. coli* [pQR368]) respectively. The increase in the level of catalytically active P450 expressed of 55 nmol per g of soluble protein for P450SU1 and 413 nmol per g of soluble protein for P450SU2 was achieved through strain selection and the introduction of the ferredoxin reductase. The addition of haem precursor alpha-aminolevulinic acid (ALA) and ferric chloride (FeCl₃) were also highlighted as enhancing active P450SU2 levels. These systems were tested for their hydroxylation activity and found to successfully convert 7-ethoxycoumarin to 7-hydroxycoumarin. They have also been successful in metabolising α -ionone to 3-hydroxy- α -ionone and β -ionone to 4-hydroxy- β -ionone with a high degree of regioselectivity (Celik et al., 2005 a). Compared to the wild type

system *Streptomyces griseolus*, no enantioselectivity was observed when catalysing β -ionone (Celik et al., 2005 a). This work is a nice demonstration of the ferredoxin reductase of *Streptomyces coelicolor* being able to donate electrons to non-native ferredoxins.

Unlike membrane-bound human counterparts the advantage of the *Streptomyces* species is the provision of soluble P450 enzymes with a broad substrate specificity. Moreover, this species is involved in producing about two-thirds of the naturally occurring antibiotics and secondary metabolites thus have a high biotechnological relevance (Bernhardt, 2006). Hussain and Ward (2003 b) state that the fused recombinant system has the potential to prepare drug metabolites in quantity to assess their toxicological effects. Alternative methods using media additions have been found to improve enzymatic expression of a range of P450 systems which could potentially further improve the method described by Hussain and Ward (2003 b).

Using P450 soyC Taylor et al. (1999) reported that components termed as P450 activators including α -benzoflavone and β -benzoflavone could stimulate activity. It was found that these P450 activators could bind near to the active site and influence the bioconversion of particular substrates. α -benzoflavone was also found a few years earlier to also activate P450 3A4 from human liver (Ueng et al., 1997). It is well documented that haem precursors such as ALA, and the iron containing media supplements hemin and FeCl_3 improve P450 yields. ALA is most predominately used in many studies where there are reports of two fold (Imai et al., 1993), four fold (Taylor et al., 1999, Richardson et al., 1995) and even 20 fold (Jansson et al., 2000) increases in expression levels of various P450s. Gillam et al. (1995) actually report it being essential for heamoprotein production. This haem precursor is also typically used in combination with FeCl_3 where a 32 % increase in active P450 was reported when ALA and FeCl_3 were used in combination (Hussain and Ward, 2003 b). Jansson et al. (2000) also reported an increase in the active P450 yield on addition of both ALA and FeCl_3 . Zhang et al. (2010) found that the expression of P450SMO was increased by 10 % when media was supplemented with FeCl_3 . It is possible that FeCl_3

increases the yield of active P450 by providing a source of iron for correct haem formation, as iron levels regulate ALA synthase which is an important enzyme in haem synthesis. It has also been suggested that it compensates for the lack of iron in *E. coli* (Kubota et al., 2005). In the case of hemin, which is the oxidised form of haem, this cofactor can trigger other enzymes in the haem biosynthetic pathway as well as increase haem enzyme activity (Lu et al., 2010). Reports using a Baculovirus expression system for human cytochrome P450 have indicated the advantage of using hemin where a 10-fold increase in P450 content was observed when hemin was added to the culture. In the same study the time of addition was also found to affect expression (Chen et al., 1996). Controversial information has been published regarding the inclusion of trace elements and thiamine during culture and have been noted to enhance P450 expression (Shimada et al., 1998; Gillam et al., 1995; Fischer et al., 1992), although other sources do state they are not essential for expression (Phillips and Shephard, 2006; Jansson et al., 2000). Finally, P450 gene expression has been found to be enhanced by glycerol and sugar supplementation (Kagawa and Cao, 2001). In the case of a microsomal P450, arabinose was found to enhance expression by inducing an osmotic stress response and was reported to play a crucial part in formation of functional proteins (Kagawa and Cao, 2001). The availability of a high-throughput approach would be beneficial to rapidly test a number of these media supplements and could be used to optimise P450 expression and bioconversion performance.

1.2.3.1.2.3 Application of High-throughput Approaches

Due to the associated complexities of the P450 electron transport systems so far it has been difficult to select target P450 enzymes from large variant libraries and effectively carry out preparative scale biotransformation (Speight et al., 2004). Therefore, work has been carried out in an attempt to speed up this process by developing rapid P450 identification methods. Speight et al. (2004) initially developed a method whereby fully randomized active site libraries were generated and biotransformation were carried out in 96-well plates to identify P450cam variants having the desired activity. Celik et al. (2005 b) has proposed

an alternative approach based on the production of an indigo dye from P450cam mutants. Celik et al. (2005 b) claimed this method increased the number of mutants that could be screened in parallel by conducting the screen directly from agar plates. In order to increase the dealkylation activity of CYP116B3 a high-throughput screening system was used to test 7800 variants (Liu et al., 2010). This system involved cultivation of variants in microwell plates followed by a fluorescence assay based on the production of 7-hydroxycoumarin.

There is a current interest in gaining more information in a timely manner about novel P450 systems due to the catalytic activity they may possess. High-throughput approaches have been used to screen libraries of P450 enzymes for bioconversion activity. However, as yet there has been little emphasis on whole bioprocess evaluation of a P450 expression system for eventual large-scale production. In order for a biocatalytic process to be effectively utilised there needs to be a distinct process in place where cells are cultured, enzyme is expressed, bioconversion conducted and products extracted. Each step needs to be tested to identify constraints and process interactions for the creation of an optimised process and by establishing high-throughput methods capable of this, can this goal be achieved. Therefore it is of interest in the present study that an automated microwell process sequence for kinetic evaluation of whole cell P450 biocatalysts is developed. There is a particular emphasis on working towards being able to predicatively scale-up the microwell process so that information collected can inform large-scale process development. This approach is required if an industrially relevant process is to be designed and optimised in a shortened timeframe.

1.3 Conclusions of the Literature Survey

It is evident from a detailed review of the literature that miniaturisation is a clear route able to meet the demands for lower costs and reduced biologic developmental timelines. When a new biologic is identified, whether this is a compound of biopharmaceutical interest or a biocatalyst capable of metabolising a pivotal step in the production of antibiotics, the experimental burden can be

quite significant. The biological nature inherently means an investigation of growth conditions, expression conditions, product stability, product half-life and purification methods is necessary to name a few. It has been found that microscale technologies can be applied in all these areas. In particular microtiter plates are a promising format that enable parallel investigation of multiple variables while requiring a reduced quantity of often scarce and expensive raw materials. Plate formats have an unmatched high-throughput capacity not only because of the number of wells available as miniature bioreactors but because multiple plates can be stacked for storage and then used or analysed in sequence. Furthermore, the range of geometries available help cater for the needs of multiple organisms or application purposes. While geometrical differences to conventional stirred systems do present variations in fluid hydrodynamics and mixing regimes this has not hindered the reproduction of data collected between both configurations indicating microtiter plates as a tool for predictive scale-up. Moreover, their standard size and shape means they can be readily incorporated with robotic platforms for automated processing. Thus moving towards automation is crucial in terms of increasing consistency and productivity, whereby mundane repetitive tasks can be automated and manpower potentially delegated to developmental activities requiring problem solving and critical thinking.

The area of oxidative bioconversion was highlighted due to the vast biotechnological potential including fine chemical synthesis, bioremediation, antibiotic and steroid synthesis, drug metabolism and flavour and detergent production. While some industrial processes do utilise steps catalysed by oxidative enzymes, this has taken over a decade of developmental research to generate the necessary knowledge for effective implementation and this is due to two distinct reasons. Firstly, this is due to biocatalyst properties such as instability, low catalytic rates and system complexity and, secondly, to the slow speed at which libraries are screened and operational conditions for production and bioconversion selected. It is of interest to develop cleaner, cheaper and more specific environmentally compatible biocatalytic approaches for oxidative reactions. This is considering the undesirable features of chemical routes including the requirement of toxic and unstable solvents/reagents which poses

safety issues making large-scale production undesirable, the lack of regioselectivity making access to particular products impossible, and the operation under extreme conditions. In an effort to accelerate the implementation of sustainable oxidative biocatalytic processes, automated microscale technologies are highlighted for process development and investigation and will be the focus of this thesis.

1.4 The Present Contribution

Presently, the majority of microscale based technologies have been used either as screening tools or to characterise individual unit operations. There has been a limited focus on linking microscale unit operations to enable an investigation of process interactions and to be used as an effective small-scale model for bioprocess design and development. The aim of this thesis is to apply such approaches to novel biocatalytic systems, which has not been previously reported, and could be used for systematic characterisation prior to committing time and resources to large-scale biological improvement strategies.

The first objective of the thesis is the development of a fully automated generic microscale platform. Specific aims of this platform would include a demonstration of robustness to enable process consistency, an increased throughput enabling multiple conditions to be evaluated in a single run and the ability to save time and effort compared to manual operations without compromising precision and accuracy of data collection. Due to the vast biotechnological applications of oxidative biocatalysts and with a wider view for better exploitation of the catalytic versatility, the microscale platform was initially developed using the CHMO expressing recombinant strain *E. coli* TOP10 [pQR210]. Fernandes and Cabral (2006) have stated that ‘the core of most bioprocesses is a biotransformation or fermentation step and its characterisation and optimisation is a key issue for the design of an effective and competitive process’. The second objective was to demonstrate the platform could be used for whole bioprocess optimisation to enable quicker identification of process constraints and limitations. With a working generic platform in place the third objective was to demonstrate it could be applied to novel systems in

particular those which have yet to be investigated or probed for specific growth, expression and activity requirements. The number of P450 catalysed reactions used in industrial synthesis is low, however, the availability of self-sufficient systems overcoming inherent limitations could be a way forward to increase the industrial uptake. A number of novel self-sufficient systems have recently been reported, therefore it was considered important to show the methodology could be applied to the P450 systems developed by Hussain and Ward (2003 b). This included *E. coli* [pQR367] expressing P450SU1 and *E. coli* [pQR368] expressing P450SU2 where the microscale approach was adapted to culture, express and conduct whole cell bioconversions using these novel systems. It is important that optimisation objectives perform similarly in model and production systems (Freyer et al., 2004) if they are to effectively inform developmental activities at a reduced cost and within a shortened timeframe. Thus the fourth and final objective was to investigate the potential for automated microscale approaches to be predictive of laboratory and pilot scale operations.

1.5 Outline of the Thesis

The thesis will examine the hypothesis that high-throughput automated microscale approaches can be used for the development and investigation of novel oxidative biocatalytic processes.

Chapter 1 presented the overall context of the research with an introduction to the thesis hypothesis. It details a literature survey reviewing the current advancements in the areas of microscale technologies, automation and bioconversion and highlights those requiring further investigation. This chapter concludes with the major findings of the literature survey and the present contribution of this thesis to the field of research.

Chapter 2 documents the materials and methods used to conduct all experimental procedures used in the generation of thesis results discussed in Chapters 3 to 6.

Chapter 3 describes the methodology used in the design and development of a fully automated generic microscale platform for the investigation of whole cell oxidation biocatalytic processes. *E. coli* TOP10 [pQR210] expressing CHMO is used as an exemplary system to test the platform.

Chapter 4 describes how the generic microscale platform developed in Chapter 3 was used for the whole bioprocess evaluation of the oxidative biocatalyst CHMO expressed from the recombinant system *E. coli* TOP10 [pQR210].

Chapter 5 describes the application of the generic microscale platform for the investigation of two novel cytochrome P450 expression systems *E. coli* [pQR367] expressing P450SU1 and *E. coli* [pQR368] expressing P450SU2. In particular the microscale platform is used to improve the biocatalytic performance by assessing the impact of media supplementation on the O-dealkylation of 7-ethoxycoumarin to 7-hydroxycoumarin.

Chapter 6 describes the methodology used to examine the potential for predictive scale-up of automated microscale approaches. A optimised process sequence identified from whole bioprocess evaluation of *E. coli* TOP10 [pQR210] expressing CHMO is scaled up to 75 L pilot plant scale, and a improved system for 7-ethoxycoumarin bioconversion using *E. coli* [pQR367] expressing P450SU1 and *E. coli* [pQR368] expressing P450SU2 is scaled up to 7.5 L laboratory scale.

Chapter 7 presents the overall thesis conclusions and suggestions for future work.

2 Materials and Methods

2.1 Materials

2.1.1 Chemicals

Yeast extract, tryptone (LP0042), bacteriological peptone (LP0037) and bacteriological agar were obtained from Oxoid limited (Basingstoke, UK). Sodium chloride, ampicillin sodium salt, bicyclo[3.2.0]hept-2-en-6-one (98 %), (-)-(1*S*,5*R*)-2-oxabicyclo[3.3.0]oct-6-en-3-one (99 %), sodium phosphate monobasic and dibasic, potassium phosphate monobasic and dibasic, (1*R*)-(+)-camphor (98 %), (1*R*)-(-)-fenchone (98 %), (3*R*,6*RS*)-(+)-dihydrocarvone (98 %), norcamphor (98 %), cyclohexanone (99.5 %), cycloheptanone (99 %), cyclooctanone (98 %), ϵ -caprolactone (99 %) dimethyl sulfoxide (DMSO), broadbean peptone (50209041), tryptone pancreatic digest from casein (LP0042R), 5-aminolevulinic acid hydrochloride (ALA), D-ribose, D-glucose, D-fructose, maltose, Bradford reagent, dithiothreitol (DTT) α -naphthoflavone, ethylenediaminetetraacetic acid (EDTA), trace elements, thiamine, polypropylene glycol 2000 (PPG), Laemmli 2X concentrate sample buffer, isopropylthiogalactoside (IPTG) and bovine serum albumin (BSA) were obtained from Sigma-Aldrich Company Ltd (Poole, UK). Glycerol, ethyl acetate, hemin and naphthalene were obtained from Alfa Aesar (Lancashire, UK). Soyabean peptone (70178), peptone from casein pancreatic digest (21509031), peptone from casein tryptic digest (70172) and tryptone enzymatic digest from casein (95039) were obtained from Fluka (Poole, UK). Peptone (P/1160/48), Iron (III) chloride hexahydrate (FeCl_3), phenylmethylsulfonyl fluoride (PMSF), 7-hydroxycoumarin (99 %) and TRIS base were obtained from Fischer Scientific (Loughborough, UK). BD Bacto-yeast extract and BD Bactotryptone were obtained from Becton Dickinson (New Jersey, USA). β -naphthoflavone, acetonitrile, methanol, hexane, 7-ethoxycoumarin (99 %) and TRIS HCL were obtained from VWR International (Leicestershire, UK). Sodium dithionite (sodium hydrosulphite) was obtained from SLS LTD (Nottingham, UK).

Tricine, chloramphenicol and NADPH tetrasodium salt were obtained from Merck Chemicals LTD (Nottingham, UK).

2.1.2 Microorganisms

E. coli TOP10 was originally obtained from Invitrogen (Groningen, The Netherlands) and *Acinetobacter calcoaceticus* NCIMB 9871 from NCIMB (Aberdeen, Scotland, UK). The CHMO gene was cloned into *E. coli* TOP10 from *Acinetobacter calcoaceticus* NCIMB 9871 using the vector, pKK223-3, as reported by Doig et al. (2001) to produce *E. coli* TOP10 [pQR210].

E. coli BL21 Star (DE3)pLysS was originally obtained from Invitrogen (Groningen, The Netherlands). Construction of expression vectors harboring the genes for P450SU1 its adjacent ferredoxin Fd1 from *Streptomyces griseolus* and ferredoxin NADP reductase SCF15A gene from *Streptomyces coelicolor* as well as the transformation into *E. coli* BL21 Star (DE3)pLysS to create *E. coli* BL21 Star (DE3)pLysS [pQR367] has been described previously by Hussain and Ward (2003 b). Construction of expression vectors harboring the genes for P450SU2 its adjacent ferredoxin Fd2 from *Streptomyces griseolus* and ferredoxin NADP reductase SCF15A gene from *Streptomyces coelicolor* as well as the transformation into *E. coli* BL21 Star (DE3)pLysS to create *E. coli* BL21 Star (DE3)pLysS [pQR368] has been described previously by Hussain and Ward (2003 b).

2.2 General Methods

2.2.1 *E. coli* TOP10 [pQR210]

2.2.1.1 Seed Stock Preparation

The overnight culture was prepared by inoculating a single colony of *E. coli* TOP10 [pQR210] in LB-glycerol (10 gL⁻¹ tryptone, 10 gL⁻¹ sodium chloride, 10 gL⁻¹ yeast extract, 10 gL⁻¹ glycerol and 50 mgL⁻¹ ampicillin added after

sterilisation through a 0.2 micron sterile filter) medium pH 7 and grown for a total of 14 hours at 37 °C and 200 rpm in an orbital shaker (New Brunswick Scientific, Edison, USA). Forty % v/v glycerol solution was added to an overnight culture (20 % v/v final glycerol concentration) and 1 mL aliquots were transferred aseptically to sterile eppendorf tubes and stored at -80 °C.

2.2.1.2 Sequencing Analysis

The seed stock prepared as described in section 2.2.1.1 was streaked on fresh LB-glycerol agar plates (10 gL⁻¹ tryptone, 10 gL⁻¹ sodium chloride, 10 gL⁻¹ yeast extract, 10 gL⁻¹ glycerol, 15 gL⁻¹ agar and 50 mgL⁻¹ ampicillin added after sterilisation through a 0.2 micron sterile filter). Plates were left to grow for 14-16 hours at 37 °C until single colonies were visualised. Single colonies were then transferred to 10 mL fresh LB-glycerol media and grown for a further 12-16 hours at 37 °C and 200 rpm in an orbital shaker. Cells were centrifuged for 5 minutes at 4000 rpm and the cell pellet processed to extract the plasmid DNA using a standard QIAprep Spin miniprep kit protocol. Plasmid DNA samples at a concentration of 50 ngμL⁻¹ along with primers at a concentration of 5 pmolesμL⁻¹ were sent for sequencing analysis at the Wolfson Institute for Biomedical Research and results showed the presence of the CHMO gene and sequence homology to the vector, pKK223-3. This confirmed the plasmid vector to be pQR210 as described by Doig et al. (2001) and was used for all CHMO studies.

2.2.1.3 Inoculum Preparation

A 1 mL frozen stock of *E. coli* TOP10 [pQR210] was inoculated into LB-glycerol growth media under sterile conditions. Shake flasks were incubated for 14-16 h overnight at 200 rpm and 37 °C in an orbital shaker until an optical density (OD) of 5-6 was reached. The broth from these cultures was subsequently used to inoculate both microscale and pilot plant scale cultivations.

2.2.1.4 Shake Flask Cultivations and Bioconversions

100 mL of LB-glycerol media was inoculated with 5 % inoculum in a 500 mL baffled shake flask at 200 rpm and 37 °C in an orbital shaker. Samples were taken hourly and used to measure the OD. Cells were left to grow for a total of 6 hours after which glycerol was added to the culture to achieve a final concentration of 10 gL⁻¹. The culture was left to incubate with glycerol for 15 minutes and then a stock of bicyclo[3.2.0]hept-2-en-6-one pre-dissolved in 50 mM sodium phosphate buffer was added to the culture to a final concentration of 1 gL⁻¹. The bioconversion was left for a total of 1 hour where samples were taken every 15 minutes for OD measurement and metabolite analysis by gas chromatography (GC).

2.2.2 *E. coli* BL21 Star (DE3)pLysS [pQR367] and *E. coli* BL21 Star (DE3)pLysS [pQR368]

Note: *E. coli* BL21 Star (DE3)pLysS [pQR367] will be referred to as *E. coli* [pQR367] and *E. coli* BL21 Star (DE3)pLysS [pQR368] will be referred to as *E. coli* [pQR368] in the remainder of the thesis.

2.2.2.1 Production of *E. coli* [pQR367] and *E. coli* [pQR368]

Single colonies from agar plates containing *E. coli* TOP10 [pQR367] and *E. coli* TOP10 [pQR368] were cultured in LB medium pH 7 (10 gL⁻¹ tryptone, 10 gL⁻¹ sodium chloride, 5 gL⁻¹ yeast extract and 100 mgL⁻¹ ampicillin added after sterilisation through a 0.2 micron sterile filter) and plasmid DNA extracted using a standard QIAprep Spin miniprep kit protocol. Competent cells of *E. coli* BL21 Star (DE3)pLysS were streaked onto LB agar plates with chloramphenicol (pre-dissolved in ethanol) and left to grow at 37 °C until single colonies were visible. Single colonies were picked and cultured in shake flasks containing LB medium (10 gL⁻¹ tryptone, 10 gL⁻¹ sodium chloride, 5 gL⁻¹ yeast extract and 10 mgL⁻¹ chloramphenicol (pre-dissolved in ethanol)) at 37 °C and 200 rpm in an orbital shaker for 14 hours. 40 % v/v glycerol solution was added to the culture (20 %

v/v final glycerol concentration) and stored in 1 mL aliquots at -80 °C. A 1 mL aliquot of competent *E. coli* BL21 Star (DE3)pLysS cells and the plasmid DNA of the constructs [pQR367] and [pQR368] were used for transformation (kindly conducted by Professor John Ward). Competent cells and constructs were put on ice, 5 µL of each plasmid DNA was added to separate aliquots of competent cells, mixed and left for 30 minutes on ice. The cells were heat shocked by placing them in a water bath at 37 °C for 30 seconds to enable the plasmid to be taken up by the competent cells and then placed back on ice. The transformed cells were combined with SOC nutrient media. The vials were left to incubate at 37 °C and 200 rpm for an hour. Both transformed cells were then spread on LB agar plates with ampicillin and chloramphenicol and left to incubate at 37 °C overnight until small colonies were visible. Plates with successful transformants were stored at 4 °C in the fridge.

2.2.2.2 Seed Stock Preparation

The overnight culture was prepared by inoculating a single colony of *E. coli* [pQR367] or *E. coli* [pQR368] in LB (10 gL⁻¹ tryptone, 10 gL⁻¹ sodium chloride, 5 gL⁻¹ yeast extract, 10 mgL⁻¹ chloramphenicol (pre-dissolved in ethanol) and 100 mgL⁻¹ ampicillin added after sterilisation through a 0.2 micron sterile filter) medium pH 7 and grown for a total of 14 hours at 37 °C and 200 rpm in an orbital shaker (New Brunswick Scientific, Edison, USA). Forty % v/v glycerol solution was added to an overnight culture (20 % v/v final glycerol concentration) and 1 mL aliquots were transferred aseptically to sterile eppendorf tubes and stored at -80 °C.

2.2.2.3 Sequencing Analysis

The seed stock prepared as described in section 2.2.2.2 was streaked on fresh LB agar plates (10 gL⁻¹ tryptone, 10 gL⁻¹ sodium chloride, 5 gL⁻¹ yeast extract, 15 gL⁻¹ agar, 10 mgL⁻¹ chloramphenicol (pre-dissolved in ethanol) and 100 mgL⁻¹ ampicillin added after sterilisation through a 0.2 micron sterile filter). Plates were left to grow for 14-16 hours at 37 °C until single colonies were visualised.

Single colonies were then transferred to 10 mL fresh LB media and grown for a further 12-16 hours at 37 °C and 200 rpm in an orbital shaker. Cells were centrifuged for 5 minutes at 4000 rpm and the cell pellet processed to extract the plasmid DNA using a standard QIAprep Spin miniprep kit protocol. Plasmid DNA samples at a concentration of 50 ng μ L⁻¹ along with primers at a concentration of 5 pmole μ L⁻¹ were sent for sequencing analysis at the Wolfson Institute for Biomedical Research. Using the T7 terminator primer of pET21a 5'-gctagtattgctcagcgg-3' results showed the presence of the ferredoxin NADP reductase SCF15A gene from *Streptomyces coelicolor* in sequences obtained using [pQR367] and [pQR368] samples. Using the T7 universal primer of pET21a 5'-taatacgactcactataggg-3' results showed the presence of the genes for P450SU1 and P450SU2 from *Streptomyces griseolus* in sequences obtained using [pQR367] and [pQR368] respectively. Seed stock samples therefore contained plasmid DNA with the presence of P450, ferredoxin and ferredoxin reductase genes and were used for all subsequent cytochrome P450 studies.

2.2.2.4 Inoculum Preparation

A 1 mL frozen stock of *E. coli* [pQR367] and *E. coli* [pQR368] were inoculated into LB growth media with chloramphenicol and ampicillin under sterile conditions. Shake flasks were incubated for 14 hours overnight at 200 rpm and 37 °C in an orbital shaker until an OD of 4-5 was reached. The broth from these cultures was subsequently used to inoculate both microscale and laboratory scale cultivations.

2.2.2.5 Shake Flask Cultivations and Bioconversions

100 mL Terrific broth (TB) (12 gL⁻¹ tryptone, 24 gL⁻¹ yeast extract, 4 mL⁻¹ glycerol, 2.3 gL⁻¹ potassium phosphate monobasic, 12.5 gL⁻¹ potassium phosphate dibasic, 10 mgL⁻¹ chloramphenicol (pre-dissolved in ethanol) and 100 mgL⁻¹ ampicillin, salts and ampicillin were added after autoclaving and filter sterilised using 0.2 micron sterile filters) pH 7 was inoculated with 1 % inoculum in 500 mL shake flasks and incubated at 37 °C and 250 rpm in an orbital shaker

until the cells reached a OD of 0.6-0.8. The temperature was dropped to 25 °C and the agitation to 180 rpm to achieve optimum expression conditions. Once the incubator had reached the correct temperature 1 mM ALA and 0.5 mM FeCl₃ was added to the culture to enhance cytochrome P450 expression and incubated at 25 °C and 180 rpm for 20 minutes. Following this the culture was induced using 1 mM IPTG and after 10 minutes of induction 1 mM 7-ethoxycoumarin (pre-dissolved in ethanol) added to begin bioconversion. The culture was left for a total of 30 hours where samples were taken regularly to monitor the OD of cells and the bioconversion progression.

2.3 Microscale Process Sequences

2.3.1 *E. coli* TOP10 [pQR210]

2.3.1.1 Manual Operations

2.3.1.1.1 Microwell Based Temperature Study

Wells in five areas of a 96-DSW plate (96-DSW, Becton Dickenson, Franklin Lakes, NJ, USA) were filled with 1 mL LB-glycerol medium and left to agitate at 1000 rpm and 37 °C on an Eppendorf Thermomixer Comfort (Eppendorf AG, Hamburg, Germany) with a orbital shaking pattern and throw of 3 mm. Using a thermocouple the temperature of each well was measured every 10 minutes for the first hour and then every hour for a total of 7 hours. Results of this study are shown in Figure 3.6 and indicated a 30-minute warming period was required to ensure the medium in the wells was being incubated at the correct temperature. A similar study was conducted to determine the time required to cool the medium down to 30 °C after a period of incubation at 37 °C.

2.3.1.2 Automated Microscale Linked Process Sequence

A Tecan Genesis platform was used for process automation and setup with all required polypropylene 96-DSW culture plates, 96-Standard round well plates

(96-SRW, Sarstedt group, Leicester, UK), reagent troughs (Tecan, Reading, UK) and disposable microconductive tips (Tecan, Reading, UK). A sterile environment was maintained by using UV sterilisation within a Bigneat class 2 biosafety cabinet equipped with a laminar airflow system and HEPA filtration. The UV sterilisation step was found to be appropriate as LB-glycerol agar plates left open for a seven-hour period after a 20-minute sterilisation process showed no signs of contamination. A schematic representation of the process is shown in Figure 3.11. The process begins by addition of 950 μ L LB-glycerol media to wells of a 96-DSW plate agitated by an Eppendorf Thermomixer Comfort. The plate was left uncovered during the process due to the expected high oxygen demand, and the contained environment was thought to eliminate the risk of contamination. Less than 2 % of the fill volume has previously been found to evaporate over the entirety of the process and this is not considered to have a significant effect (Ferreira, 2008). The plate was agitated at 37 °C and 1000 rpm for 30 minutes to warm the media. Fifty μ L of overnight prepared culture was then added to wells and shaken at 37 °C and 1000 rpm for 6 hours. Automatic sampling was done hourly using the sacrificial well approach (Doig et al. 2002) and the OD measured using a Tecan microplate reader. After 6 hours of growth aliquots were transferred to new wells or a new plate depending on the number of samples required and glycerol added to allow the regeneration of NADPH cofactor. The plate was also cooled to 30 °C at this stage, which reduces evaporation of the ketone substrate during bioconversion (Ferreira, 2008). The cells were incubated with glycerol for 15 minutes at 1000 rpm and 30 °C after which the ketone substrate (pre-dissolved in 50 mM sodium phosphate buffer) was added and bioconversion followed for a total of 1 hour where OD readings were taken and 200 μ L aliquots transferred to a new 96-DSW plate and frozen to stop the reaction. Following the 1 hour bioconversion the plate containing the frozen samples was removed from the freezer and placed back on the deck of the robotic platform and left to defrost. 400 μ L of ethyl acetate was automatically added to all samples in the plate, the plate was sealed using a chemical resistant silicone sealing mat (Axygen, California, USA) and automatically transferred to the Eppendorf Thermomixer Comfort where it was shaken at 1200 rpm for 3 minutes. The plate was then automatically transferred to a Rotanta 46 RSC microwell centrifuge (Hettich, Tuttlingen, Germany) and centrifuged for 15

minutes at 4000 rpm and 4 °C which was sufficient to separate organic and aqueous phases. The plate was automatically removed from the centrifuge and transferred to the platform and the top organic layer from each sample dispensed into GC vials for sample analysis.

2.3.1.3 Bioprocess Evaluation using Automated Sequence

The process sequence was adapted accordingly to evaluate different substrates and substrate concentrations, growth regimes, well fill volumes and media formulations. The media formulations examined were identical to LB-glycerol media, as described in section 2.2.1.1, except for tryptone which was replaced by each of the amino acid sources listed in Table 4.2. The effect of fill volume on growth kinetics was investigated by using a range of liquid volumes from 400 µL to 1000 µL at a constant agitation and shaking diameter, after 6 hours of growth aliquots of culture were transferred to a new plate to achieve a constant fill volume of 500 µL for bioconversion. Volumes lower than 400 µL could have resulted in inaccuracies due to an excess of evaporation. The effect of fill volume on bioconversion kinetics was investigated by growing cells at a constant fill volume of 1000 µL and then after 6 hours of growth aliquots of culture were transferred to a new plate to achieve fill volumes from 200 µL up to 1000 µL for bioconversion.

2.3.2 *E. coli* [pQR367] and *E. coli* [pQR368]

2.3.2.1 Manual Operations

2.3.2.1.1 Microwell Based Temperature Study

The temperature study was similar to that described in section 2.3.1.1.1 the only difference being that wells were filled with TB medium and the temperature of incubation tested was 25 °C.

2.3.2.1.2 Microwell Based Evaporation study

Wells of a 96-DSW plate were filled with 1 mL sterile TB medium. The plate was left to agitate at 25 °C and 800 rpm for a period of 1 hour, 10 hours and 24 hours. After each time period the well contents from each well area was removed and weighed and the liquid loss calculated. The results of this study are discussed in section 5.2.2.4.

2.3.2.2 Automated Microscale Linked Process Sequence

A Tecan Genesis platform was used for process automation and setup with all required polypropylene 96-DSW culture plates, 96-SRW plates, reagent troughs and disposable microconductive tips. A schematic representation of the process is shown in Figure 5.15. The process begins by addition of 990 µL TB media to wells of a 96-DSW plate agitated by an Eppendorf Thermomixer Comfort. The plate was left uncovered during the process due to the high oxygen demand, and the contained environment eliminates the risk of contamination. The plate was agitated at 37 °C and 1000 rpm for 30 minutes to warm the media. Ten µL of overnight prepared culture was then added to wells and shaken at 37 °C and 1000 rpm until the cell OD reached 0.6-0.8. Automatic sampling was conducted using the sacrificial well approach (Doig et al. 2002) and the OD measured using a Tecan microplate reader. The plate was cooled to 25 °C and the agitation changed to 800 rpm which were the conditions used for enzyme expression. Components found to enhance expression/bioconversion were added at this stage including 1 mM ALA and 0.5 mM FeCl₃. The cells were incubated for 20 minutes with the components at 800 rpm and 25 °C after which enzyme expression was induced with 1 mM IPTG. Following a 10-minute induction period, 1 mM 7-ethoxycoumarin (pre-dissolved in ethanol) was added to begin bioconversion. The culture was left to continue for a total of 30 hours where OD readings were taken every 5 hours and 200 µL bioconversion samples taken every hour during the last 5 hours of culture and transferred to a new 96-DSW plate and frozen to stop the reaction. After a total of 30 hours of culture, final samples were taken including a 1 mL aliquot which was dispensed into

ependorfs, centrifuged and the supernatant discarded and frozen in pellets for later analysis using a carbon monoxide (CO) based assay. The plate containing the frozen samples was removed from the freezer and placed back on the deck of the robotic platform and left to defrost. 400 μ L of ethyl acetate was automatically added to all samples in the plate, the plate was sealed using a chemical resistant silicone sealing mat and automatically transferred to the Eppendorf Thermomixer Comfort where it was shaken at 1200 rpm for 3 minutes. The plate was then automatically transferred to a Rotanta 46 RSC microwell centrifuge and centrifuged for 15 minutes at 4000 rpm and 4 °C which was sufficient to separate organic and aqueous phases. The plate was automatically removed from the centrifuge and transferred to the platform, then the top organic layer from each sample was dispensed into eppendorfs. These eppendorfs were then transferred to a fume cupboard and left overnight for the ethyl acetate to evaporate for at least 12 hours. The next day 200 μ L of acetonitrile was added to re-dissolve the bioconversion metabolites and these samples analysed by high pressure liquid chromatography (HPLC).

2.3.2.3 Automated Screening Approach

The automated screening approach is similar to that described in section 2.3.2.2. Due to the fact that the whole plate was being utilised to test a range of components once cells has been induced and the bioconversion substrate added no OD readings were taken. Samples were only taken after 30 hours of growth to test the OD, and bioconversion samples transferred to a new 96-DSW plate which was processed using the automated liquid-liquid extraction as described in section 2.3.2.2.

During the screening studies stocks of α -naphthoflavone and β -naphthoflavone were prepared dissolved in DMSO. Stocks of Hemin were prepared in 50 mM sodium hydroxide. Trace elements were prepared by dissolving 2.7 g $\text{FeCl}_3 \cdot 6\text{H}_2\text{O}$, 0.2 g ZnCl_2 , 0.2 g $\text{CoCl}_2 \cdot 6\text{H}_2\text{O}$, 0.2 g $\text{Na}_2\text{MoO}_4 \cdot 2\text{H}_2\text{O}$, 0.1 g $\text{CaCl}_2 \cdot 2\text{H}_2\text{O}$, 0.13 g $\text{CuCl}_2 \cdot 2\text{H}_2\text{O}$ and 0.05 g H_3BO_3 in 100 mL RO water with 10 % hydrochloric acid.

2.4 Parallel Process Sequences at Matched $K_L a$

2.4.1 *E. coli* TOP10 [pQR210]

2.4.1.1 75 L Operation

For the pilot plant process a 75 L (LH Fermentation, Reading, UK) 0.33 m internal diameter bioreactor was used, stirred by three six-bladed Rushton turbine impellers attached to a bottom-driven impeller shaft. The aspect ratio (vessel height/ vessel diameter) H_V/D_V was 2.8 and the impeller diameter to vessel diameter ratio D_i/D_V was 0.3. The bioreactor was filled with LB-glycerol medium (final working volume 45 L) and 0.2 mL⁻¹ of the antifoam polypropylene glycol (PPG) and sterilised in-situ at a temperature of 121 °C for 20 minutes. The vessel was inoculated with 5 % of the working volume with overnight prepared inoculum and the conditions of the fermenter were set to 37 °C, 384 rpm, pH 7 and 1 vvm. The selected operating conditions correspond to a Reynolds (Re) number in the turbulent region of 77,440. pH was monitored but not controlled to ensure a realistic comparison to the microwell process to be made. Due to differences in inoculum preparation, media sterilisation and use of antifoam agents a sample was taken and used to inoculate a parallel manual microwell process, as described in section 2.4.1.2 to ensure both processes would begin under identical conditions. Cells were cultured for 6 hours. Glycerol was then added to a final concentration of 10 gL⁻¹. The cells were incubated with glycerol for 15 minutes after which the ketone substrate was added to a final concentration of 0.5 gL⁻¹. Bioconversion took place for a total of 1 h where samples were taken for OD readings and 300 µL aliquots frozen for offline analysis.

2.4.1.2 Microwell Linked Process Sequence

This process was conducted manually and in parallel to the 75 L process. The operation was similar to that described in section 2.3.1.2 except that a constant fill volume of 500 µL was used for the duration of the process and the inoculum

was obtained from the 75 L bioreactor. In order for the processes to be matched the bioconversion stage was carried out at 37 °C and at a substrate concentration of 0.5 gL⁻¹.

2.4.2 *E. coli* [pQR367] and *E. coli* [pQR368]

2.4.2.1 7.5 L Operation

For the laboratory scale process a 7.5 L (New Brunswick Scientific Co, New Jersey, USA) 0.18 m internal diameter bioreactor was used, stirred by two six-bladed Rushton turbine impellers connected to a top-driven impeller shaft. The aspect ratio H_v/D_v was 1.6 and the D_i/D_v was 0.3. The bioreactor was filled with TB medium minus the salts (final working volume 5 L) and 0.2 mL⁻¹ PPG. The pH probes were calibrated using standard buffers at pH 4 and 7. The dissolved oxygen tension (DOT) probe was calibrated at 0 % in nitrogen and 100 % using gaseous air. The probes were placed in the holders within the vessel and the whole vessel sterilized by autoclaving. Once sterilisation was complete and the vessel had cooled the potassium phosphate salts and 100 mgL⁻¹ ampicillin which had been filter sterilized through a 0.2 micron filter were added to the vessel aseptically. An aliquot of 10 mgL⁻¹ chloramphenicol (pre-dissolved in ethanol) was also added. Both probes were finally checked and re-calibrated as appropriate if required. The vessel was inoculated with 1 % of the working volume with overnight prepared inoculum (*E. coli* [pQR367] or *E. coli* [pQR368]) and the conditions of the fermenter were set to 37 °C, 763 rpm, pH 7 and 1 vvm. The selected operating conditions correspond to a Re number in the turbulent region of 44,278. pH was monitored but not controlled to ensure a realistic comparison with the microwell process. Due to differences in inoculum preparation and use of antifoam agents a sample was taken and used to inoculate a parallel manual microwell process, as described in section 2.4.2.2 to ensure both processes would begin under identical conditions. Cells were cultured until they reached an OD of 0.6-0.8. The temperature was dropped to 25 °C and the agitation changed to 571 rpm which were the conditions used for enzyme expression. Components found to enhance expression/bioconversion were added

at this stage including 5 mM ALA and 20 gL⁻¹ glycerol. The cells were incubated for 20 minutes with the components at 571 rpm and 25 °C after which enzyme expression was induced with 1 mM IPTG. Following a 10-minute induction period 1 mM 7-ethoxycoumarin (pre-dissolved in ethanol) was added to begin bioconversion. The culture was left to continue for a total of 30 hours where samples were taken for OD readings and 300 µL aliquots frozen for offline analysis.

2.4.2.2 Microwell Linked Process Sequence

This process was conducted manually and in parallel to the 7.5 L process. The operation was similar to that described in section 2.3.2.2 except the inoculum was obtained from the 7.5 L bioreactor.

2.5 Substrate Solubility Studies

(1*R*)-(-)-Fenchone, (1*R*)-(+)-Camphor and (+)-(3*R*,6*RS*)-Dihydrocarvone were all added pre-dissolved in DMSO rather than 50 mM sodium phosphate buffer because they were all poorly water soluble. A number of other solvents were tested including ethanol, methanol, isopropyl alcohol (IPA) and dimethyl formamide (DMF) where different concentrations of solvent and buffer were made in an attempt to reduce the amount of cosolvent used. However, in all cases 100 % solvent was required to get full solubilisation of the poorly water soluble substrates and DMSO was chosen as it was considered to have the least damaging effect on the cells and substrates. 7-ethoxycoumarin was also found to be poorly water soluble and pre-dissolved in ethanol.

2.6 Analytical Techniques

2.6.1 Optical Density Measurement

The OD of cell samples was measured using an Ultraspec 1100 Pro UV/Visible spectrophotometer (Amersham Biosciences, Buckinghamshire, UK) at 600 nm

during laboratory and pilot plant scale operations or a Tecan microplate reader (Tecan, Reading, UK) at 600 nm during microscale operations. To enable results from a spectrophotometer to be directly compared to those obtained from a microplate reader the pathlength of a 200 μ L well volume in a 96-SRW microplate was calculated and used to obtain a conversion factor of 1.8. This factor was used to convert all microplate readings to standard spectrophotometer readings. Reverse osmosis (RO) water was used as a blank and for sample dilution.

2.6.2 Dry Cell Weight Measurement

Cells from a 1 L shake flask culture (working volume 200 mL) were used to determine the dry cell weight of *E. coli* TOP10 [pQR210], *E. coli* [pQR367] and *E. coli* [pQR368] cells. Cells of different OD were filtered on pre-weighed glass microfiber filter discs grade GF/F with a pore size of 0.7 micron using a vacuum pump. The filter discs were left to dry overnight in an oven at 80 °C and then weighed again the next day where the dry cell weight was determined. The results were used to produce dry cell weight calibration curves of OD versus biomass concentration as shown in appendix A. The maximum error of duplicate OD readings was ± 4 %.

2.6.3 Automated Robotics

Two robotic arms are utilised by the Tecan automated system. The first is a liquid handling arm (LiHa) with 8 pipetting heads and the ability to do single and multipipetting with a maximum pipetting speed of 900 μ Ls⁻¹. It can be setup with disposable microconductive tips or stainless steel fixed tips and moves on the x, y and z planes. The Tecan Gemini software has a number of pre-set liquid classes which are liquid handling parameters specifying speeds, airgaps and detection modes for a range of liquids. Depending on the liquid properties specific liquid classes can be developed however the standard water class with aspiration and dispense speed of 150 μ Ls⁻¹ and 600 μ Ls⁻¹, respectively, were used for the majority of liquids unless otherwise stated. The second is a robotic

manipulator arm (RoMa), which can be fitted with a range of grips depending on the plates to be processed. This has planar movements on the x, y and z planes with a maximum movement speed of 400 mm s^{-1} , and rotational movements on the x plane with a rotator speed of 60 $^{\circ} s^{-1}$.

The accuracy and precision of pipetting was tested using a method which has been described previously (Nealon et al., 2005) with two disposable microconductive tips P1000 which can dispense up to 990 μL volumes and P200 which can dispense up to 190 μL volumes. The accuracy and precision of all tips was confirmed for all working volumes and the coefficient of variance was found to be 5 % or below and therefore the liquid handling precision and accuracy was considered acceptable (Olsen, 2000).

2.6.4 Gas Chromatography (GC)

2.6.4.1 Sample Preparation for GC

Aqueous samples from the bioconversion were prepared by mixing equal volumes of sample and a 1 g L^{-1} naphthalene and ethyl acetate solution. Naphthalene was used as an internal standard. The sample was vortex mixed for 30 seconds and centrifuged at 13000 rpm for 2 minutes. 100 μL of the top solvent layer was transferred to vials and analysed using GC as described in section 2.6.4.2. The flame ionization detector (FID) response to samples was measured as an integrated peak area. Bicyclo[3.2.0]hept-2-en-6-one, (1*R*)-(+)-camphor, norcamphor, cyclohexanone, cycloheptanone, cyclooctanone and (1*R*)-(-)-fenchone were used for ketone standards and (1*S*,5*R*)-2-oxabicyclo[3.3.0]oct-6-en-3-one and ϵ -caprolactone was used for the lactone standards. (+)-(3*R*,6*SR*)-Dihydrocarvone is comprised of two isomers however the combination of both isomers was used for the calibration standard. Lactone products produced from norcamphor and cycloheptanone were not commercially available. Shake flask cultures using these substrates were run to completion and the products 2-oxabicyclo[3.2.1]octan-3-one and oxocan-2-one were extracted into ethyl acetate and used to create calibration curves after characterisation by nuclear magnetic

resonance spectroscopy, mass spectrometry and infra red spectroscopy.

2.6.4.2 GC Operation and Quantification

A Perkin-Elmer autosystem XL-2 gas chromatograph (Perkin-Elmer, Connecticut, USA), fitted with an Heliflex AT-1701 column 30 m x 0.54 mm (Alltech Associates Applied Science Ltd, UK) was used to analyse the bioconversion substrate and product samples. One μL samples were injected at a temperature of 200 °C by an integrated autosampler and a FID was used to detect compounds leaving the column. The oven temperature and detection temperature were set at 100 °C and 280 °C, respectively. The temperature programme used involved a hold for 5 minutes at 100 °C and was then increased at 10 °C min^{-1} to 240 °C. Both data capture and analysis were conducted using the Perkin-Elmer Nelson TurbochromTM software.

For stock solutions the standard deviation for a single peak area measurement was determined from triplicate measurements of five sample solutions (concentration range 0.2-1 gL^{-1}) in ethyl acetate. The maximum standard deviation of triplicate stock preparations varied between 1.8 % and 10.6 %. Sample calibration curves and chromatograms can be found in the appendix A and B, respectively. The ethyl acetate partition coefficients of bicyclo[3.2.0]hept-2-en-6-one and (1*S*,5*R*)-2-oxabicyclo[3.3.0]oct-6-en-3-one have been determined previously as described by Lander (2003) to be tending to infinity and 8.17 ± 0.08 respectively, and have been accounted for in all calculations. In the case of all other ketone substrates tested and ϵ -caprolactone in this work, the ethyl acetate partition coefficient was found to also be infinity while the partition coefficient for lactone products was not determined due to limited yields.

2.6.5 High Pressure Liquid Chromatography (HPLC)

2.6.5.1 Sample Preparation for HPLC

Aqueous samples from bioconversions were prepared by mixing a 500 μL sample with 1 mL ethyl acetate solution. The sample was vortex mixed for 30 seconds and centrifuged at 14000 rpm for 2 minutes. 500 μL of the top solvent layer was transferred to eppendorfs and left to evaporate overnight for at least 12 hours. 500 μL of acetonitrile was then added to the eppendorfs and vortex mixed for 10 seconds to re-dissolve the metabolite pellets. Samples were then centrifuged for 2 minutes at 14000 rpm and analysed using HPLC as described in section 2.6.5.2. The UV-Vis detector response to samples was measured as an integrated peak area. 7-ethoxycoumarin was used for substrate standards and 7-hydroxycoumarin was used for product standards.

2.6.5.2 HPLC Operation and Quantification

A Agilent 1200 series HPLC (Agilent, West Lothian, UK), fitted with an Packard Bell nucleosil 100-5 C18 reverse phase column 4.0 x 125 mm (Agilent, West Lothian, UK) was used to analyse the bioconversion substrate and product samples. The mobile phases used were A: water with 0.1 % acetic acid (pH 3.3) and B: methanol with 0.1 % acetic acid. The column was equilibrated for 20-30 minutes with 2 % mobile phase B and 98 % mobile phase A prior to sample analysis. The column was maintained at a temperature of 40 $^{\circ}\text{C}$ and 5 μL samples were injected onto the column at a flow rate of 1 mLmin^{-1} . A gradient programme was used as shown in Table 2.1 and metabolites were detected at a wavelength of 320 nm using a UV-Vis detector.

Table 2.1 HPLC gradient programme

Time (min)	% B	% A	Stage
0	2	98	Gradient
5	50	50	
10	50	50	Isocratic Hold
11	2	98	Re-equilibration
16	2	98	

For stock solutions the standard deviation for a single peak area measurement was determined from triplicate measurements of seven sample solutions (concentration range 0.0125-1 gL⁻¹) in acetonitrile. The maximum standard deviation of triplicate stock preparations was 0.8 %. Sample calibration curves and chromatograms can be found in the appendix A and B, respectively.

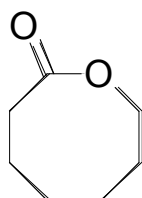
2.6.6 Thin Layer Chromatography (TLC)

TLC was used for quick identification of 7-ethoxycoumarin and 7-hydroxycoumarin which both fluoresce under UV light. Cell samples were extracted with equal volumes of ethyl acetate for 60 seconds. The sample was centrifuged for 1 min and 13000 rpm and the top organic layer transferred to another vial and left to evaporate overnight. Samples were then concentrated to 100 mM with the appropriate volume of ethyl acetate. A solvent system of hexane and ethyl acetate in a 3:2 ratio was used and 10 mL of this added to a 50 mL jar and left closed for a few minutes to saturate the air in the jar with the solvents. Using a glass spotter 1-2 µL of each sample were spotted onto the bottom of a silica gel TLC (TLC plate silica gel 60, Merck) sheet. The TLC sheet was then placed in the jar with the solvent just touching the bottom few millimeters of the sheet and the lid was placed gently on top. The TLC sheet was left in the jar until the solvent had been draw up the TLC sheet and the substrate and products separated. The TLC sheet was then removed carefully from the jar and the spots visualized under UV light in a wavelength of 300-320 nm.

2.6.7 Product Identification

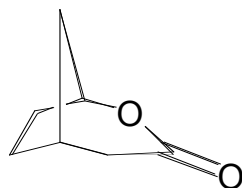
New products identified from GC analysis were isolated and purified using silica chromatography, then characterised by NMR spectroscopy and mass spectrometry and IR spectroscopy to be predominantly 2-oxabicyclo[3.2.1]octan-3-one from the norcamphor bioconversion and oxocan-2-one (correlated by chemical synthesis) from cycloheptanone.

2.6.7.1 Oxocan-2-one



Cycloheptanone (1.00 g, 8.93 mmol) and *m*-chloroperbenzoic acid (0.168 g, 9.74 mmol) in dichloromethane (10 mL) were stirred for 24 hours at room temperature. The mixture was washed with saturated sodium carbonate solution (3 x 10 mL) and saturated sodium chloride solution (10 mL). The organic layer was dried (Na₂SO₄) and concentrated *in vacuo* (Harikrishna et al., 2009). The crude product was purified by flash silica chromatography (ethyl acetate:hexane, 1:1) to give oxocan-2-one as a colourless oil (0.620 g, 54 %). $n_{\max}(\text{neat})/\text{cm}^{-1}$ 2931, 1725; ¹H NMR (600 MHz; CDCl₃) δ 1.58–1.66 (4H, m) 1.74–1.90 (4H, m) 2.54 (2H, t, *J* 6.4, CH₂CO) 4.34 (2H, t, *J* 5.7, CH₂O); ¹³C NMR (150 MHz; CDCl₃) δ 24.0, 25.9, 28.4, 31.0, 31.4, 68.0 (CH₂O), 176.9 (C=O); *m/z* (HRCI) found [MH]⁺ 129.09101. C₇H₁₃O₂ requires 129.09155. GC retention time: 10.4 min.

2.6.7.2 2-Oxa-bicyclo[3.2.1]octan-3-one



After baffled shake flask cultures equivalent to that described in section 2.2.1.4 with racemic norcamphor as a substrate, a whole cell solution (200 mL) was centrifuged and the supernatant was extracted with ethyl acetate (200 mL). The organic layer was dried (Na_2SO_4) and concentrated *in vacuo*. The crude product was purified by flash silica chromatography (ethyl acetate:hexane, 1:1) to give the major isomer 2-oxa-bicyclo[3.2.1]octan-3-one and minor isomer 3-oxabicyclo[3.2.1]octan-2-one in a ratio of 15:1, as a colourless oil in 43 % isolated yield (50 mg). $n_{\text{max}}(\text{neat})/\text{cm}^{-1}$ 2950, 1730; ^1H NMR (600 MHz; CDCl_3) (major isomer) d 1.61–1.75 (2H, m) 1.88–2.00 (3H, m) 2.08–2.20 (1H, m) 2.42–2.52 (1H, m) 2.52–2.57 (1H, m) 2.68–2.74 (1H, m) 4.86 (1H, m, CHOCO); ^{13}C NMR (150 MHz; CDCl_3) (major isomer) d 29.4, 31.9, 32.6, 36.0, 40.8, 81.1 (CHO), 171.0 (C=O); m/z (HREI) found $[\text{M}]^+$ 126.06814. $\text{C}_7\text{H}_{10}\text{O}_2$ requires 126.06808. GC retention time (major isomer): 14.62 min.

2.6.8 NADPH Consumption Microscale Assay

2.6.8.1 Sample Preparation

1 mL samples from cultures were centrifuged at 4 °C for 2 minutes at 13000 rpm. The supernatant was discarded and the cell pellet re-suspended in 50 mM TRIS-HCL pH 9. The sample was sonicated (Soniprep 150) on ice for 5*10s on and 5*10s off at 8 μm . The sample was centrifuged to remove the cell debris at 4 °C for 2 minutes and 13000 rpm and the supernatant kept on ice or frozen at – 20 °C until used in the assay.

2.6.8.2 NADPH Consumption Assay

The intracellular CHMO activity can be quantified by following the substrate induced consumption of NADPH. Donoghue and Trudgill (1975) previously reported that the oxidation of 1 μmol of cyclohexanone by CHMO is accompanied by the consumption of 1 μmol of NADPH and 0.84 μmol of O_2 . Therefore the consumption of NADPH is stoichiometrically linked to product formation in CHMO catalysed reactions. NADPH absorbs strongly at 340 nm whereas NADP does not and this can therefore be used in a spectrophotometric assay. The method used is based on that previously reported by Donoghue and Trudgill (1975) however has been adapted to a microscale approach.

A Tecan microplate reader was used for sample analysis. The microplate reader was set to 30 °C. 100 μL of 50mM TRIS-HCL pH 9, 20 μL of 1.6 mM NADPH and 60 μL of sample prepared as described in section 2.6.8.1 were added to wells of a 96-SRW plate and left to warm to 30 °C for 10 minutes. 20 μL of 20 mM cyclohexanone (or substrate of interest) was added to three wells containing sample and 20 μL water was added to another three wells containing sample to monitor the background rate and the decrease in absorbance at 340 nm was monitored for a total of 30 minutes or until NADPH has been fully consumed. The activity of the enzyme was expressed in Units (U) where one unit is equivalent to the number of μmoles of NADPH consumed per minute. Sample calculations are shown in the appendix C.

This assay was adapted depending on the substrates tested. If substrates were dissolved in a alternative buffer or DMSO (for those with poor solubility) then control experiments were also conducted where cyclohexanone was also dissolved in buffer or DMSO.

2.6.9 Carbon Monoxide (CO) Assay

2.6.9.1 Sample Preparation

All buffers and reagents used for this assay were made fresh on the day of the assay. Samples from cytochrome P450 cultivations were centrifuged for 1 minute at 14000 rpm at 4 °C. The supernatant was discarded and resuspended in 1 mL buffer (80 % 100 mM potassium phosphate buffer pH 7.5, 20 % glycerol, 2 mM EDTA, 1.5 mM DTT and 0.4 % Triton X-100). The sample was left on ice for 30 minutes as PMSF is unstable at room temperature and after 30 minutes of cooling 1 mM PMSF was added to the sample. The sample was sonicated on ice for 10*10s on and 10*10s off at 8 µm. The sample was then centrifuged for 1 hour at 14000 rpm and 4 °C and the pellet discarded. The supernatant was used in the CO assay and stored on ice when not in use or frozen at – 20 °C until needed.

2.6.9.2 CO Assay

Omura and Sato (1964) first reported the presence of distinct Soret peaks at 420 nm and 450 nm when cytochrome P450s are bound with CO. This observation is now used to assay for the presence and quantification of active cytochrome P450. During the development of this assay a few experiments were conducted to get the best possible spectrum. It has been found that incubation time with CO can affect the results (Phillips and Shephard, 2006) therefore CO was incubated with the sample for various time periods and it was found that 5 minutes was appropriate to ensure full CO binding and no change in spectrum results as shown in the appendix C. The majority of works previously reported also use substrate free samples when this assay is conducted as the presence of substrates can cause spectral changes (McLean et al., 1996). This was tested and it was found that the assay should only be conducted with substrate free samples as when substrates are present a poor spectrum is produced making cytochrome P450 quantification difficult as shown in the appendix C.

Prior to running the assay samples were left to reach room temperature. All samples were run in UV-transparent cuvettes. The Cecil Aquarius 190-1100 nm UV-Vis spectrophotometer (Cecil Instruments LTD, Cambridge, UK) was blanked using buffer (80 % 100 mM potassium phosphate buffer pH 7.5, 20 % glycerol, 2 mM EDTA, 1.5 mM DTT and 0.4 % Triton X-100) and the baseline run between 400 and 500 nm. The sample was reduced by adding 25 mM (final concentration) sodium hydrosulphite (dissolved in 80 % 100 mM potassium phosphate buffer pH 7.5, 20 % glycerol, 2 mM EDTA and 1.5 mM DTT) was mixed gently and left for 1 minute. The sample was then scanned between 400 to 500 nm. CO was bubbled through the sample at a rate of 1 bubble per second (achieved using a needle valve for fine control) for 30 seconds and the sample left for 5 minutes to allow the CO to bind and then the sample was scanned again between 400 to 500 nm. The CO difference spectrum was calculated by subtracting the reduced spectrum from that achieved when CO was bubbled and an extinction coefficient of $91 \text{ mM}^{-1}\text{cm}^{-1}$ was used. Protein content was estimated by using the Bradford assay as described in section 2.6.10. P450 expression in nmol g^{-1} represents the nmol of active P450 detected from the CO assay per gram of soluble protein. Sample calculations and CO difference spectrums are shown in the appendix C.

2.6.10 Bradford Assay

1 mL cell samples were centrifuged for 2 minutes at 13000 rpm and 4 °C. The supernatant was discarded and the pellet resuspended in 50 mM sodium phosphate buffer pH 7 (or 50 mM TRIS buffer pH 7 for P450 samples). The sample was sonicated on ice for 5*10s on and 5*10s off at 8 μm and then centrifuged for 2 minutes at 13000 rpm and 4 °C to remove the cell debris. BSA standards from 0.1 gL^{-1} up to 1.4 gL^{-1} were made in appropriate buffer in triplicate to allow quantification of protein samples. The Bradford reagent was removed from the fridge and allowed to come to room temperature. 5 μL of samples, 5 μL of each BSA standard and 5 μL of buffer (blanks) were added to wells in triplicate of a 96-SRW plate. 250 μL of Bradford reagent was added to all wells and the plate was immediately placed in a Tecan microplate reader for

analysis. The plate was mixed for 30 seconds and left to incubate for 5 minutes and the absorbance was measured at 595 nm. Using the BSA standard curve the protein concentration of each sample was determined. In the case of concentrated samples these were diluted appropriately with buffer and the assay repeated.

2.6.11 K_{La} Measurements

2.6.11.1 Microscale Measurements

In order to measure the K_{La} at a range of operating conditions at the microscale a 96-DSW plate was adapted to enable DOT measurements. A diagram of the adapted plate which was based on previously reported designs (Ferreira-Torres, 2008; Islam, 2007) and was constructed by the Biochemical Engineering Workshop in UCL is shown in Figure 2.1 A and B. A 3 mm diameter hole was drilled into the side of one well of the plate and a non-invasive oxygen sensing spot (Precision Sensing) was mounted flush to the inside wall of the plate via a Perspex transparent support. This would enable the liquid to be in contact with the spot while preventing any leakage from the plate. A miniature polymer optical fibre (POF) (Precision Sensing) was then mounted inline with the spot via a PVC mounting screw. The spot and fibre were both light sensitive and thus were stored in the dark when not in use. During measurements the POF illuminates the sensing spot with a blue LED exciting it to emit fluorescent pulses. The principle of the oxygen sensing involves quenching of these fluorescence pulses when oxygen molecules are detected. These signals are transferred via the POF to a transmitter box (Precision Sensing OXY-4 4 channel oxygen meter) and then a computer which records the signals and converts them to DOT values. Sterile medium containing 0.2 mL^{-1} PPG was added to the well with the oxygen sensing spot and used for all K_{La} measurement studies. The POF was first calibrated at 100 % by first sparging air into the headspace of the well and then calibrated at 0 % by sparging a stream of nitrogen into the headspace of the well. The probe response time (prt) was then determined. The plate was shaken until the DOT reached 100 %. According to Van't Riet (1979)

the prt is the time needed to record a percentage change in DOT of 63 % (for example 100 % down to 37 %). Nitrogen was then sparged into the headspace of the well until 37 % was reached. This was done in triplicate and the mean prt was calculated to be 3 s. This was a very fast response time and thus was considered negligible. According to Tribe et al. (1994) prts greater than 10 s can cause considerable errors in $K_L a$ quantification and thus must be accounted for in these instances.

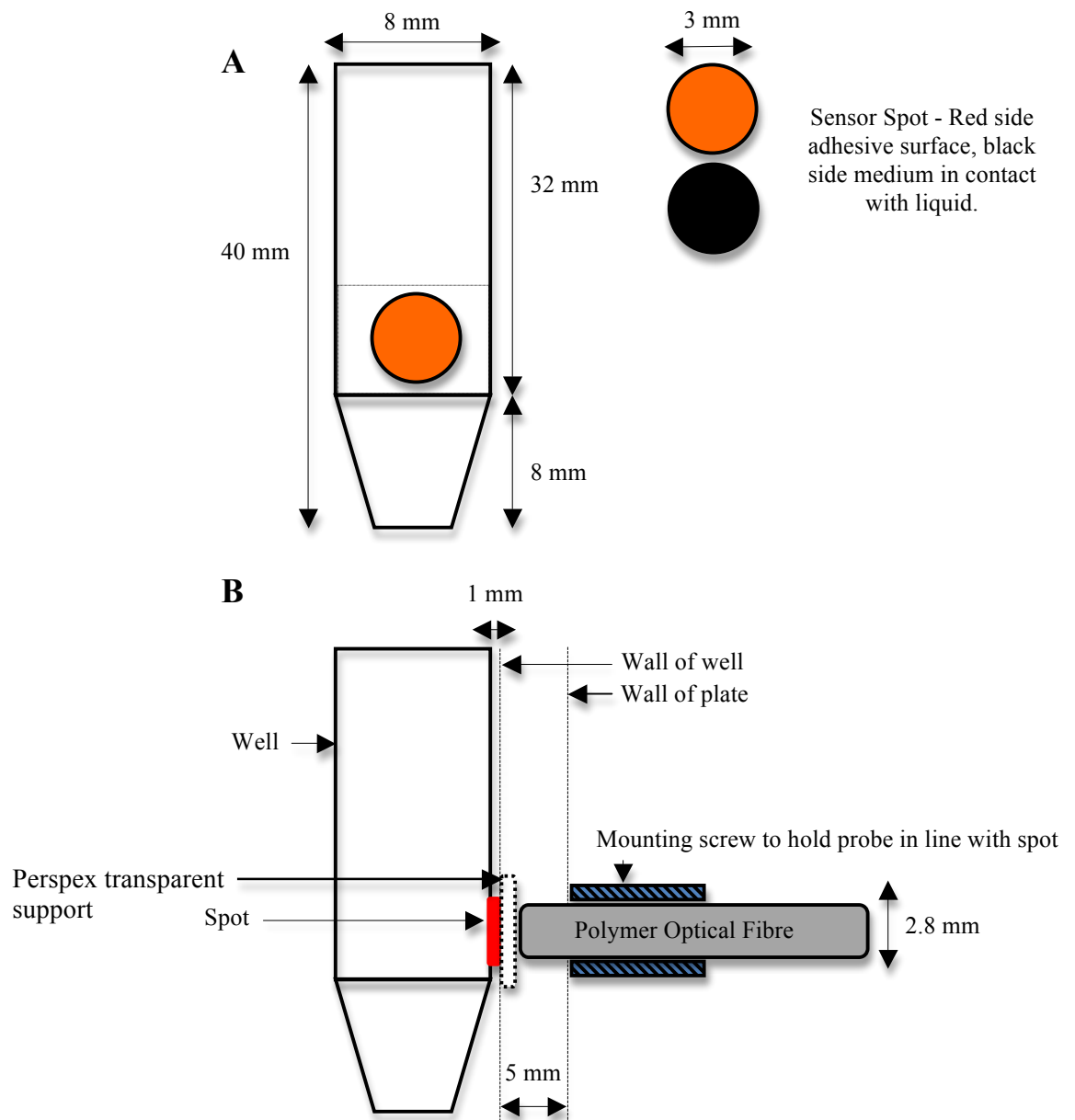


Figure 2.1 (A) Front view of a single well with oxygen sensing spot and (B) cross-sectional view of a single well with oxygen sensing spot and adjacent miniature polymer optical fibre for fluorescent signal transmission.

Dynamic gassing out studies (Van't Riet, 1979) were conducted at a range of fill volumes (500 μL – 1000 μL), shaker speeds (400 – 1000 rpm), temperatures and mediums depending on the conditions required and results are presented in Chapter 6. The modified plate was shaken using an Eppendorf Thermomixer Comfort. Each condition was setup and the plate agitated at the required shaker speed and nitrogen sparged into the well until the DOT reached 0 %, at this point the nitrogen was removed and the rate at which DOT increased up to 100 % was recorded. Each measurement was conducted in triplicate. The prt was found to be negligible, therefore Equation 2.1 (Garcia-Ochoa and Gomez, 2009) can be used to determine the $K_L a$, where $\frac{\Delta C_L}{\Delta t}$ ($\text{mmolesdm}^{-3}\text{h}^{-1}$) is the change in oxygen concentration with time, C_L^* (mmolesdm^{-3}) is the saturated dissolved oxygen concentration, and C_L (mmolesdm^{-3}) is the concentration of oxygen in the broth.

$$\frac{\Delta C_L}{\Delta t} = K_L a (C_L^* - C_L) \quad (\text{Eq. 2.1})$$

Intergrating Equation 2.1 gives Equation 2.3.

$$C_L = (C_L^* - C_L) e^{-K_L a(t)} \quad (\text{Eq. 2.3})$$

Taking the natural log and rearranging gives Equation 2.4.

$$\ln(C_L^* - C_L) = K_L a(t) + \ln C_L \quad (\text{Eq. 2.4})$$

Using the DOT measurements $C_L^* = 100 \%$ and $C_L = \text{DOT}$ at each time point and if the $\ln(C_L^* - C_L)$ is plotted versus time the $K_L a$ can be determined from the gradient of the linear part of the graph.

2.6.11.2 Laboratory Scale Measurements

For the laboratory scale measurements a 7.5 L (New Brunswick Scientific Co, New Jersey, USA) stirred tank fermenter was used. The vessel was filled with

4.5 L TB medium excluding the salts and 0.2 mL⁻¹ PPG. The DOT probe was calibrated at 0 % in nitrogen and 100 % using gaseous air. The probes were placed in the holders within the vessel and the whole vessel sterilised by autoclaving. Once sterilisation was complete and the vessel had cooled the potassium phosphate salts which had been filter sterilised through a 0.2 µm filter were added to the vessel aseptically. Both probes were finally checked and re-calibrated as appropriate. The probe response time was determined by agitating the medium until the DOT reached 100 %. Nitrogen was then sparged into the vessel through sterile filters and the time taken for the oxygen concentration to reach 37 % was recorded. This was done in triplicate and the mean prt was calculated to be 20 s.

Dynamic gassing out studies were conducted at a range of shaker speeds (400 – 800 rpm) and temperatures depending on the conditions required and results are presented in Chapter 6. Each condition was setup such as 200 rpm, 37 °C and 1 vvm and nitrogen was sparged into the vessel through sterile filters until the DOT reached 0 %. The nitrogen was then switched off and rate at which DOT increased up to 100 % was recorded. Each measurement was conducted in triplicate. Due to the extended prt it was required to consider this in the K_La calculation. This was achieved by using a correlation developed by Lamping et al. (2003) as shown in Equation 2.5, where $C_p \left(= \frac{100 - DOT}{100} \right)$ is the undissolved fraction of oxygen at time t , t_p is the probe response time and $t_m = \frac{1}{k_L a}$. An iterative approach was used to solve this equation for K_La at each time point between 20 % and 80 % saturation. These results were used to calculate the mean K_La at each condition tested.

$$C_p = \frac{1}{t_m - t_p} \left[t_m \exp\left(\frac{-t}{t_m}\right) - t_p \exp\left(\frac{-t}{t_p}\right) \right] \quad (\text{Eq. 2.5})$$

2.6.11.3 Pilot Plant Scale Measurements

For the pilot plant scale measurements a 75 L (LH Fermentation, Reading, UK) stirred tank fermenter was used. The vessel was filled with 45 L LB-glycerol medium and 0.2 mL⁻¹ PPG. The DOT probe was calibrated at 0 % in nitrogen and 100 % using gaseous air. The probes were placed in the holders within the vessel and the whole vessel sterilised in situ. Once sterilisation was complete and the vessel had cooled probes were finally checked and re-calibrated as appropriate. The probe response time was determined by agitating the medium until the DOT reached 100 %. Nitrogen was then sparged into the vessel through sterile filters and the time taken for the oxygen concentration to reach 37 % was recorded. This was done in triplicate and the mean prt was calculated to be 15 s.

Dynamic gassing out studies were conducted at a range of shaker speeds (200 – 800 rpm) depending on the conditions required and results are presented in Chapter 6. Each condition was setup such as 200 rpm, 37 °C and 1 vvm and nitrogen was sparged into the vessel through sterile filters until the DOT reached 0 %. The nitrogen was then switched off and rate at which DOT increased up to 100 % was recorded. Each measurement was conducted in triplicate. K_{La} was calculated as described for laboratory scale measurements in section 2.6.11.2.

2.6.12 Enzyme Units

A Unit (U) is defined as μmol of product formed/minute.

3 Design and Development of a Automated Microscale Platform for Investigation of Whole Cell Oxidative Biocatalytic Processes[†]

3.1 Introduction

A unique feature of automated microscale approaches is the potential to establish whole process sequences which would allow a more rapid investigation into novel oxidative biocatalytic processes. The environmental impact of chemical oxidations requiring highly reactive and/or toxic reagents makes the identification of sustainable biocatalytic alternatives for industrial pharmaceutical synthesis a useful application of microscale automation (Baboo et al., 2012). Incentives such as reduced developmental costs and accelerated process development have thus prompted continual progress in this area of research. A preliminary demonstration of process automation using *E. coli* TOP10 [pQR239] was achieved with the Multiprobe II EX liquid handling robot (Ferreira-Torres et al., 2005). The developed sequence was successful in evaluating oxidative biocatalysts libraries however, had a limited level of automation and lacked an aseptic processing environment, making it less applicable to extended culture times. Reproducibility of data collection is crucially important during parallel cultivations at the microscale. Studies have been done using robotic liquid handling to ensure liquid phase homogeneity by jet macro-mixing (Nealon et al., 2006) and a greater throughput and higher sensitivity when using reduced sample and reagent volumes compared to manual alternatives (Nealon et al., 2005). The Tecan automated robot has also previously been used for the automated culture of *E. coli* JM107:pQR706 overexpressing transketolase (Micheletti et al., 2006). This is a sophisticated platform with increased functionality, particularly suited for process automation for a range of unit operations and was used in the present work. Successful

[†] Some of the results presented in this chapter are included in Baboo et al (2012), 'An automated microscale platform for evaluation and optimization of oxidative bioconversion processes', *Biotechnology Progress*, 28, 392-405, DOI: 10.1002/btpr.1500.

integration of the miniature bioreactor system BioLector within an automated platform has resulted in the development of Robo-Lector. The system enabled the collection of kinetic data on biomass and fluorescent protein formation during microbial cultivation (Huber et al., 2009). A number of important advancements have already been made however continual efforts are required in this area if there is to be a greater uptake for characterisation and optimisation studies and a move away from traditional shake flask experimentation.

In view of this objective, the focus of this chapter was to design a generic microscale automated platform which was robust, allowed increased throughput and saved time and effort compared to manual operations without compromising precision and accuracy of data collection. To achieve this goal the oxidative biocatalyst cyclohexanone monooxygenase (CHMO) was used as a model system for process development. *E. coli* TOP10 [pQR210] is a recombinant whole cell biocatalyst expressing CHMO from *Acinetobacter calcoaceticus* NCIMB 9871. CHMO was used to catalyse the reaction of the ketone bicyclo[3.2.0]hept-2-en-6-one to two regioisomeric lactones (-)-(1*S*,5*R*)-2-oxabicyclo[3.3.0]oct-6-en-3-one and (-)-(1*R*,5*S*)-3-oxabicyclo[3.3.0]oct-6-en-2-one as shown in reaction Scheme 1.2 in section 1.2.3.1.1.1. Due to the stereoselective Baeyer-Villiger oxidation of numerous ketones (Alphand et al., 2003), CHMO is an industrially attractive biocatalyst as discussed in section 1.2.3.1.1.1. The production of this biocatalyst will be described in section 3.2 to demonstrate its similarity to *E. coli* TOP10 [pQR239] (Doig et al., 2001), which shares the host strain and CHMO enzyme. The main difference is that L-arabinose is required for *E. coli* TOP10 [pQR239] induction, whereas CHMO has been found to be constitutively expressed from *E. coli* TOP10 [pQR210], thus was used in this work.

Factors influencing microwell microbial cultivation and bioconversion have been investigated previously including microwell geometry, inoculum concentration, evaporation effects and temperature (Ferreira-Torres, 2008). In Chapter 1 the need for optimisation early during process development and high-throughput methods useful to achieving such needs were discussed. Nevertheless, being able to deal with the data generated by high-throughput techniques is still a

challenge. It was therefore of interest to develop an improved approach with a higher degree of automation of multiple processing steps to enable ‘walk away operation’. In this approach operator dependent tasks are focused on data analysis and process improvement rather than sampling, culture maintenance and data collection. By utilising the Tecan automated robot this study will examine the capability of the robotic platform and how it can be applied to achieve a fully automated approach for whole cell CHMO production and evaluation.

3.2 Results and Discussion

3.2.1 Production of Cyclohexanone Monooxygenase

Limited research has been conducted using *E. coli* TOP10 [pQR210], it was therefore of interest to initially determine the growth and bioconversion kinetics of CHMO using the model substrate bicyclo[3.2.0]hept-2-en-6-one using conventional shake flask culture. Previous work has focused on the strain *E. coli* TOP10 [pQR239] (Doig et al., 2001, Ferreira-Torres, 2008) which is a derivative construct of *E. coli* TOP10 [pQR210] (Doig et al., 2001). Due to the similarities between the strains established conditions from previous work were used as a starting point for these studies and as a reference data set with which to compare the present results against. *E. coli* TOP10 [pQR210] seed stocks were created and confirmed by sequence analysis to carry the correct plasmid as described in section 2.2.1.1. 100 mL of LB-glycerol media was inoculated with 5 % inoculum prepared as described in section 2.2.1.4 in a 500 mL baffled shake flask and incubated at 200 rpm and 37 °C. The growth kinetic data of a typical shake flask culture is shown in Figure 3.1 A. The specific growth rate was calculated from the first three hours of growth to be 0.86 h⁻¹ and the final biomass concentration achieved was 4.91 g_{DCW}L⁻¹. These values compare well with results obtained using a similar *E. coli* TOP10 [pQR239] shake flask culture by Ferreira-Torres (2008) and using a 1.5 L stirred tank reactor culture by Doig et al. (2001). Table 3.1 shows a summary of the results obtained in these studies. The only difference in the culture conditions used in this work was that no

inducer addition was required as cells were found to express CHMO constitutively.

Whole cells have the ability to recycle NADPH intracellularly making them more attractive than isolated systems if the correct reductant and reductant concentration are used prior to bioconversion. Doig et al. (2003) found that 10 gL⁻¹ glycerol allowed for optimum cofactor regeneration and thus this amount of glycerol was added after 6 hours of growth. Following a 15 minute incubation period, 1 gL⁻¹ ketone substrate was added and the bioconversion kinetics monitored for an hour. Figure 3.1 B shows the bioconversion kinetics data in terms of bicyclo[3.2.0]hept-2-en-6-one consumption and lactone formation. The chromatograms obtained for ketone and lactone at three time points are shown in Figure 3.2. The lactone refers to the combination of the two regioisomers produced (-)-(1*S*,5*R*)-2-oxabicyclo[3.3.0]oct-6-en-3-one and (-)-(1*R*,5*S*)-3-oxabicyclo[3.3.0]oct-6-en-2-one as it was not possible to separate them by the GC method adopted for quantification as shown in Figure 3.2 C. Complete conversion was achieved in 1 hour where final values of 0.06 ± 0.01 gL⁻¹ and 1.13 ± 0.01 gL⁻¹ were obtained for the final ketone and lactone concentrations respectively. These findings are consistent with those obtained by Ferreira-Torres (2008). A CHMO specific activity of 34.0 Ug_{DCW}⁻¹ was calculated from the initial rate of lactone formation.

Table 3.1 Comparison of *E. coli* TOP10 [pQR210] culture to *E. coli* TOP10 [pQR239].

Reference	Culture Format	Specific Growth Rate (h ⁻¹)	Final Biomass Concentration (g _{DCW} L ⁻¹)
This work	500 mL shake flask	0.86	4.9
Ferreira-Torres (2008)	500 mL shake flask	0.69	4.5
Doig et al. (2001)	1.5 L bioreactor	0.90	5.5

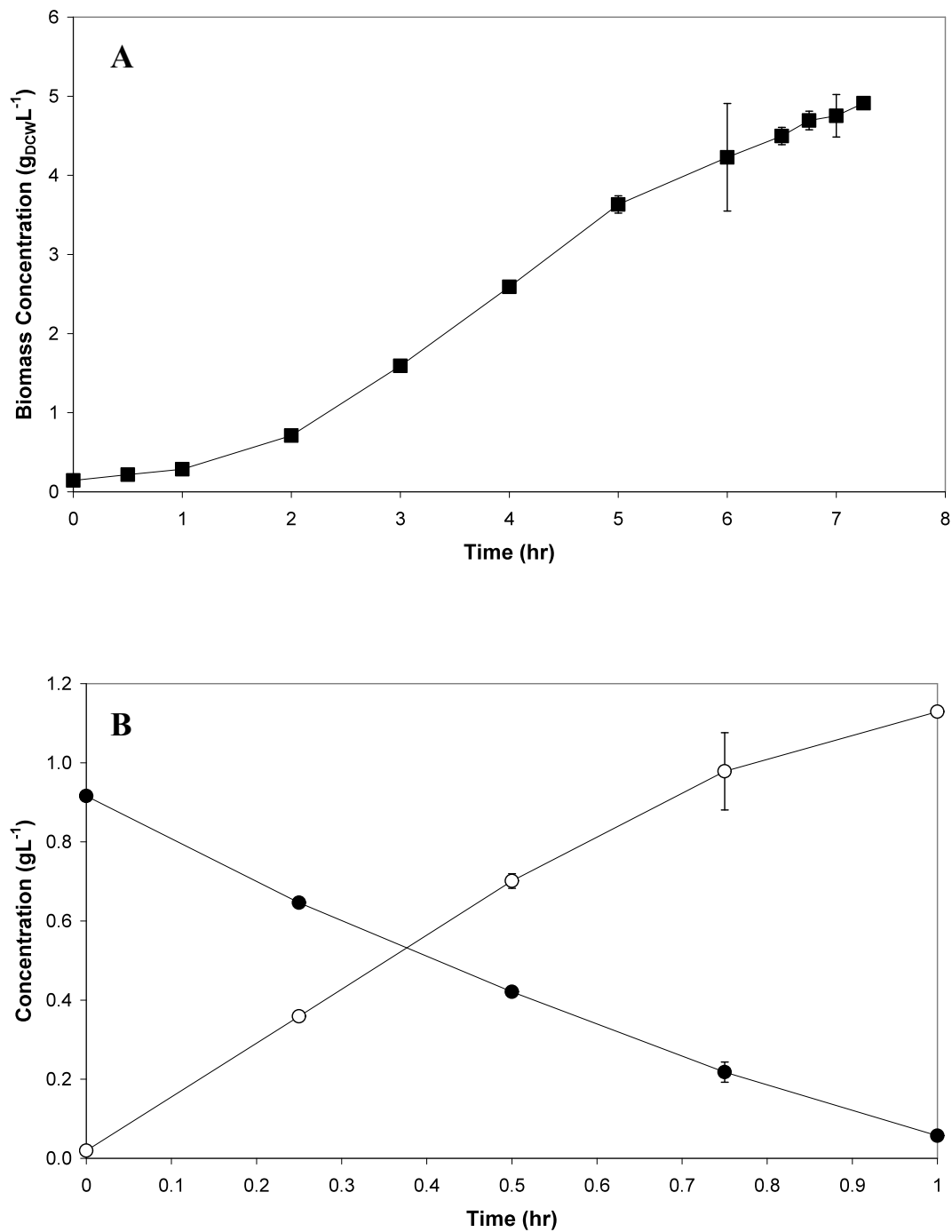


Figure 3.1 Growth (A) and bioconversion kinetics (B) of *E. coli* TOP10 [pQR210] biocatalyst catalysing bicyclo[3.2.0]hept-2-en-6-one (filled symbols) to lactone product (unfilled symbols) collected during a typical shake flask culture. Error bars indicate the range of measured values about the mean.

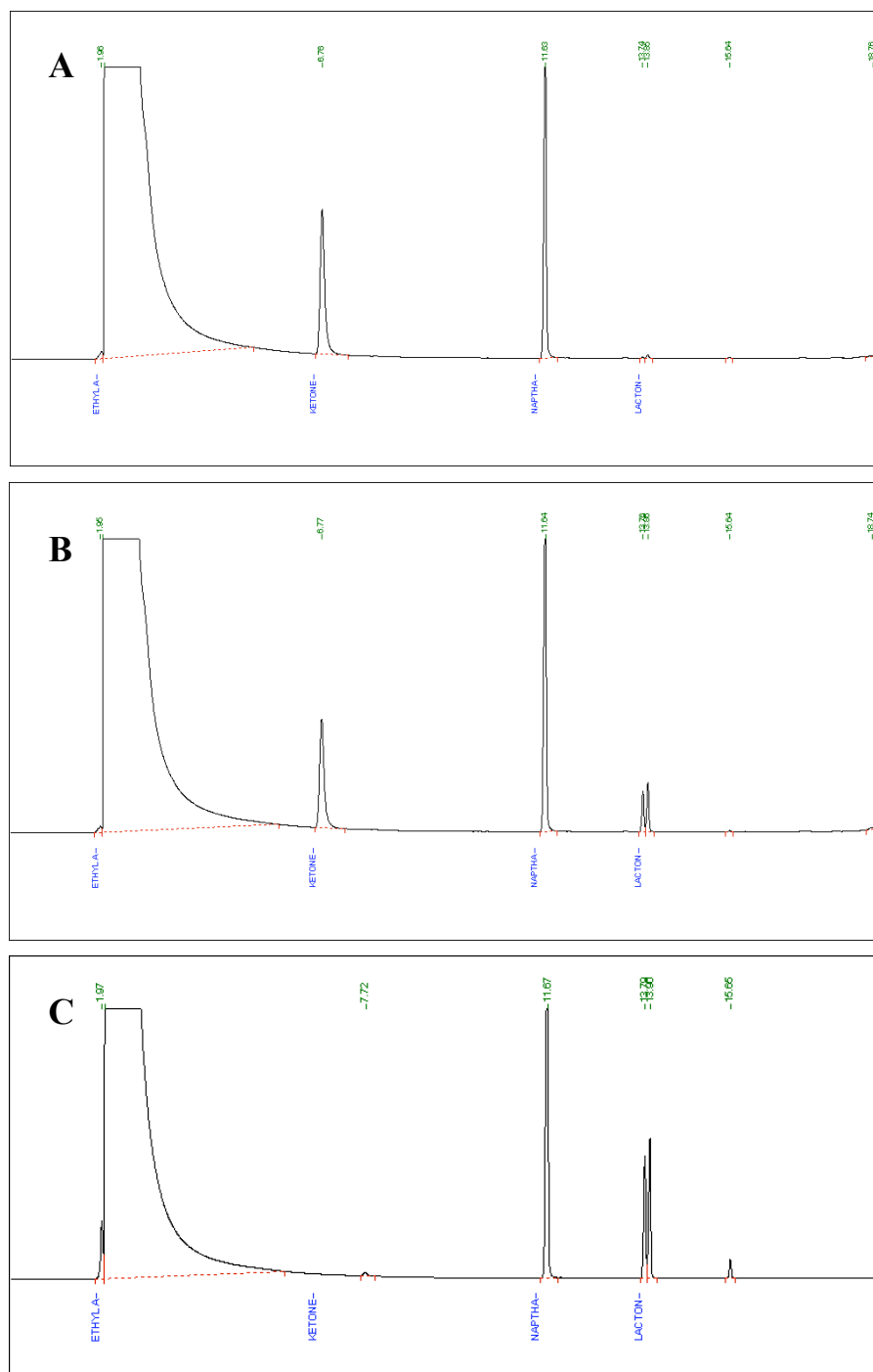


Figure 3.2 Chromatograms displaying the conversion of 1 gL^{-1} bicyclo[3.2.0]hept-2-en-6-one (retention time: 6.7 min) to (-)-(1*S*,5*R*)-2-oxabicyclo[3.3.0]oct-6-en-3-one and (-)-(1*R*,5*S*)-3-oxabicyclo[3.3.0]oct-6-en-2-one (retention times: 13.7 min and 13.8 min) at (A) 0 minutes, (B) 15 minutes and (C) 60 minutes of bioconversion. Peak present at 11 minutes corresponds to naphthalene which was used as an internal standard and added to all samples.

The similarity in terms of growth and bioconversion kinetics of *E. coli* TOP10 [pQR210] to *E. coli* TOP10 [pQR239] was confirmed from these initial shake flask studies. This system was therefore used to test the design of the newly developed automated microscale platform.

3.2.2 A Robotic Platform for Microscale Process Development

The Tecan Genesis automated liquid handling platform equipped with Gemini software was used to develop a fully automated microscale process using the *E. coli* TOP10 [pQR210] strain. The system is completely contained within a Bionet class 2 biosafety cabinet equipped with a laminar airflow system and HEPA filtration making it ideal for aseptic processing. Two robotic arms that can move over the entire workstation with an approximate footprint of 1.3 m² and access all ancillary devices on the platform were utilised for process automation. The platform has 69 grid locations and can be setup with a range of carriers for multiple plates, tips racks and devices. This platform is equipped with a Tecan microplate reader, a Tecan microplate centrifuge with 4 plate locations, an Agilent 1200 series HPLC, a Tecan vacuum separator and an Eppendorf thermomixer enabling a high degree of process automation and analysis. Figure 3.3 shows the external and internal view of the platform along with ancillary equipment.

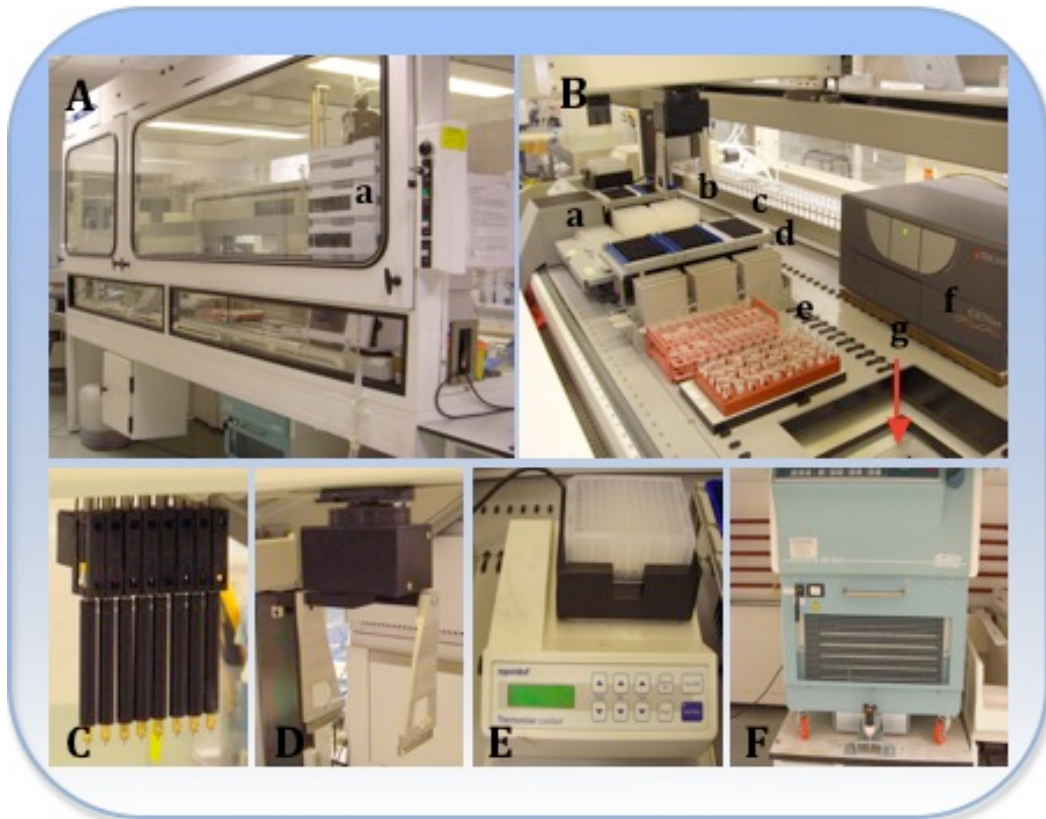


Figure 3.3 Tecan Genesis automated platform. **(A)** Front view of enclosed platform within Bigneat Biosafety Cabinet with (a) HPLC. **(B)** Internal view of robotic platform with ancillaries including (a) pipette waste station (b) plate carrier and plates, (c) disposable tip racks, (d) reagent reservoirs, (e) eppendorf and vial carriers, (f) microplate reader, (g) access hole for centrifuge. **(C)** LiHa. **(D)** RoMa. **(E)** Thermomixer. **(F)** Centrifuge.

To build confidence in the data collected using the automated approach, the accuracy and precision of the LiHa pipetting was tested by applying a method which has been described previously using two disposable microconductive tips (Nealon et al., 2005). The precision and accuracy of the automated pipetting system were calculated from three individual dispenses of the same volume for a range of volumes using Equations 3.1 and 3.2, respectively. Figure 3.4 and 3.5 show the results from the volumes tested with P1000 and P200 tips respectively. For all working volumes the coefficient of variance was found to be 5 % or below, therefore the liquid handling precision and accuracy was considered acceptable (Olsen, 2000). The pipetting accuracy was regularly checked after process runs to enable any pipetting problems to be rectified.

$$\text{Precision \% CV} = [(\text{mean} - \text{target}) / \text{mean}] * 100 \quad (\text{Eq. 3.1})$$

$$\text{Accuracy \% CV} = [\text{standard deviation} / \text{mean}] * 100 \quad (\text{Eq. 3.2})$$

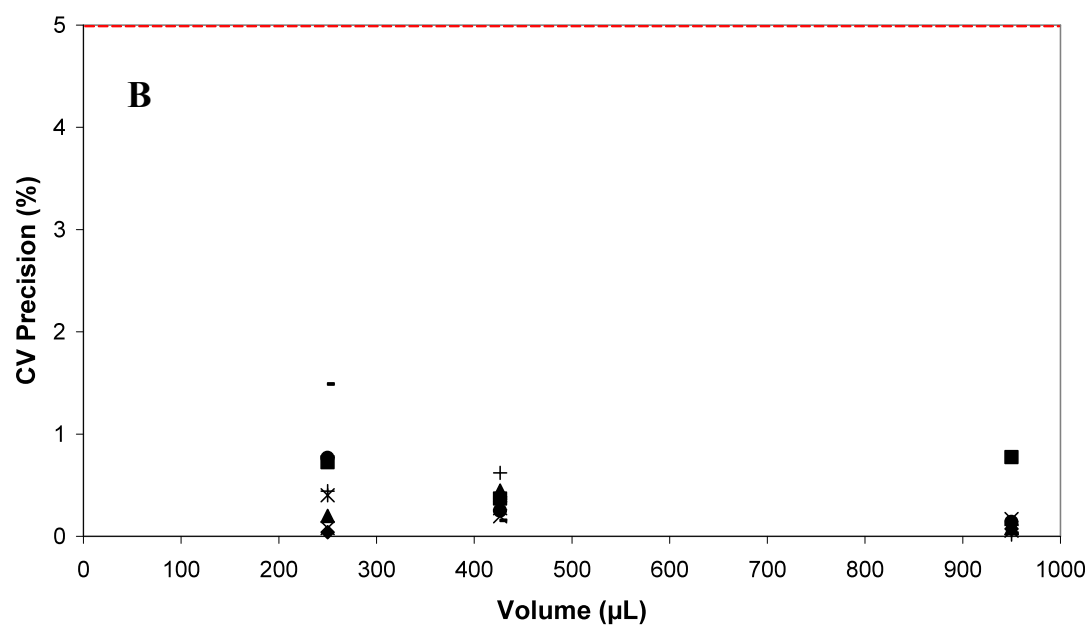
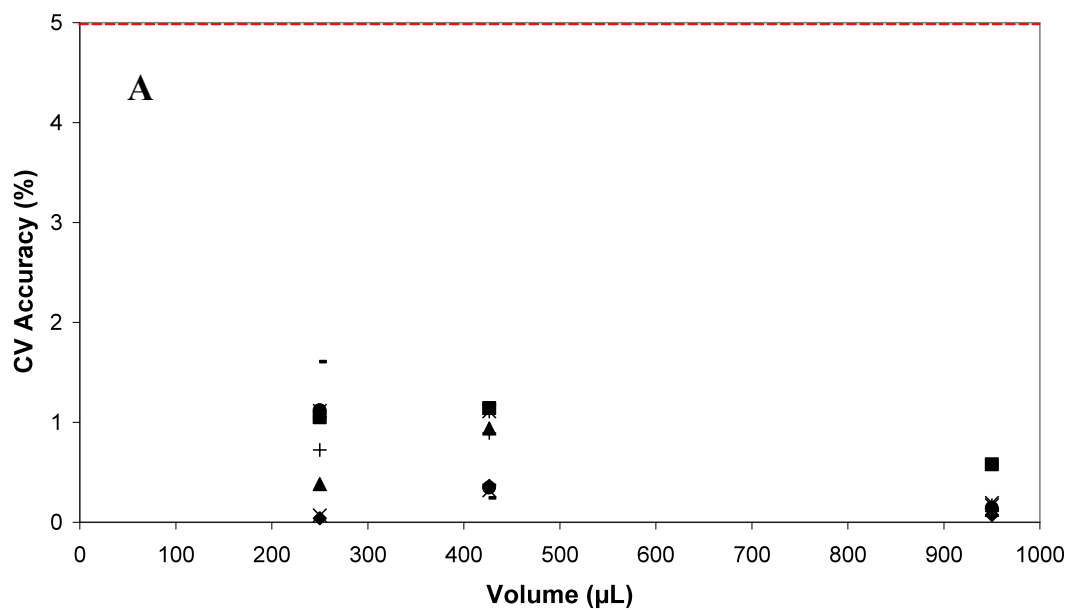


Figure 3.4 P1000 single dispense accuracy (A) and precision (B). Accuracy and precision calculated over three separate dispenses. Tip 1 (◆), tip 2 (■), tip 3 (▲), tip 4 (×), tip 5 (*), tip 6 (●), tip 7 (+) and tip 8 (-). The dashed line displays 5 % coefficient of variance for precise and accurate liquid handling.

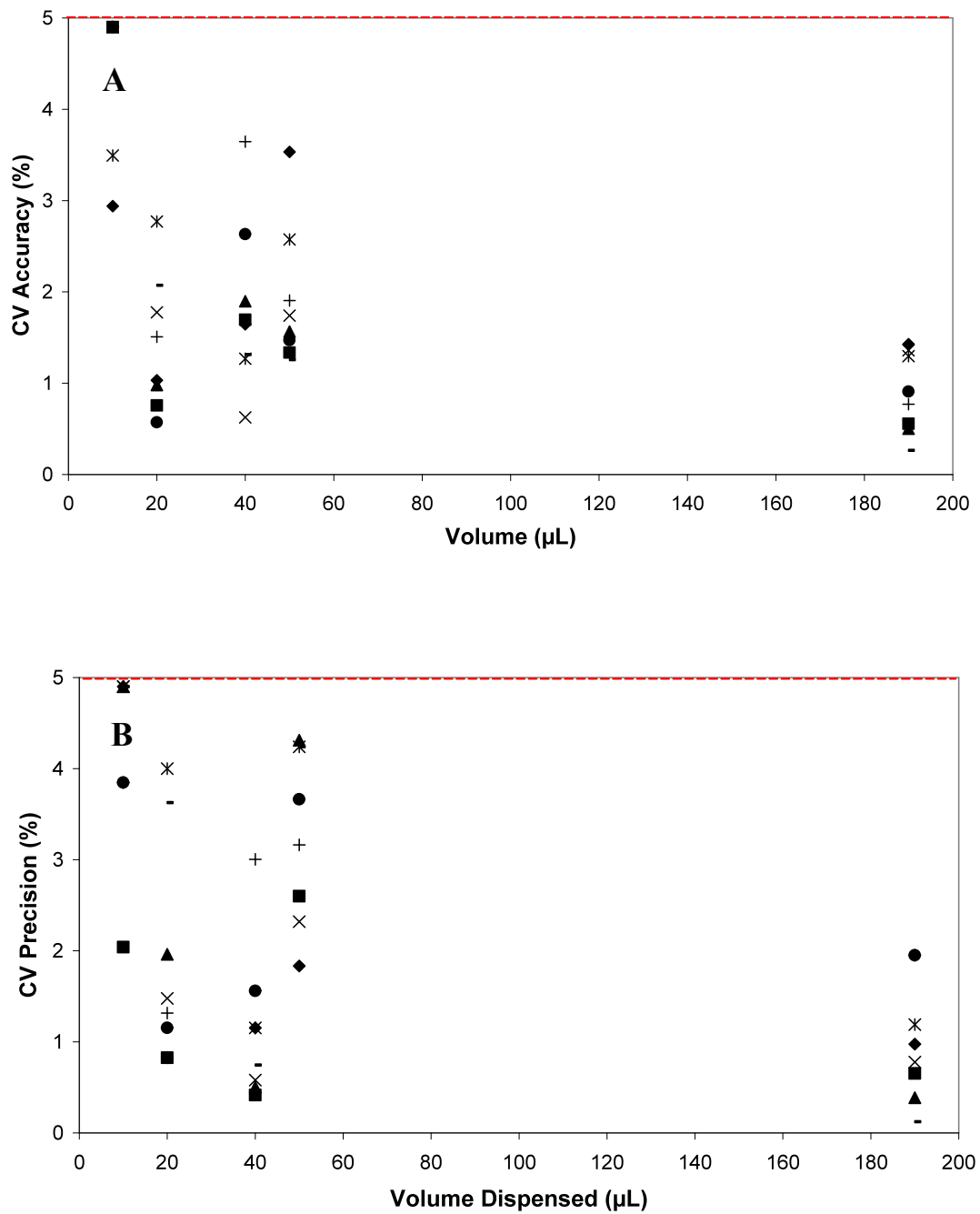


Figure 3.5 P200 single dispense accuracy (A) and precision (B). Accuracy and precision calculated over three separate dispenses. Tip 1 (◆), tip 2 (■), tip 3 (▲), tip 4 (×), tip 5 (*), tip 6 (●), tip 7 (+) and tip 8 (-). The dashed line displays 5 % coefficient of variance for precise and accurate liquid handling. For 20 μL and 10 μL a wash was used between each dispense.

3.2.3 Automated Microwell Cultivation

96-Deep square well (96-DSW) plates have been found to be a suitable culture format for aerobic microbes (Micheletti et al., 2006; Ferreira-Torres, 2008). Firstly, the square geometry has been found to ensure the best condition for oxygen transfer (Duetz and Witholt, 2001) by promoting gas-liquid mass transfer where the corners of the wells act as baffles would in a fermenter (Doig et al., 2002). The deep well format is better suited to sampling over extended periods, without the early onset of evaporation or cell settling effects which have been observed when using standard round well (SRW) plates (Ferreira-Torres, 2008). In addition, the use of 96 wells increases the throughput, enabling increased data collection from a single experiment which is of particular interest in this study. However, a common problem associated with microwells is the phenomenon of “edge effects”. “Edge effects” occur when results obtained from wells at the peripheries of a plate are different from those obtained from wells located in the centre of the plate. This effect may be due to temperature differences, compound photosensitivity or evaporation (Girard et al., 2001). The optimal growth temperature for *E. coli* TOP10 [pQR239] was reported to be 37 °C (Doig et al., 2001, 2002; Ferreira-Torres, 2008) and a temperature study was designed to ensure edge effects were not occurring in the chosen well plate format. A temperature study was conducted as described in section 2.3.1.1.1 where the temperature of wells containing 1 mL LB-glycerol media in five areas of the plate was monitored over a seven-hour period and results are shown in Figure 3.6. Figure 3.6 demonstrates that after approximately 30 minutes at 1000 rpm a temperature of 37 °C is reached in all wells and it then remains constant for the remaining 6.5 hours. Results do indicate slight differences in temperatures between well positions in the plate, where wells in the top left corner are the coolest and those in the top right are the hottest. However, the difference is at most ± 2 °C and this is not considered to cause a significant effect on the growth of *E. coli* TOP10 [pQR210].

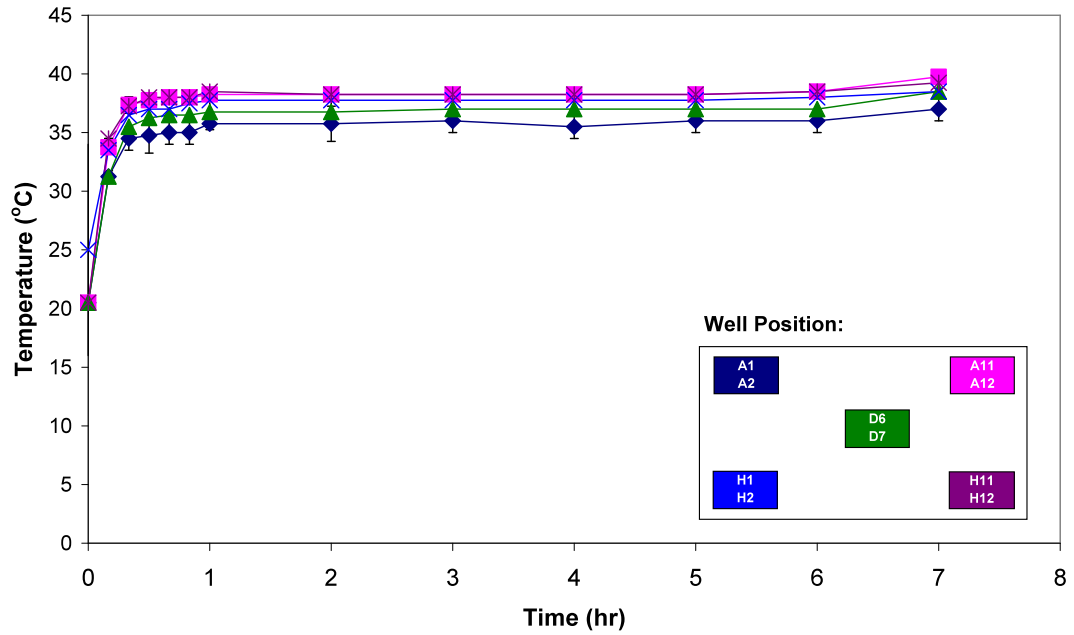


Figure 3.6 The effect of well position on well temperature. Top left (dark blue), top right (pink), bottom left (light blue), bottom right (purple), middle (green). Error bars indicate the range of measured values about the mean.

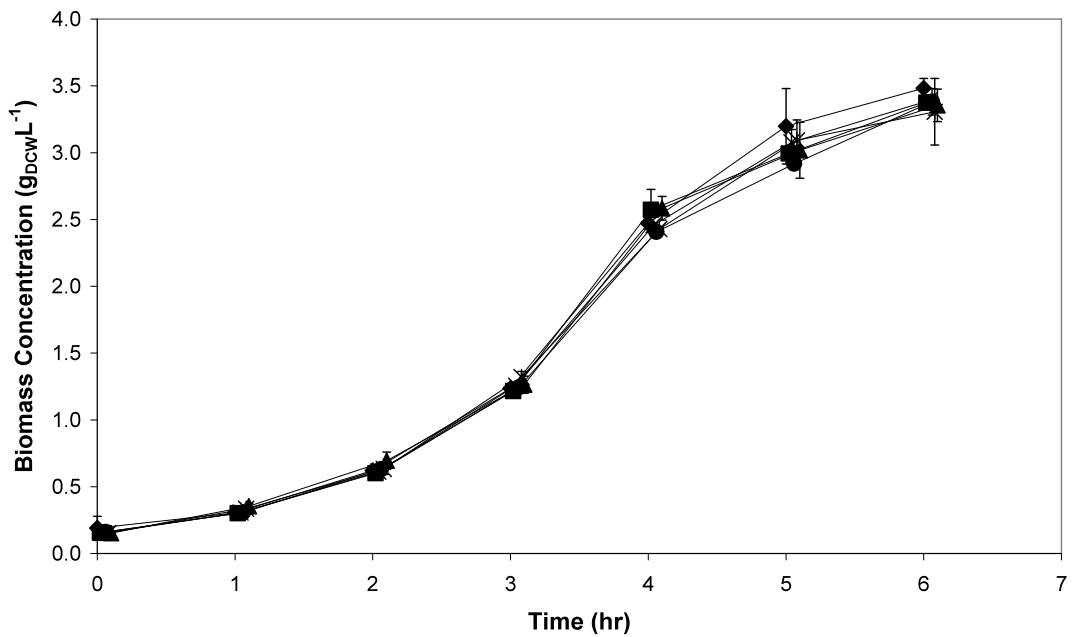


Figure 3.7 Reproducibility of growth kinetics of *E. coli* TOP10 [pQR210] across a 96-DSW plate collected during an automated culture. Columns 1-2 (◆), columns 3-4 (■), columns 5-6 (×), columns 7-8 (●), columns 9-10 (*), columns 11-12 (▲). Error bars indicate the range of measured values about the mean.

The first stage of process automation was to develop an effective method of monitoring the growth of *E. coli* TOP10 [pQR210] cells. It was important to ensure that growth was reproducible across the plate. A 96-DSW plate was first automatically filled with 1 mL LB-glycerol media and heated until a temperature of 37 °C was reached. This volume ensured no spillage from the wells which could result in well-to-well contamination at an agitation of 1000 rpm. Automatic addition of 5 % v/v overnight prepared inoculum of *E. coli* TOP10 [pQR210] followed and the growth monitored using the sacrificial well approach (Doig et al., 2002) for six hours. Samples were diluted accordingly into 96-SRW plates and these transferred via the RoMa to a Tecan microplate reader for analysis at hourly intervals. Culture sterility was tested previously (Ferreira-Torres, 2008) and found to not be compromised due to the use of antibiotic. The same antibiotic along with the contained environment, as described in section 3.2.2, ensured that no culture contamination was observed in the present work. Figure 3.7 displays the growth kinetics across a 96-DSW plate demonstrating that the well position has no effect on the growth of cells allowing the entire plate to be used for analysis.

The reproducibility of data collected on different days is an important issue to consider to ensure repeated walk-away operation was possible. The growth kinetic data were obtained in triplicate on three separate days as described in section 2.3.1.2 and results are shown in Figure 3.8. Similar growth profiles were observed for each of the three runs. From the three runs, an average of 0.72 h⁻¹ and 4.04 g_{DCW}L⁻¹ were calculated for the mean specific growth rate (μ) and the mean final biomass concentration respectively, and are similar to those reported previously (Ferreira-Torres et al, 2005). Using data from these runs the calculated average and maximum error were 5 % and 12 % respectively and are representative of the day-to-day variations attributing to differences in media and inoculum preparations. In section 3.2.2 the error of robotic dispenses was established to be less than 5 %. Day-to-day robotic performance should be consistent and significant changes from the average error would indicate a fault. The preparatory manual steps conducted prior to automated processing are thus a likely source of error. For example, slight differences in cell maturity, due to differences in overnight inoculum preparation could be responsible for the error.

A potential solution to reduce the variation observed would be to automate the overnight culture.

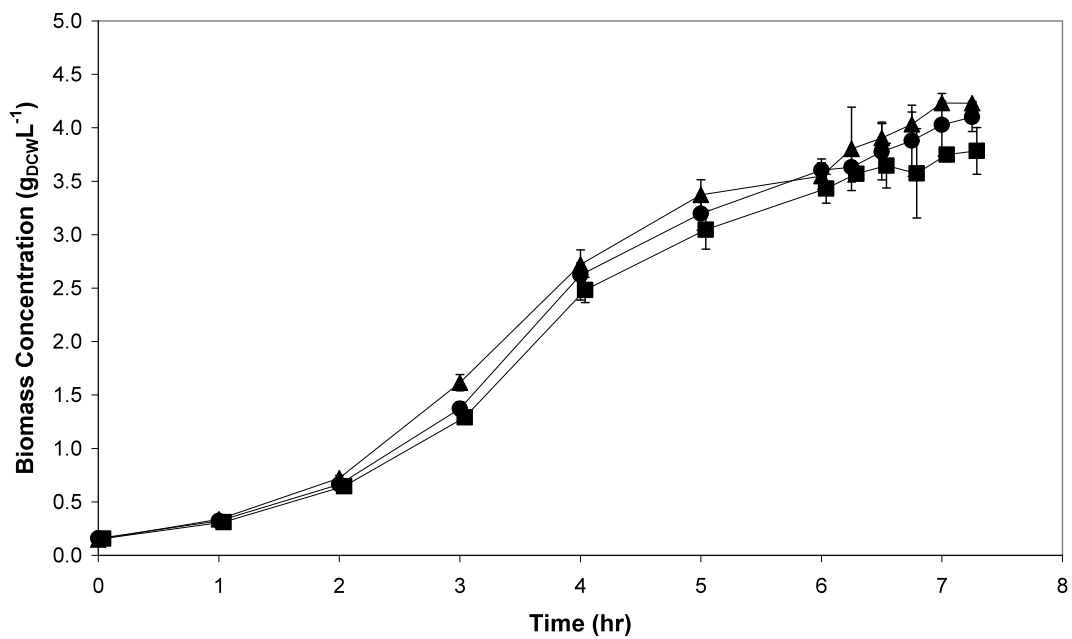


Figure 3.8 Growth kinetics of *E. coli* TOP10 [pQR210] biocatalyst collected using the automated process sequence from three separate runs (run 1 (square), run 2 (circle) and run 3 (triangle)). Error bars indicate the range of measured values about the mean.

3.2.4 Automated Microwell Bioconversion

Once the cultivation stage had been developed the second objective was to fully automate the bioconversion of bicyclo[3.2.0]hept-2-en-6-one. In preparation for this step, cell aliquots were automatically transferred to new wells as described in section 2.3.1.2 and incubated with glycerol at 30 °C. A similar temperature study to that described in section 3.2.3 was conducted to confirm that 30 °C was reached at the end of the incubation period. Glycerol is more viscous than water and thus a different liquid class was used where the aspiration and dispense speed of the LiHa were set to ensure adequate dispensing performance. 1 gL⁻¹ bicyclo[3.2.0]hept-2-en-6-one was added to the wells and Figure 3.9 shows the bioconversion kinetics data in terms of ketone consumption and lactone formation using cells obtained after six hours of growth. Both substrate consumption and product formation follow a linear behaviour (potentially due to mass transport issues into the cell) and similar final concentrations were achieved for the three runs after 1 hour of bioconversion. The impact of changing variables could be assessed from the data collected on the initial bioconversion kinetics within this timeframe. Mean final values of 0.27 ± 0.04 gL⁻¹ and 0.47 ± 0.06 gL⁻¹ were obtained for the ketone and lactone respectively, corresponding to a final product yield of 47 %. Using the mean initial lactone formation rate obtained from the three runs the calculated mean CHMO specific activity was 15.0 Ug_{DCW}⁻¹. The sum of the experimental errors in sample preparation and GC analysis are believed to be responsible for the increased error observed for the bioconversion stage in comparison to the cultivation step. Inaccuracies are likely to derive from the ethyl acetate extraction due to the volatility of the solvent used causing a change in sample concentrations. In order to avoid such inaccuracies an automated ethyl acetate extraction step was developed and it will be discussed in section 3.2.5.

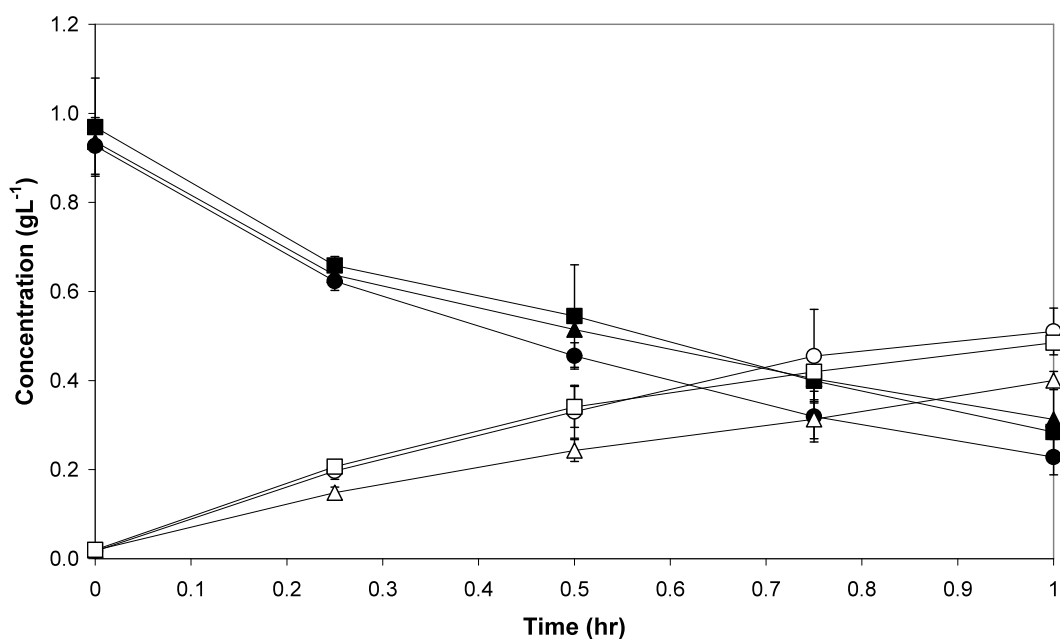


Figure 3.9 Bioconversion kinetics of *E. coli* TOP10 [pQR210] biocatalyst catalysing bicyclo[3.2.0]hept-2-en-6-one (filled symbols) to lactone product (unfilled symbols) collected using the automated process sequence from three separate runs (run 1 (square), run 2 (circle) and run 3 (triangle)). Error bars indicate the range of measured values about the mean.

3.2.5 Automated Liquid-liquid Extraction

The method employed to manually extract the bioconversion metabolites is described in section 2.6.4.1 and involves vortex mixing of individual cell samples with ethyl acetate. Automated microscale approaches can generate large sample numbers, which need to be processed in a short timeframe if they are to generate reliable results. In order to prevent this step from becoming the process bottleneck it was of interest to develop an automated alternative step. It was also desirable to increase the consistency and accuracy of data collection, as the manual processing may have been responsible for the increased error reported in section 3.2.4.

Ethyl acetate is a volatile solvent, consequently, a liquid class was developed so that this solvent could be aspirated and dispensed with appropriate accuracy/precision. The LiHa works with microconductive tips. While such tips are appropriate for most of the fluids used in this work, for ethyl acetate it was necessary to remove the conductivity sensing. The aspiration of a set volume of ethyl acetate was conducted in triplicate. Results were compared with those obtained from the same experiment conducted manually and the percentage difference was found to be 1 %, confirming that the developed liquid class properties were suitable for the liquid handling of ethyl acetate.

Figure 3.10 shows a comparison of results obtained using a manual procedure with those obtained as described in section 2.3.1.2 using a 96-DSW plate agitated at 1200 rpm on an Eppendorf thermomixer for 0.5 up to 3 minutes. Following extraction the plate was transferred via the RoMa to a microplate centrifuge and centrifuged for 15 minutes at 4000 rpm and 4 °C. This was found to separate organic and aqueous phases. A total of 3 minutes was the time required to fully extract both ketone and lactone using the thermomixer. Ketone concentration remains approximately constant from 1 minute up to 3 minutes whereas there is a greater degree of variation when using the manual vortex extraction. This new extraction method was also tested throughout the plate in different well locations and an average error of less than 5 % was calculated between the target and

extracted ketone concentration. The thermomixer method was therefore used for the further processing of all samples with the added benefit of being able to process up to 96 samples in one extraction. An alternative method to combat the error arising from the volatility of the ethyl acetate would be to adjust metabolite concentrations in relation to changes in the concentration of internal standard added to each sample detected by GC. Therefore deviations in the concentration of the internal standard would give a quick indication on how much a sample may have been concentrated by due to solvent evaporation and this could be considered to calculate the true concentration of ketone and lactone.

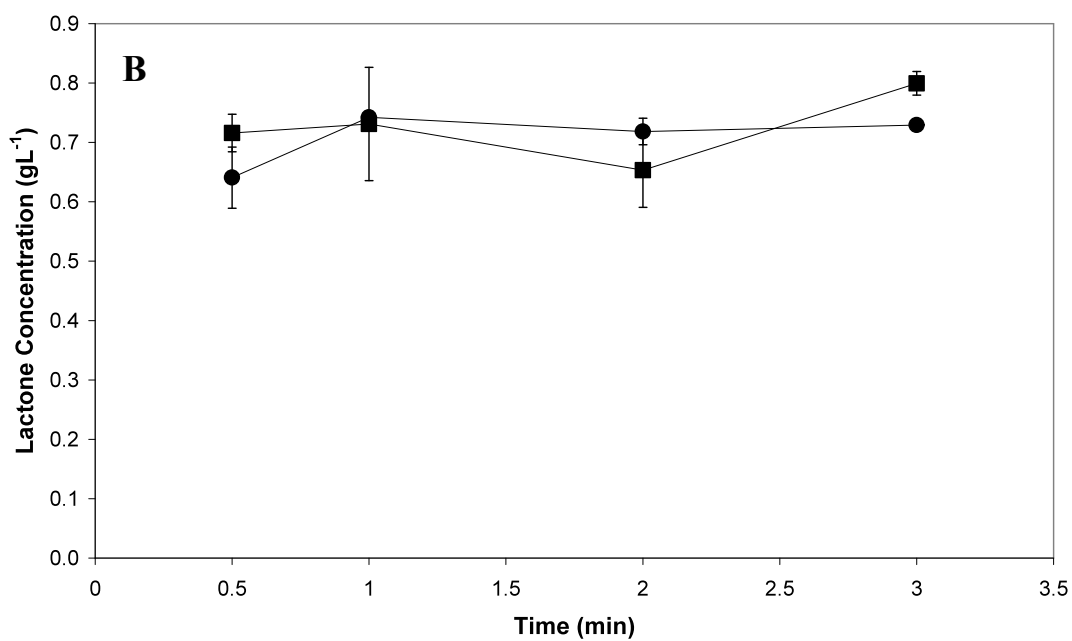
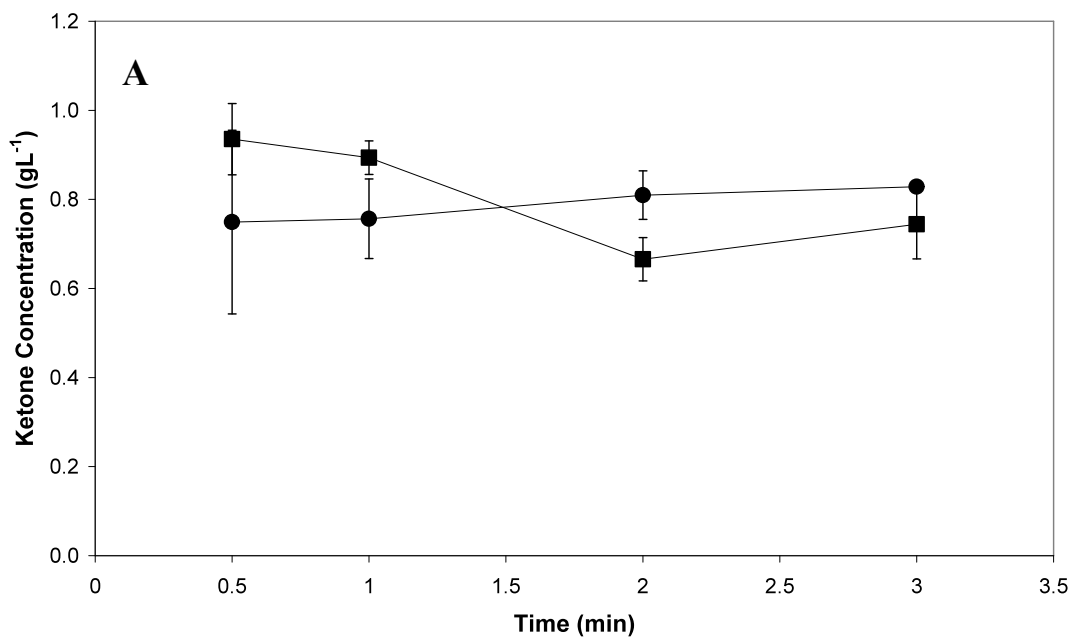


Figure 3.10 The effect of agitation time on the concentration of ketone (A) and lactone (B) extracted into ethyl acetate using a vortex mixer (■) and a Eppendorf thermomixer (●). For each data point the same sample was extracted with both devices. Error bars indicate the range of values about the mean of duplicate well measurements for the thermomixer results and duplicate samples for the vortex mixer results.

3.2.6 Automated Linked Process of Cultivation, Bioconversion and Liquid-liquid Extraction

The complete automated approach for evaluation of *E. coli* TOP10 [pQR210] using each of the steps described in sections 3.2.3 to 3.2.5 is shown in Figure 3.11. ‘Walk away operation’ was achieved once the Tecan platform had been setup and prepared for aseptic processing as described in section 2.3.1.2. The preparation of culture plates (96-DSW) and analysis plates (96-SRW), reagent addition including inoculum, glycerol, substrate and ethyl acetate as well as sampling and OD measurements were all automated. Data was automatically collected throughout the culture and bioconversion samples were frozen every 15 minutes. The frozen bioconversion samples were defrosted and an automated liquid-liquid extraction followed. At the end of the process GC vials containing ethyl acetate with the extracted metabolites were collected from the platform, capped and loaded onto the GC instrument for analysis.

The automated microwell approach has been confirmed to rapidly collect reproducible data on different days as described in sections 3.3 to 3.6. A manually run experiment conducted within the Tecan enclosed environment was also found to be in good agreement with the automatically collected data. From three manually conducted runs an average error of 21 % and maximum error of 27 % was calculated which represents the error arising from the inconsistency in plate preparation and sampling, and inaccuracies in manual pipetting. The day-to-day deviations are greater during manual operations thus the reliability of the automated approach makes it a superior method for process investigation.

There are notable benefits from using this approach over the traditional shake flask experimentation. The effects of six parameters can be tested simultaneously in duplicates in 8 hours with minimal error, low chance of contamination and significantly reduced manual operations. The traditional manual approach would require twelve shake flasks cultures, which, due to manual processing would cause a larger error and risk of contamination. Additionally, keeping the culture mixing and at constant growth conditions

prevents cellular stresses whereby during the automated approach no interruptions in shaking are required. It has been reported when shaking is stopped during sample collection there can be a reduction in oxygen uptake rate due to oxygen limitation which can become quite significant when screening multiple vessels (Büchs, 2001; Wittmann et al., 2003; Fernandes and Cabral, 2006). Automation reduces these risks where operators are only required for preparation, setup and monitoring. The seven-hour processing time conducted by the robot can be spent in analysing results and carrying out analytical measurements such as GC and preparation for other experiments. Moreover, system downtime is decreased where automated sequences can be run almost back-to-back after platform setup and sterilisation and overnight processing is possible, thus maximising system productivity. Furthermore, working at the microscale reduces raw material requirements and multiple plates can be processed in parallel increasing throughput within the same process time.

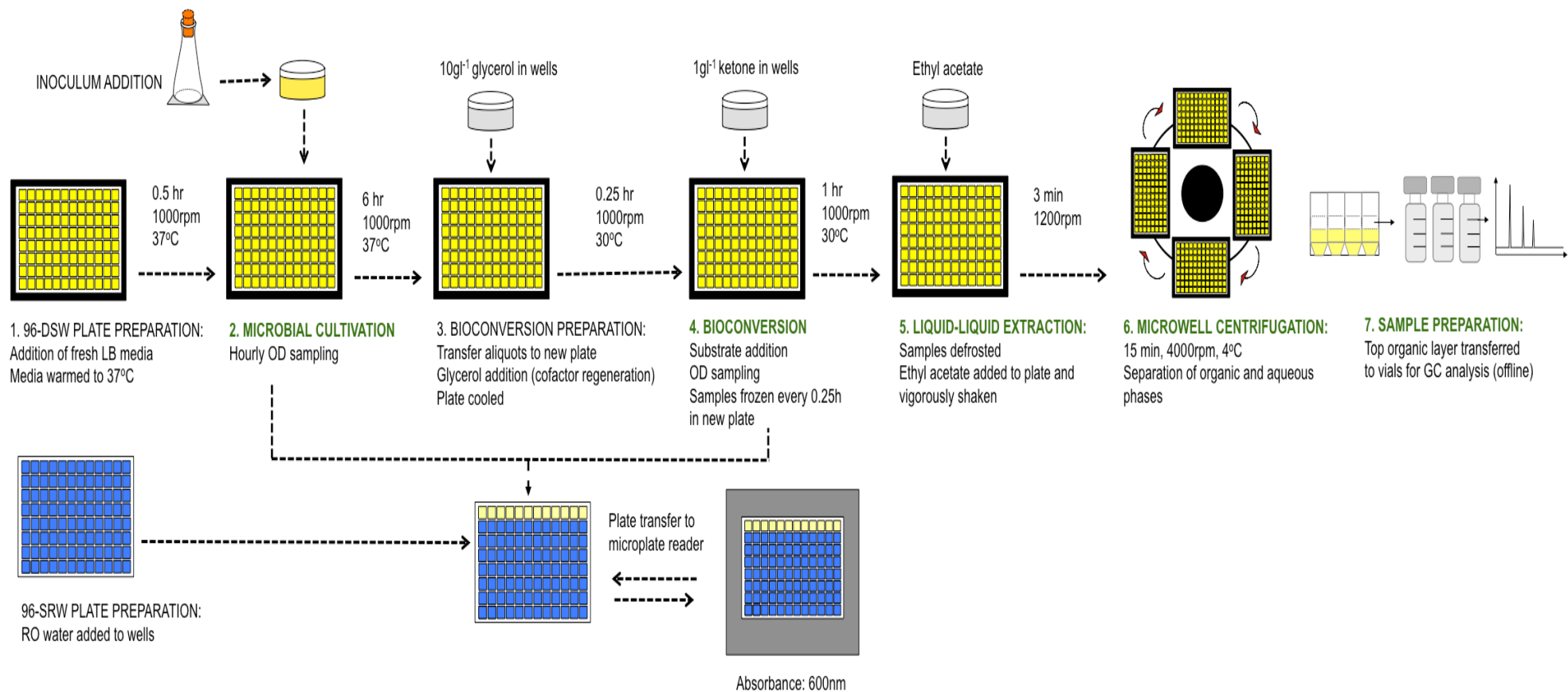


Figure 3.11 Schematic representation of the fully automated linked process sequence using *E. coli* TOP10 [pQR210] expressing cyclohexanone monooxygenase. Coloured wells represent filled wells as an example (yellow: media and culture, blue: RO water).

3.3 Concluding Remarks

The commercialisation of biologics is a long process. Hence the biotechnology industry is under constant pressure to reduce developmental timelines and cut costs if they are to meet market demands and gain competitive advantage. One strategy is to use a combination of miniaturisation to cut costs and automation to speed processing consistency and reduce downtime. In line with this approach, the objective of this work was to design and develop a generic microscale automated platform for bioprocess investigation. The key achievements included a demonstration of robustness, increased throughput and accuracy of data collection on multiple upstream process steps.

E. coli TOP10 [pQR210] was found to be a suitable system for the production of CHMO. The Tecan automated liquid handling platform was chosen due to its applicability to process automation and high degree of functionality. The LiHa liquid dispense was established to have an error below 5 % and thus was an acceptable system (Olsen, 2000) to begin process automation for the microscale production of CHMO using *E. coli* TOP10 [pQR210]. Working from established microscale microbial culture, 96-DSW plates were found to allow reproducible culture conditions across the plate with no adverse “edge effects”. The automated approach was further found to rapidly collect data on different days reproducibly in spite of differences in media and overnight inoculum preparations. Moreover, when compared to manual runs the error between triplicates was reduced from an average of 21 % down to 5 %. The collection of reproducible bioconversion kinetics was established. However, the error observed between triplicate bioconversion data sets prompted the development of an automated liquid-liquid extraction allowing 96 samples to be processed in one run of the automated method. From automated data collection cells of *E. coli* TOP10 [pQR210] grew at a specific rate of 0.72 h^{-1} to a final biomass concentration of $4.04 \text{ g}_{\text{DCW}}\text{L}^{-1}$ and were found to metabolise 1 gL^{-1} bicyclo[3.2.0]hept-2-en-6-one to the respective lactone in a yield of 47 % and with a specific activity of $15 \text{ Ug}_{\text{DCW}}^{-1}$.

The developed platform has the potential to be applied to multiple microbial and oxidative biocatalytic systems. Whole cell recombinant proteins are used for the production of fine chemicals, drug synthesis and bioremediation to name a few applications (Duetz et al., 2001). The majority of production processes involve a growth, expression and bioconversion phase all of which have been automated in this study and can be rapidly assessed. Depending on the process requirements this generic approach could be used in its current state or adjusted to suite the requirements of each individual system. In particular, novel strains which have yet to be fully investigated would clearly benefit from rapid evaluation using this automated approach and as such this will be covered in Chapter 5. It can therefore be used to test the constraints and limitations of a system to enable full process optimisation.

Using the Tecan robotic system fully automated microbial culture, bioconversion and metabolite liquid-liquid extraction has been achieved. This allows the rapid collection of process data with increased throughput, accuracy and reproducibility making it superior to traditional approaches reliant on manual operations prone to error and contamination. More importantly, this approach enables the majority of the process time to be used for data analysis, further experimentation or analytics. Once the automated microscale platform was in place, it was of interest to apply it for whole bioprocess evaluation. The initial microwell results collected in this study will form the basis for strain growth and bioconversion kinetics. These will be used for further studies covered in Chapter 4 where the optimised process conditions for the oxidative biocatalyst CHMO will be defined.

4 Whole Bioprocess Evaluation Using an Automated Microscale Platform[†]

4.1 Introduction

The development of a high-throughput robust automated microscale platform for rapid data collection on upstream unit operations was described in Chapter 3. Preliminary microwell based results were collected, forming a basis for growth and bioconversion kinetics on a CHMO-expressing system. Whole bioprocess evaluation is important to test system constraints and limitations to enable optimal process conditions to be identified. In particular, the selected conditions can then be tested in large-scale conventional bioreactors to ensure the reproduction of kinetic results in geometrically different formats. This aspect will be covered in Chapter 6. This illustrates the benefits of microscale automation where time consuming developmental stages can be accelerated at reduced cost and large-scale cultivations focussed on production.

In the last few years there has been significant interest in CHMO from *A. calcoaceticus* NCIMB 9871 resulting in CHMO becoming the best characterised BVMO to date (Alphand et al., 2003). This is predominantly because it can catalyse the Baeyer-Villiger oxidation without conventional toxic and/or unstable oxidants in an enantioselective manner. Due to intrinsic limitations, namely a pathogenic nature and requirement of the toxic carbon source cyclohexanol (Trudgill, 1990), use of the wild type organism is avoided while recombinant systems have enabled considerable progress since the 1990s (Stewart et al., 1998; Mihovilovic et al., 2001; Doig et al., 2001). *E. coli* expression systems have been studied to determine conditions for biocatalyst expression, activity and bioconversion. In the case of *E. coli* TOP10 [pQR239] a number of factors have been investigated using the model substrate bicyclo[3.2.0]hept-2-en-6-one. Firstly, culture conditions will have an impact on whole cell CHMO specific

[†] Some of the results presented in this chapter are included in Baboo et al (2012), 'An automated microscale platform for evaluation and optimization of oxidative bioconversion processes', *Biotechnology Progress*, 28, 392-405, DOI: 10.1002/btpr.1500.

activity. This has been found to reach a maximum at pH 7 with a broad pH optimum range between 6 and 8 (Doig et al., 2003). Similarly, while a temperature of 37 °C yields the highest activity, temperatures ranging from 30 °C to 40 °C will promote activity (Doig et al., 2003). In the case of microscale studies, due to the requirement of an open system, 30 °C is the best temperature to overcome the effects of substrate evaporation (Ferreira-Torres, 2008). The source of amino acid used in media formulations can also improve CHMO specific activity which was the case when soyabean peptone was used (Baldwin and Woodley, 2006; Berezina et al., 2007). Finally, monitoring cellular growth can often be crucial is determining the point of cell harvest as CHMO specific activity expressed from *E. coli* TOP10 [pQR239] will increase with biocatalyst concentration but only up to 2 g_{DCW}L⁻¹.

Bioconversion conditions should also be considered, such as reactant concentration, where bicyclo[3.2.0]hept-2-en-6-one has been reported to have an inhibitory limit. Doig et al. (2003) reported substrate inhibition to take place at concentrations above 0.2 - 0.4 gL⁻¹ using resuspended whole cells, whereas Shitu et al. (2009) found a greater tolerance using the same strain and substrate concentration was found to be detrimental above 2 gL⁻¹. Furthermore, the lactone product concentration can limit the reaction where specific biotransformation activity will reduce as soon as it is produced (Doig et al., 2003; Shitu et al., 2009) and the highest reaction rate has been determined in the absence of product. Whole cells can recycle NADPH intracellularly in the presence of an appropriate carbon source where Doig et al. (2003) found both the choice and concentration of reductant to influence specific activity. Both cellular growth and CHMO bioconversion are oxygen dependent, hence DOT and oxygen transfer rates play a crucial role in achieving the maximum enzymatic performance (Doig et al., 2001). Consequently, at the microscale the volumetric CHMO activity has been found to increase when increasing the surface area to volume ratio of a 96-DSW plate (Doig et al., 2002; Ferreira-Torres, 2008).

Identifying industrially relevant reactions is an area of significant interest. Moreover, there is a sustained focus in examining the substrate specificity of CHMO. Due to the fact that ketones and lactones can be applied in flavour and

fragrance production such as γ -decalactone which is used to create a peach-like flavour. In fact, CHMO can metabolise numerous substrates (Roberts and Wan, 1998). Cyclic ketones such as cyclohexanone and cyclopentanone (Doig et al., 2003; Ferreira-Torres et al., 2005), the bicyclic ketone bicyclo[3.2.0]hept-2-en-6-one (Alphand, 2003), racemic bicyclic diketones (Ottolina et al., 2005), 1,3-diathiane (Zambianchi et al., 2004) and α -substituted cyanocyclohexanones (Berezina et al., 2007) have all been tested with *E. coli* TOP10 [pQR239]. Other *E. coli*-expressed CHMO have also been reported to metabolise terpenones such as cis-dihydrocarvone, carvomenthone and methone (Cernuchova and Mihovilovic, 2007), 4-substituted-3,5-dimethylcyclohexanones (Mihovilovic et al., 2005) and racemic benzylketones (Geitner et al., 2007) to name a few.

Accordingly, few previous works have been conducted to gain a greater understanding of the CHMO system, substrate specificity and its respective constraints and limitations. The ability to complete such studies in a reduced time frame and with minimal raw materials is therefore of great importance. A robust automated microscale platform for the investigation of CHMO was developed as described in Chapter 3. In order to demonstrate the platform utility for whole bioprocess sequence evaluation, build on current research and further investigate areas which have yet to be extensively studied, a range of operating conditions and substrates were tested with *E. coli* TOP10 [pQR210] and the results are presented in this chapter.

4.2 Results and Discussion

4.2.1 Automated Investigation of CHMO Specific Activity

4.2.1.1 Impact of Oxygen Transfer Rate on Bioprocess Performance

CHMO is an oxidative biocatalyst and is expressed from an aerobic microorganism thus oxygen supply is critical. The rate at which oxygen is

supplied to a microwell system can therefore be varied to determine the extent of oxygen dependency. This was assessed by investigating the effect of well fill volume on growth kinetics as it is an important parameter shown to affect air-liquid mass transfer in microwell geometries (John et al., 2003; Kensy et al., 2005; Funke et al., 2009). The growth curves obtained from an automated run at varying fill volumes as described in section 2.3.1.3 are shown in Figure 4.1 A. Similar growth is observed at all conditions for the first 4 hours after which a clear distinction between the curves at different fill volumes can be observed. Biomass concentrations of $5.59 \text{ g}_{\text{DCWL}}^{-1}$ and $4.23 \text{ g}_{\text{DCWL}}^{-1}$ were achieved at fill volumes of 500 μL and 1000 μL , respectively. Reducing the fill volume to 600 μL caused the growth to increase, while further volume reductions have no significant effect. Oxygen therefore becomes the limiting growth factor above a 600 μL fill volume.

Decreasing the fill volume creates a larger specific interfacial area thus improving the gas liquid mass transfer coefficient ($K_{\text{L}a}$). $K_{\text{L}a}$ (s^{-1}) can be estimated using Equation 4.1 (Doig et al., 2005) for each of the operating fill volumes. The equation was developed for a range of plate geometries using a dimensionless group approach.

$$K_{\text{L}a} = 31.35 D a_i \text{Re}^{0.68} \text{Sc}^{0.36} \text{Fr}^x \text{Bo}^y \quad (\text{Eq. 4.1})$$

Where $x = 0.64$, $y = 0.15$, (Doig et al., 2005) for 96-SRW microplates and are geometry dependant coefficients, D (m^2s^{-1}) is the oxygen diffusion coefficient (Perry and Green, 1997), a_i (m^{-1}) is the initial specific surface area and Re , Sc , Fr and Bo are dimensionless numbers which have been defined for the microwell geometry adapting their definition for conventional stirred bioreactors.

Predicted $K_{\text{L}a}$ values, computed using Equation 4.1 at each fill volume, are shown in Table 4.1 at 1000 rpm shaker speed and 3 mm shaking diameter. A square geometry was used in this work and, as Equation 4.1 was developed for round wells, a 30 % increase in $K_{\text{L}a}$ was added to take into account the geometry difference (Micheletti et al., 2006). From the predicted values a 50 % decrease

in the fill volume causes the surface area to volume ratio to double, resulting in an approximately double value of K_{La} . However, it is important to note that this improvement can only be achieved with appropriate agitation to ensure significant surface disruption. This finding confirms that an improved K_{La} is responsible for improved growth. K_{La} value predictions help in the evaluation of fill volume impact on final reaction yield and provide an initial indication of how the rate of oxygen transfer will vary.

Following the growth at varying fill volumes 500 μL cell aliquots were transferred from each well to a new plate and the bioconversion results are shown in Figure 4.1 B. In Figure 4.1 B the fastest rate of substrate consumption and highest specific activity ($16.7 \text{ Ug}_{\text{DCW}}^{-1}$) were achieved at a 600 μL fill volume. This is 36 % higher than the corresponding value achieved at 1000 μL ($12.3 \text{ Ug}_{\text{DCW}}^{-1}$). A higher enzyme yield, resulting from the improved growth is responsible for this finding. Evaporation effects during the culture are thought to be responsible for the higher than expected initial substrate concentration (1.2 gL^{-1}) at a 500 μL fill volume. This reaction suffers from substrate inhibition (Doig et al., 2003) which will be discussed in detail in section 4.2.2.1 and is responsible for the results observed in this work. In this work by improving the oxygen supply through the increase in the surface to volume ratio both cell growth and bioconversion yield were considerably improved.

Adopting the same methodology as in the previous experiment the impact of fill volume on the bioconversion step was examined. Figure 4.2 A shows the rate of substrate consumption obtained where cells were initially grown at a constant fill volume of 1000 μL for the first 6 hours and then the volume varied from 200 μL up to 1000 μL during the bioconversion. The CHMO specific activities were calculated from initial rates of product formation and are shown along with the mass balance analysis in Figure 4.2 B. Predictions of K_{La} values using Equation 4.1 have confirmed that reducing the fill volume improves the gas liquid transfer rate, therefore it is expected that it will also increase the rate at which substrate can be oxidised and converted to product.

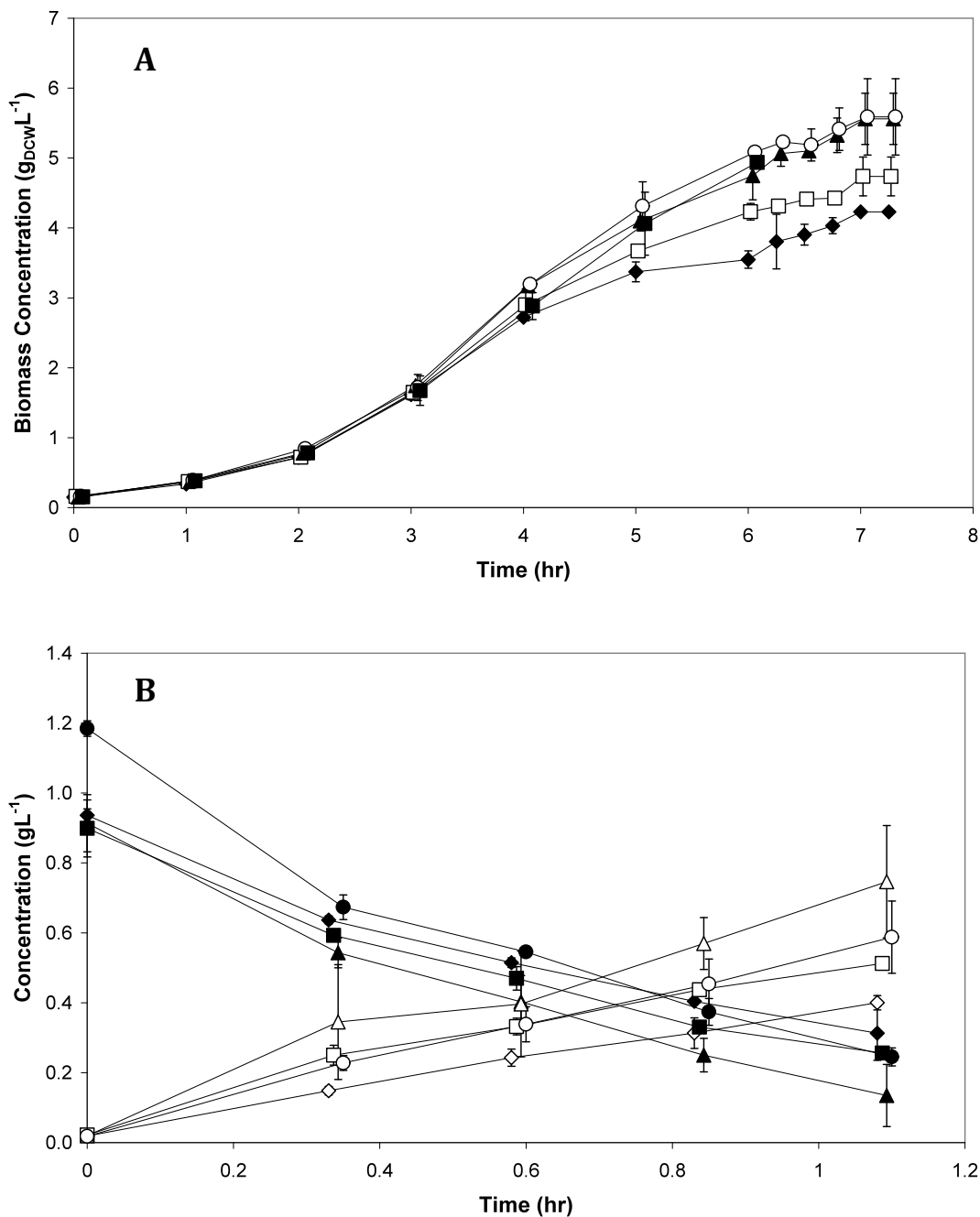


Figure 4.1 (A) Growth kinetics of *E. coli* TOP10 [pQR210] at varying fill volumes of 400 μL (■), 500 μL (○), 600 μL (▲), 800 μL (□) and 1000 μL (◆) for 6 hours of growth and **(B)** bioconversion kinetics at each of the volumes tested with 1 gL⁻¹ bicyclo[3.2.0]hept-2-en-6-one (filled symbols) to lactone product (unfilled symbols). All well volumes changed to 500 μL at 6 h time point except for 400 μL volume where well transfer was not carried out due to insufficient volume. Error bars indicate the range of measured values about the mean.

Table 4.1 Summary of calculated values for prediction of $K_{L}a$ at different well fill volumes.

Fill volume (μL)	a_i (m^{-1})	Re	Sc	Fr	Bo	$K_{L}a$ (s^{-1})
1000	64					0.085
800	80					0.107
600	107	1067	400	161	0.011	0.142
500	128					0.171
400	160					0.213

In this study, once the fill volumes were adjusted and the bioconversion initiated, oxygen was required for two competing processes, cell maintenance and bioconversion. As the fill volume reduced the rate of substrate consumption increased where at 200 μL substrate was consumed at the fastest rate. This may imply lower fill volumes enable both cell maintenance and bioconversion to occur without limitation whereas at well volumes of 400 μL and above bioconversion is compromised as oxygen is more readily used for cell maintenance. Baldwin and Woodley (2006) have also reported previously that oxygen is preferentially used for cellular maintenance and once this requirement is fulfilled oxygen will then be used for the Baeyer-Villiger oxidation.

From the mass balance results the extent of evaporation could be evaluated. A slight increase in ketone/lactone evaporation can be observed at decreasing fill volumes. This finding was not observed when a 200 μL fill volume was used as the highest specific activity was achieved at this volume.

A useful approach to control the level of oxygen transfer for both growth and bioconversion operations has been shown to be the well fill volume. The results of this work have shown that only under oxygen limited conditions a change in fill volume is required where reduced fill volumes increase $K_{L}a$ but have no further benefit on cell growth. Moreover, under non-oxygen limited conditions, further fill volume reductions could be detrimental to this particular process

where DOT above 10 % has previously be found damaging to enzyme activity (Doig et al., 2001).

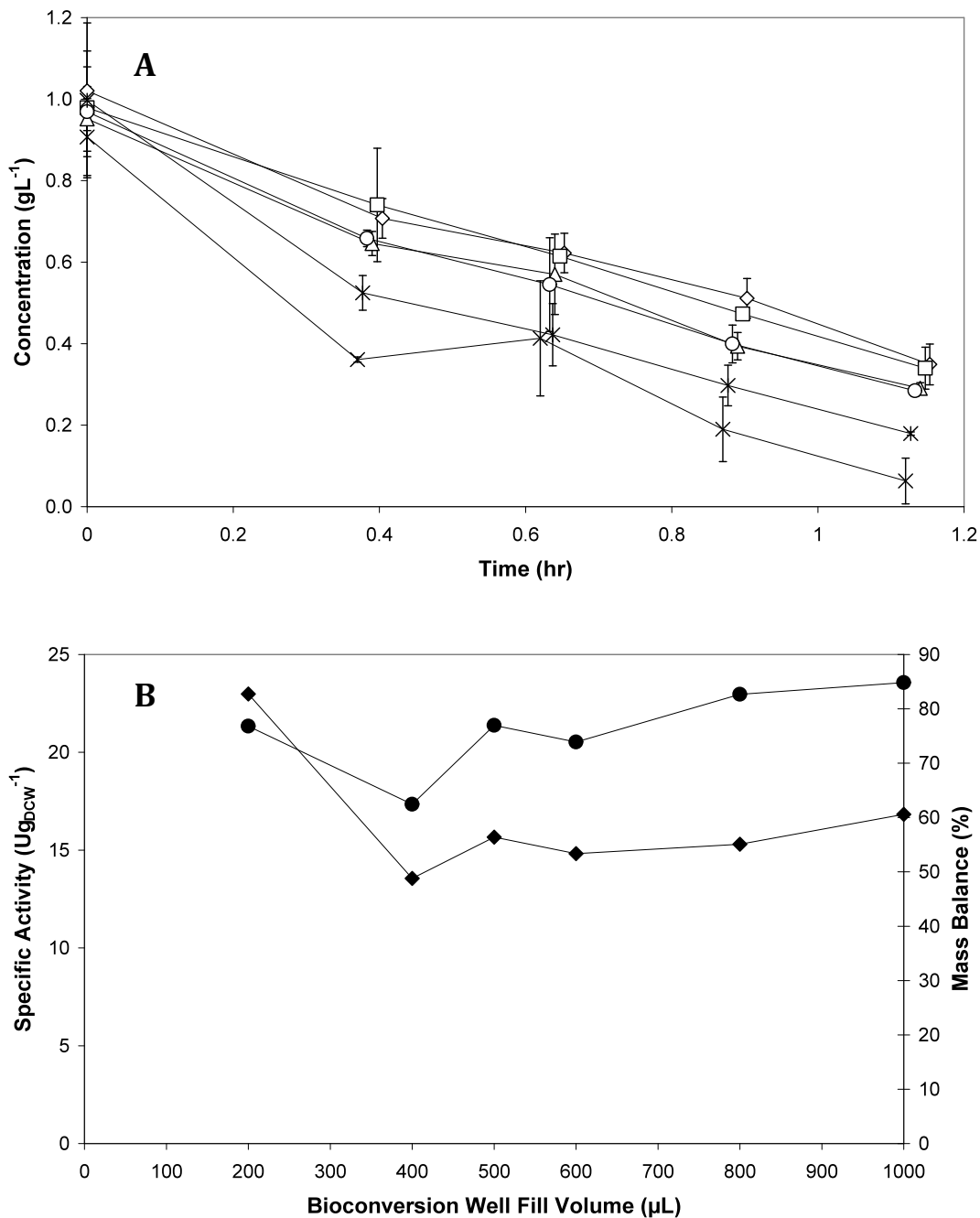


Figure 4.2 (A) Bioconversion kinetics of *E. coli* TOP10 [pQR210] with 1 gL⁻¹ bicyclo[3.2.0]hept-2-en-6-one using a well fill volume of 200 μL (×), 400 μL (*), 500 μL (○), 600 μL (△), 800 μL (□) and 1000 μL (◇). Error bars indicate the range of measured values about the mean. **(B)** Effect of bioconversion fill volume on specific activity (◆) and % mass balance (●) at different fill volumes after a 1 hour bioconversion defined as [(mass of ketone in well + mass of lactone in well) / (total ketone added to well)] * 100.

4.2.1.2 Impact of Biomass Concentration on Biocatalyst Activity

The use of whole cell systems are, in some cases, preferred to isolated enzymes because biocatalysts are believed to be in a stable environment, do not require additional cofactor regeneration systems and further costly steps (enzyme isolation and purification) can be avoided (Duetz et al., 2001). Nevertheless, maintenance of growing cells can cause challenges similar to those found in this work where oxygen limitation hindered growth above biomass concentrations of $2 \text{ g}_{\text{DCW}}\text{L}^{-1}$ and inevitably impacted biocatalysts activity.

One possible solution could be an increase in the oxygen supply, or alternatively, identifying when biocatalyst is most active. The later was therefore examined whereby the automated process was used to culture cells from 1 hour up to 6 hours as shown in Figure 4.3 A. Biomass concentrations were varied from $0.60 \text{ g}_{\text{DCW}}\text{L}^{-1}$ to $3.50 \text{ g}_{\text{DCW}}\text{L}^{-1}$ and cells were then used for a 1 hour bioconversion as shown in Figure 4.3 B. The slowest rate of product formation was observed at the lowest biomass concentration when cells were grown for just 1 hour and converted 25 % of the substrate. Full conversion of substrate to product was only achieved when cells were cultured for 3 hours to a biomass concentration of $1.85 \text{ g}_{\text{DCW}}\text{L}^{-1}$ prior to bioconversion. Below this concentration, down to $1 \text{ g}_{\text{DCW}}\text{L}^{-1}$, cells had a higher specific activity as shown in Figure 4.3 C, although the bioconversion rate was still lower due to insufficient enzyme present. However, when the biomass concentration obtained was higher than $1.85 \text{ g}_{\text{DCW}}\text{L}^{-1}$, both the specific activity and the reaction rate began to decrease. This reduction became quite significant for cells grown for 4 hours to $2.55 \text{ g}_{\text{DCW}}\text{L}^{-1}$ and above. In this case the specific activity fell to $23 \text{ U}_{\text{g}_{\text{DCW}}}^{-1}$ from the highest specific activity of $65 \text{ U}_{\text{g}_{\text{DCW}}}^{-1}$ and only 55 % of the substrate was successfully converted to product. From these results it may be concluded that the reason for a drop in specific activity at biomass concentrations above $2 \text{ g}_{\text{DCW}}\text{L}^{-1}$ is oxygen limitation as found in section 4.2.1.1.

In order to confirm the finding, samples from the automated run were removed after each designated culture time prior to bioconversion and used in a separate

NADPH consumption assay. Full details are described in section 2.6.8. Each sample was re-suspended in 50 mM TRIS-HCL buffer at pH 9, sonicated and then centrifuged to remove the cell debris. The cell lysate was incubated with 0.16 mM NADPH and, after addition of 2 mM of the natural substrate cyclohexanone, the consumption of NADPH monitored spectroscopically by following the depletion of absorbance at 340 nm. It has been found previously that the consumption of 1 μmol of NADPH is stoichiometrically linked to the oxidation of 1 μmol of cyclohexanone (Trudgill, 1975). From Figure 4.4 A a similar trend to that obtained in Figure 4.3 B can be noted where the rate at which NADPH is consumed increases with biomass concentration from 0.5 $\text{g}_{\text{DCW}}\text{L}^{-1}$ (obtained after 1 hour of culture) up to 1.6 $\text{g}_{\text{DCW}}\text{L}^{-1}$ (obtained after 3 hours of culture). At biomass concentrations higher than 1.6 $\text{g}_{\text{DCW}}\text{L}^{-1}$ the consumption rate gradually decreases. Hence, the specific activity was found to increase with biomass concentration and reduce significantly above 2 $\text{g}_{\text{DCW}}\text{L}^{-1}$, as shown in Figure 4.4 B. As the described experiments use cell-free samples, results indicate that, in addition to oxygen limitation, reduced CHMO titre at increased biomass concentrations is also responsible for the reduction in bioconversion rate. It has been reported previously that a reduction in enzyme synthesis with increased yield is a common feature of overexpressed enzymes (Micheletti et al., 2006).

The results obtained in this work suggest that extended culture reduces the level and effectiveness of the biocatalyst. It is true, as shown in section 4.2.1.1, that increasing the oxygen transfer rate can improve the bioconversion by preventing oxygen limitation conditions. However specific activities, achieved from operating at a lower biomass concentration, are significantly higher (65.0 $\text{Ug}_{\text{DCW}}^{-1}$ at 1.04 $\text{g}_{\text{DCW}}\text{L}^{-1}$) than those achieved when operating at reduced fill volumes (23.0 $\text{Ug}_{\text{DCW}}^{-1}$ at a 200 μL bioconversion fill volume). In this work, growing cells for a maximum of 3 hours ensures the biomass concentration remains below 2 $\text{g}_{\text{DCW}}\text{L}^{-1}$ and allows an adequate supply of highly active biocatalyst for bioconversion.

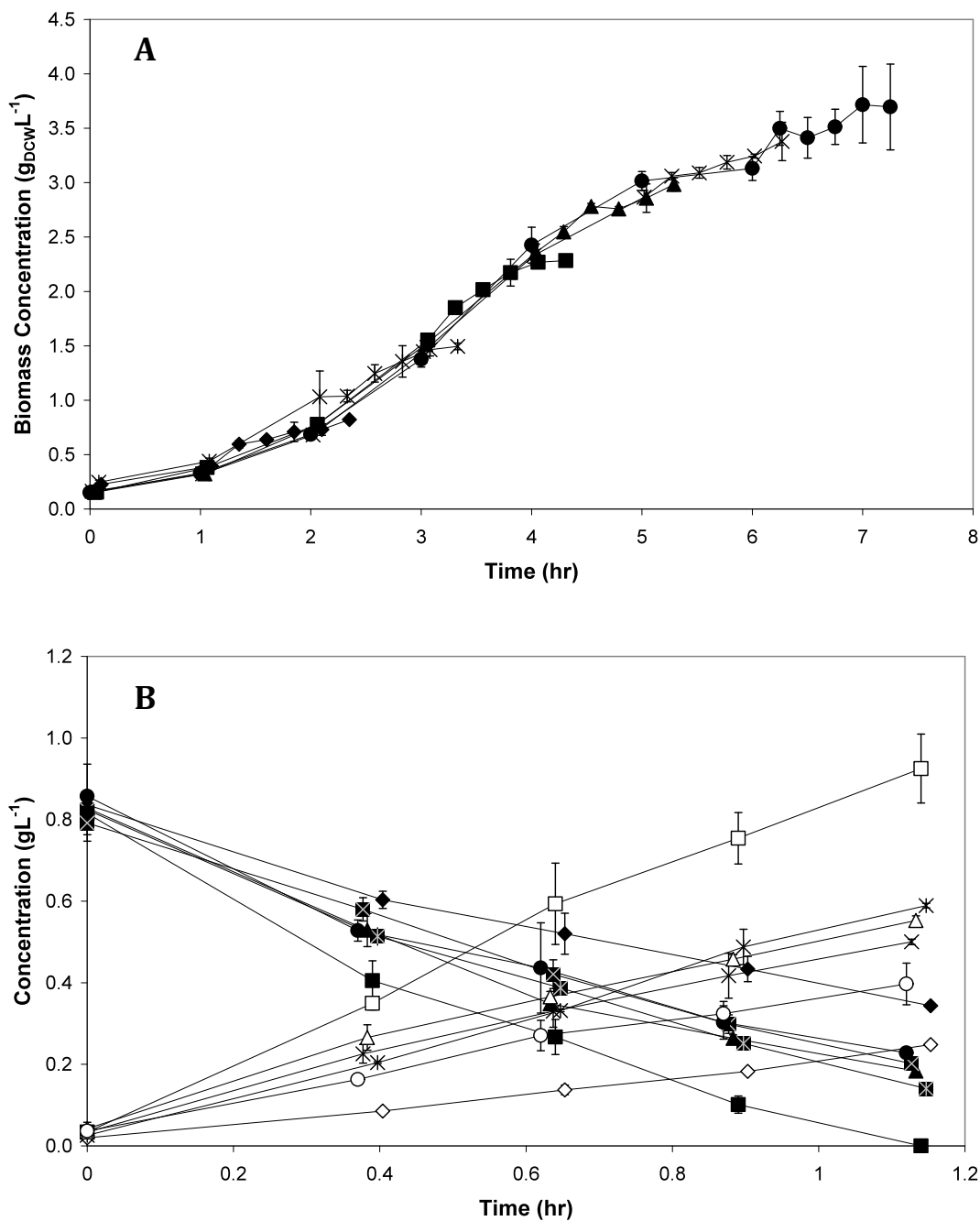


Figure 4.3 (A) Growth kinetics of *E. coli* TOP10 [pQR210] grown for a period of 1 hour (◆), 2 hours (*), 3 hours (■), 4 hours (▲), 5 hours (×) and 6 hours (●) to a biomass concentration of 0.60 g_{DCW}L⁻¹, 1.04 g_{DCW}L⁻¹, 1.85 g_{DCW}L⁻¹, 2.55 g_{DCW}L⁻¹, 3.06 g_{DCW}L⁻¹, and 3.50 g_{DCW}L⁻¹ respectively. **(B)** Bioconversion kinetics of bicyclo[3.2.0]hept-2-en-6-one (filled symbols) to lactone product (unfilled symbols) collected using cells from each culture.

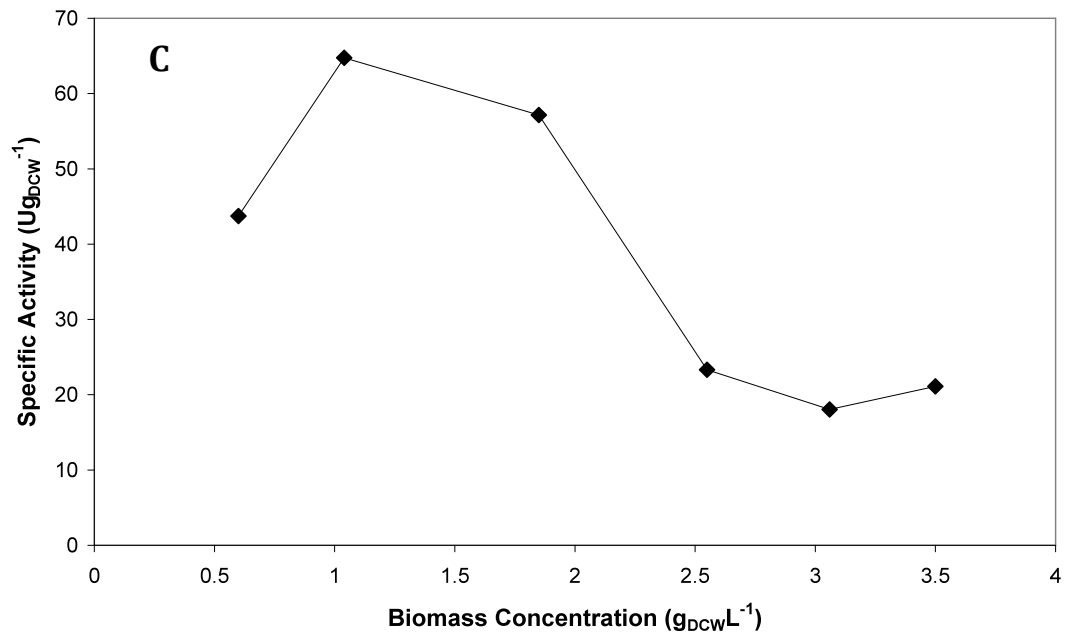


Figure 4.3 (C) Specific activity at each biomass concentration tested. Error bars indicate the range of measured values about the mean.

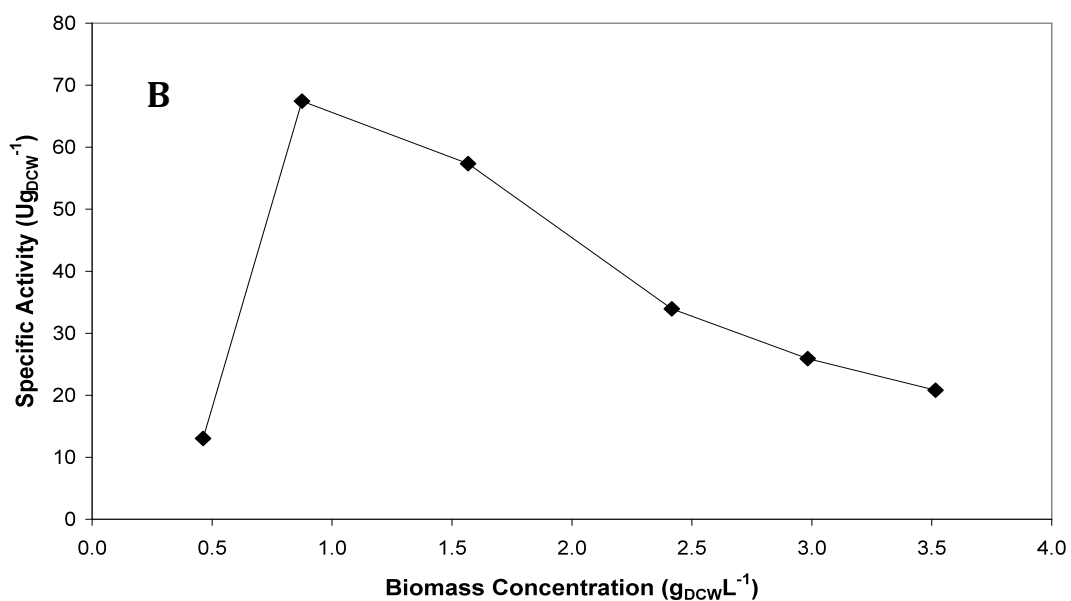
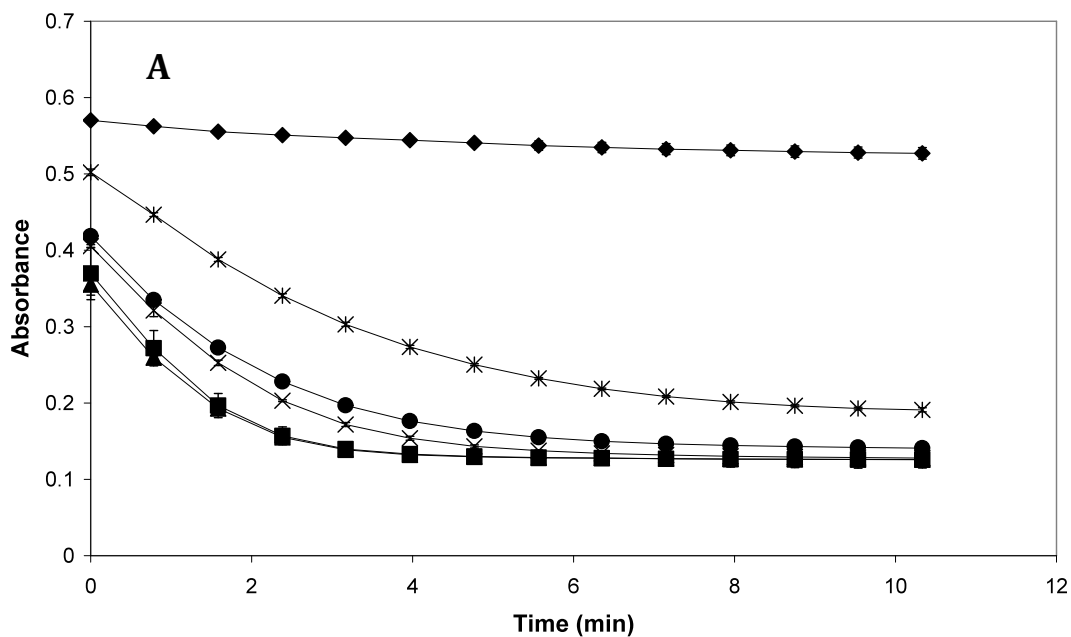


Figure 4.4 (A) The change in absorbance due to NADPH consumption by isolated CHMO samples incubated with cyclohexanone prepared as described in section 2.6.8.1 from cultures grown for 1 hour (◆), 2 hours (*), 3 hours (■), 4 hours (▲), 5 hours (×) and 6 hours (●) to a biomass concentration of $0.46 \text{ g}_{\text{DCW}}\text{L}^{-1}$, $0.88 \text{ g}_{\text{DCW}}\text{L}^{-1}$, $1.57 \text{ g}_{\text{DCW}}\text{L}^{-1}$, $2.42 \text{ g}_{\text{DCW}}\text{L}^{-1}$, $2.98 \text{ g}_{\text{DCW}}\text{L}^{-1}$, and $3.52 \text{ g}_{\text{DCW}}\text{L}^{-1}$ respectively. **(B)** Specific activity at each biomass concentration tested. Error bars indicate the range of measured values about the mean.

4.2.1.3 Evaluation of Media Composition

The amino acid source used in media formulation has been found to impact cellular growth and CHMO specific activity (Baldwin and Woodley, 2006; Berezina et al., 2007) but has not been fully investigated. Common amino acid sources found in growth media supplying nitrogen, carbon and sulfur include peptones, derived from the digestion of animal or plant proteins, and tryptones, derived from the milk protein casein. The impact of amino acid source using the automated process was investigated. *E. coli* TOP10 [pQR210] was cultured in eight media identical in composition to LB-glycerol differing only by the tryptone component which was replaced by each amino acid source listed in Table 4.2.

Table 4.2 Amino acid sources tested using automated sequence.

Amino Acid Source	Source	Preparation
Soyabean Peptone	Soyabean	Papaic digestion of Soya flour
Broadbean peptone	Broadbean	Enzymatic hydrolysis of broadbean protein concentrates
Bacteriological peptone	Animal	Enzymatic digestion of animal protein sources
Peptone	N/A	Enzymatic digest of protein
Tryptone	Casein (Milk protein)	Pancreatic digest of casein
Peptone from casein pancreatic digest	Casein (Milk protein)	Enzymatic digest of casein
Peptone from casein tryptic digest	Casein (Milk protein)	Enzymatic digest of casein
Tryptone pancreatic digest from casein	Casein (Milk protein)	Enzymatic digest of casein
Tryptone enzymatic digest from casein	Casein (Milk protein)	Enzymatic digest of casein

Figure 4.5 A shows the growth profiles obtained with each media formulation. After 3 hours of growth, once the biomass concentration reached $1.5 \text{ g}_{\text{DCW}}\text{L}^{-1}$ a

distinct change in growth with different media formulations can be observed. The reason for this finding can be attributed to a nutrient specific effect associated with each amino acid source tested. Growth was enhanced in the presence of soyabean peptone where the highest biomass concentration of $4.58 \text{ g}_{\text{DCW}}\text{L}^{-1}$ was observed, while a nutritional limitation in tryptone enzymatic digest from casein limited growth when this media formulation was used to a final biomass concentration of $2.47 \text{ g}_{\text{DCW}}\text{L}^{-1}$. Generally, casein-derived sources produced the poorest growth while those from a vegetable origin resulted in cell growth improvement. The original media formulation LB-glycerol (media composition described in section 2.2.1.1) containing tryptone constituted an exception and the growth kinetics can be found in Figure 3.8 in section 3. In line with the results presented in this work peptones derived from casein were also reported to slow *E. coli* growth by Berezina et al. (2007). Soyabean peptone has also been found to improve cell growth for *Claviceps fusiformis*, a type of fungus, and thus it can be speculated that it is beneficial for a range of organisms (Rozman et al., 1985).

The influence of each media formulation on CHMO bioconversion kinetics and specific activity, respectively, is presented in Figures 4.5 B and C. Cells cultured with tryptone pancreatic digest grew to a low biomass concentration but still produced the highest specific activity of $33.3 \text{ U}_{\text{g}_{\text{DCW}}}\text{L}^{-1}$ and product yield of 0.79 gL^{-1} . The activity was 1.7 times the activity achieved using soyabean peptone ($18.7 \text{ U}_{\text{g}_{\text{DCW}}}\text{L}^{-1}$) while the product yield (0.66 gL^{-1}) was 20 % higher. This activity was twice the activity achieved using the original LB-glycerol formulation containing tryptone ($15 \text{ U}_{\text{g}_{\text{DCW}}}\text{L}^{-1}$). The impact of biomass concentration on biocatalyst activity has already been discussed and could be contributing to the results observed in this work where slow growth prevents the onset of early oxygen limitation. In fact, specific activities over $30.0 \text{ U}_{\text{g}_{\text{DCW}}}\text{L}^{-1}$ were only measured from casein-derived amino acid sources. For media containing soyabean or broadbean biomass concentrations exceeded $3 \text{ g}_{\text{DCW}}\text{L}^{-1}$ hence the bioconversion step yielded specific activities that were less than $20 \text{ U}_{\text{g}_{\text{DCW}}}\text{L}^{-1}$.

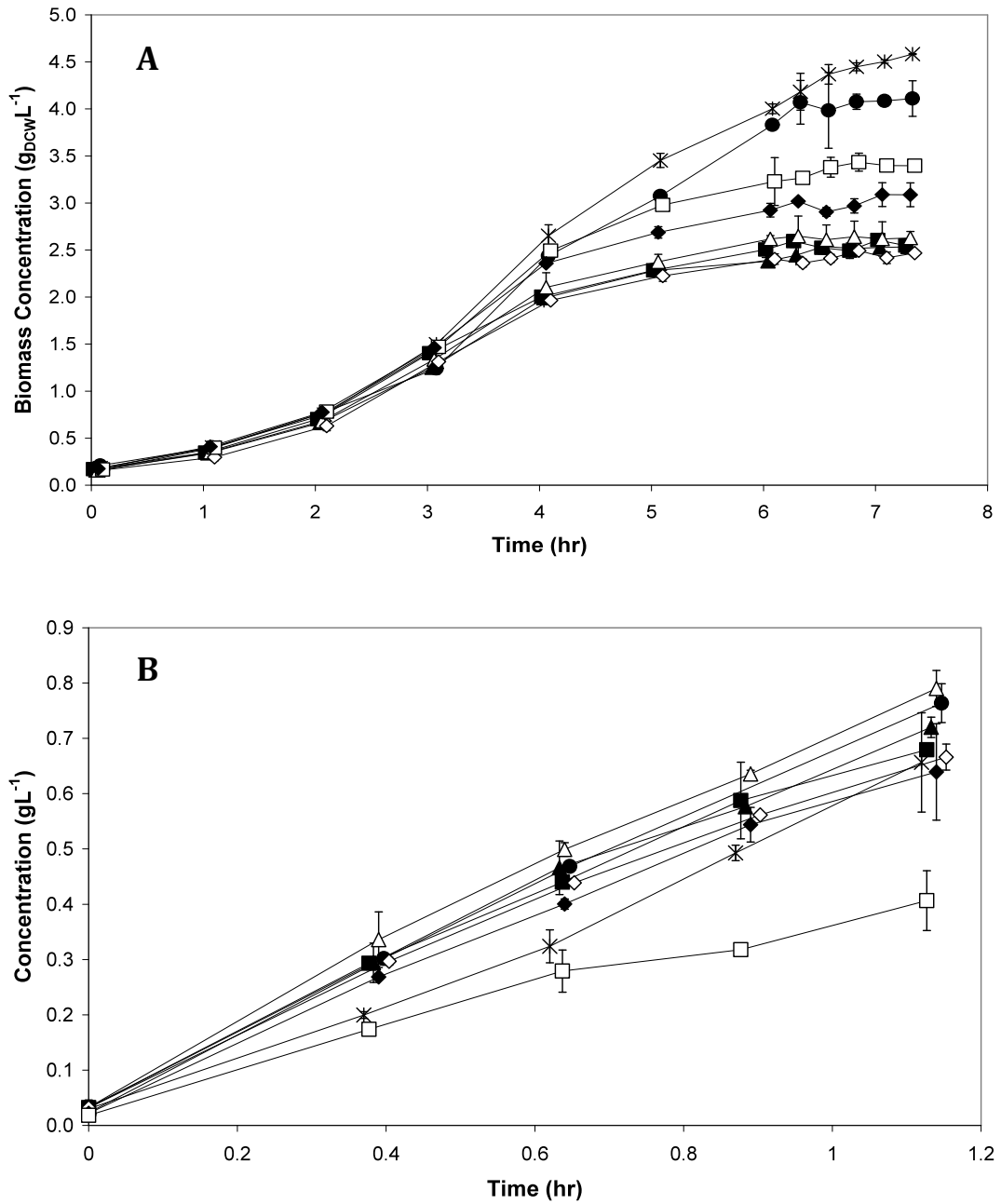


Figure 4.5 (A) Growth kinetics and **(B)** bioconversion kinetics of *E. coli* TOP10 [pQR210] grown in soyabean peptone (*), broadbean peptone (●), bacteriological peptone (◆), peptone (□), peptone from casein pancreatic digest (▲), peptone from casein tryptic digest (■), tryptone pancreatic digest from casein (△) and tryptone enzymatic digest from casein (◇) as the amino acid source. Error bars indicate the range of measured values about the mean.

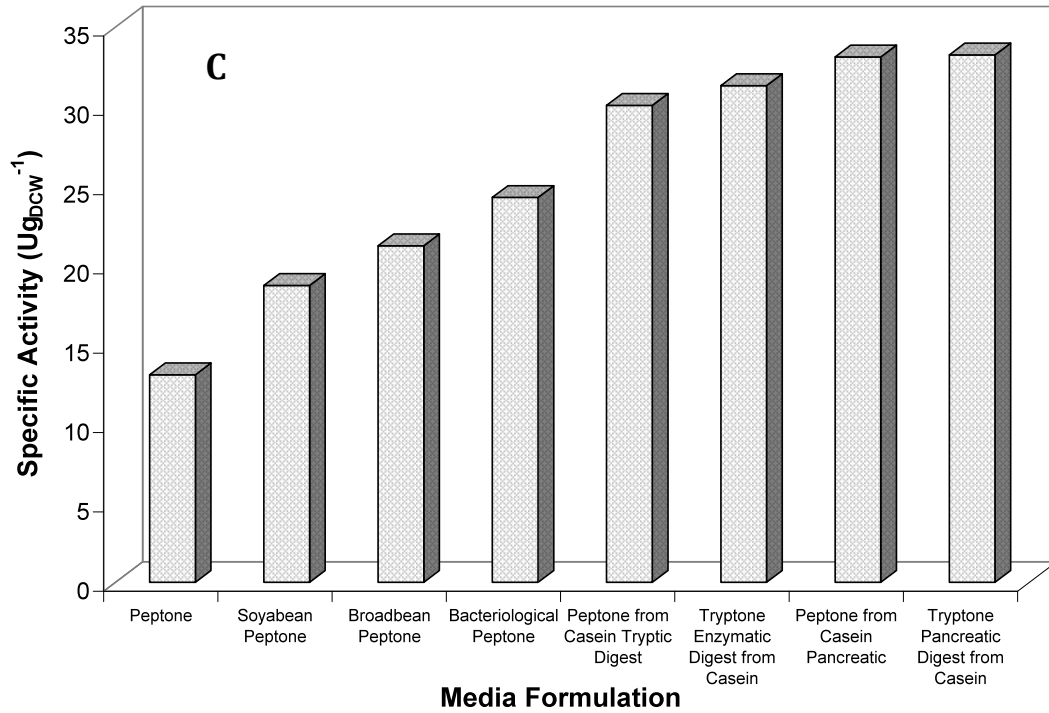


Figure 4.5 (C) Specific activities achieved using cells grown in the eight media formulations tested.

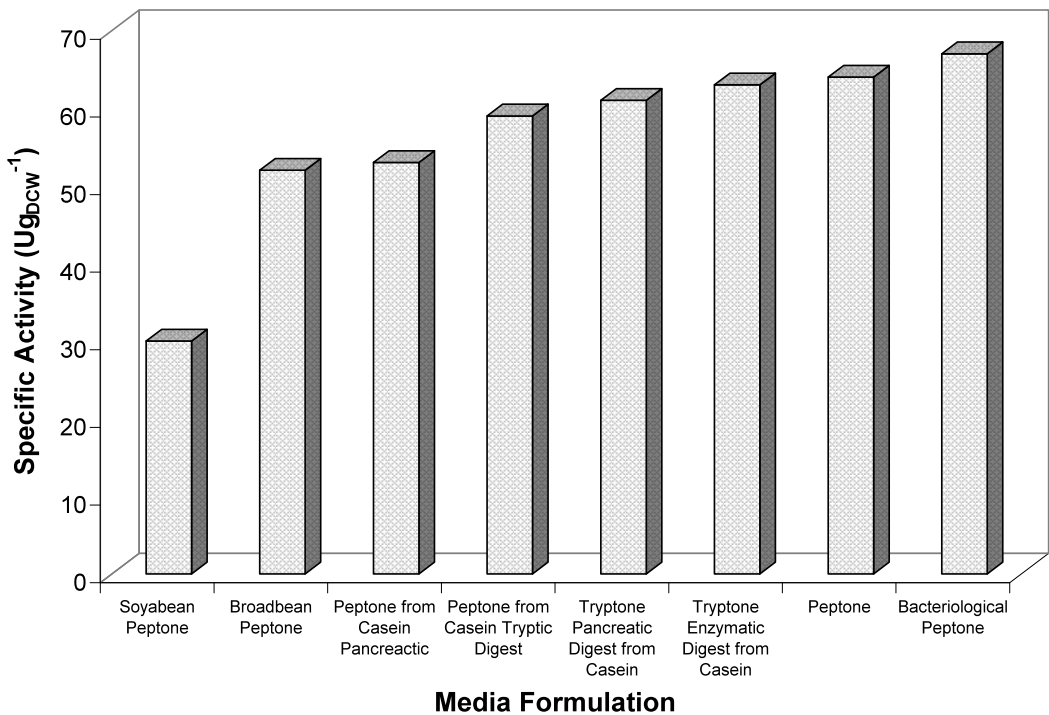


Figure 4.6 Specific activities achieved using cells grown to a similar biomass concentration in the eight media formulations tested.

In order to determine the effects of the amino acid source on bioconversion without the detrimental impact of oxygen limitation, cells were grown in each media for a period of 3 hours. At this stage of the culture (Figure 4.5 A) it is shown that there is no significant difference in biomass concentration and values remain below $2 \text{ g}_{\text{DCW}}\text{L}^{-1}$. Figure 4.6 shows the specific activity achieved in the eight media formulations when cells were grown to a similar biomass concentration. For all media tested there was an improvement in specific activity. This is expected as, by limiting the growth to a point where there is no oxygen limitation, both cell maintenance and bioconversion requirements can be easily met. The bioconversion is only limited by the level of biocatalyst and/or mass transfer to the active site. In the initial study bacteriological peptone only produced moderate specific activities but, if tested after 3 hours of growth it was the best performing media with a specific activity of $67.0 \text{ U}_{\text{g}_{\text{DCW}}}^{-1}$. Soyabean peptone at this condition is the poorest media with a specific activity of $30.0 \text{ U}_{\text{g}_{\text{DCW}}}^{-1}$, however, this is not significantly different from what was presented in Figure 4.5 C. In general, while five of the media exhibit quite similar specific activities, the source of amino acid does play a role in determining how well CHMO will perform. One potential explanation is an improvement in substrate mixing associated with the amino acid source. This could be due to the broth viscosity being affected by the choice of peptone or tryptone and thus affecting fluid hydrodynamic properties and the substrate transport to the cell.

The results presented in this section have important implications with regards to media recipe selection but they also highlight the need to study process interactions and quantify the impact of each unit operation on the final product yield. While only one media component was tested in this work the automated approach could be readily applied to test multiple formulations and media supplements for the rapid assessment of an organism's nutritional requirements. This approach could be crucial in early process design.

4.2.2 Automated Investigation of Alternative CHMO Reactions

4.2.2.1 The Impact of Substrate Concentration

In a bioprocess deterioration of whole cell biocatalysts is a potential problem due to cell damage, natural cell death and substrate inhibition/toxicity (Shitu et al., 2009). Bicyclo[3.2.0]hept-2-en-6-one has been found previously to have inhibitory effects over a threshold concentration, however, different sources report a range of upper limits of inhibition effects even when the same strain was used (Doig et al., 2003; Shitu et al., 2009). This is potentially due to differences in bioconversion conditions between the work of Shitu et al. (2009), where a greater substrate tolerance up to 2 gL^{-1} was reported before a drop in the initial product formation rate, and the work of Doig et al. (2003), who found a reduction in specific activity once the substrate concentration increased above 0.4 gL^{-1} . For this reason it was of interest to ascertain the inhibitory limit of CHMO expressed from whole cells of *E. coli* TOP10 [pQR210] in order to maintain the optimum biocatalysts efficiency for the present microscale approach.

Using the automated approach, after a 6-hour growth, bioconversion was initiated by addition of substrate concentrations ranging from 0.2 gL^{-1} to 6 gL^{-1} . Differences in substrate concentrations had a distinct effect on the growth during the 1-hour bioconversion as shown in Figure 4.7 A. At increasing substrate concentration the growth rate was found to decrease. Cellular growth continued at the lowest substrate concentration tested (0.2 gL^{-1}) reaching the highest biomass concentration of $4.42 \text{ g}_{\text{DCW}}\text{L}^{-1}$, while at the highest substrate concentration growth stopped and cell death was observed. It can therefore be concluded that bicyclo[3.2.0]hept-2-en-6-one is damaging to the cell. It was previously found, by using flow cytometry, that substrate addition caused changes in both cell physiology and metabolism (Shitu et al., 2009). In particular, a 20-fold increase in substrate concentration from 0.5 gL^{-1} up to 10 gL^{-1} resulted in over a 2-fold drop in cell viability (Shitu et al., 2009).

The effect of substrate concentration on bioconversion rates is shown in Figure 4.7 B. Full conversion of substrate to product was only achieved at substrate concentrations from 0.2 gL⁻¹ to 0.5 gL⁻¹. Above this limit the final product concentration gradually decreased and the lowest final product concentration of 0.16 gL⁻¹ was reached after a 1-hour bioconversion at the highest substrate concentration tested (6 gL⁻¹). The maximum specific activity of 25 U_{gDCW}⁻¹ was measured at a 0.5 gL⁻¹ substrate concentration and it was found to decrease to just 4 U_{gDCW}⁻¹ at 6 gL⁻¹ substrate as shown in Figure 4.7 C. Two contributory factors have been reported as being responsible for the findings observed, including the reduced cell viability and a compromised cofactor (NADPH) regeneration ability due to a poorly functioning cell membrane caused by substrate toxicity (Shitu et al., 2009). This effect is not exclusive to bicyclo[3.2.0]hept-2-en-6-one where 1,3-dithiane has also been found to have inhibitory effects (Zambianchi et al., 2004). In order to maintain the maximum productivity of the CHMO system using whole cells at the microscale the substrate concentration should be operated at 0.5 gL⁻¹.

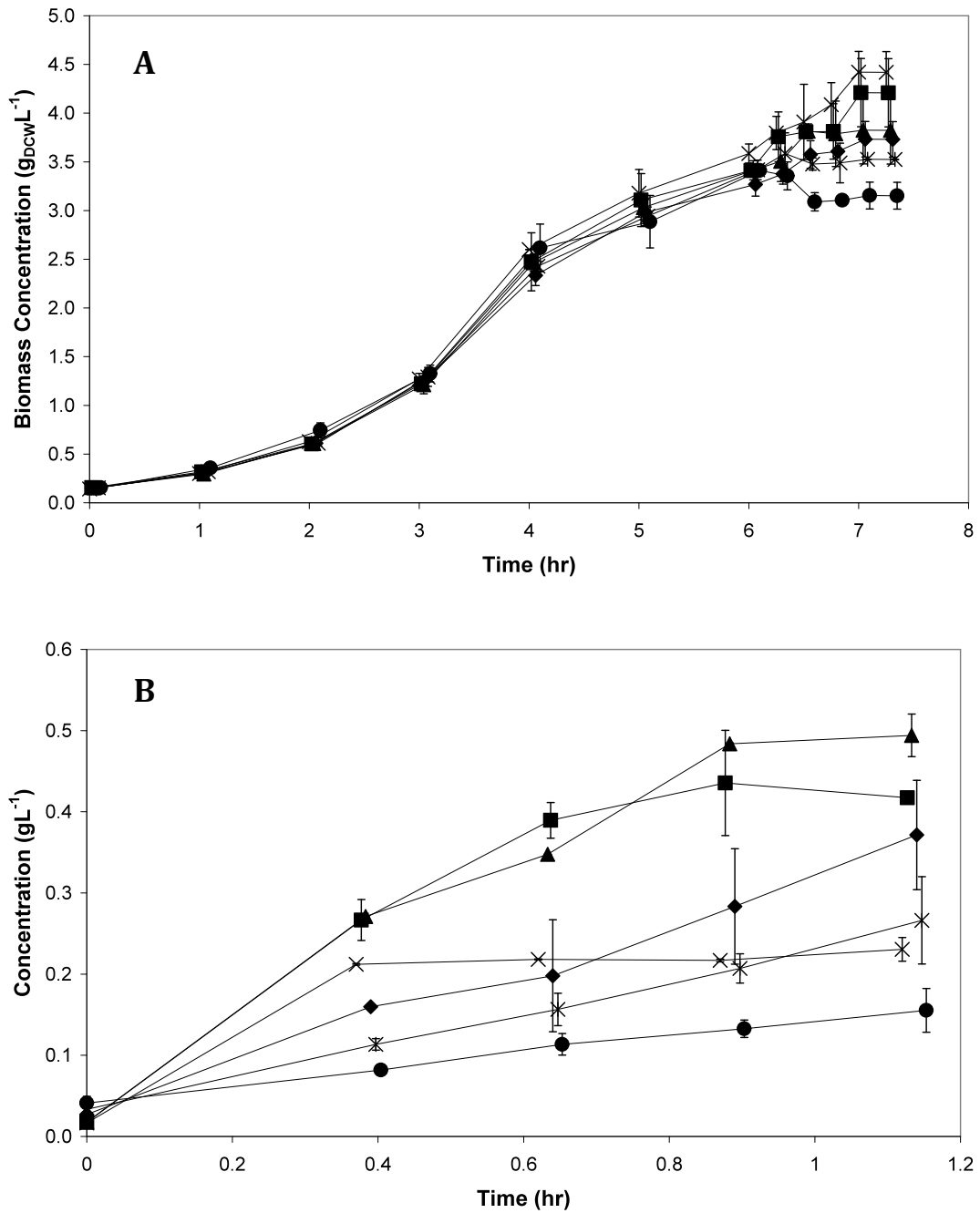


Figure 4.7 (A) Growth and (B) Bioconversion kinetics of *E. coli* TOP10 [pQR210] at varying substrate (bicyclo[3.2.0]hept-2-en-6-one) concentrations of 0.2 gL⁻¹ (×), 0.4 gL⁻¹ (■), 0.5 gL⁻¹ (▲), 2 gL⁻¹ (◆), 4 gL⁻¹ (*), and 6 gL⁻¹ (●). Substrate addition was at the 6.25 h time point. Error bars indicate the range of measured values about the mean.

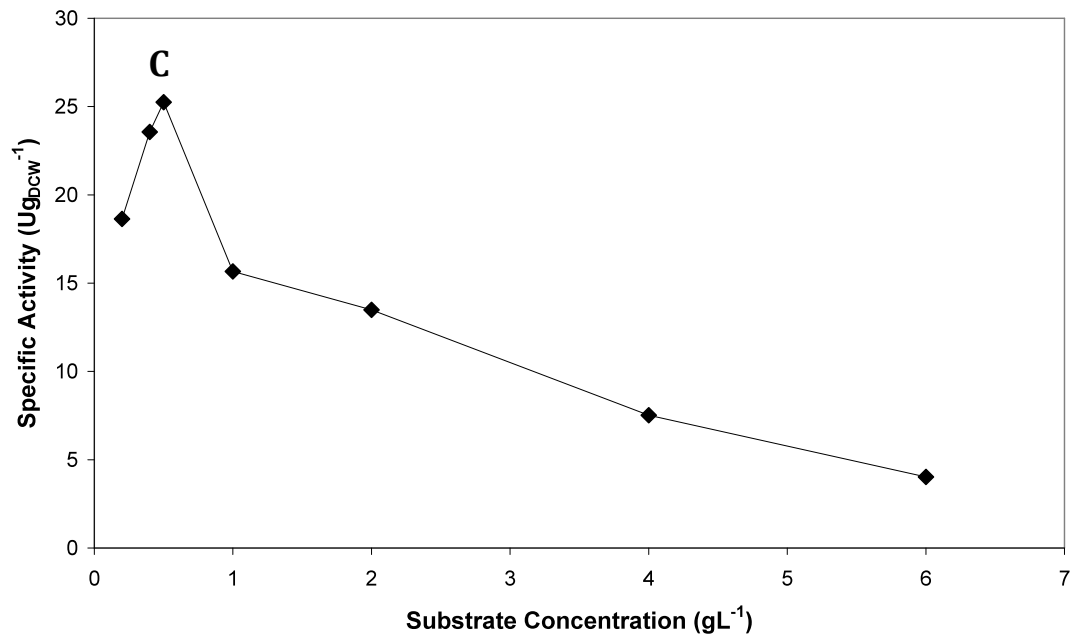
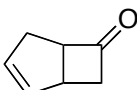
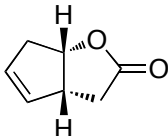
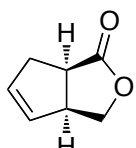
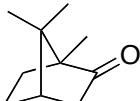
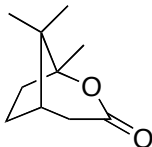
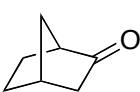
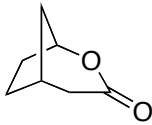
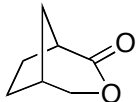


Figure 4.7 (C) The effect of substrate concentration on specific activity.

4.2.2.2 High-throughput Screening of Baeyer-Villiger Substrates

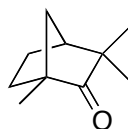
Identification of enzyme substrates is an industrially relevant application of automated microwell based techniques. Over 100 CHMO substrate candidates have previously been identified (Kamerbeek et al., 2003) and, from these, those yet to be tested with CHMO expressed by *E. coli* TOP10 [pQR210] were investigated. Chemical structures of the selected ketone substrates as well as reported or resulting products are shown in Table 4.3, together with the model substrate bicyclo[3.2.0]hept-2-en-6-one and the natural substrate cyclohexanone. These include (1*R*)-(+)-camphor, (1*R*)-(-)-fenchone and (+)-dihydrocarvone which have applications in the food and cosmetic industry as the CHMO catalysed products are flavour active lactones (Gatfield, 1997). For instance, when treated under acidic conditions in the presence of alcohol, pleasant scents are produced from (1*R*)-(+)-camphor and (1*R*)-(-)-fenchone. 2-oxabicyclo[3.2.1]octan-3-one the product of CHMO-catalysed racemic norcamphor has also been reported in the synthesis of prostaglandins (Newton and Roberts, 1980) and nucleosides (Levitt et al., 1990). Additionally cycloheptanone and cyclooctanone were also selected for testing and, while the respective products do not have direct applications, many can be further metabolised to useful products. For example the metabolism of oxocan-2-one from cycloheptanone can produce pimelic acid whose derivatives are used in the biosynthesis of amino acids (Hasegawa et al., 1982).

Table 4.3 Selected ketone substrates oxidised by CHMO.

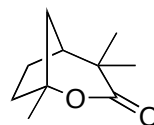
Substrate	Products*
(Doig et al., 2003)	
bicyclo[3.2.0]hept-2-en-6-one	(1 <i>S</i> ,5 <i>R</i>)-2-oxabicyclo[3.3.0]oct-6-en-3-one
	
	(1 <i>R</i> ,5 <i>S</i>)-3-oxabicyclo[3.3.0]oct-6-en-2-one
	
(Abril et al., 1989)	
(1 <i>R</i>)-(+)-camphor	2-oxabicyclo[3.2.1]1,7,7-trimethyloctan-3-one
	
(Abril et al., 1989; Mihovilovic et al., 2008)	
racemic norcamphor	2-oxabicyclo[3.2.1]octan-3-one
	
	3-oxabicyclo[3.2.1]octan-2-one
	

(Abril et al., 1989)

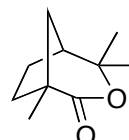
(1*R*)-(-)-fenchone



1,2-fencholide

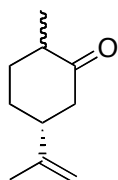


2,3-fencholide

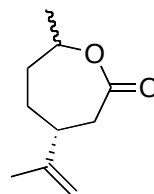


(Abril et al., 1989; Cernuchova and Mihovilovic, 2007)

(+)-(3*R*,6*RS*)-dihydrocarvone

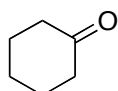


6-isopropenyl-3-methyl-2-oxacycloheptanone

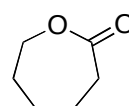


(Kim et al., 2008)

cyclohexanone

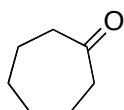


ϵ -caprolactone

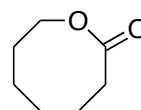


(Hasegawa et al., 1982; Kim et al., 2008)

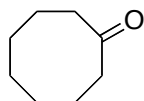
cycloheptanone



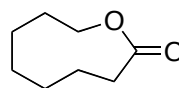
oxocan-2-one



cyclooctanone



1-oxa-2-oxo-cyclononane



* Indicates products produced only when oxidised by CHMO.

Six new substrates were tested using the automated approach and, along with cyclohexanone, the growth kinetic results are shown in Figure 4.8 A. It is important to note that substrates were only added after 6.25 hours of growth. The final biomass concentrations obtained from all substrates were similar, ranging from $4.06 \text{ g}_{\text{DCW}}\text{L}^{-1}$ in the presence of norcamphor to $3.49 \text{ g}_{\text{DCW}}\text{L}^{-1}$ in the presence of (1*R*)-fenchone. In agreement with the established protocol described in Chapter 3, the slightly higher biomass concentration obtained with cyclohexanone can be attributed to differences in inoculum and media preparations as experiments were run on different days. Due to poor water solubility the substrates (1*R*)-fenchone, (1*R*)-camphor and (+)-dihydrocarvone had to be added pre-dissolved in DMSO. To identify any possible inhibitory effects of DMSO on growth and bioconversion a control experiment was carried out. DMSO was found to have no significant effect on growth, however, it caused a reduction in enzyme specific activity. As dissolving substrates in DMSO was the only suitable method of adding them to the culture such method was adopted in this work. The progress of substrate consumption and product formation of the six new substrates and cyclohexanone are shown in Figure 4.8 B.

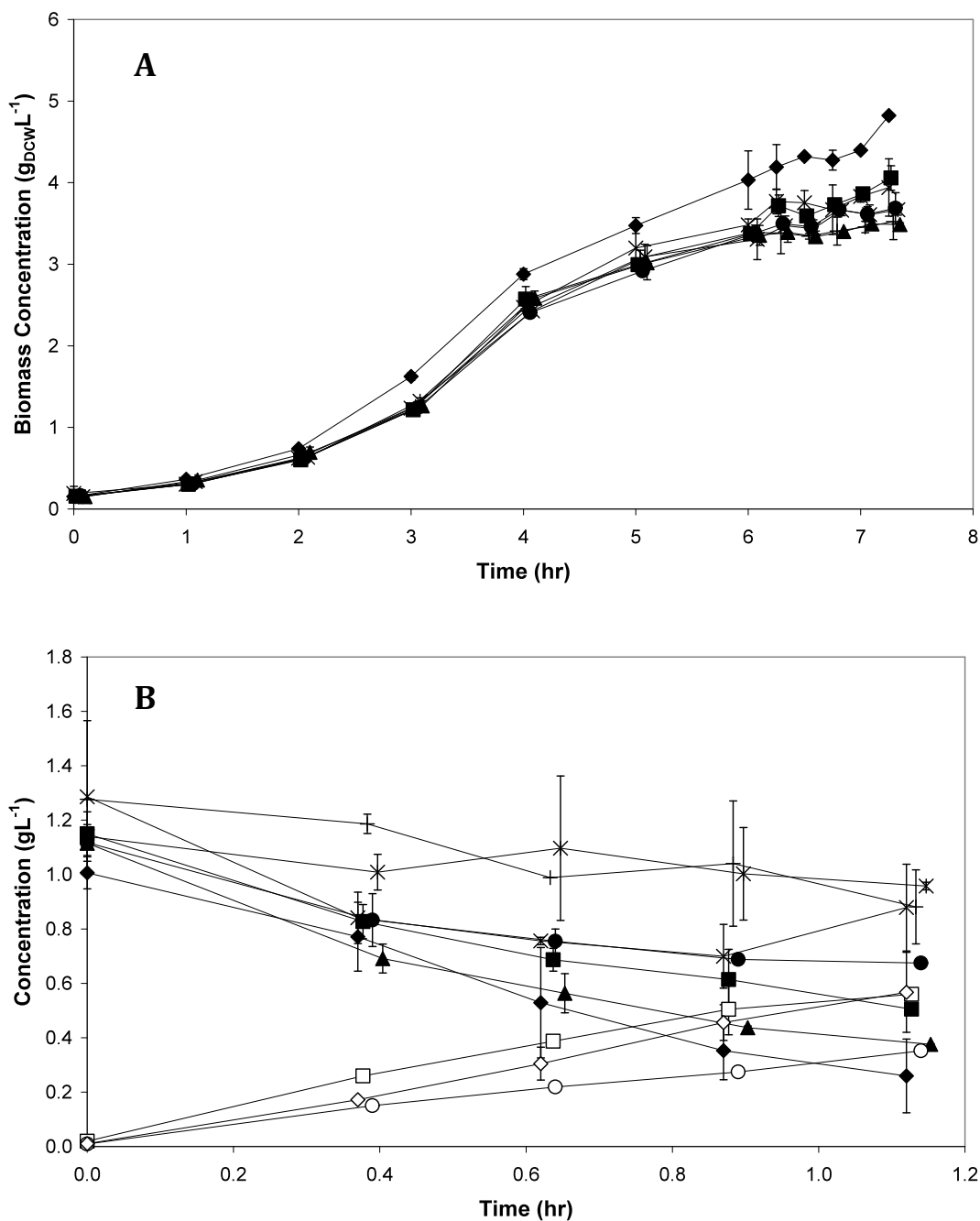


Figure 4.8 (A) Growth and (B) bioconversion kinetics of *E. coli* TOP10 [pQR210] with substrates (1*R*)-camphor (+), (1*R*)-fenchone (▲), (+)-dihydrocarvone (×), cyclooctanone (*), norcamphor (■) to 2-oxabicyclo[3.2.1]octan-3-one (□), cycloheptanone (●) to oxocan-2-one (○) and cyclohexanone (◆) to ϵ -caprolactone (◇). The results of cyclohexanone presented here were collected in a separate automated run to that of the other six substrates. Substrate addition was at the 6.25 h time point. Error bars indicate the range of measured values about the mean.

Together with the natural substrate cyclohexanone, products were only observed from norcamphor and cycloheptanone catalysis. Single product peaks were observed in the GC chromatograms for these two substrates (see appendix B for sample chromatograms) and, by analogy with previously reported work, these were identified as 2-oxabicyclo[3.2.1]octan-3-one (Abril et al., 1989) and oxocan-2-one (Hasegawa et al., 1982), respectively. The nature and chemical structures of the two products obtained were confirmed by Mass Spectroscopy (MS), Nuclear Magnetic Resonance (NMR) and Infrared Spectroscopy (IR) analysis or by correlation to a chemically synthesised standard. The final product yield achieved from microscale experiments was too low to produce sufficient material for MS and NMR analysis, thus shake flask bioconversions were conducted and the resulting products purified by flash silica chromatography and used as described in section 2.6.7.2. NMR, MS, and IR spectrums of purified norcamphor products can be found in appendix D. Mihovilovic et al. (2008) reported the formation of two regioisomers which they termed “normal” (the major isomer 2-oxabicyclo[3.2.1]octan-3-one) and “abnormal” (3-oxabicyclo[3.2.1]octan-2-one) lactones using CHMO from a range of sources including *Acinetobacter* NCIMB 9871 expressed in a recombinant *E. coli* strain. The major product detected by GC and NMR analysis in this work was confirmed to be the “normal” lactone observed by Mihovilovic et al. (2008), which was produced in a ratio of approximately 15:1 (“normal” : “abnormal”) from a 2-hour shake flask bioconversion. This is consistent with the work of Mihovilovic et al. (2008) where a ratio of 97:3 was achieved using CHMO from *Acinetobacter* NCIMB 9871. The theoretical mass of 2-oxabicyclo[3.2.1]octan-3-one and 3-oxabicyclo[3.2.1]octan-2-one ($C_7H_{10}O_2$) is $126.06808 \text{ gmol}^{-1}$ and from the MS analysis it was measured to be $126.06814 \text{ gmol}^{-1}$.

In the case of cycloheptanone, the yield of product achieved from a 100 mL initial shake flask culture was insufficient to produce a NMR spectra confirming the presence of oxocan-2-one. Therefore oxocan-2-one was chemically synthesised from pure cycloheptanone as described in section 2.6.7.1. NMR and MS spectrums of the chemically synthesised oxocan-2-one can be found in appendix D. The theoretical mass of oxocan-2-one ($C_7H_{13}O_2$) was 129.09155

g mol^{-1} and from the MS analysis it was measured to be $129.09101 \text{ g mol}^{-1}$ for the chemically synthesised product. Once a chemical standard was available, biologically synthesised oxocan-2-one could be directly compared to it. Four 100 mL shake flask bioconversions were conducted with cycloheptanone to produce a maximum final oxocan-2-one yield of 0.2 g. A sample of chemically and biologically-synthesised oxocan-2-one were mixed in ethyl acetate and run on the GC and, as shown in Figure 4.9, only one peak was visualised at 10.04 minutes, confirming both products had identical retention times. NMR, MS, and IR spectrums of purified oxocan-2-one from CHMO catalysed cycloheptanone can be found in appendix D. From the MS analysis the mass of biologically produced oxocan-2-one was measured to be $129.09101 \text{ g mol}^{-1}$. MS and proton NMR compared well to the chemically synthesised standard confirming that oxocan-2-one can be produced from cycloheptanone using CHMO.

From the initial rate of product formation specific activities of $17.3 \text{ U g}_{\text{DCW}}^{-1}$ and $10.9 \text{ U g}_{\text{DCW}}^{-1}$ were calculated from the bioconversion of norcamphor and cycloheptanone, respectively, producing final concentrations of 0.56 g L^{-1} and 0.35 g L^{-1} of the respective lactones. There are similarities in terms of yield and specific activity between the norcamphor and bicyclo[3.2.0]hept-2-en-6-one bioconversions. Additionally, norcamphor results were in good agreement with CHMO-catalysed cyclohexanone results which produced a specific activity of $16.2 \text{ U g}_{\text{DCW}}^{-1}$ and final ϵ -caprolactone yield of 0.57 g L^{-1} . Similarities between the norcamphor and cyclohexanone bioconversion data may be due to the fact that they both possess six-membered-ring ketone moieties, despite the bridged bicyclic functionality in norcamphor restricting conformational flexibility. Bicyclo[3.2.0]hept-2-en-6-one and norcamphor are able to adopt similar orientations within the active site as both are bicyclic ketones with no methyl side groups. The relationship between ketone structure and substrate specificity has been previously observed (Trower et al., 1989; Kostichka et al., 2001). Some monooxygenases can show substrate specificity for those compounds which are cyclic (Trower et al., 1989) rather than straight chained, have a specific carbon chain length or ring size (Kostichka et al., 2001), while the size of the enzyme has also been proposed to play a role in substrate specificity.

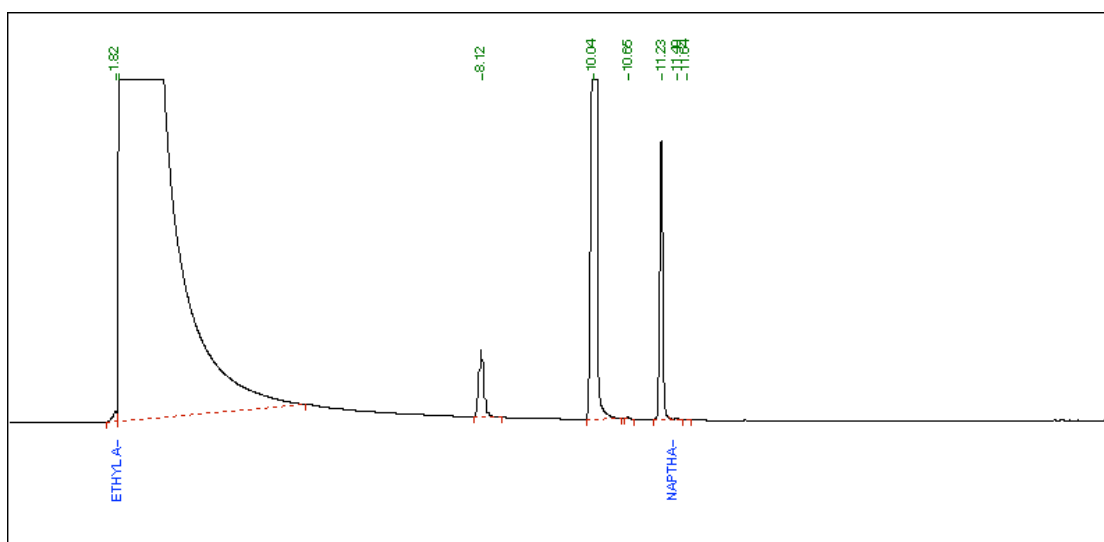


Figure 4.9 GC chromatogram of mixed chemically synthesised and biologically produced oxocan-2-one (retention time: 10.04 minutes) from cycloheptanone (retention time: 8.12 minutes). Naphthalene was used as an internal standard (retention time: 11.23 minutes).

The substrates tested in this work have been tested before using alternative microorganisms. Whole cells of the strain KUC-7N of the *Norcadia* genus completely converted 2 gL⁻¹ cycloheptanone to 1-oxa-2-oxo-cyclooctane in two days of growth (Hasegawa et al., 1982). Compared to the present study the conversion rate is eight times slower and is likely to be due to the strain and growth conditions used. From the results of this study it was assumed that full conversion would have been possible if the reaction had been operated below the inhibitory limit and the reaction conducted for just over 2 hours. This presumption was tested and will be discussed in section 4.2.3. In the case of isolated enzyme CHMO expressed from *Acinetobacter* NCIB 9871 was immobilised and reported to catalyse 11 gL⁻¹ norcamphor over a five-day period to 2-oxabicyclo[3.2.1]octan-3-one in a 81 % yield (Abril et al., 1989). The slower conversion rates achieved by Abril et al. (1989) may be due to the use of purified enzyme which requires the use of a NADPH regeneration system for cofactor recycling, the activity of immobilised enzyme and the rate of NADPH regeneration.

No products were detected from bioconversions with (1*R*)-fenchone, (1*R*)-camphor, (+)-dihydrocarvone or cyclooctanone after GC analysis. To elucidate the reason for this the percentage evaporation of each of the substrates was measured from evaporation studies and is shown in Table 4.4. It was confirmed that out of the four substrates which failed to react, all evaporated with time and only the results from (1*R*)-fenchone indicated cell metabolism. CHMO is able to bioconvert (+)-dihydrocarvone, (1*R*)-fenchone, (1*R*)-camphor and cyclooctanone as shown by Abril et al. (1989), Kim et al. (2008) and Donoghue et al. (1976). Therefore there are a number of explanations why no conversion was observed in this work. Firstly, the expression host has been reported to alter specific activity (Kim et al., 2008) and these substrates have not been previously tested with *E. coli* TOP10 [pQR210]. Many of these substrates are hydrophobic in nature, making them less accessible to the cell, and more vigorous mixing may be required to ensure effective substrate mixing (Marques et al., 2007). CHMO has been found to have the lowest affinity for cyclooctanone and successful bioconversion has also been reported when using purified enzyme (Donoghue et al., 1976). This implies mass transfer limitations may be preventing the uptake

of cyclooctanone, thus a longer reaction time or specific reaction conditions may be required to promote conversion of this substrate. One (or a combination) of these factors may be responsible for the lack of conversion observed. The setup of the automated platform means it can now be routinely used to further investigate the exact cause and identify conditions to promote product formation.

Table 4.4 Percentage evaporation of substrates tested.

Substrate	% Evaporation
Bicyclo[3.2.0]hept-2-en-6-one	10
(1 <i>R</i>)-(+)-camphor	29
Norcamphor	2
(1 <i>R</i>)-(-)-fenchone	51
(+)-dihydrocarvone	31
Cyclohexanone	6
Cycloheptanone	26
Cyclooctanone	8

Substrates were added to LB-glycerol media and shaken for 1 hour at 30 °C and 1000 rpm. Percentage Evaporation is the percentage difference between the initial concentration and final concentration of substrate after 1 hour of incubation.

The identification of new substrates for whole cell biotransformations capable of undergoing the Baeyer-Villiger oxidation represents a major finding of this work. In addition, the use of whole cells is an important advantage whereby the need for expensive NADPH regeneration systems is eliminated. The automated approach can be used to systematically evaluate a range of conditions to optimise conversion with norcamphor and cycloheptanone, identify those needed to achieve conversion from (+)-dihydrocarvone, (1*R*)-fenchone, (+)-camphor and cyclooctanone and test more reaction substrates or CHMO expressing systems.

4.2.3 Automated Process Optimisation

It has been established that the automated process can effectively collect data on a range of parameters influencing CHMO expression and on CHMO-mediated reactions. From such data the impact on growth and bioconversion stages can be rapidly assessed. The final aim in this work was to demonstrate automated process optimisation by selecting the best conditions from each of the studies with the view to scale-up those conditions. Therefore the optimised process involved a 3-hour growth at a 500 μL fill volume to ensure the highest CHMO activity and no oxygen limitation. In view of process scale-up at matched $K_{\text{L}}a$ conditions, it was also of interest to keep a constant fill volume for both growth and bioconversion steps. This is why 500 μL was preferred to 600 μL for the growth fill volume as studies have shown there is no significant difference between the results achieved at these volumes. Following growth, a 1-hour bioconversion was carried out at a bicyclo[3.2.0]hept-2-en-6-one concentration of 0.5 gL^{-1} , which is the highest working substrate concentration before inhibition effects occur and substrate toxicity become detrimental to the process. A range of amino acid formulations were tested in section 4.2.1.3. However, although bacteriological peptone was found to be the best medium, LB-glycerol was used for all other experiments and in order to avoid unexpected effects resulting from interactions between the parameters, as already observed in section 4.2.1.3, it was decided to select LB-glycerol media for the scale-up study. In Figure 4.10 A and B the results of the optimised automated run are shown alongside the original non-optimised process. By adopting the best conditions found in this study, full conversion was achieved in just over 24 minutes within a 1-hour bioconversion time and the process time was almost halved. This was not possible originally due to a combination of substrate and product inhibition. The specific CHMO activity also increased to 78.6 $\text{Ug}_{\text{DCW}}^{-1}$ from 15 $\text{Ug}_{\text{DCW}}^{-1}$ (over a 400 % increase) achieved in the original process which was due to the improvement in biocatalysts activity and prevention of oxygen limitation. Following on from the success of the automated approach for process optimisation in this study it was of interest to apply it to the substrates tested in section 4.2.2.2.

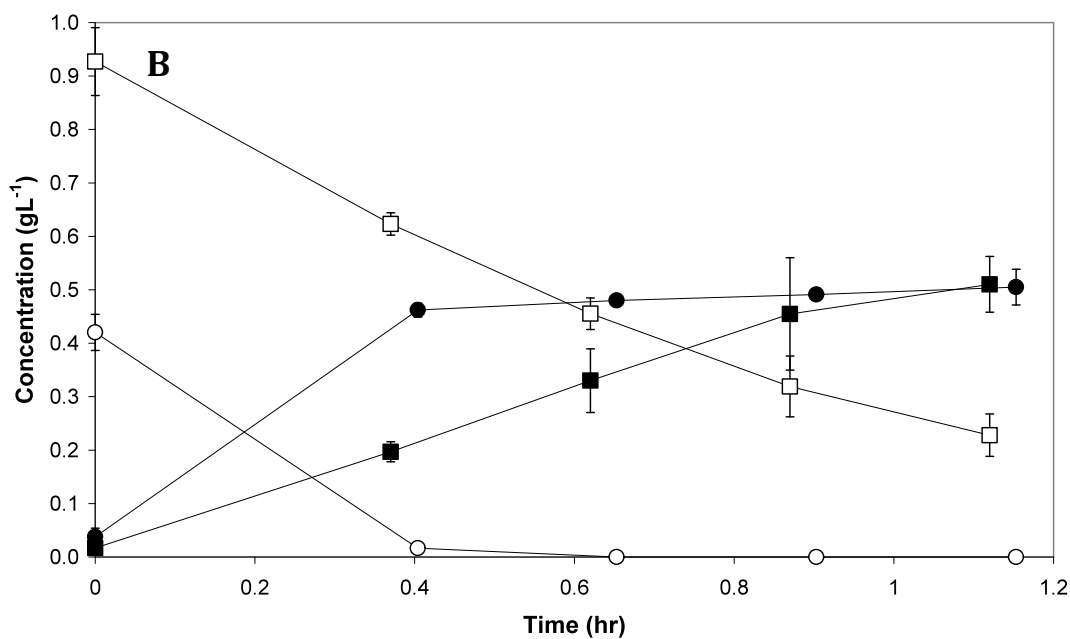
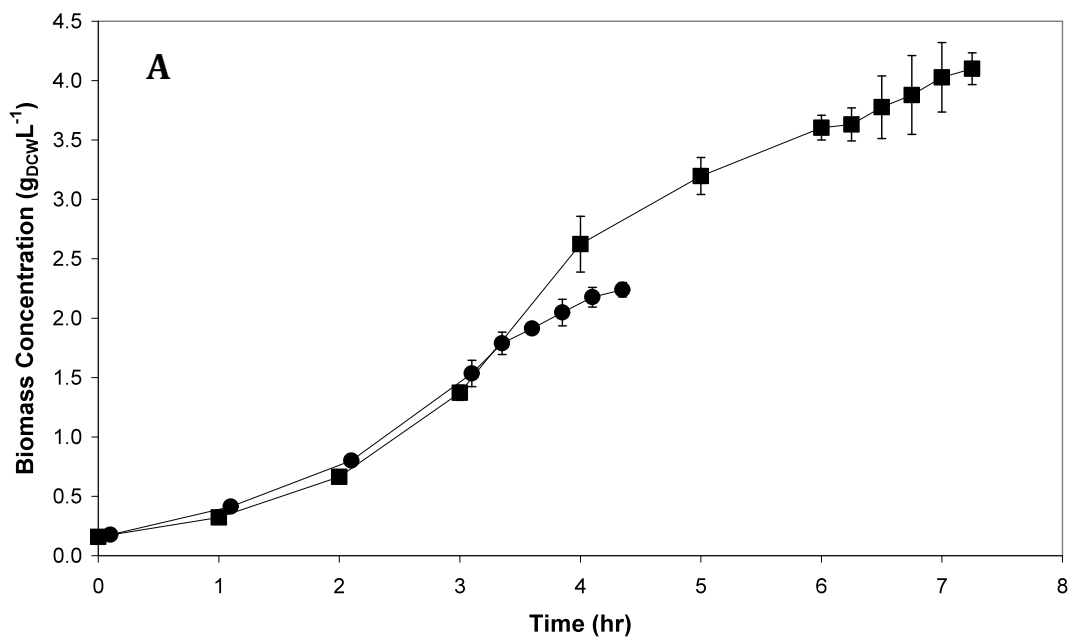


Figure 4.10 Growth (A) and bioconversion kinetics (B) of *E. coli* TOP10 [pQR210] biocatalyst catalysing bicyclo[3.2.0]hept-2-en-6-one (unfilled symbols) to lactone product (filled symbols) collected from a optimised (●) and non-optimised run (■). Error bars indicate the range of measured values about the mean.

An adapted automated run was conducted with the six new substrates. In line with the findings of section 4.2.1.2 and 4.2.2.1, the effect of a longer bioconversion time, reduced substrate concentration and increased biocatalyst activity were investigated. The growth was allowed to continue for only three hours at a fill volume of 1000 μL . The effect of substrate concentration was not tested with all the substrates, however, initial studies with cycloheptanone indicated substrate inhibition effects. For this reason after the growth stage, 0.5 gL^{-1} of each substrate was added to cells and the bioconversion conducted at a 500 μL fill volume and left to run for a total of 4 hours. This approach was adopted to determine if a longer bioconversion time would promote conversion from the unproductive substrates. In Figure 4.11 A the growth kinetics during the 3-hours of growth and 4-hours of bioconversion are shown. In the original experiment, as shown in Figure 4.8 A, only minor changes in growth were observed during the 1-hour bioconversion whereas in the newly obtained results the difference is more significant. Growth continues in the presence of both norcamphor and cycloheptanone, both of which have already been successfully bioconverted in the original study in section 4.2.2.2. In the case of all the other substrates growth was found to be reduced and the lowest biomass concentration of 2.02 $\text{g}_{\text{DCW}}\text{L}^{-1}$ is observed from (+)-dihydrocarvone. Results indicate that because the least amount of growth is observed from substrates that are not readily metabolised they may be damaging to the cell, preventing cell uptake. In fact (+)-dihydrocarvone has been shown to have antimicrobial activity and is a common constituent of mint essential oils found in herbs which were traditionally used in food preservation (Sivropoulou et al., 1995).

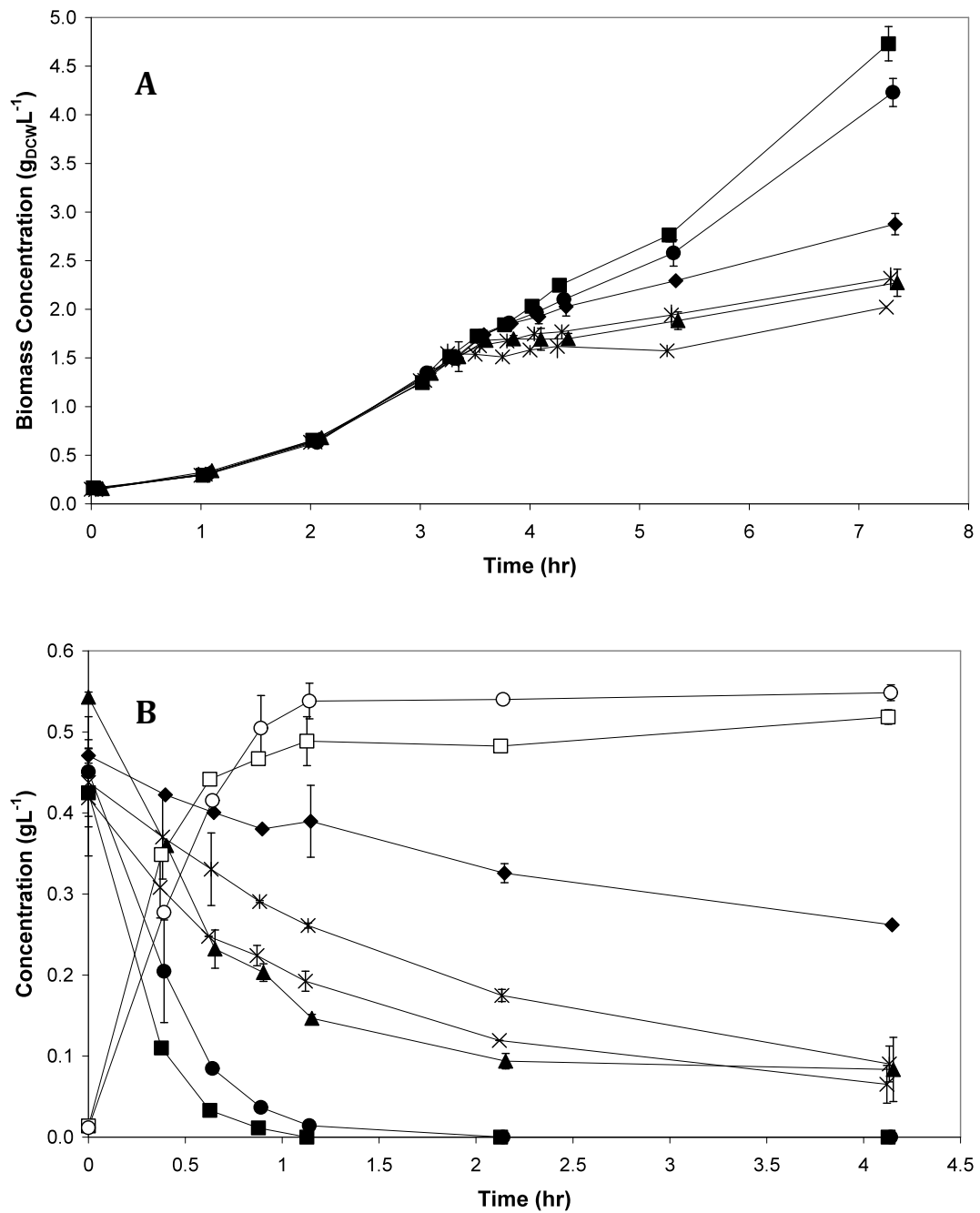


Figure 4.11 (A) Growth and (B) bioconversion kinetics of *E. coli* TOP10 [pQR210] with substrates (1R)-camphor (*), (1R)-fenchone (▲), (+)-dihydrocarvone (×), cyclooctanone (◇), norcamphor (■) to 2-oxabicyclo[3.2.1]octan-3-one (□) and cycloheptanone (●) to oxocan-2-one (○). Substrate addition was at the 3 h time point. Error bars indicate the range of measured values about the mean.

The substrate consumption and product formation profiles for each substrate are shown in Figure 4.11 B. Norcamphor and cycloheptanone were metabolised at the fastest rate and full conversion of both was observed in just over an hour. The specific activities calculated from the initial rate of 2-oxabicyclo[3.2.1]octan-3-one and oxocan-2-one formation were $61.2 \text{ U}_{\text{gDCW}}^{-1}$ and $56.0 \text{ U}_{\text{gDCW}}^{-1}$, 3 and 5 times higher respectively, if compared to activity values typical of the original process. From Figure 4.11 B results show that the improved conditions have resulted in an improvement in substrate depletion. For cyclooctanone the reduction was found to be due to evaporation. In the case of (1*R*)-camphor, (1*R*)-fenchone and (+)-dihydrocarvone after evaporation losses, results did indicate that substrate was being consumed. In fact a potential product peak was visualised in the GC chromatograms from (1*R*)-camphor as shown in Figure 4.12 at a retention time of 9.23 minutes. NMR and MS analysis would be required to determine if this was in fact a true product, namely 2-oxabicyclo[3.2.1]1,7,7-trimethyloctan-3-one as observed previously (Abril et al., 1989). However, because the level produced was very low and could not be quantified without a product standard these studies were not conducted as part of this work.

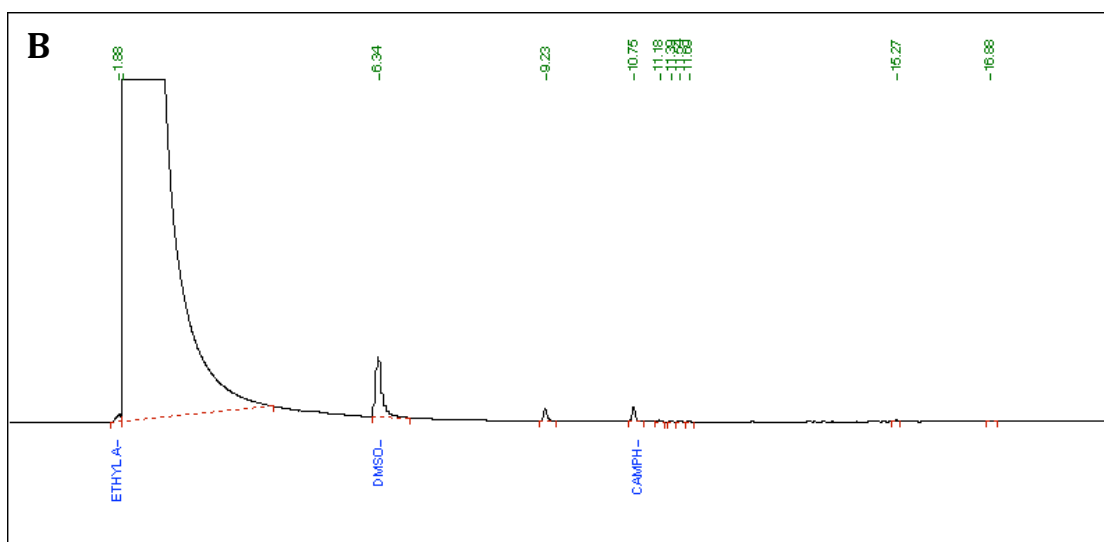
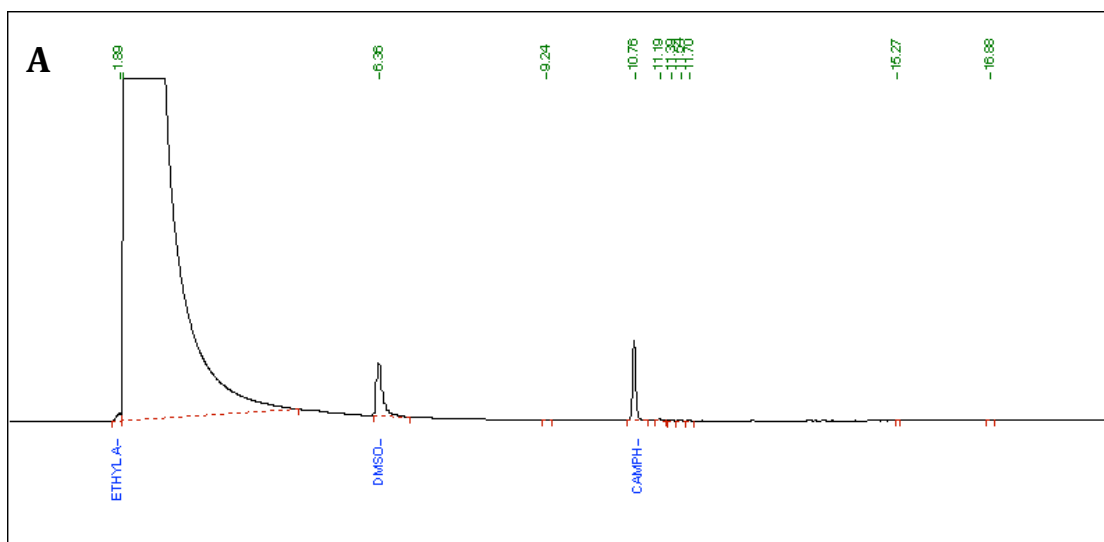


Figure 4.12 GC chromatogram of (1*R*)-camphor (retention time: 10.76 minutes) bioconversion after (A) 0 hours and (B) 4 hours. Peak at a retention time of 9.23 minutes is a potential camphor product and peak at 6.34 minutes is DMSO used to solubilise camphor during the bioconversion.

Successful bioconversion of (1*R*)-camphor, (1*R*)-fenchone, (+)-dihydrocarvone and cyclooctanone have been reported using purified enzyme. It was therefore of interest to determine if the lack of bioconversion observed in this work was due to mass transfer limitations to the cell. The NADPH consumption assay, conducted as described in section 2.6.8, was used to assess this effect. Cell samples taken from the automated run after 3 hours of growth, and prior to bioconversion, were prepared accordingly, as described in section 2.6.8.1, and the cell lysate containing CHMO was used in the assay. Due to solubility issues two experiments were done. Norcamphor, cycloheptanone and cyclooctanone were all dissolved in 50 mM TRIS-HCL pH 9 when added to the assay and compared to the natural substrate cyclohexanone also dissolved in buffer. (1*R*)-Camphor, (1*R*)-fenchone and (+)-dihydrocarvone were all poorly water soluble and were dissolved in DMSO. In order to consider any effects of DMSO, cyclohexanone was also dissolved in this solvent and used for comparison purposes. Once substrate was added to the assay, NADPH consumption was monitored and the specific activity calculated as shown in Table 4.5. Figure 4.13 shows the percentage relative activity of each substrate compared to cyclohexanone which was set to 100 %. Similar to the bioconversion results norcamphor was found to be the best substrate out of the six tested, followed by cycloheptanone in terms of specific activity. Interestingly, (1*R*)-camphor, (1*R*)-fenchone and (+)-dihydrocarvone also had specific activities which were not far from that achieved with cycloheptanone. Cyclooctanone produced the lowest observed specific activity and was just 9 % of that achieved with cyclohexanone. Product formation was not tested however a measurable specific activity implies the enzyme is oxidising the substrate and CHMO does show activity to all the substrates tested in this work. These results confirm that mass transfer limitation into the cell is a contributory factor in preventing successful metabolism as reported previously with bicyclo[3.2.0]hept-2-en-6-one (Doig et al., 2002). Furthermore, the hydrophobic nature of certain substrates is potentially hindering the reaction by preventing effective dispersion and thus contact with the cell (Marques et al., 2007).

Table 4.5 CHMO specific activity in the presence of substrates.

Substrate	Specific Activity* (U_{gDCW}⁻¹)
Dissolved in Buffer	
Cyclohexanone	22.0
Norcamphor	18.6
Cycloheptanone	14.8
Cyclooctanone	2.1
Dissolved in DMSO	
Cyclohexanone	26.1
(1 <i>R</i>)-(-)-fenchone	17
(+)-dihydrocarvone	15.6
(1 <i>R</i>)-(+)-camphor	17.7

* Calculated from CHMO assay results.

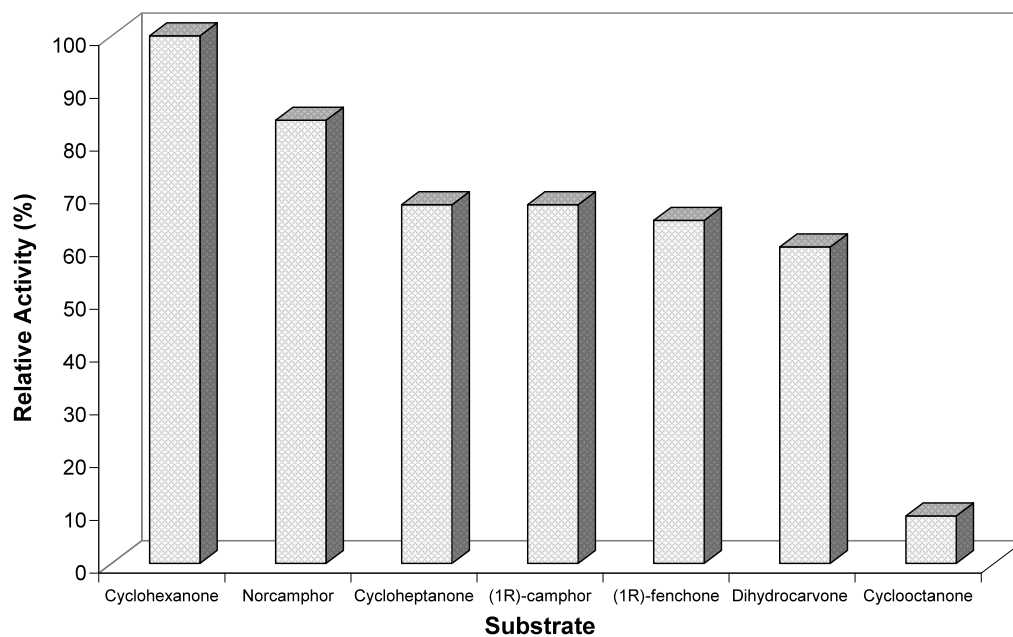


Figure 4.13 Percentage relative activity of CHMO in the presence of each substrate compared to the natural substrate cyclohexanone.

4.3 Concluding Remarks

An automated platform for rapid microscale data collection was established in Chapter 3. This was shown to generate reproducible results on multiple days with a higher degree of consistency and accuracy if compared to manual alternatives. In line with reducing production costs, a current challenge is the development of more efficient bioprocesses and the automated platform could be an ideal tool for achieving this goal. In order to demonstrate its potential, the approach was used for whole bioprocess evaluation in view of defining optimised process conditions for the CHMO-based system.

Three factors influencing CHMO specific activity were chosen including oxygen transfer rate, biomass concentration and amino acid source. The dependence on oxygen was found to be critical where, in the event of oxygen limitation, both growth and biocatalyst activity were compromised. It was found that reducing the microwell fill volume could overcome this issue due to an increase in oxygen transfer rate. However, this was only effective for volumes as low as 600 μL fill volume while further volume reductions had no significant improvement. The biomass concentration was also found to be a rate-limiting step where once 2 $\text{g}_{\text{DCW}}\text{L}^{-1}$ had been exceeded the decrease in specific activity was considerable. This was partly due to oxygen limitation, where oxygen is supplied in preference for growth rather than biocatalysis, but also because the CHMO titre was found to decrease at increasing biomass concentrations. Improving the oxygen supply was a reasonable solution, although a more effective approach was to reduce the level of growth before oxygen limitation became detrimental. Finally, the performance of CHMO was affected by the media formulation where a change in amino acid source from the original tryptone to bacteriological peptone caused a 17 % improvement in specific activity. Once the CHMO specific activity had been optimised it was important to consider a wide range of reactions. Substrate inhibition is a common problem and in this work it was found to limit the reaction above 0.5 gL^{-1} of bicyclo[3.2.0]hept-2-en-6-one due to detrimental effects on cell viability. Due to the industrial interest a clear use of the automated approach is to screen for new CHMO substrates and six substrates,

previously untested with this strain, were investigated. Two out of the six were successfully metabolised and the respective products confirmed by NMR, MS and IR analysis to be consistent with those reported from other CHMO expressing systems.

By combining the best conditions from each of the studies the ultimate aim was to develop an optimised bioprocess for eventual scale-up. The growth was carried out for 3 hours at a 500 μL fill volume to prevent the onset of oxygen limitation and to produce highly active CHMO for a bioconversion operated at 0.5 gL^{-1} , below the substrate inhibitory limit. A almost 2-fold drop in processing time and over a 5-fold increase in CHMO specific activity was observed where full conversion of bicyclo[3.2.0]hept-2-en-6-one to the respective lactones was achieved in under 25 minutes. This represented a considerable improvement on the original process. Optimised conditions were also found to benefit the conversion of norcamphor and cycloheptanone while mass transfer limitations were identified as being responsible for the lack of product formation from (1*R*)-camphor, (1*R*)-fenchone, (+)-dihydrocarvone and cyclooctanone.

In conclusion, automated microscale approaches have proved effective for media recipe selection, substrate specificity studies and most importantly process optimisation. However, the development of novel oxidative systems presents an important challenge where there is limited research and would clearly benefit from rapid evaluation. In Chapter 5 the automated platform will be applied to two novel cytochrome P450 biocatalysts illustrating its potential for a range of systems. Chapter 6 includes results focussing on the scale-up of the optimised microscale work presented in this chapter.

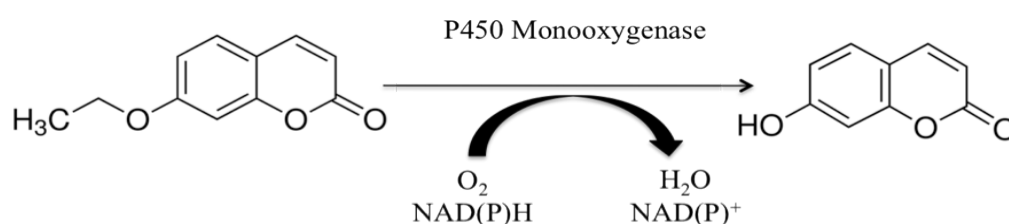
5 Microscale Process Development of Novel Cytochrome P450 Biocatalysts

5.1 Introduction

The ability to rapidly generate data on whole bioprocesses using automated microscale technologies was presented in Chapters 3 to 4. The approach could be applied to a range of biocatalytic systems to allow quicker identification of optimised process conditions, making them more applicable for large-scale development. One group of enzymes that could particularly benefit from the approach are cytochrome P450s.

Cytochrome P450s are a superfamily of haemoprotein monooxygenases which have been studied for over 50 years due to their vast reaction ability which includes hydroxylations, isomerisations, dehydrogenations and carbon-carbon bond cleavage (Klingenberg, 1958; Garfinkel, 1958; Werck-Reichhart and Feyereisen, 2000). However, as discussed in section 1.2.3.1.2.1, exploiting the reaction ability can be a challenging task. Specific P450s biocatalysts are membrane bound and the requirement for complex electron transport systems makes heterologous expression difficult. In addition, isolated enzymes require efficient NAD(P)H regeneration systems. The use of whole cell systems can overcome some of these issues while physiological problems concerning substrate uptake, product/substrate toxicity, product degradation and poor substrate solubility may arise (van Beilen et al., 2003). The original expression system may not be the optimal producer of the target P450 biocatalyst. For example, mammalian cytochrome P450s can metabolise drugs (Parikh et al., 1997), steroids (Williams et al., 2000) and herbicides (Inui et al., 2000), however their expression yields can be limited (Fischer et al., 1992; Jansson et al., 2000). The discovery of novel self-sufficient P450s which have been cloned into *E. coli* expression systems makes them attractive for further research (Roberts et al., 2002; Liu et al., 2006; Zhang et al., 2010). Hussain and Ward (2003 b) developed two such systems where the cytochrome P450 and adjacent ferredoxin from *Streptomyces griseolus* were combined with the ferredoxin reductase from

Streptomyces coelicolor and successfully expressed in *E. coli*. It was found that the inclusion of the ferredoxin reductase along with the choice of *E. coli* host strain enabled high level expression of the two P450s, cytochrome P450SU1 and cytochrome P450SU2. In addition, both were found to catalyse the O-dealkylation of 7-ethoxycoumarin, a xenobiotic compound, to the fluorescent 7-hydroxycoumarin as shown in reaction scheme 5.1. There are a number of beneficial reactions associated with dealkylations including drug metabolism (La et al., 1955). In particular, 7-ethoxycoumarin has typically been used to monitor P450 activity in hepatic and extrahepatic tissues (Phillips and Shephard, 2006). In the original host strain P450SU1 and P450SU2 were able to metabolise sulfonylurea herbicides to compounds less poisonous to plants, thus highlighting them as potential bioremediation biocatalysts (O'keefe et al., 1991).



Reaction Scheme 5.1 P450 catalysed O-dealkylation of 7-ethoxycoumarin to 7-hydroxycoumarin.

The number of industrial processes utilising P450s is limited. Traditionally, P450 monooxygenases have been utilised in toxicity determination or to elucidate the effects of xenobiotic compounds *in vivo* (Urlacher and Sabine, 2006). Commercial examples include the biotransformation of the steroid hydrocortisone produced at 100 ton/yr by Bayer Pharmaceuticals using P450 monooxygenases to conduct 11 β -hydroxylation (Sonomoto et al., 1983), the production of cortisone from progesterone by Pfizer (Peterson, 1952), and production of Pravastatin by microbial oxidation of compactin by Bristol-Myers Squibb Company. Considering the P450 reaction repertoire as addressed in section 1.2.3.1.2.1 there is great potential for increased industrial uptake. Future applications could include antibiotic synthesis (Andersen et al., 1993), anticancer drug synthesis (Jennewein et al., 2005), bioremediation (Guengerich, 1995;

Kellner et al., 1997), polymer (Picataggio et al., 1992) and flavour (Wust and Croteau, 2002) production where P450s have been found to catalyse useful steps in these areas. Further research in this area is needed to develop strategies aimed at optimising yields and overcoming the shortcomings.

The aim of this chapter is to adapt the established automated approach developed in Chapter 3 for the investigation of cytochrome P450s. In this study the recombinant strains developed by Hussain and Ward (2003 b), *E. coli* BL21 Star (DE3)pLysS [pQR367] (referred to here on as *E. coli* [pQR367]) expressing P450SU1 its ferredoxin from *Streptomyces griseolus* and the ferredoxin reductase SCF15a from *Streptomyces coelicolor*, and *E. coli* BL21 Star (DE3)pLysS [pQR368] (referred to here on as *E. coli* [pQR368]) expressing P450SU2 its ferredoxin from *Streptomyces griseolus* and the ferredoxin reductase SCF15a from *Streptomyces coelicolor*, were used. The bioconversion of 7-ethoxycoumarin was only touched upon in previous work. Hence, strategies to improve this bioconversion were employed to demonstrate the utility of the adapted automated process. The experimental approach and methodology used in this work have been described in Chapter 3. The results are presented and discussed in section 5.2 and the chapter closes with a summary of findings in section 5.3.

5.2 Results and Discussion

5.2.1 Production of Cytochrome P450SU1 and P450SU2

Prior to the development of microscale cultivations it was important to test the growth and bioconversion of *E. coli* [pQR367] and *E. coli* [pQR368] following the established culture and expression protocols reported by Hussain and Ward (2003 b). The presence of the correct P450 and ferredoxin reductase genes were confirmed by sequence analysis (as described in section 2.2.2.3) after transformation of the plasmid into *E. coli* BL21 Star (DE3)pLysS for both strains. Figure 5.1 shows an example of the shake flask growth kinetics results of induced and non-induced cultures of *E. coli* [pQR367] and *E. coli* [pQR368]

along with an induced negative control culture of *E. coli* BL21 Star (DE3)pLysS. 100 mL Terrific broth (TB) was inoculated with 1 % inoculum (as described in section 2.2.2.4) in 500 mL shake flasks and incubated at 250 rpm and 37 °C. Similar growth profiles were observed from all cultures, characterised by a one hour lag phase potentially due to different inoculum and culture medium (LB and TB, respectively). Cells were grown until an OD of 0.6-0.8 (typically after 2.7-3 hours of growth). Specific growth rates for induced cultures of 1.18 h⁻¹, 1.21 h⁻¹ and 1.22 h⁻¹ were calculated for *E. coli* [pQR367], *E. coli* [pQR368] and *E. coli* BL21 Star (DE3)pLysS, respectively.

At an OD of 0.6-0.8 conditions were changed to promote expression. Cytochrome P450s have a haem prosthetic group, which is the essential active-oxygen carrying group of these P450s, and haem precursors such as δ -aminolevulinic acid (ALA) and ferric chloride (FeCl₃) supplementation have been found to increase the level of spectrally measurable P450 (Imai and Sato, 1993; Jansson et al., 2000; Hussain and Ward, 2003 b). Hence, both ALA and FeCl₃ were added to the culture 20 minutes prior to IPTG induction of the respective P450s and incubated at 25 °C and 180 rpm for the remainder of the culture. This change in culture condition is responsible for the slight reduction in growth present in Figure 5.1 from the third hour of growth onwards. The time of IPTG addition was previously found to have no effect on biocatalyst expression (Hussain and Ward, 2003 b). However, the optimal expression of P450SU2 was measured between 24 and 35 hours of induction (Hussain and Ward, 2003 b) therefore in the present work cultures were run for a total of 30 hours. A significant decrease in growth is observed after 25 hours of culture due to a increased dead cell population. Cells were harvested after 30 hours of growth where induced cultures of *E. coli* [pQR367], *E. coli* [pQR368] and *E. coli* BL21 Star (DE3)pLysS reached a final biomass concentration of 3.16 g_{DCW}L⁻¹, 3.41 g_{DCW}L⁻¹ and 2.91 g_{DCW}L⁻¹, respectively. Figure 5.1 shows little difference between induced and non-induced culture indicating that enzymatic expression has no effect on the growth of these strains.

In order to quantify the level of active P450 expression, samples were analysed spectroscopically using a carbon monoxide (CO) based assay as described in

section 2.6.9 and the amount of active P450SU1 and P450SU2 was calculated from the CO difference spectrums shown in Figure 5.2 A and B respectively. Cytochrome P450s can exist in two states, an active high spin state termed 'cytochrome P450' and an inactive low spin state termed 'cytochrome P420'. This terminology originates from the presence of soret peaks at wavelengths of 450 nm and 420 nm in CO difference spectra as described by Omura and Sato (1964). Both forms can be observed in the spectrum for P450SU1 with 25 ± 1.1 nmol of active P450 per gram of soluble protein (nmol g^{-1}) whereas only the active form is visible in the P450SU2 spectrum with 391 ± 1.6 nmol of active P450 per gram of soluble protein. Values achieved in this work are lower than those reported previously and are summarised in Table 5.1, however this may be attributed to differences in sample harvest time. While this effect was observed on P450SU2 expression, P450SU1 expression was found to be less than half the value achieved previously. P450SU1 is the less productive biocatalysts and, as shown in Figure 5.2 A, susceptible to forming the inactive P420. Hence, a longer expression time was considered to be beneficial for this biocatalyst.

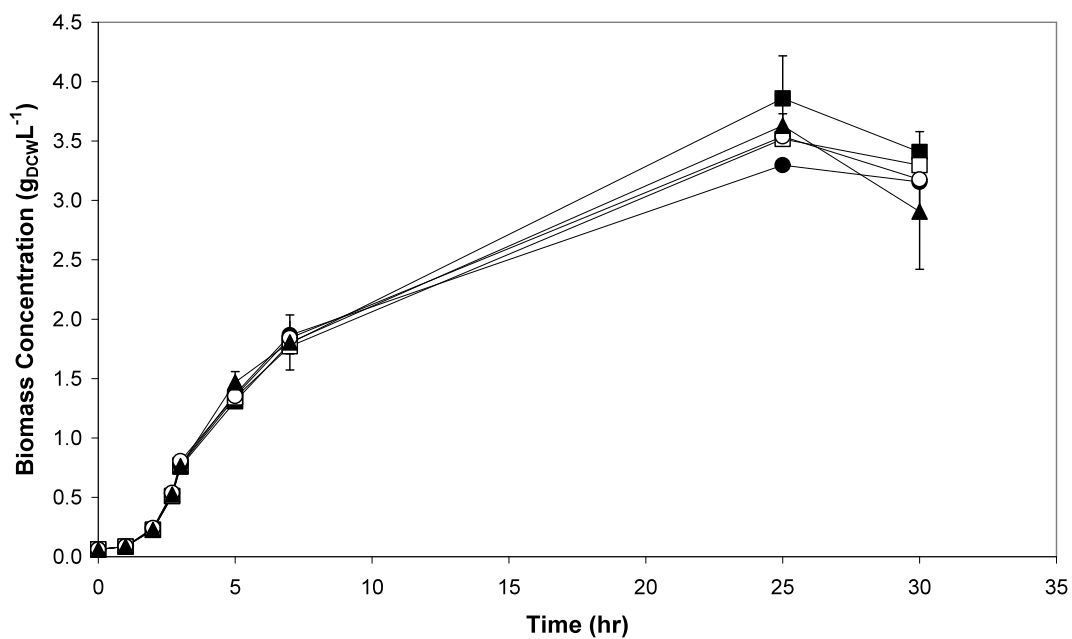


Figure 5.1 Growth kinetics of *E. coli* [pQR367] (●), *E. coli* [pQR368] (■) and *E. coli* BL21 Star (DE3)pLysS (control) (▲) during a induced (closed symbol) and non-induced (open symbol) shake flask culture catalysing 7-ethoxycoumarin to 7-hydroxycoumarin. Error bars indicate the range of measured values about the mean.

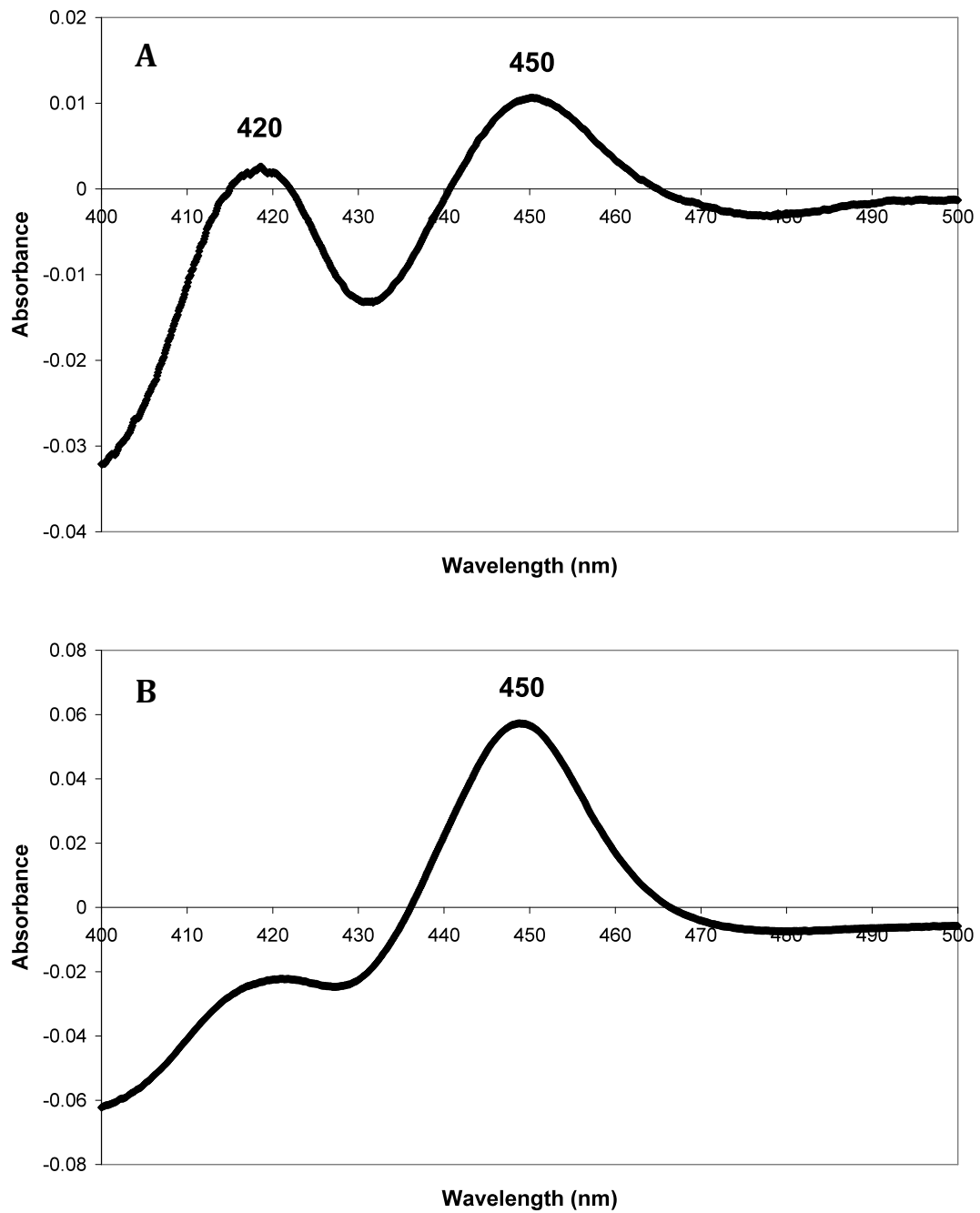


Figure 5.2 Representative CO difference spectra of **(A)** P450SU1 expressed in *E. coli* [pQR367] and **(B)** P450SU2 expressed in *E. coli* [pQR368]. Samples were from cultures where no 7-ethoxycoumarin was added.

Table 5.1 Summary of P450 expression from shake flask cultures.

Strain	P450 Expression (nmol g ⁻¹)
pQR368	391 ± 1.6
pQR367	25 ± 1.1
pQR368*	413
pQR367*	55

* Represents results from Hussain and Ward, (2003 b).

The bioconversion was initiated by the addition of 1 mM of 7-ethoxycoumarin to cultures 10 minutes after induction. In Figure 5.1 7-ethoxycoumarin was present in all cultures from the third hour of growth onwards. TLC analysis of culture samples (prepared as described in section 2.6.6) was used as a quick test for the production of 7-hydroxycoumarin, more commonly known as Umbelliferone, as shown in Figure 5.3 prior to HPLC. Using standards of 7-hydroxycoumarin (column P), product spots were only detected in induced cultures. TLC sheets were stained with permanganate for better visualisation of the substrate which, as shown in Figure 5.3 B, was present in all samples. HPLC analysis (as described in section 2.6.5) was used to quantify the final product yield after 30 hours of culture as shown in Figure 5.4 (sample HPLC chromatograms of shake flask bioconversions can be found in appendix B). No product was detected in non-induced or control cultures in agreement with results obtained from TLC. A total of 1.6 mgL⁻¹ and 4.3 mgL⁻¹ was produced from induced cultures of *E. coli* [pQR367] and *E. coli* [pQR368] respectively.

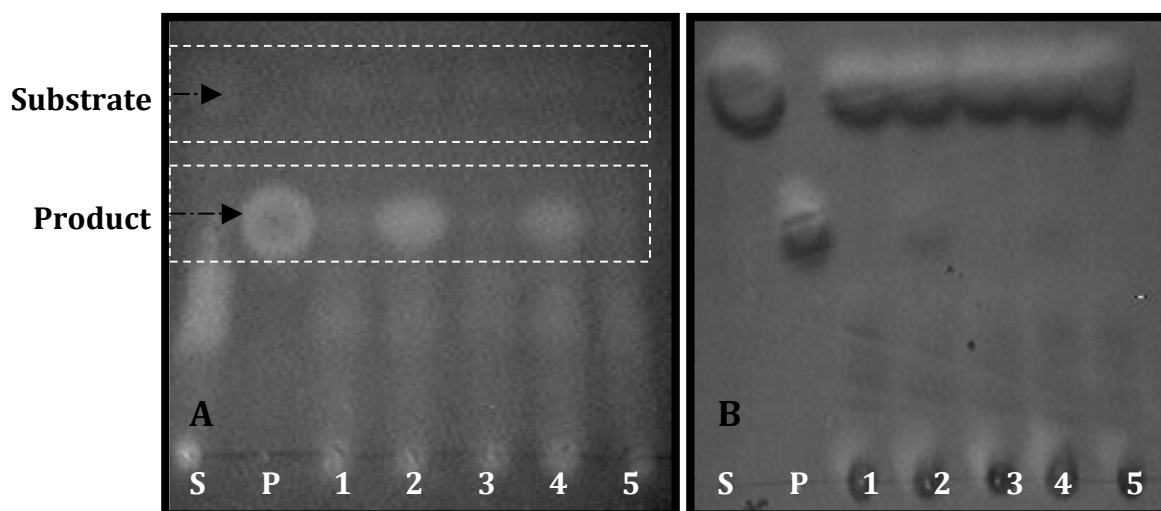


Figure 5.3 TLC analysis showing the bioconversion of 7-ethoxycoumarin to 7-hydroxycoumarin. **(A)** Shows compounds under UV light. Column S and P contain standards of 7-ethoxycoumarin and 7-hydroxycoumarin in ethyl acetate. **(B)** Shows compounds stained with permanganate and visualised under UV light. Columns 2, 4 and 5 are from induced cultures of *E. coli* [pQR368], *E. coli* [pQR367] and *E. coli* BL21 Star (DE3)pLysS (control). Columns 1 and 3 are from non-induced cultures of *E. coli* [pQR368] and *E. coli* [pQR367].

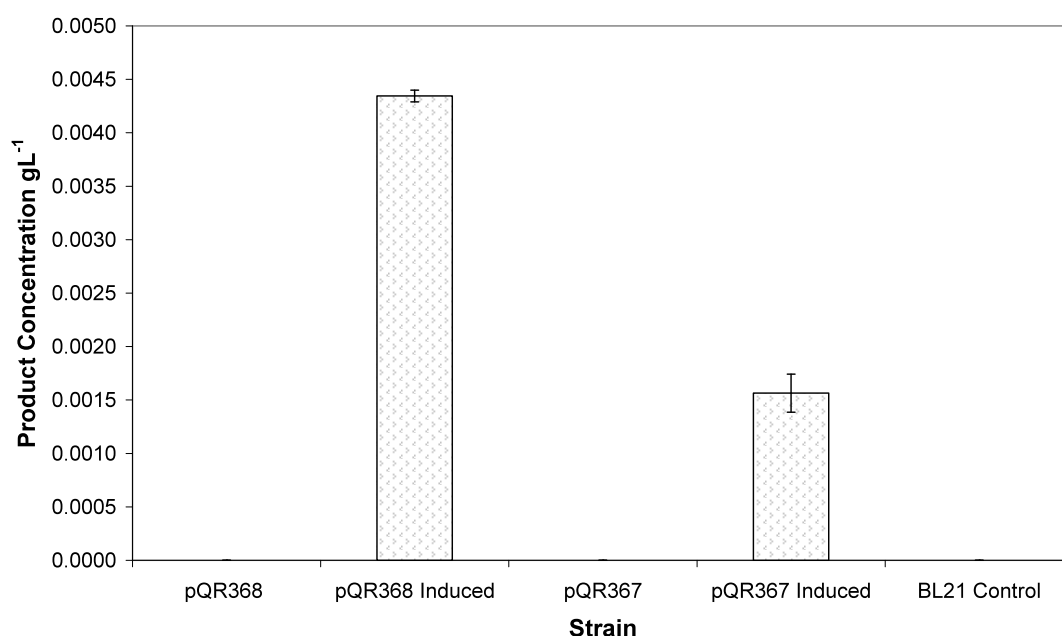


Figure 5.4 7-hydroxycoumarin concentration after 30 hours of induced and non-induced culture of *E. coli* [pQR368], *E. coli* [pQR367] and induced culture of *E. coli* BL21 Star (DE3)pLysS (control). Error bars indicate the range of measured values about the mean.

Hussain and Ward (2003 b) reported the successful O-dealkylation of 7-ethoxycoumarin to 7-hydroxycoumarin, however they did not report the yield obtained. Results from a group using the same strains with 7-ethoxycoumarin were also reported by the University of Edinburgh (unpublished data), where low 7-hydroxycoumarin yields between 2 and 5 % from *E. coli* [pQR368] and no conversion from *E. coli* [pQR367] were achieved. This is in agreement with the results presented in Figure 5.4 whereby P450SU2 was found to be a better biocatalyst than P450SU1. The results can be explained by the associated ferredoxin as it has been reported that Fd-2, which is adjacent to P450SU2, is more effective at restoring monooxygenase activity to mixtures of purified P450 (O'keefe et al., 1991). In addition, the low level expression of P450SU1 compared to P450SU2 has been attributed to rare codons present in the P450SU1 gene which may not be provided for by the expression strain (Hussain and Ward, 2003 b).

The high level expression of P450SU1 and P450SU2 as shown here has been reported previously and yet the biotransformation ability of 7-ethoxycoumarin is poor. Increasing biotransformation efficiency is important if environmentally compatible alternatives to chemical synthesis are to be exploited for industrial application. Poor bioconversion can inevitably be due to poor substrate specificity. However, it was of interest to investigate if the O-dealkylation could be improved considering the benefits of this reaction. This includes increasing molecule hydrophilicity, improving their pharmaceutical activities and increasing the industrial applicability (Niraula et al., 2001). Section 5.2.2 will outline the methodology used to develop the automated approach for the investigation of P450SU1 and P450SU2 in view of applying it for biotransformation improvement as addressed in section 5.2.3.

5.2.2 Automated Microscale Production of Cytochrome P450s

5.2.2.1 The Effect of Temperature During Expression

The automated process described in section 3.2.6 was used as an initial platform to develop the process automation of cytochrome P450s. 96-DSW plates were selected among other microwell formats as found suitable for both aerobic culture and bioconversion demands. It was considered appropriate to use similar microwell culture conditions to those established in Chapter 3 due to host similarities. In particular, as described in section 2.3.2.2, wells were automatically filled with 1 mL TB and inoculated with 1 % v/v *E. coli* [pQR368] and/or *E. coli* [pQR367]. Cells were incubated at 1000 rpm and 37 °C until an OD of 0.6-0.8 was reached. The conditions under which biocatalyst expression can be initiated are important, temperature in particular. The expression temperature of 25 °C was used in shake flask cultures and it has been reported that culture temperature must be returned to 30 °C prior to induction with IPTG (Phillips and Shephard, 2006). This is because recombinant *E. coli* protein expression at 37 °C can often lead to inactive protein aggregates, known as inclusion bodies, and a decrease in temperature has been found to prevent inclusion body formation (Schein, 1989; Vasina and Baneyx, 1996; Delcarte et al., 2003). Furthermore, Lu and Mei (2007) found that the optimum induction temperature for the expression of P450 BM3 was 30 °C. When a temperature of 37 °C was used a significant decrease in specific activity was observed. However, Taylor et al. (1999) reported the presence of P420 (inactive P450) in inclusion bodies formed after induction. Additionally, it is recommended by the manufacturer of the pET vector system as used in this work that the temperature is lowered during expression to ensure production of soluble enzyme and 25 °C was found by Zhang et al. (2010) to be optimum for P450SMO expression who also used the pET vector system. A temperature study as described in section 2.3.2.1.1 was conducted to ensure the correct expression incubation temperature was reached prior to induction. Figure 5.5 shows that after an initial incubation at 37 °C it took approximately 20 minutes for a temperature of 25 °C to be reached in all wells which then remained constant. A 20 minute incubation

period with ALA and FeCl₃ was required before induction which was also sufficient time for the correct induction temperature to be reached.

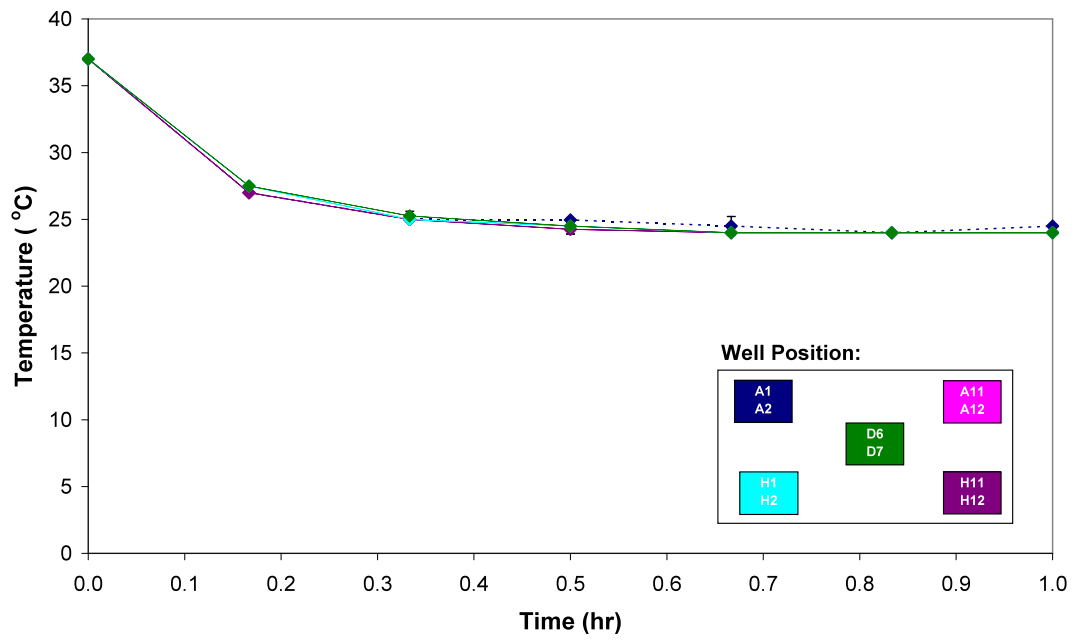


Figure 5.5 Cooling time required to achieve the correct induction temperature of 25 °C.

5.2.2.2 The Effect of Agitation Speed

The agitation speed used during expression is cytochrome P450 dependant where both gentle and fast shaker speeds have been found beneficial for expression. For example with P450c17 (a microsomal steroidogenic P450) low shaking speeds of 150 rpm were found optimal for expression whereas higher shaking speeds of 210 rpm were found optimal for P450scc (a mitochondrial steroidogenic P450) (Phillips and Shephard, 2006). Similarly, Jansson et al. (2000) found the best shaker speed for CYP1B1 (a human heamoprotein) was 150 rpm whereas CYP101 (cytochrome P450cam) expression was poor at this shaker speed and required higher rates from 175 rpm to 200 rpm. In the case of P450SU1 and P450SU2 expression following the original protocol (Hussain and Ward, 2003 b) which was replicated in section 5.2.1 demonstrated a gentle shaking speed was required. In Figure 5.6 and Figure 5.7 the effect of agitation speed during expression on the growth and bioconversion using both strains is presented.

Three agitation speeds were tested. At 600 rpm a clear reduction in growth can be observed compared to results obtained at 800 rpm and at 1000 rpm. This is probably due to an oxygen limitation as insufficient agitation results in inefficient gas-liquid mass transfer (Duetz and Witholt, 2004). When the agitation speed is reduced an increase in cell sedimentation in wells was also observed in some cases. This is probably due to the extended culture times of over 30 hours required for P450 expression. Additionally, as cell numbers increase low agitation rates are unable to keep all cells in suspension. This effect was described by Marques et al. (2007) who observed that reducing agitation rates resulted in cell cluster formation and accumulation on the well bottom. At 800 rpm there is no oxygen limitation, while further increases in agitation up to 1000 rpm had no further improvement in growth.

The formation of 7-hydroxycoumarin was next assessed at each agitation speed tested. Figure 5.7 shows that increasing the agitation rate from 600 rpm to 800 rpm causes a 65 % increase in product concentration expressed from P450SU2,

whereas there is little change from P450SU1. However, further agitation increases up to 1000 rpm caused a drop in product concentration from P450SU2, lower than that achieved at the lowest agitation rate tested of 600 rpm. Moreover, no product was detected from P450SU1, at least at levels that could be detected by the HPLC assay. This result demonstrates the importance of agitation rate selection in P450 bioconversion. Jansson et al. (2000) described that high agitation rates inhibited expression of human P450 CYP1B1 expressed in *E. coli* and suggested that cell integrity was damaged due to incorporation of haemoprotein in the cytoplasmic membrane. In this work low agitation rates can lead to non-homogenous mixtures, cell settling and oxygen limitation. Hence, 800 rpm was chosen for microwell expression as it promoted good mixing, oxygen limitation did not occur and the yield of 7-hydroxycoumarin was improved.

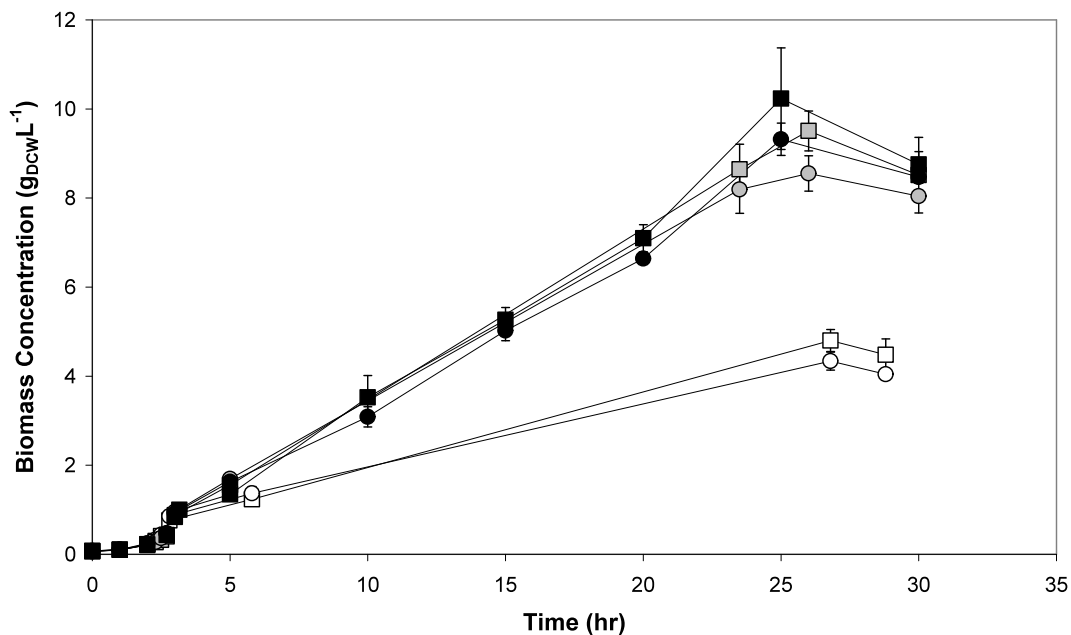


Figure 5.6 The effect of microwell agitation rate on growth of *E. coli* [pQR367] (●) and *E. coli* [pQR368] (■). 600 rpm (unfilled symbols), 800 rpm (grey filled symbols), 1000 rpm (black filled symbols). Error bars indicate the range of measured values about the mean.

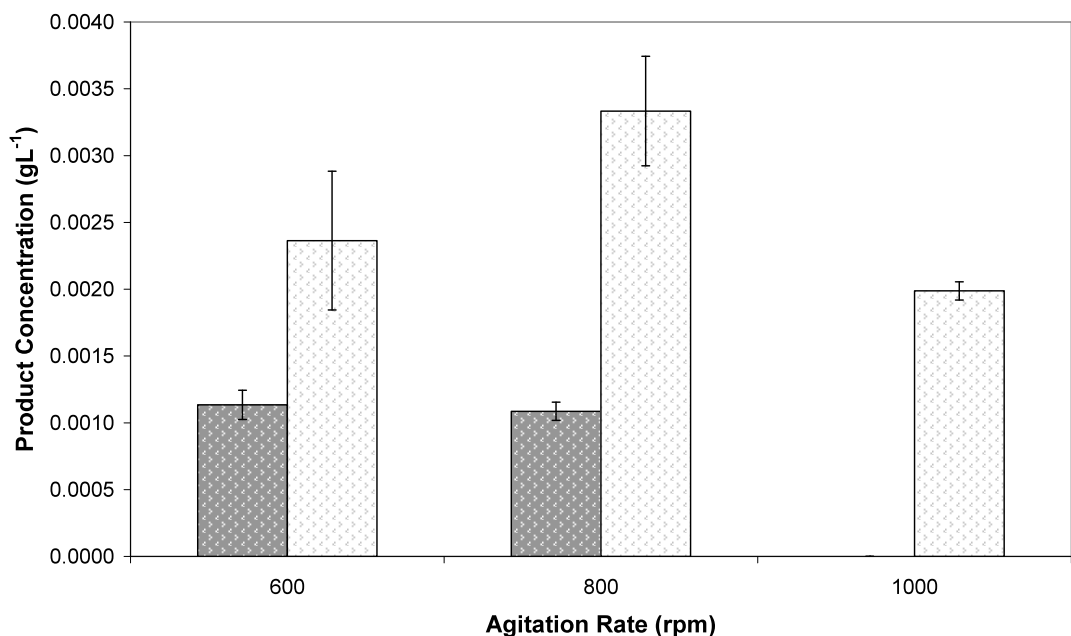


Figure 5.7 The effect of microwell agitation rate on 7-hydroxycoumarin production from *E. coli* [pQR367] expressing P450SU1 (grey bars) and *E. coli* [pQR368] expressing P450SU2 (white bars). Error bars indicate the range of measured values about the mean.

5.2.2.3 The Influence of Microwell Fill Volume

In Chapter 4 microwell fill volume was found to be an important parameter in controlling oxygen levels. The effect of microwell fill volume was thus investigated in this work to determine the optimal working volume for the system. In the study initial fill volumes ranged from 400 μL up to 1000 μL and cells were cultured at 1000 rpm and 37 °C until an OD of 0.6-0.8. The agitation and temperature was dropped to 800 rpm and 25 °C for expression and incubated with ALA and FeCl_3 which was followed by induction and then bioconversion. Figure 5.8 shows the effect of fill volume on *E. coli* growth kinetics. Results do not show a significant effect of fill volume, however the highest and lowest biomass concentrations were achieved at the highest and lowest fill volume, respectively. In Chapter 4 it was found that decreasing the fill volume increased the oxygen transfer rate resulting in an increase in growth. This effect was not observed with *E. coli* BL21 Star (DE3)pLysS where the effect of evaporation on larger volumes is reduced and can sustain higher cell concentrations. Whereas, the effect of evaporation on low volumes is pronounced due to increased gas/liquid interfacial area (Marques et al., 2007) and the concentrating effect on media components such as salts may be detrimental to growth. The increased headspace as a result of reduced volumes in microwells has also been reported to cause void formation where the centrifugal force will project liquid towards the walls (Marques et al., 2007) this may also be responsible for the reduced growth.

Figure 5.9 shows increased well volumes have a beneficial effect on product yields. The concentration of solutes which may be detrimental for growth may also be responsible for the reduction in bioconversion where a 40 % reduction in fill volume causes a 42 % decrease in product concentration. Due to the beneficial effects of reduced fill volumes observed during the CHMO studies these results are difficult to elucidate without further investigations. It is speculated that high oxygen transfer rates may be damaging to the P450 biocatalysts. In section 5.2.2.2 (Figure 5.7) increasing the agitation rate to 1000 rpm resulted in no product formation from *E. coli* [pQR367] and in the present study reductions in fill volume also reduced the product level. Increasing

agitation and reducing the fill volume should both result in increased oxygen transfer however in these studies particular conditions (above 800 rpm and below 1000 μ L) are detrimental to product formation. Further studies need to be done to measure the DOT at each condition and also the activity of the biocatalyst to confirm if high DOT is responsible for a reduction in bioconversion performance. From these findings 1000 μ L was used as the culture working volume due to increased product concentrations and the reduced impact of evaporation over extended culture times.

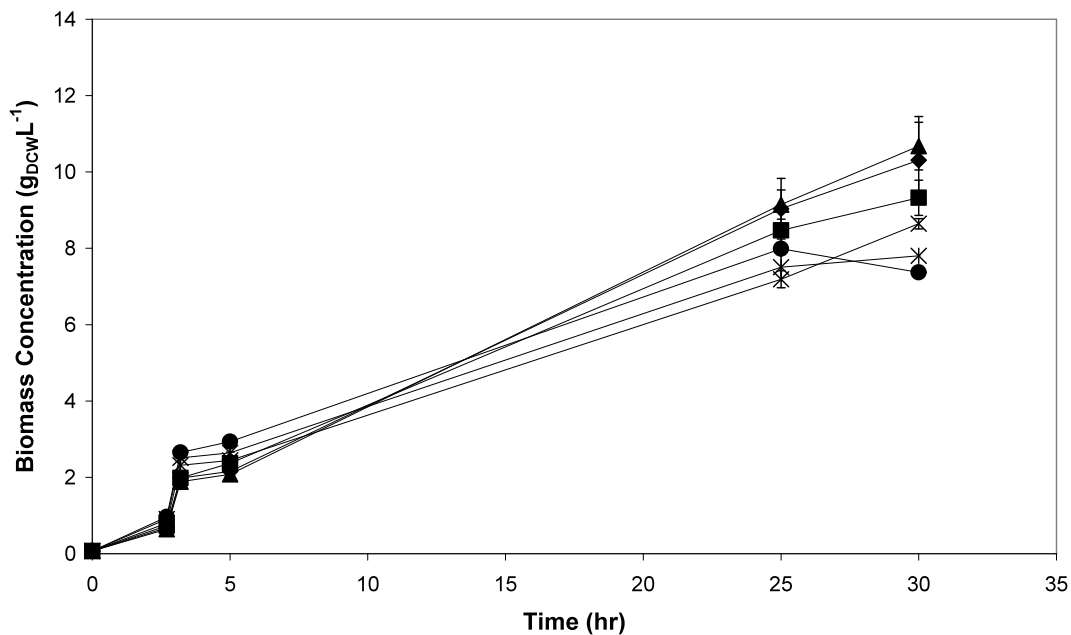


Figure 5.8 The effect of microwell fill volume on growth *E. coli* [pQR367]. 1000 μL (▲), 800 μL (◆), 700 μL (■), 600 μL (×), 500 μL (*), 400 μL (●). Error bars indicate the range of measured values about the mean.

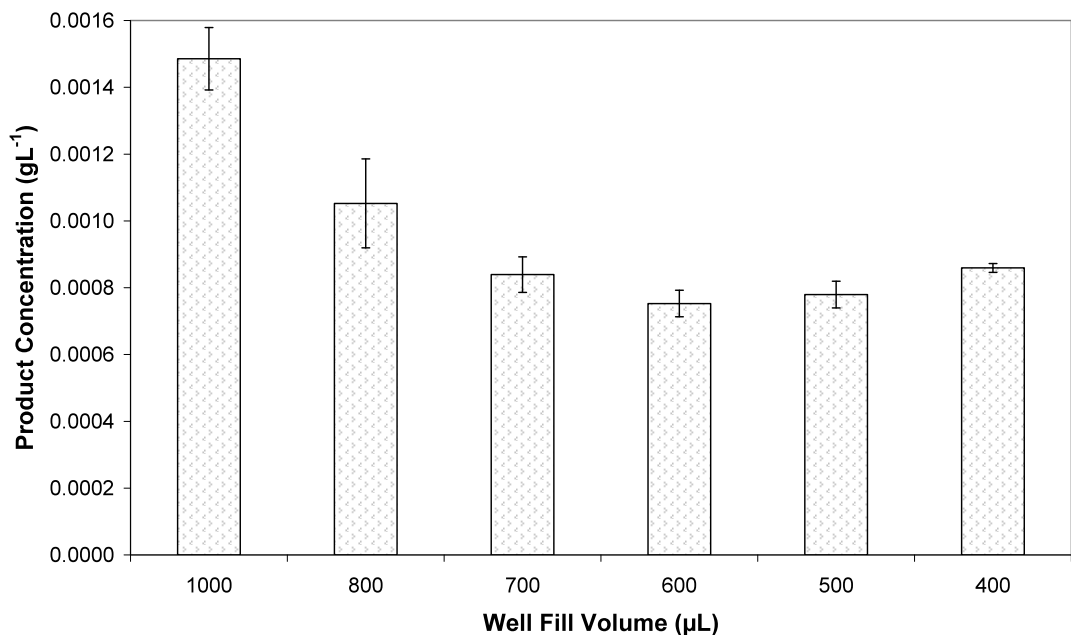


Figure 5.9 The effect of microwell fill volume on 7-hydroxycoumarin production from *E. coli* [pQR367] expressing P450SU1. Error bars indicate the range of measured values about the mean.

5.2.2.4 The Effect of Microwell Evaporation

Considering the extended culture times involved in the production of the cytochrome P450s it was considered important to quantify the effects of evaporation. Wells of a 96-DSW plate were filled with 1000 μL TB and shaken at 25 °C and 800 rpm for a total period of 24 hours as described in section 2.3.2.1.2. The well content was weighed after 1, 10 and 24 hours and the liquid loss calculated. Figure 5.10 shows the effect of evaporation in different wells of the plate over the 24 hour time period. A difference in evaporation associated with the well position can be observed. The highest evaporation rate of 5 uLh^{-1} was calculated for wells located at the top left of the plate and the lowest evaporation rate of 4 uLh^{-1} for wells located in the middle right section of the plate. On average a rate of evaporation of 5 uLh^{-1} can be calculated from all wells. This value amounts to 15 % of the wells contents in a total of 30 hours of culture. Duetz and Witholt (2001) reported after 20 days of culture a total loss of 27 % of the well contents whilst using an appropriate cover to prevent excessive evaporation and humidified conditions. A maximum liquid loss of 15 % was considered acceptable for this work however cultures should not be run for considerably longer than 30 hours. Nevertheless, it is important to quantify the level of evaporation and to evaluate methods to reduce it.

A potential solution to excessive evaporation in microwell format could be the use of a membrane. A gas permeable membrane (Breath-easy) was selected which allows the diffusion of oxygen and reduces evaporation. A culture was carried out in a 96-DSW plate where half of the plate was covered with a Breath-easy membrane and the other half was left open. The results of the study are shown in Figure 5.11. The use of a permeable membrane has a significant effect on the cell growth of both strains causing a reduction by nearly 50 % when the membrane is used. Similarly Marques et al. (2009) reported a 50 % reduction in oxygen transfer rates when using a sealing tape on microwell plates to prevent evaporation.

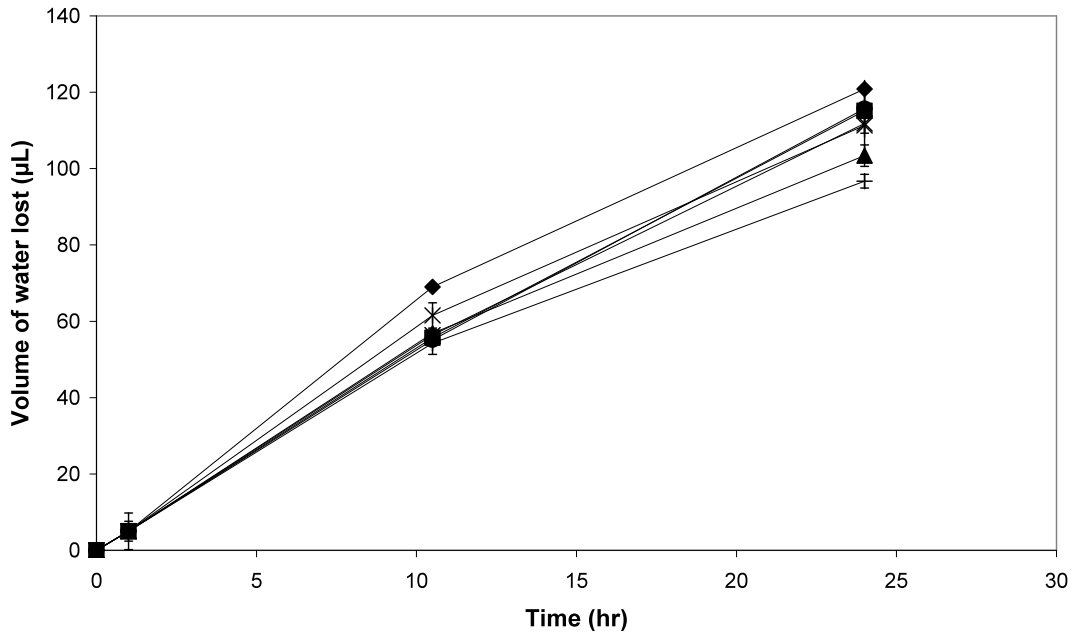


Figure 5.10 The effect of well position on the amount of liquid evaporated from a 96-DSW plate at 25 °C and 800 rpm. Plate locations: top left (◆), top right (■), middle left (▲), middle (×), middle right (+), bottom left (●), bottom right (*). Error bars indicate the range of measured values about the mean.

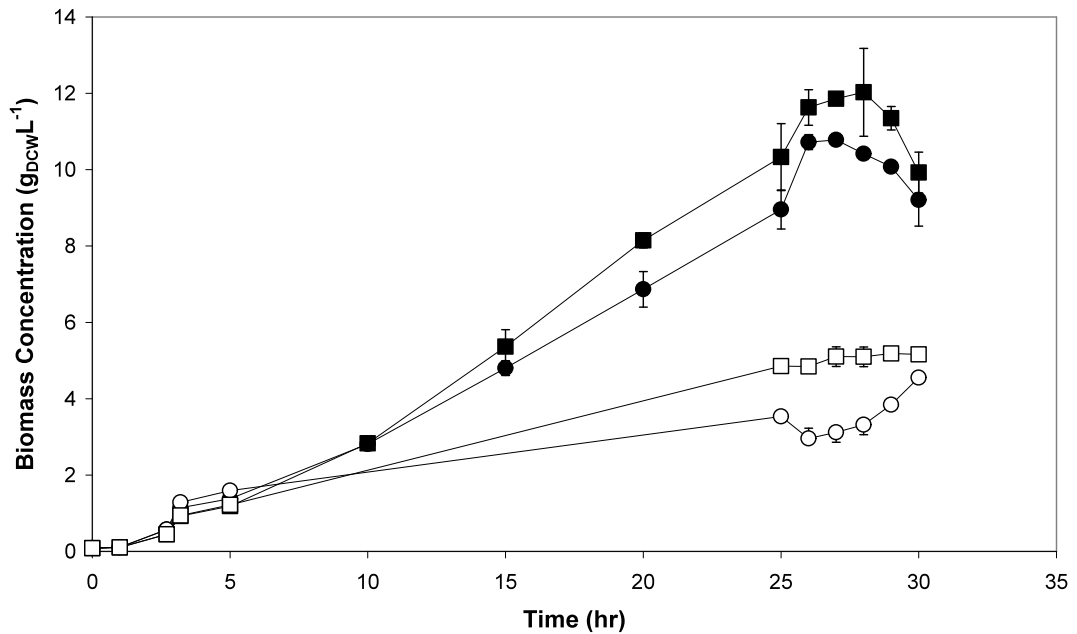


Figure 5.11 The effect of covering wells with a gas permeable membrane (open symbols) on the culture of *E. coli* [pQR367] (●) and *E. coli* [pQR368] (■) compared to uncovered wells (closed symbols). Error bars indicate the range of measured values about the mean.

Zimmerman et al. (2003) tested a range of plastic seals and concluded that none of the products tested could provide both high oxygen permeability and high water vapour retention. Using an open system enables overnight sampling which would have been otherwise impossible using the robotic disposable tips with a sealed plate. Fixed tips can be installed, however, there is a risk of well-to-well contamination due to sample carry over thus reducing the number of samples that can be withdrawn. Continual piercing of membranes may also result in damage over time. Overcoming problems such as evaporation is an important practical issue and an interesting solution would be the development of an automated plate opening/closing system with an appropriate gas permeable lid. A lid similar to that developed by Duetz et al. (2000), who reported evaporation rates of 20 μL per well per day and has been widely employed for mammalian and bacterial culture would be worth investigating. It is important to note that these rates were achieved at a humidity of 50 % and accurate control of humidity was not available in the system used in this work. For this reason it was decided to conduct the experiments with no permeable membrane which would significantly alter the oxygen transfer rate and consequently impact the cell growth and biocatalyst productivity.

5.2.2.5 Automated Data Collection on Cytochrome P450s

From the studies already discussed in sections 5.2.2.1 to 5.2.2.4 the automated run used in this work involved a microwell growth phase at 1 mL, 37 °C and 1000 rpm until an OD of 0.6-0.8 then a expression phase at 1 mL, 25 °C and 800 rpm followed by induction and substrate bioconversion. Considering the extended culture time it was important to develop a sampling strategy which would allow data to be collected on both growth and bioconversion during a 30 hour culture for bioprocess evaluation. The first strategy was to sample every 5 hours of culture using a sacrificial well approach. This would allow the impact of three factors on two strains or six factors on one strain to be tested in a single plate/automated run. Figure 5.12 shows the product formation results obtained during 30 hours of culture. No product was detected prior to 20 hours of culture.

A likely reason for this finding could be due to the product levels being too low to be detected. Alternatively, product may have only been produced after 20 hours of culture due to very slow metabolism or reduced enzyme titre. To investigate this further the initial protocol was altered. Rather than adding the substrate after 3 hours of culture it was added after 25 hours of culture which is the point of optimal enzyme expression as reported previously (Hussain and Ward, 2003 b). An additional benefit of this approach is that as 7-ethoxycoumarin is poorly water soluble, it had to be added dissolved in 100 % ethanol thus adding the substrate at a higher cell biomass would alleviate any adverse effects caused by the ethanol.

Figure 5.13 shows the results of this study. Product was only detected when substrate addition took place after 3 hours of culture, when substrate was added at the 25th hour nothing was detected. This indicated that not only was the biocatalyst expression important but the substrate incubation time was also a crucial factor in bioconversion. It has been reported that certain P450s are induced by xenobiotic compounds (Bolwell et al., 1994), particularly plant P450s, as expression is initiated as a means of protection to metabolise environmental pollutants. In fact, the wild type organism *Streptomyces griseolus* expresses P450SU1 and P450SU2 when induced with sulfonylurea herbicides. Uno et al. (2008) also reported that the P450 1A expression increased when exposed to environmental pollutants. However, in the *E. coli* expression system the P450 genes were separated from the native transcription control sequences and replaced with the artificial T7 promoter sequence thus 7-ethoxycoumarin is unlikely to induce P450SU1 and P450SU2 in this work. The increased incubation time is most likely responsible for the increased bioconversion. Additionally, other factors including poor substrate solubility, inefficient transport into cells (Urlacher and Girhard, 2012) and slow dealkylation are likely explanations for the observed behaviour.

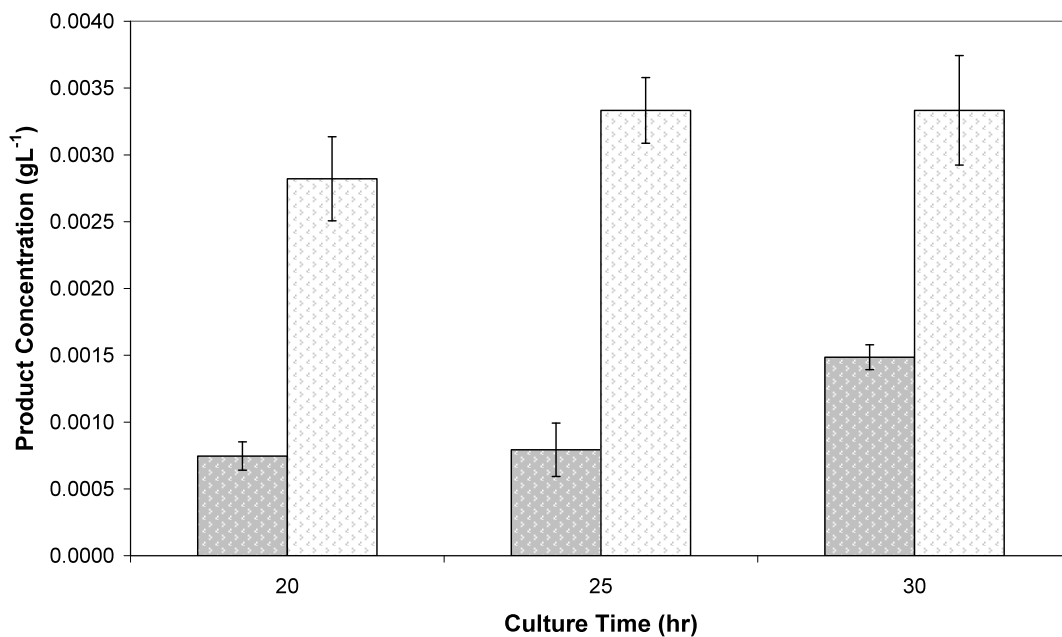


Figure 5.12 7-hydroxycoumarin production from *E. coli* [pQR367] (grey bars) and *E. coli* [pQR368] (white bars). Substrate addition took place after 3 hours of culture. No product detected prior to 20 hours of culture. Error bars indicate the range of measured values about the mean.

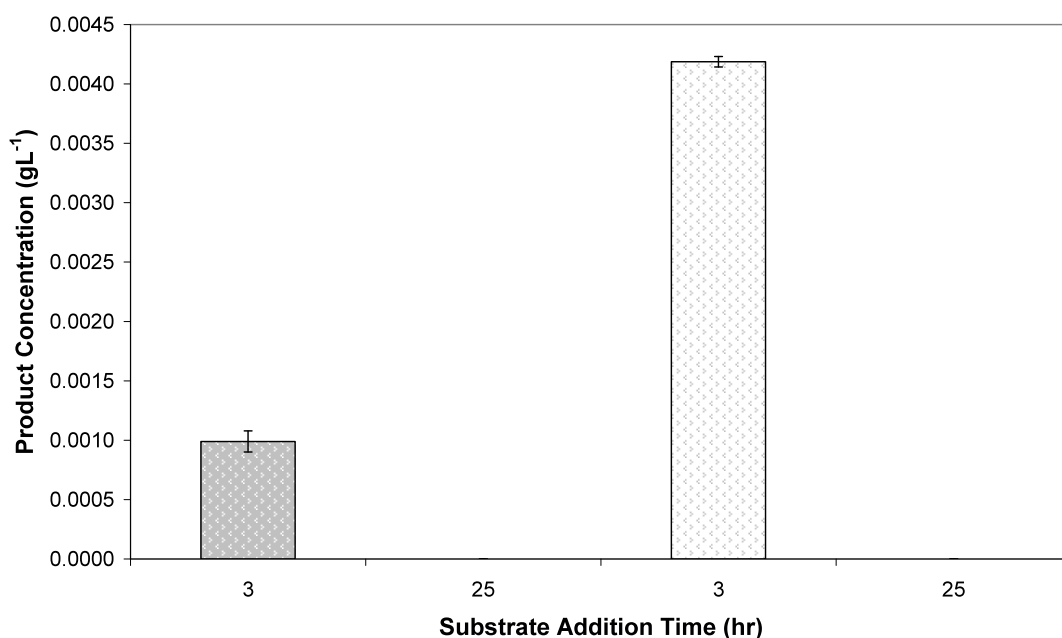


Figure 5.13 The effect of substrate addition time on 7-hydroxycoumarin production from *E. coli* [pQR367] (grey bars) and *E. coli* [pQR368] (white bars). Error bars indicate the range of measured values about the mean.

It was therefore decided that the sampling strategy would involve OD samples to be taken every 5 hour interval until the 25th hour and then every 1 hour for the remaining culture. Bioconversion samples would only be taken at 0 hours and hourly during the last 5 hours of culture when there was a sufficient level of product to be detected by HPLC. A schematic representation of the adapted automated approach for the evaluation of *E. coli* [pQR367] expressing P450SU1 and *E. coli* [pQR368] expressing P450SU2 is shown in Figure 5.14.

Similar to what was achieved for the CHMO process ‘walk away operation’ was developed in this work for cytochrome P450 studies. Initially the platform is setup with the required plates and reagent reservoirs and an aseptic processing environment is prepared as described in section 2.3.2.2. Samples are automatically collected throughout the culture and OD measured using the plate reader to obtain kinetic cell growth data. User prompts are used to enable the operator to initiate the expression phase once the cells have reached a preset OD of 0.6. Figure 5.15 shows an example of the user prompt used. The prompt will appear at stage two in Figure 5.14. Inserting a value lower than 0.6 will result in OD sampling to continue, while inserting a value greater than or equal to 0.6 will initiate the expression phase. Due the nature of certain reagents the operator is required to add reagent reservoirs when they are needed to avoid likely degradation at room temperature. However, apart from reagent addition, an operator is only needed for regular monitoring. The system works independently for 30 hours and at the end of the process the operator will collect and freeze bioconversion samples at designated time points as shown in Figure 5.14. At 30 hours of culture the final OD and bioconversion samples are taken and a 1 mL aliquot frozen for analysis of CO reduced spectra as described in section 2.6.9. The process continues with an automated liquid-liquid extraction on samples collected during the bioconversion as described in section 2.3.2.2 for metabolite extraction and the organic layer automatically dispensed into eppendorfs after centrifugation. These are then transferred to a fume cupboard for overnight evaporation and re-dissolved in acetonitrile for HPLC analysis. Upstream and downstream process steps and analytical measurements (which include plate preparation, reagent addition, sampling) are all fully automated.

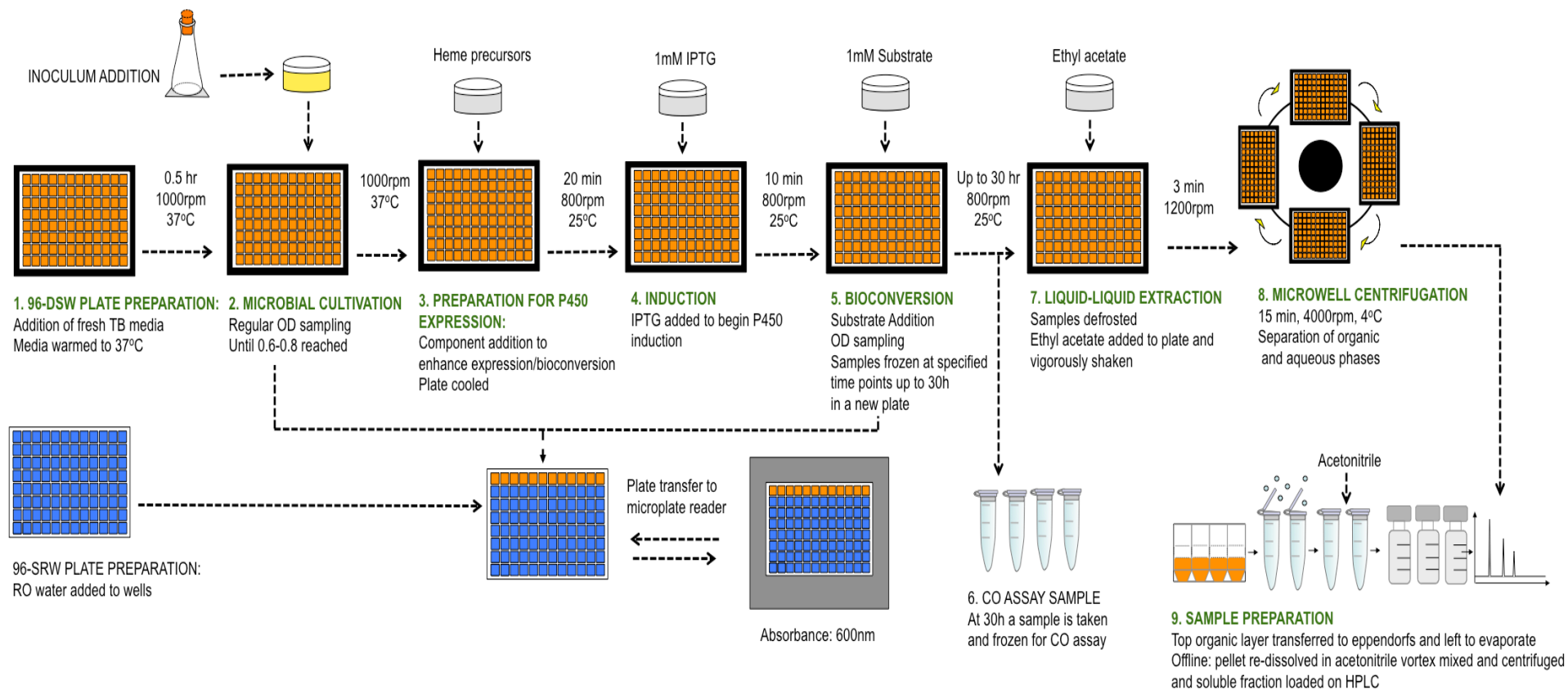


Figure 5.14 Schematic representation of the fully automated linked process sequence using *E. coli* [pQR367] and *E. coli* [pQR368] expressing cytochrome P450SU1 and P450SU2 respectively. Coloured wells represent filled wells as an example (orange: media and culture, blue: RO water).

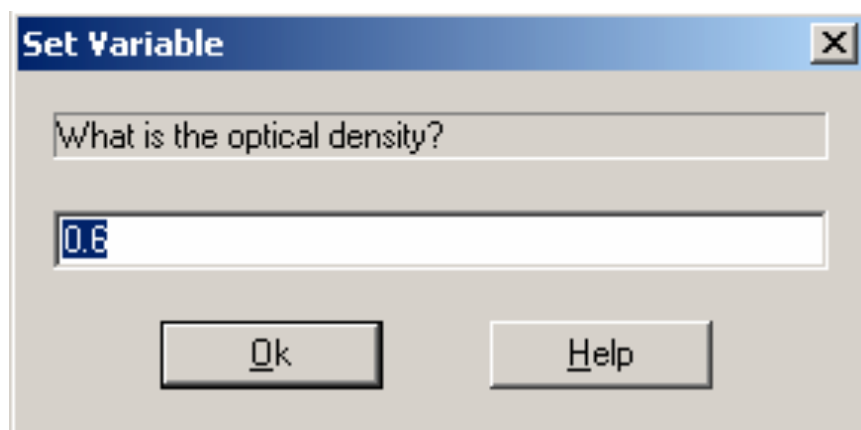


Figure 5.15 User prompt to initiate expression phase.

The time required to obtain a sufficient number of cells for biocatalyst production and detectable bioconversion is 30 hours and this extended time period causes several challenges when working with microlitre amounts of material. The reproducibility of data collection was assessed to ensure the data collected was not adversely affected by evaporation. In particular, it was important to test both the reproducibility of growth and bioconversion on different days and from different areas of the plate to evaluate any “edge effects”. From Figures 5.16 A and B the growth of both *E. coli* [pQR367] and *E. coli* [pQR368] is very similar between triplicate data sets collected on three separate days in three separate areas of the plate using the automated approach shown in Figure 5.14. A mean specific growth rate of 1.56 h⁻¹ and 1.84 h⁻¹ and final biomass concentration of 9.33 g_{DCW}L⁻¹ and 9.01 g_{DCW}L⁻¹ were obtained from the cultures of *E. coli* [pQR367] and *E. coli* [pQR368] respectively. The calculated average and maximum errors were 5 % and 13 % for *E. coli* [pQR367] and 6 % and 13 % for *E. coli* [pQR368] between triplicate runs.

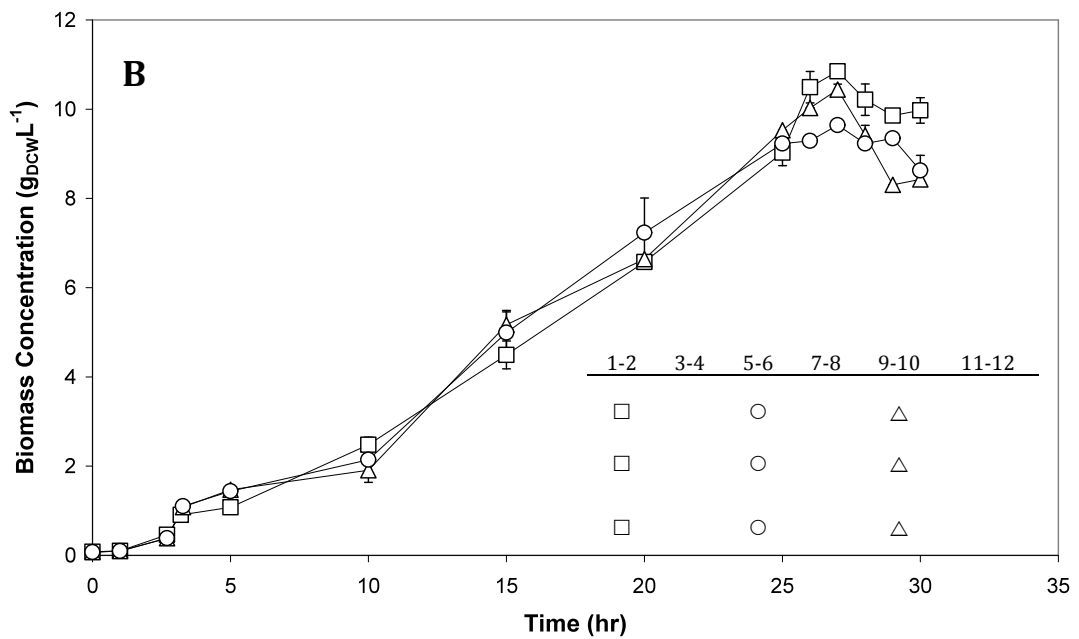
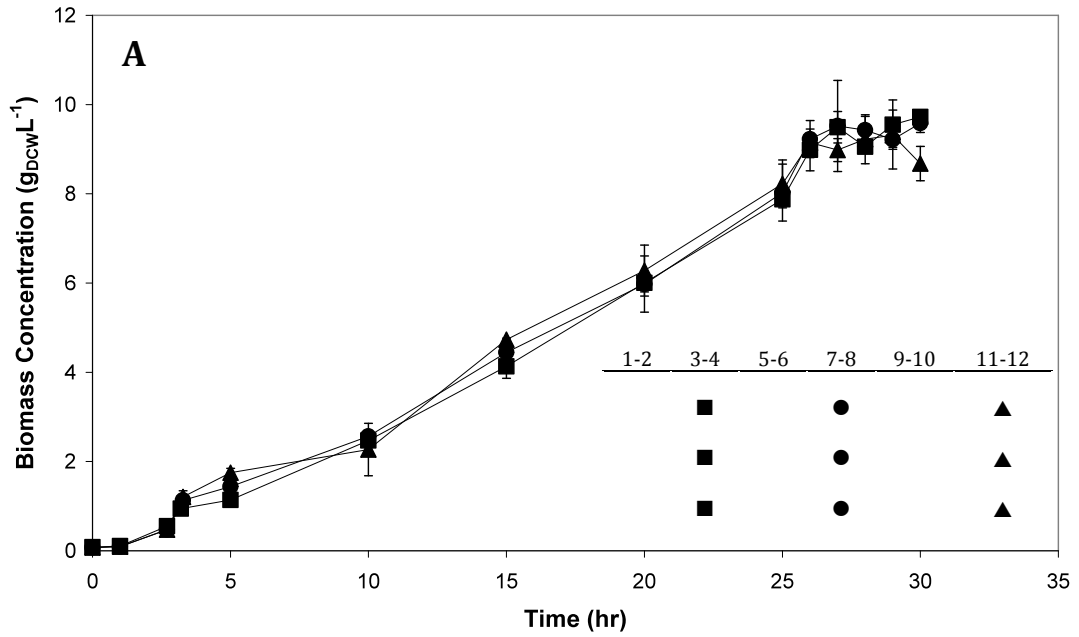


Figure 5.16 Reproducibility of growth kinetic data collected from three separate runs on the culture of (A) *E. coli* [pQR367] in different areas of a 96-DSW plate (■) columns 3-4, (●) columns 7-8 and (▲) columns 11-12 and (B) of *E. coli* [pQR368] in different areas of a 96-DSW plate (□) columns 1-2, (○) columns 5-6 and (△) columns 9-10. Error bars indicate the range of measured values about the mean.

The reproducibility of bioconversion kinetic data is shown in Figure 5.17. The rate of product formation is quite slow and there is a very slow increase in product yield during the last 5 hours of growth. The mean final concentration of 7-hydroxycoumarin produced from P450SU1 and P450SU2 was $0.98 \pm 0.06 \text{ mgL}^{-1}$ and $3.55 \pm 0.17 \text{ mgL}^{-1}$ representing product yields of 0.5 % and 1.9 % respectively. The calculated average and maximum errors were 5 % and 10 % for *E. coli* [pQR367] and 4 % and 5 % for *E. coli* [pQR368] between triplicate runs.

The samples collected after 30 hours of growth were analysed using a CO assay and the expression of P450SU1 and P450SU2 are shown in Figure 5.18 A and B. Similar to the spectrums achieved from shake flask cultures, P450SU1 displays the presence of soret peaks at 420 nm and 450 nm whereas P450SU2 only has a distinct peak at 450 nm. The calculated level of active P450 was 29 nmolg^{-1} from P450SU1 and 53 nmolg^{-1} from P450SU2.

The results collected using the automated microwell platform confirmed that reproducible growth and bioconversion kinetic data can be collected on two P450 biocatalysts. The automated approach could also be used to produce samples for CO difference spectrum analysis. A number of parameters could potentially be investigated using the automated sequence however it was decided to use the approach to improve the product yield at the bioconversion stage. Investigation of enzyme expression has been looked at (Hussain and Ward, 2003 b). A microscale CO assay was not developed in this work thus samples had to be processed manually using the original spectrophotometric approach. Due to the number of sample preparation steps required for this assay including sonication and sparging CO into every sample this can become the limiting step in sample analysis. Thus at present the automated approach is more suitable for assessment of bioconversion effectiveness using HPLC which is dependant on enzymatic expression and activity. However, research into microscale sonication techniques is in progress (Ordidge, 2012) and a microscale CO assay has been reported (Choi et al., 2003). It would therefore be worthwhile to develop microscale approaches for additional processing steps which could be included in this automated sequence to enable a more efficient analysis of samples for CO

difference spectrum analysis, the 'gold standard' for assessing the level of active P450.

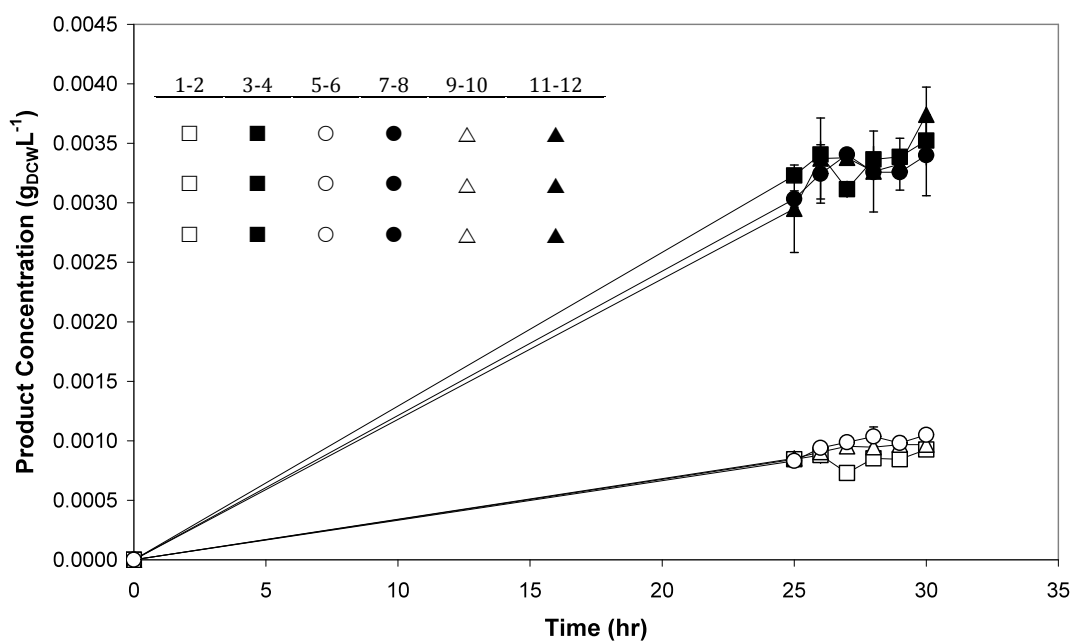


Figure 5.17 Reproducibility of bioconversion kinetic data collected on the culture of *E. coli* [pQR367] in different areas of a 96-DSW plate (□) columns 3-4, (○) columns 7-8 and (△) columns 11-12 and the culture of *E. coli* [pQR368] (■) columns 1-2, (●) columns 5-6 and (▲) columns 9-10. Error bars indicate the range of measured values about the mean.

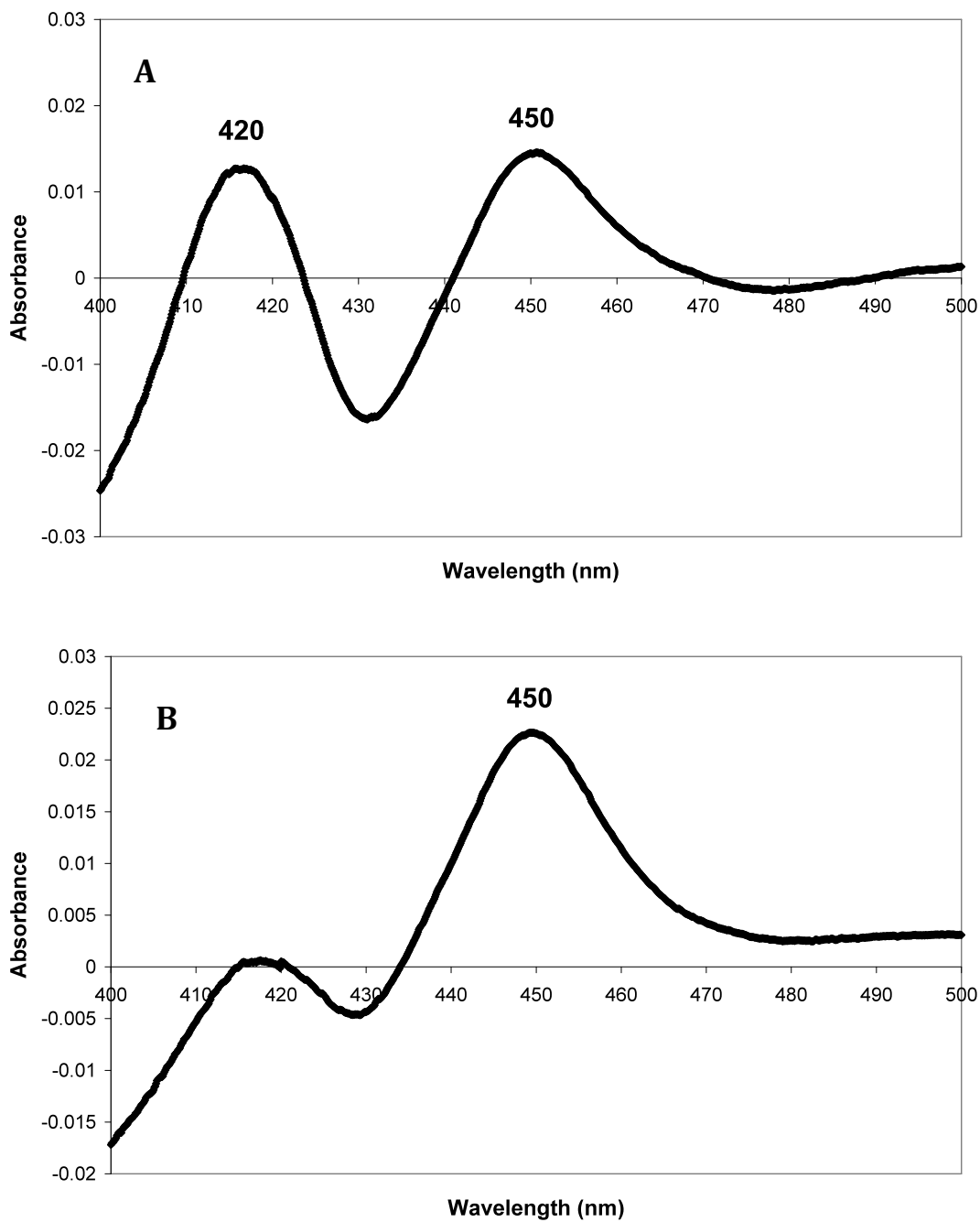


Figure 5.18 Representative CO difference spectra of **(A)** P450SU1 expressed in *E. coli* [pQR367] and **(B)** P450SU2 expressed in *E. coli* [pQR368] during automated process sequence. Samples were from cultures where no 7-ethoxycoumarin was added.

5.2.3 Applying the Automated Approach for Bioconversion Improvement

There has been limited research on methods aimed to improve the O-dealkylation activity and bioconversion efficiency was found to be poor in section 5.2.2.5. Bioconversion effectiveness is inevitably linked to enzymatic expression and activity thus factors associated with improved expression were used as a starting point in an attempt to improve O-dealkylation activity where the conversion of 7-ethoxycoumarin to 7-hydroxycoumarin was used as a model system.

From a review of published findings particular media additions were found to be successful in promoting improved enzymatic expression as discussed in Chapter 1. Firstly, components termed as P450 activators including α -benzoflavone and β -benzoflavone were reported by Taylor et al. (1999) to stimulate the activity of P450 SOY from *Streptomyces griseus*. Haem precursors such as ALA (Taylor et al., 1999, Richardson et al., 1995), and the iron containing media supplements hemin (Chen et al., 1996) and FeCl₃ (Jansson et al., 2000; Hussain and Ward, 2003 b; Zhang et al., 2010) are well documented at improving P450 yields. In fact up to a 20-fold improvement in expression levels has been reported when using ALA (Jansson et al., 2000) and it has been termed essential for haemoprotein production (Gillam et al., 1995). Thirdly, trace elements and thiamine are often added in the culture medium (Shimada et al., 1998; Gillam et al., 1995; Fischer et al., 1992). However, some sources do claim these components may not be essential for expression (Phillips and Shephard, 2006; Jansson et al., 2000). Finally, glycerol and sugar supplementation have been found to enhance P450 gene expression (Kagawa and Cao, 2001). In particular arabinose was found to enhance the expression of a microsomal P450 by inducing an osmotic stress response and was reported to play a crucial part in formation of functional proteins (Kagawa and Cao, 2001).

Therefore, a number of factors have been found to be beneficial in the expression of active P450 however the aim in this study was to assess if they could improve the bioconversion ability of P450SU1 and P450SU2. It was first of interest to

conduct an initial screen where an increased number of factors could be tested simultaneously for their bioconversion ability. The automated approach developed in section 5.2.2.5 was purposefully modified and the method used for the automated screens is described in section 2.3.2.3. Once cells had reached an OD of 0.6-0.8 (corresponding to stage 3 in Figure 5.14) each of the factors shown on the x-axis in Figure 5.19 A and B and Figure 5.20 A and B were added to wells in duplicate. However, in the case of trace elements and thiamine these were added to the TB medium during preparation as thus were present in the medium from the start of the process.

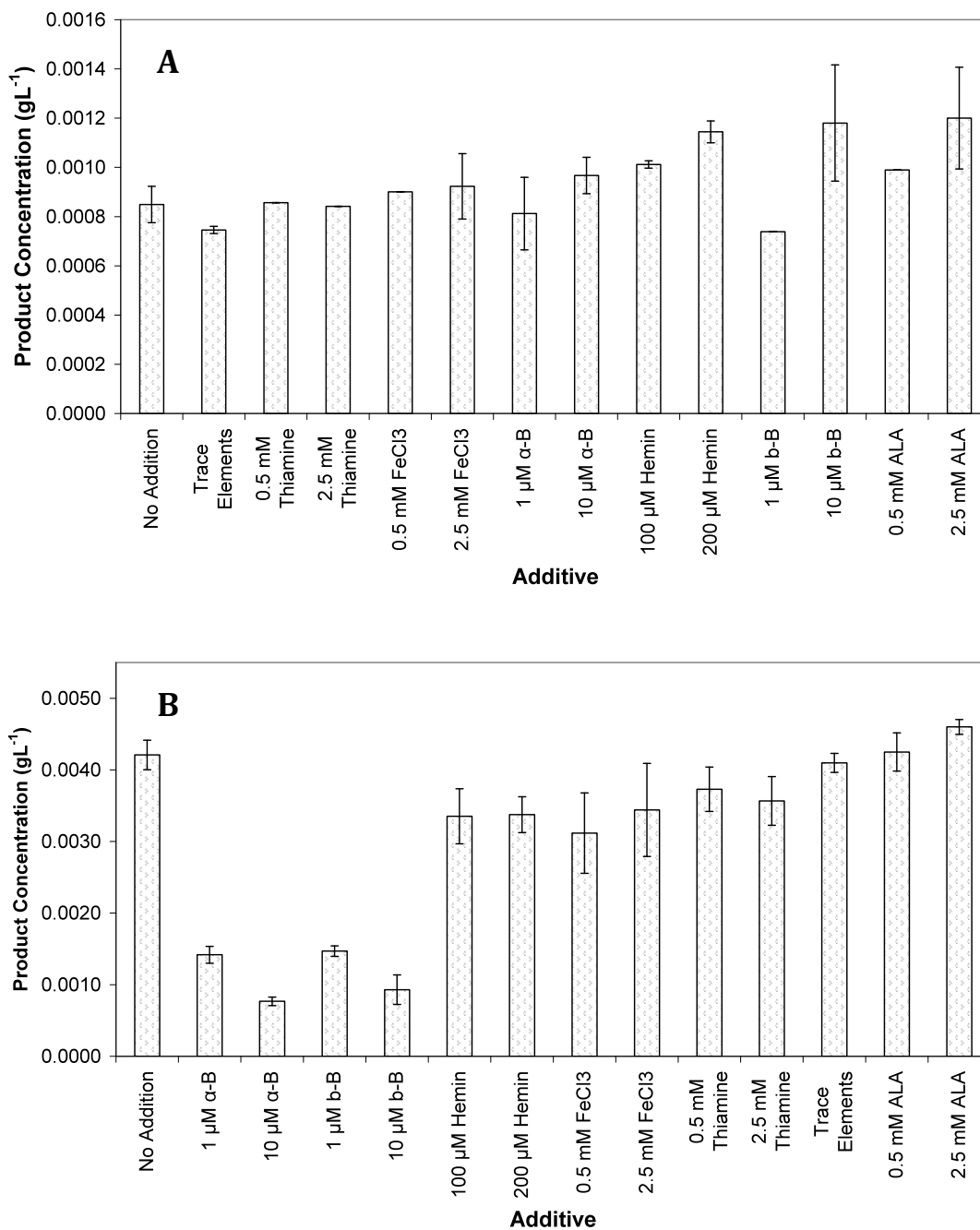


Figure 5.19 The effect of α -benzoflavone (α -B), β -benzoflavone (b-B), ALA, hemin, FeCl₃, thiamine, and trace elements on 7-hydroxycoumarin production from (A) *E. coli* [pQR367] expressing P450SU1 and (B) *E. coli* [pQR368] expressing P450SU2. Error bars indicate the range of measured values about the mean.

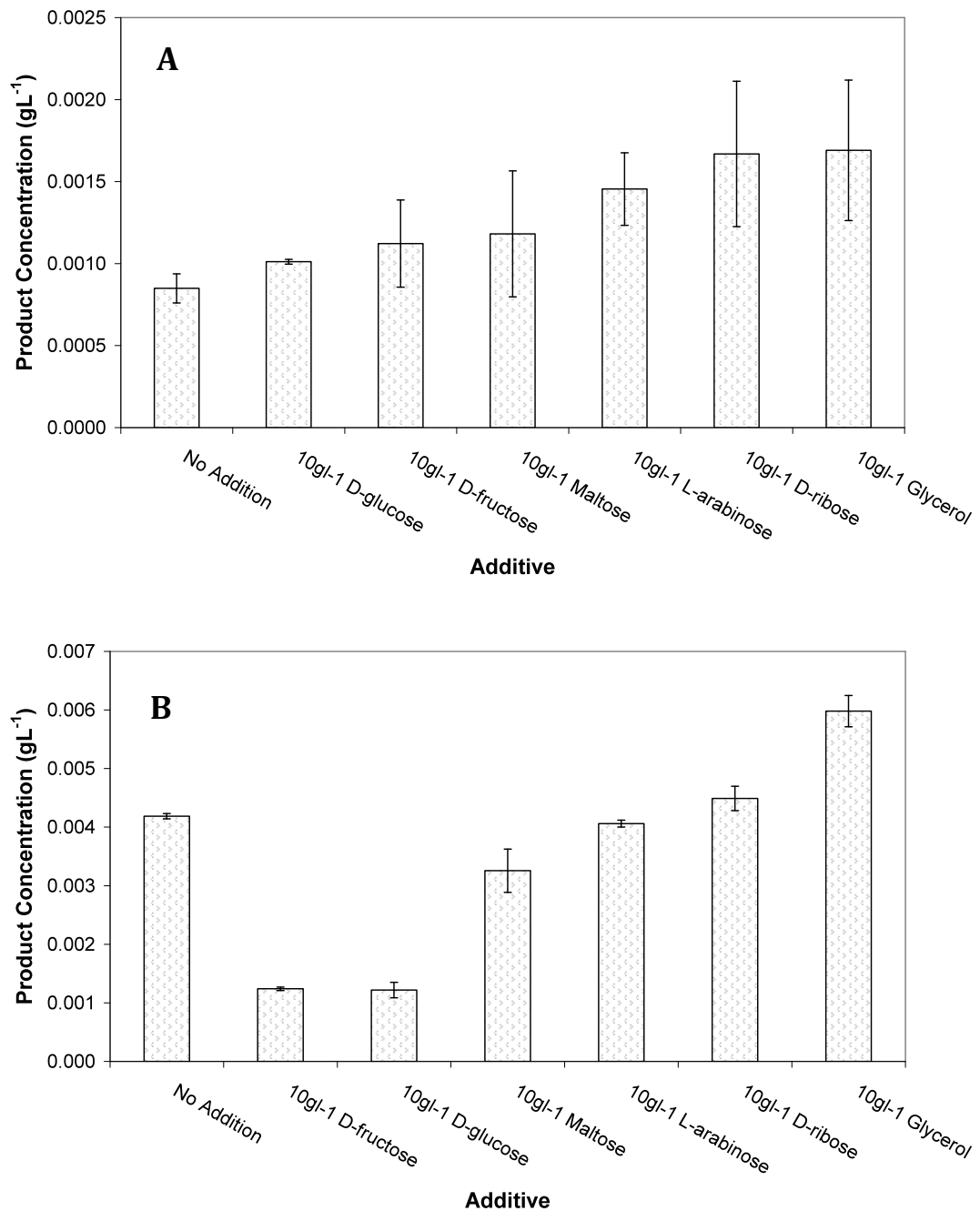


Figure 5.20 The effect of the sugars D-fructose, D-glucose, maltose, L-arabinose, D-ribose and glycerol on 7-hydroxycoumarin production from (A) *E. coli* [pQR367] expressing P450SU1 and (B) *E. coli* [pQR368] expressing P450SU2. Error bars indicate the range of measured values about the mean.

Factors were tested alongside control cultures of *E. coli* [pQR367] and *E. coli* [pQR368] grown following the original protocol but with no haem precursor addition. The factors thiamine, trace elements, hemin and FeCl₃ were found to have little or no significant effect on 7-hydroxycoumarin production from both strains. The result with FeCl₃ was unexpected as studies with *E. coli* [pQR368] have shown an improved yield of active P450 (Hussain and Ward, 2003 b). This result seems to imply that FeCl₃ is only beneficial when added with ALA where improvements have been reported previously (Jansson et al., 2000; Hussain and Ward, 2003 b). P450 activators were found to result in a significant decrease in 7-hydroxycoumarin production from *E. coli* [pQR368]. The opposite was observed with *E. coli* [pQR367] where increases in both α -benzoflavone and β -benzoflavone caused an increase in product concentrations.

Among all factors tested ALA was found to be the most effective at improving the production of 7-hydroxycoumarin from both P450SU1 and P450SU2. ALA has a crucial role in haem production where it is one of the first components in a series of events for the final formation of haem. Supplementation of this acid is an efficient method to increase the yield especially if intracellular production becomes a limiting factor.

Figure 5.20 shows the effect of a range of sugars and glycerol. Glycerol and D-ribose were both found to improve product formation from P450SU1 while only glycerol had a significant effect on P450SU2 product formation. The addition of 10 gL⁻¹ glycerol resulted in over a 2-fold and a 1.4-fold increase from P450SU1 and P450SU2, respectively, while the addition of 10 gL⁻¹ D-ribose caused over a 2-fold increase from P450SU1. The additions of D-glucose, D-fructose and maltose caused minimal improvements of P450SU1 bioconversion and a reduction in product formation from P450SU2. The result with D-glucose is expected as it indirectly represses the transcription of the lac operon by reducing the catabolite activator protein level which is required to assist RNA polymerase binding during protein synthesis. Therefore a reduced biocatalyst titre could be responsible for the significant drop in bioconversion from P450SU2.

Kagawa and Cao (2001) suggest that sugar addition increases P450 expression by two possible mechanisms. Firstly, they provide an effective carbon source and secondly they can induce an osmotic stress response which has been linked to the formation of functional proteins. Table 5.2 shows a summary of the final biomass concentration reached after 30 hours of culture in the presence of each carbon source. The lowest biomass concentrations were achieved in the presence of D-glucose and D-fructose and as a result significant reductions in product concentration were obtained with P450SU2. In the case of glycerol increased biomass concentrations were observed and glycerol was also found to promote product formation from both strains. It is important to note that this is not an absolute trend and an increase in biomass concentration does not mean a direct increase in product formation. This is seen from maltose experiments which resulted in one of the highest biomass concentrations but had no significant effect on final product concentration.

Table 5.2 Summary of the effect of carbon source on growth.

Carbon Source	Final Biomass	Final Biomass
	Concentration ($\text{g}_{\text{DCW}}\text{L}^{-1}$)	Concentration ($\text{g}_{\text{DCW}}\text{L}^{-1}$)
	<i>E. coli</i> [pQR368]	<i>E. coli</i> [pQR367]
No additional carbon source	9.07	7.84
Maltose	10.11	9.86
Glycerol	11.28	8.82
L-arabinose	11.48	8.55
D-ribose	9.45	7.92
D-fructose	3.00	3.17
D-glucose	2.87	2.91

From the results of these preliminary experiments, described in Figures 5.19 and 5.20, it was decided to further investigate those which showed the greatest improvement in bioconversion. These included ALA and glycerol additions. β -benzoflavone was found to be beneficial for P450SU1 bioconversion however due to solubility issues this was not investigated further. A study on the effects

of varying concentrations of ALA and glycerol as well as a glycerol feeding regime on growth, bioconversion and active P450 expression using the automated sequence shown in Figure 5.14 will be discussed in section 5.2.3.1.

5.2.3.1 The Effect of δ -aminolevulinic Acid (ALA)

P450SU1 and P450SU2 biocatalysts are both hemo proteins and will only actively function with a haem prosthetic group. Haem synthesis begins with the synthesis of ALA from glutamic acid via the C-5 pathway in *E. coli* (Woodard and Dailey 1995; Delcarte et al., 2000). Shin et al. (2007) suggested that the rate-limiting step in this process is the formation of ALA where ALA supplementation to the cell culture has been used to by-pass this issue. Therefore this factor was selected for further studies.

A range of ALA concentrations from 1 mM up to 5 mM were investigated and the growth kinetics are shown in Figure 5.21 A and B. Increasing ALA concentrations from 1 mM up to 5 mM had little effect and similar growth profiles were obtained at each condition tested for both strains where cells grew linearly to a maximum biomass concentration at the 25th hour, after which cell death began.

The effect on bioconversion during the last 5 hours of growth is shown in Figure 5.22 A and B. There is a clear trend where increases in ALA concentration result in increases in product concentration and 5 mM ALA generates the highest product levels. At 5 mM ALA a 63 % and 26 % improvement in 7-hydroxycoumarin concentration was achieved, respectively, after 30 hours of culture compared to when no ALA addition was made.

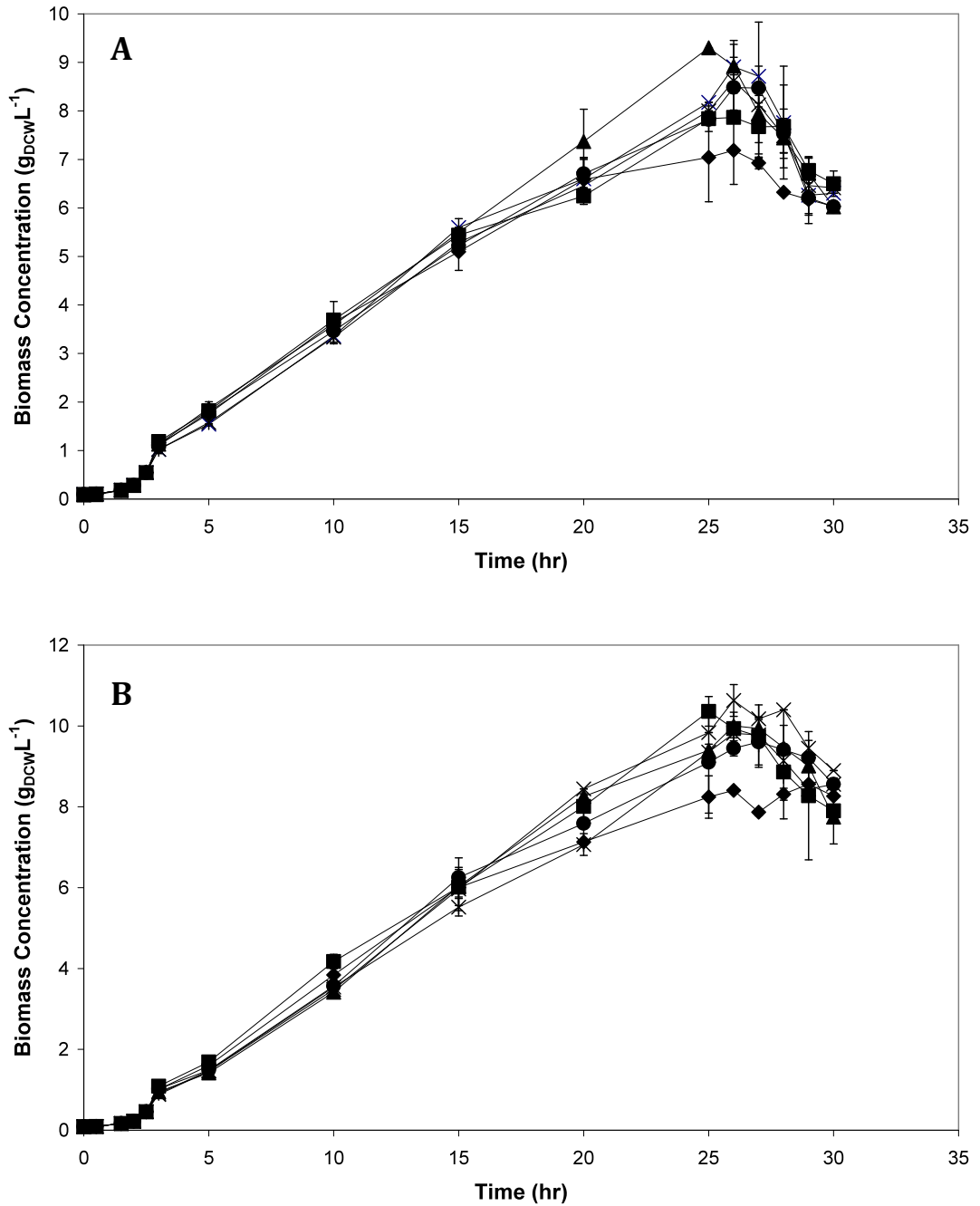


Figure 5.21 The effect of ALA concentration on the culture of **(A)** *E. coli* [pQR367] and **(B)** *E. coli* [pQR368]. 0 mM (\blacktriangle), 1 mM (\times), 2 mM ($*$), 3 mM (\bullet), 4 mM (\blacklozenge), 5 mM (\blacksquare). Error bars indicate the range of measured values about the mean.

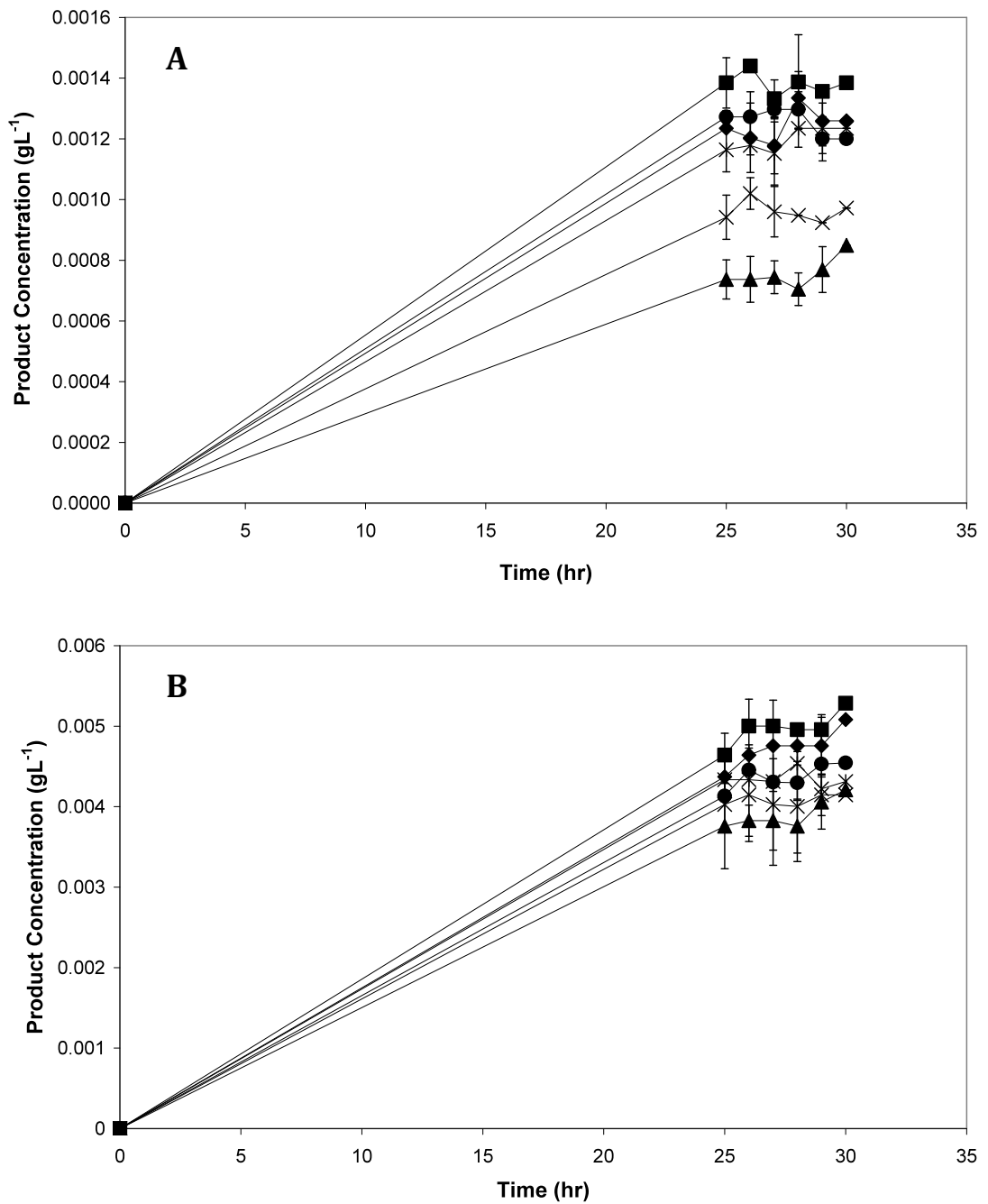


Figure 5.22 The effect of ALA concentration on 7-hydroxycoumarin production from (A) *E. coli* [pQR367] and (B) *E. coli* [pQR368]. 0 mM (▲), 1 mM (×), 2 mM (*), 3 mM (●), 4 mM (◆), 5 mM (■). Error bars indicate the range of measured values about the mean.

Samples collected after 30 hours of growth were analysed using the CO assay at each of the ALA concentrations tested and results are shown in Figure 5.23 A and B. The calculated level of active P450 expression is shown in Table 5.3 for ALA concentrations from 0 to 5 mM. The yield of active P450SU1 and P450SU2 biocatalysts increases at increasing ALA concentration. This result is not in agreement with previous work where ALA was found to have no impact on P450SU1 expression (Hussain and Ward, 2003 b). This finding can be explained by the fact that a low concentration of ALA (1 mM) was previously used whereas significant improvements were observed in this work when ALA concentrations above 2 mM were used. In this study 5 mM ALA was found to be the best concentration for active expression of P450SU2 resulting in a 3-fold improvement. 4 mM ALA was found to be the best concentration for P450SU1 displaying a 3.2-fold improvement over conditions when ALA was not added.

A similar trend was reported by Jansson et al. (2000) but a smaller concentration range was studied from 0.5 mM to 2.5 mM. In their work a 20-fold increase in the expression of the human P450 CYP1B1 was observed at 2.5 mM ALA compared to no ALA addition. Richardson et al. (1995) stated that the influence of ALA may be bigger or smaller depending on the form of cytochrome P450 expressed as observed in this work where a larger improvement was found with P450SU1 compared to P450SU2. Jansson et al. (2000) also found that out of the two cytochrome P450s they investigated human P450 CYP1B1 and cytochrome P450cam (CYP101), there was a more significant improvement on CYP1B1 expression from ALA addition. It has been speculated by Richardson et al. (1995) that poorly expressed enzymes are more prone to degradation. Therefore ALA addition increases haem concentration which promotes protein folding, thus reducing the susceptibility to protease degradation. Due to the fact that ALA is the first committed intermediate in the haem biosynthesis pathway (Lu et al., 2010) it is reasonable to presume that the rate-limiting step in the production of correctly folded active P450 is the synthesis of the haem prosthetic group (Hussain and Ward, 2003 b). Furthermore, Hussain and Ward (2003 b) report that ALA addition causes a combined increase in protein expression and correctly folded holoenzyme with haem in its correct protein environment.

Results obtained in this work confirm that ALA has a positive effect on the level of active holoenzyme which is then utilised for improved bioconversion.

Cornelissen et al. (2011) reported previously that the P450 concentration of CYP153A6 did not directly correspond to specific hydroxylation activity. The authors postulated this to be due to physiological parameters such as substrate mass transfer into the cell or cofactor regeneration limiting the hydroxylation rather than cytochrome gene expression. This could also explain why in this study, even though ALA increases both the expression and bioconversion, a 2-fold increase in expression yield does not result in a 2-fold increase in product formation.

Table 5.3 P450 expression a varying ALA concentrations.

ALA Concentration (mM)	P450SU1 Expression (nmolg⁻¹)	P450SU2 Expression (nmolg⁻¹)
0	27	57
1	34	64
2	49	74
3	58	93
4	88	156
5	87	173

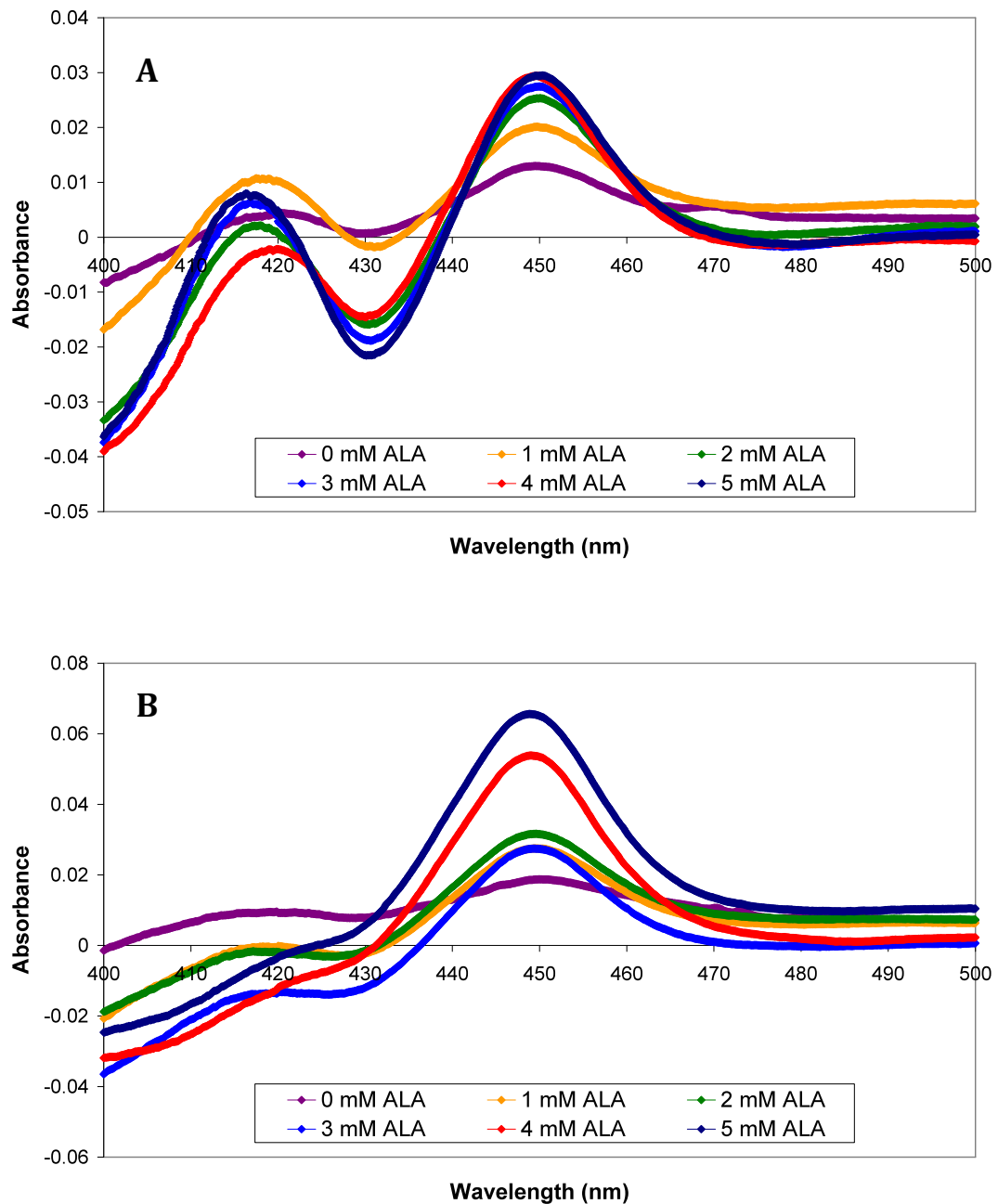


Figure 5.23 Representative CO difference spectra of **(A)** P450SU1 expressed in *E. coli* [pQR367] and **(B)** P450SU2 expressed in *E. coli* [pQR368] cultured at varying ALA concentrations. Samples were from cultures where no 7-ethoxycoumarin was added.

5.2.3.2 The Effect of Glycerol

From the study discussed in section 5.2.3 glycerol was highlighted as a factor beneficial for 7-hydroxycoumarin production. For this reason different glycerol concentrations were tested varying from 2.5 gL⁻¹ to 20 gL⁻¹. In addition a 10 gL⁻¹ glycerol feeding strategy was also evaluated.

Growth kinetics achieved at each of the concentrations tested are shown in Figure 5.24 A and B. Glycerol concentration does not seem to have a significant effect during the main growth phase however there are some differences observed during the last 5 hours of growth. Glycerol might provide an energy source and sustain cell growth for a longer period of time. In the case of *E. coli* [pQR367] cells continue to grow at 2.5 gL⁻¹ and 5 gL⁻¹ glycerol up until the 30th hour whereas typically cell death would begin from the 25th hour onwards. The lower glycerol concentrations tested also seem to promote higher final biomass concentrations. For instance, 5 gL⁻¹ glycerol enabled a final biomass concentration of 10 g_{DCW}L⁻¹ from *E. coli* [pQR367] to be reached compared to only 6.54 g_{DCW}L⁻¹ at 20 gL⁻¹ glycerol concentration. A similar result was achieved with *E. coli* [pQR368] only that 2.5 gL⁻¹ glycerol resulted in the highest final biomass concentration.

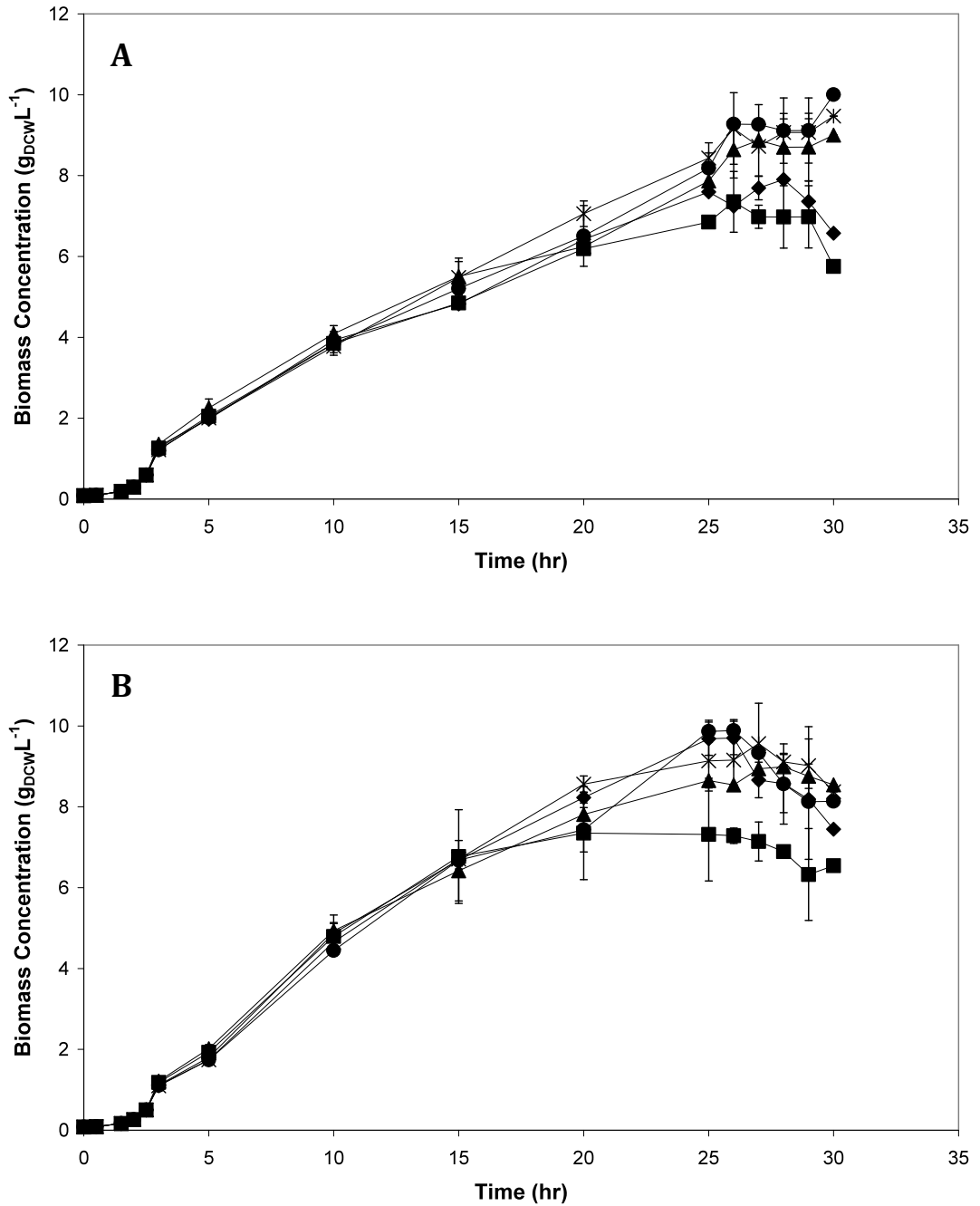


Figure 5.24 The effect of glycerol concentration on the culture of **(A)** *E. coli* [pQR367] and **(B)** *E. coli* [pQR368]. 2.5 gL⁻¹ (*), 5 gL⁻¹ (●), 10 gL⁻¹ (◆), 20 gL⁻¹ (■), fed 10 gL⁻¹ every 5 hours (▲). Error bars indicate the range of measured values about the mean.

From assessing the bioconversion kinetic data shown in Figure 5.25 A and B glycerol feeding and adding 20 gL⁻¹ glycerol to the culture produced the highest levels of 7-hydroxycoumarin from both strains. Glycerol enhances the bioconversion with P450SU2 more than P450SU1 where an 8-fold increase in glycerol concentration leads to a 57 % and 13 % improvement, respectively, in 7-hydroxycoumarin production. In section 5.2.2.5 it was found that product formation begins between the 15th and 20th hour of growth. 20 gL⁻¹ glycerol resulted in the highest levels of product yet a reduction in growth can be observed in Figure 5.24 at this concentration. The benefits of glycerol on the bioconversion could be a result of cells allocating more energy into substrate metabolism and less to growth, accounting for the reduction observed in biomass concentration from the 15th hour. However, this effect was not observed at any other glycerol concentration nor when a glycerol feeding approach was used. This may be because continual or intermittent feeding satisfies the cells increasing demand for energy (Shiloach and Fass, 2005) rather than the rapid depletion of nutrients from the start of exponential growth.

Whole cell bioconversions via P450 monooxygenases are NAD(P)H-dependant where NAD(P)H is generated endogenously and recycled intracellularly as shown in reaction scheme 5.1. Glycerol can be utilised as a reductant and enable NAD(P)H to be regenerated from NAD(P)⁺. In this study, conducted at different glycerol concentrations, whole cell bioconversion yield improved implying that exogenous glycerol may enhance the rate of NAD(P)H regeneration. A similar result has been described by Mouri et al. (2006) where exogenous glycerol was found to improve the oxygenation of the substrate camphor. Mouri et al. (2006) used resting whole cells of *E. coli* expressing P450cam and a glycerol dehydrogenase-mediated NADH regeneration system. This is different from the present work where growing cells and no additional regeneration system were used, however, both display the benefits of glycerol supplementation which can increase the cells natural NAD(P)H regeneration ability.

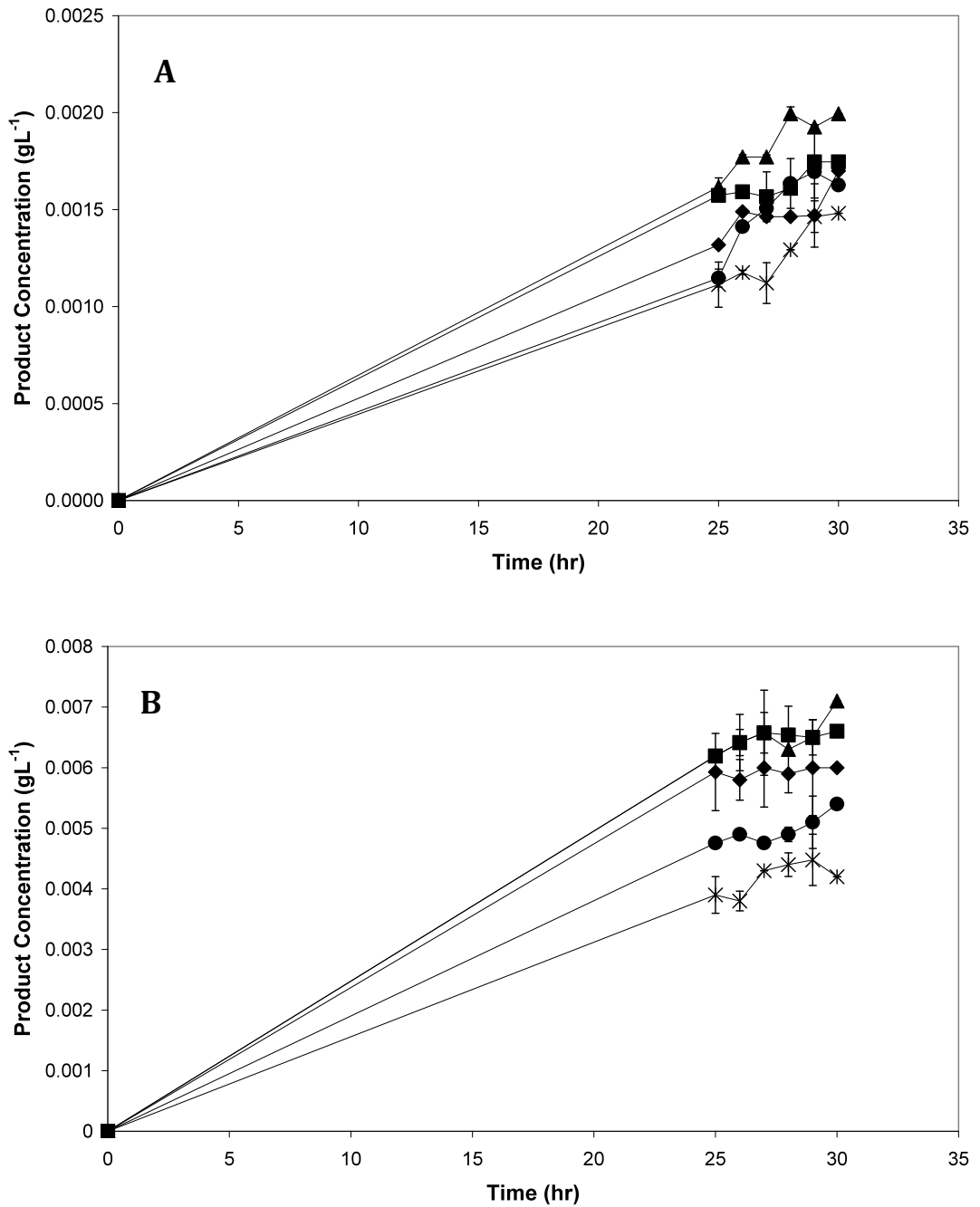


Figure 5.25 The effect of glycerol concentration on 7-hydroxycoumarin production from (A) *E. coli* [pQR367] and (B) *E. coli* [pQR368]. 2.5 gL⁻¹ (*), 5 gL⁻¹ (●), 10 gL⁻¹ (◆), 20 gL⁻¹ (■), fed 10 gL⁻¹ every 5 hours (▲). Error bars indicate the range of measured values about the mean.

Figure 5.26 shows the CO difference spectra achieved at each of the conditions tested with glycerol for P450SU2. The spectra for P450SU1 were found to be of poor quality thus have not been included in this work. Table 5.4 shows the active yield of P450SU2 where both a concentration of 20 gL⁻¹ and glycerol feeding method produced the highest yields of active P450. The addition of glycerol to the culture is proposed to improve protein folding as previously reported by Kagawa and Cao (2001) and Vail et al. (2005). As observed from the ALA study the level of active protein expression is responsible for the improvements in bioconversion observed.

Table 5.4 P450 expression at varying glycerol concentrations.

Glycerol Concentration* (gL ⁻¹)	P450 Expression (nmolg ⁻¹)
2.5	47
5	47
10	99
20	104
10 Feed	122

* Concentration does not include the 4 mL⁻¹ glycerol in TB media formulation.

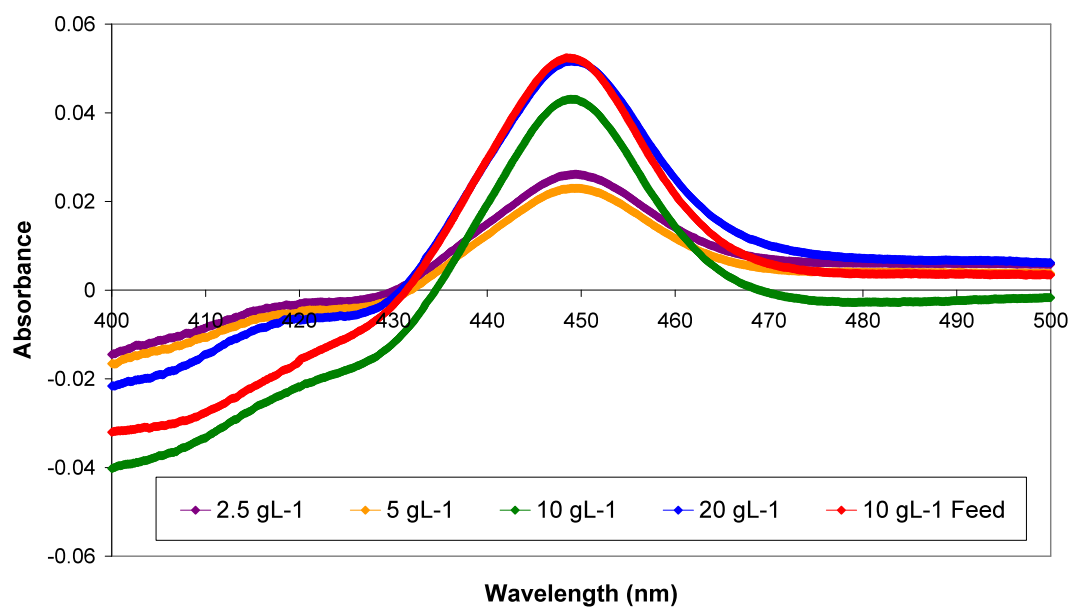


Figure 5.26 Representative CO difference spectra of P450SU2 expressed in *E. coli* [pQR368] cultured at varying glycerol concentrations. Samples were from cultures where no 7-ethoxycoumarin was added.

5.2.3.3 The Effect of 7-ethoxycoumarin Concentration

To evaluate any substrate inhibition effects 7-ethoxycoumarin was tested at three initial concentrations (0.1 mM, 1 mM and 2 mM). The concentration of product was found to increase with substrate concentration from 0.1 mM up to 1 mM as shown in Figure 5.27. In the case of 0.1 mM substrate concentration no product was detected from P450SU1 bioconversion, probably due to very low product levels or poor substrate contact with the cell. Doubling the substrate concentration from 1 mM up to 2 mM further reduced the product concentration by 13 % for P450SU1 and 55 % from P450SU2, indicating potential substrate inhibition effects. To determine the operating substrate concentration a study was designed to test a range of substrate concentrations. This study was only conducted with P450SU2 as although product concentrations differed a similar trend was achieved from P450SU2 and P450SU1 as presented in Figure 5.27. Additionally, product levels achieved at reduced substrate concentrations (0.1 mM) were undetectable with P450SU1 making accurate assessment of usable substrate concentrations difficult.

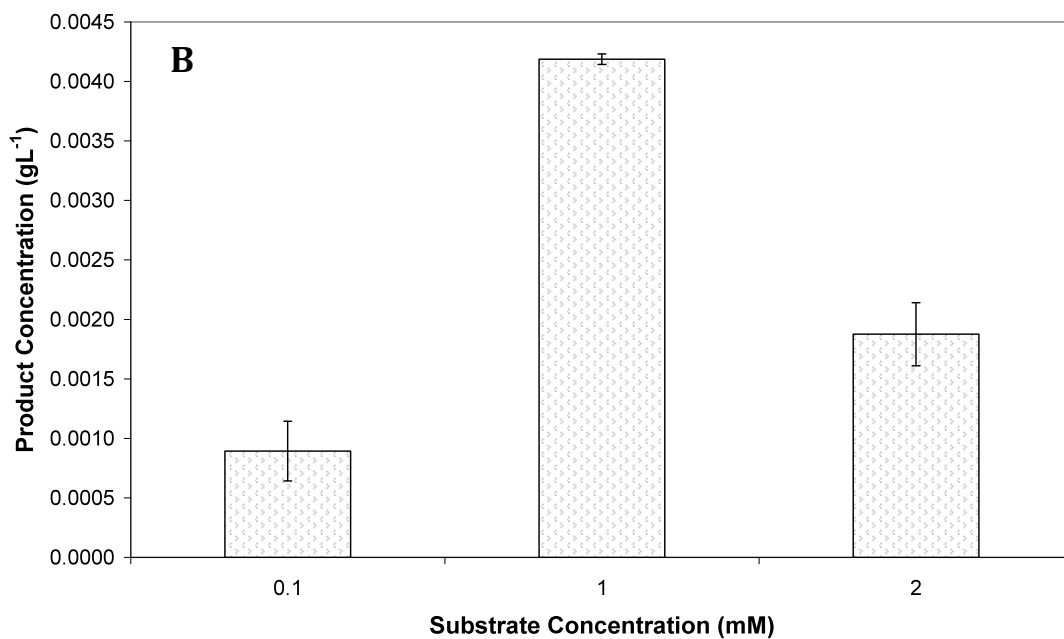
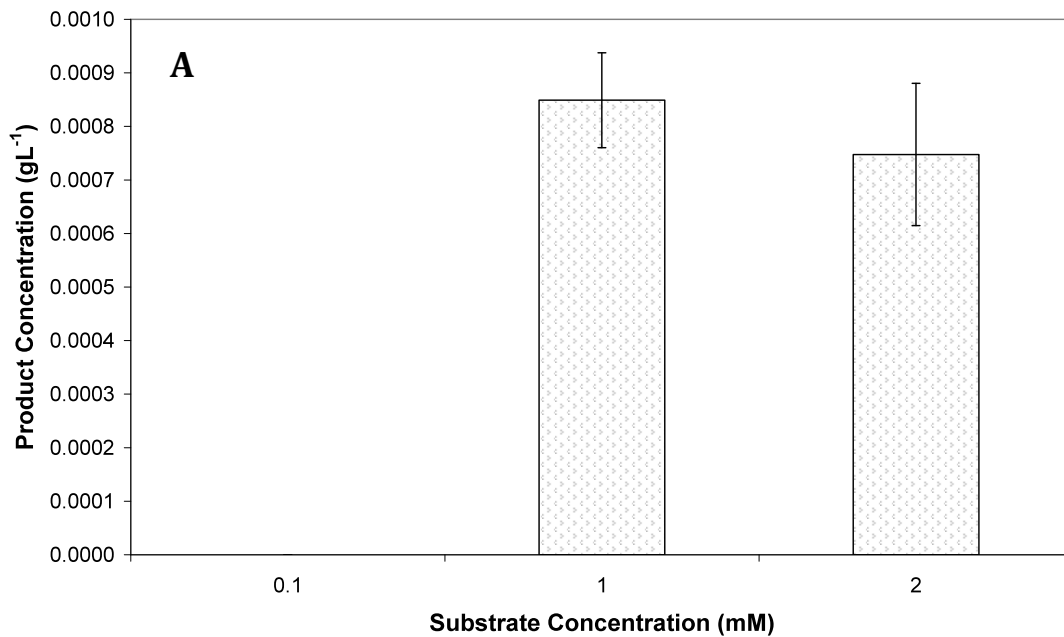


Figure 5.27 The effect of substrate concentration on 7-hydroxycoumarin production from (A) *E. coli* [pQR367] expressing P450SU1 and (B) *E. coli* [pQR368] expressing P450SU2. Experiments were conducted as described in section 2.3.2.3. Error bars indicate the range of measured values about the mean.

According to the results obtained the best operating concentration was likely to be between 0.1 mM and 1 mM therefore concentrations from 0.5 mM up to 1 mM were tested using the automated approach shown in Figure 5.14. It is important to note that no haem precursors were added in this study, cells were induced and substrate was added at the appropriate time points. Figure 5.28 shows the effects of substrate concentration on the growth of cells. The highest biomass concentration was achieved at 1 mM substrate and the lowest at 0.5 mM substrate. This may imply that 7-ethoxycoumarin is utilised as a carbon source.

The bioconversion kinetic data is shown in Figure 5.29 where a 2-fold increase in substrate concentration causes over a 2-fold increase in final product concentration. Studies on the effects of substrate concentration were not reported with P450SU1 or P450SU2 making it challenging to draw realistic and meaningful conclusions. However, Yamazaki et al. (1999) found that the rate of O-dealkylation by human liver cytochrome P450 increases with increasing 7-ethoxycoumarin concentration up to 1 mM, and the rate increase reduces as concentrations approach 1 mM. It was thus decided that the original protocol using 1 mM substrate would continue to be used as it was demonstrated that this is below any potential substrate inhibitory limits.

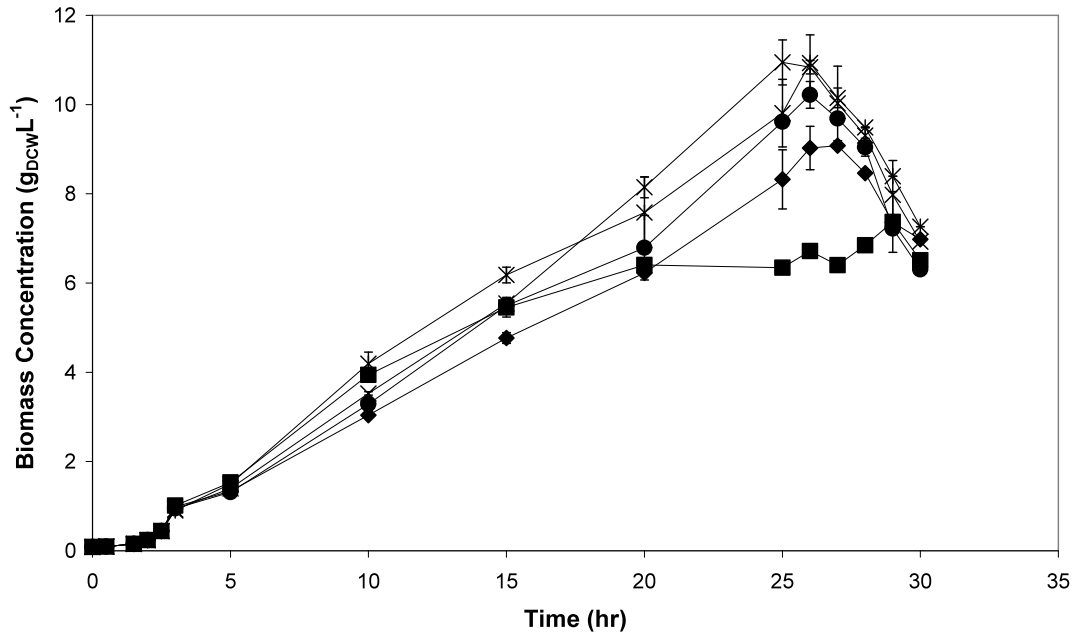


Figure 5.28 The effect of 7-ethoxycoumarin concentration on the culture of *E. coli* [pQR368]. 0.5 mM (■), 0.6 mM (◆), 0.7 mM (●), 0.8 mM (*), 1 mM (×). Error bars indicate the range of measured values about the mean.

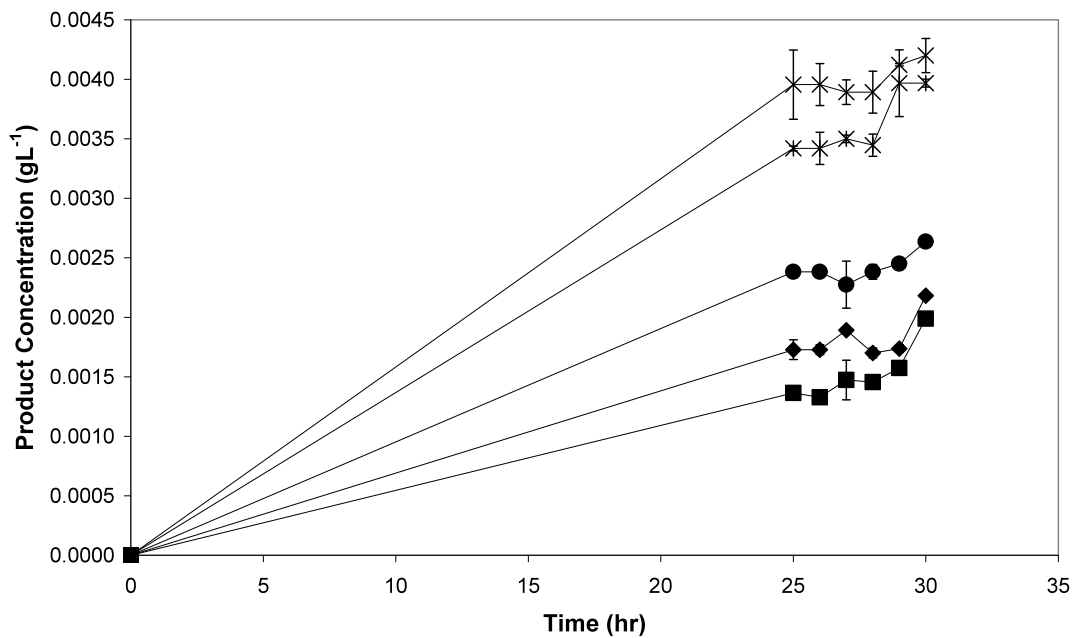


Figure 5.29 The effect of substrate concentration on 7-hydroxycoumarin production from *E. coli* [pQR368]. 0.5 mM (■), 0.6 mM (◆), 0.7 mM (●), 0.8 mM (*), 1 mM (×). Error bars indicate the range of measured values about the mean.

5.2.3.4 Improved Bioconversion of 7-ethoxycoumarin

A number of factors were tested (haem precursors, sugars, media additions) and some were shown to cause an improvement in the bioconversion yield of P450SU1 and P450SU2. It was then thought appropriate to run a process using those factors which were found to promote both biocatalyst expression and bioconversion product yield improvement. This included additions of 5 mM ALA to prevent haem formation from becoming limiting, 20 gL⁻¹ glycerol, which was found to enhance NAD(P)H regeneration and drive correct protein folding, and 1 mM substrate concentration which was below substrate inhibitory limits. The improved process was carried out alongside a control process with no factor addition. The growth kinetics for both processes are shown in Figure 5.30 A. The addition of glycerol is presumed to be responsible for sustaining the growth of cells up until the 30th hour, however this result was surprising as in section 5.2.3.2 this results was not seen when cells were grown at 20 gL⁻¹ glycerol. The onset of cell death at the 25th hour is observed in cultures where ALA and glycerol were absent.

A comparison of the bioconversion kinetics in Figure 5.30 B shows a clear improvement in product formation from cultures containing both ALA and glycerol. The final concentration of 7-hydroxycoumarin produced from P450SU1 with and without media supplementation was 4.02 ± 0.19 mgL⁻¹ and 0.85 ± 0.09 mgL⁻¹ corresponding to product yields of 2.1 % and 0.4 % respectively. The final concentration of 7-hydroxycoumarin produced from P450SU2 with and without media supplementation was 6.50 ± 0.10 mgL⁻¹ and 4.20 ± 0.03 mgL⁻¹ corresponding to product yields of 3.4 % and 2.2 % respectively. There is an overall 5-fold and 1.5-fold improvement from *E. coli* [pQR367] expressing P450SU1 and *E. coli* [pQR368] expressing P450SU2, respectively. Additionally, in the case of *E. coli* [pQR367] where typically there is little increase during the last 5 hours of culture, the culture additions also increased the rate of product formation.

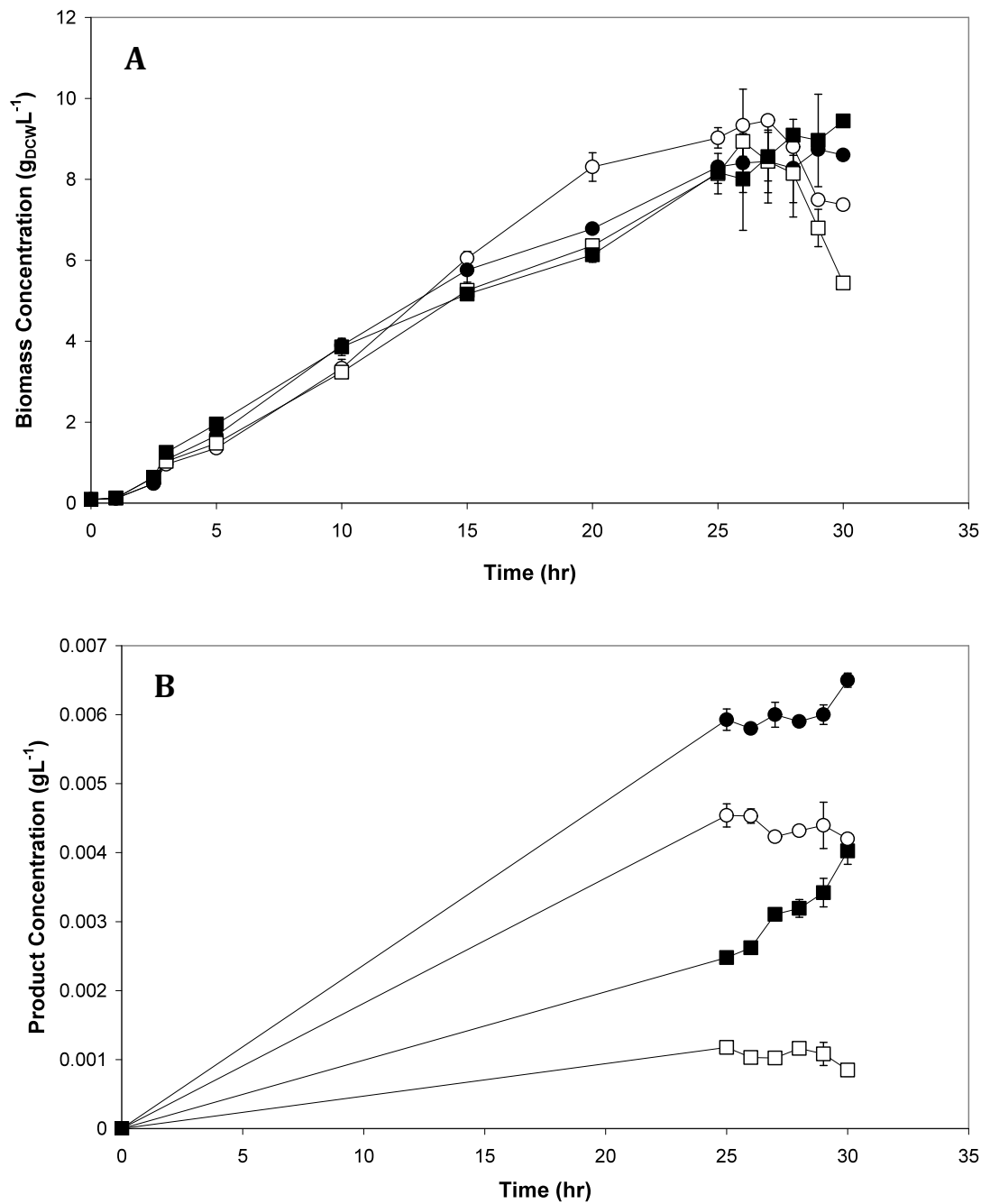


Figure 5.30 (A) Growth kinetics and (B) time course of 7-hydroxycoumarin production from *E. coli* [pQR367] (■) and *E. coli* [pQR368] (●) with 20 gL⁻¹ glycerol, 5 mM ALA and 1 mM 7-ethoxycoumarin (closed symbols) and no media supplementation with 1 mM 7-ethoxycoumarin (open symbols). Error bars indicate the range of measured values about the mean.

Finally, the media additions resulted in significant improvements to the level of active P450 expression shown in Figure 5.31. The corresponding yields are presented in Table 5.5. A 5-fold increase is observed from both cytochrome P450s. It is interesting that, even though the yield of active P450SU1 has been significantly increased, the inactive P420 peak is present in the CO spectra. The addition of ALA should enable an adequate supply of correctly formed haem prosthetic group, however, the presence of apoenzyme indicates there is still some variable preventing the formation of fully functioning holoenzyme. Potentially, even if more haem is formed, the limiting step could be when incorporating it into the active site as previously described by Healy et al. (2002). Healy et al. (2002) also refers to particular conditions which cause the transition of the active P450 to the P420 state, including pressure, temperature variations or extreme pH values. These are not thought to be likely causes considering identical culture conditions for *E. coli* [pQR367] and *E. coli* [pQR368] were setup and no P420 was detected from *E. coli* [pQR368]. It therefore must be a factor specific to P450SU1 which makes it more susceptible to converting to the inactive P420 form.

Table 5.5 Comparison of P450 study with media additions.

[ALA] (mM)	[Glycerol] (gL ⁻¹)*	P450SU1		
		X _{Final} (gDCwL ⁻¹)	P _{Final} (mgL ⁻¹)	Expression (nmolg ⁻¹)
0	0	5.44	0.85	27
5	20	9.44	4.02	134
		P450SU2		
		X _{Final} (gDCwL ⁻¹)	P _{Final} (mgL ⁻¹)	Expression (nmolg ⁻¹)
0	0	7.37	4.20	57
5	20	8.60	6.50	293

* Concentration does not include the 4 mL⁻¹ glycerol in TB media formulation.

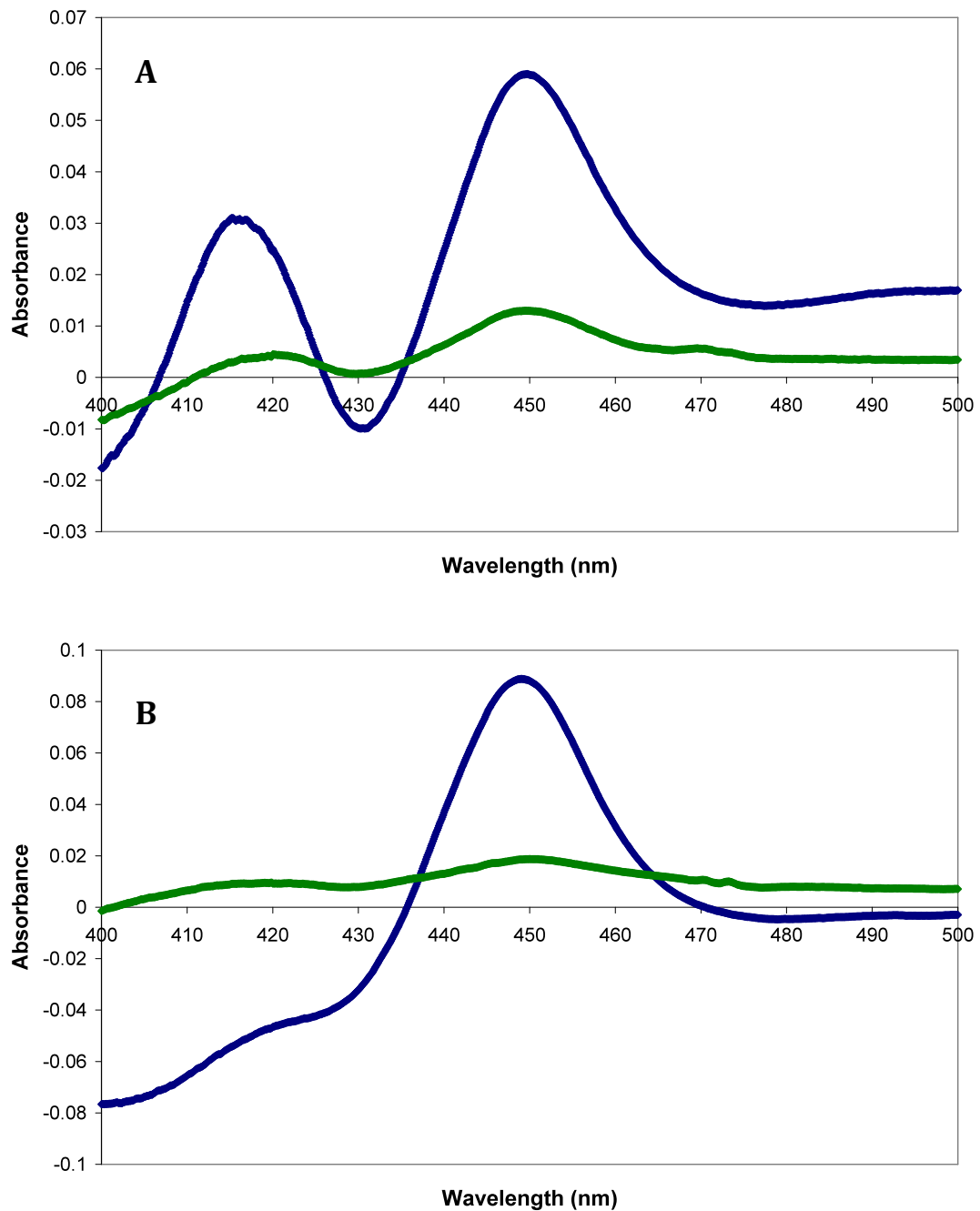


Figure 5.31 CO difference spectra of **(A)** P450SU1 expressed in *E. coli* [pQR367] and **(B)** P450SU2 expressed in *E. coli* [pQR368] with (blue line) and without (green line) the addition of 5 mM ALA and 20 gL⁻¹ glycerol. Samples were from cultures where no 7-ethoxycoumarin was added.

5.3 Concluding Remarks

In Chapter 4 it was found that automated approaches could be used to rapidly optimise the production of the oxidative biocatalyst CHMO. Cytochrome P450s have versatile catalytic properties however have failed to be successfully utilised to their full potential at an industrial scale. Little is known on novel P450s and the ability to rapidly collect process data on novel strains and biocatalysts is a desirable feature. Automated approaches enable data collection during the initial development stage, where strains, which initially would be rejected due to poor yields, can be further investigated for determination of their true potential. Additional benefits include a greener and sustainable approach to chemical synthesis of target compounds without the need for dangerous or toxic reagents. For these reasons the initial automated approach was applied to two novel P450 expression systems *E. coli* [pQR367] expressing P450SU1 and *E. coli* [pQR368] expressing P450SU2.

Shake flask cultures, as described by Hussain and Ward (2003 b), were successfully reproduced confirming the conditions for active P450 expression and bioconversion. Using these initial culture conditions the microscale approach was developed where 96-DSW plates enabled the collection of reproducible growth and bioconversion kinetics across the plate and on different days. Due to the extended culture times there was an issue of evaporation, however, the use of a gas permeable membrane was found to adversely affect the oxygen transfer. By limiting the culture to 30 hours, using a sacrificial well approach along with the maximum fill volume of 1000 μL liquid loss did not exceed more than 15 % of the well contents and was within reported ranges enabling valid data to still be collected. Using the automated approach cells of *E. coli* [pQR367] and *E. coli* [pQR368] grew at a specific growth rate of 1.56 h^{-1} and 1.84 h^{-1} and reached final biomass concentrations of $9.33 \text{ g}_{\text{DCW}}\text{L}^{-1}$ and $9.01 \text{ g}_{\text{DCW}}\text{L}^{-1}$ respectively. P450SU1 and P450SU2 were actively expressed at a yield of 29 nmol g^{-1} and 53 nmol g^{-1} producing $0.98 \pm 0.062 \text{ mgL}^{-1}$ and $3.55 \pm 0.17 \text{ mgL}^{-1}$ respectively of 7-hydroxycoumarin. This represented 7-ethoxycoumarin

conversions of 0.5 % and 1.9 % from P450SU1 and P450SU2, respectively and further studies were conducted to improve this bioconversion yield.

An initial study was performed and 14 factors previously found to positively affect enzymatic expression, were tested. Three of these were selected for a complete analysis of growth, expression and bioconversion. The automated approach successfully identified limitations in haem prosthetic group formation, NAD(P)H regeneration and substrate inhibitory limits enabling the correct concentrations of the haem precursor ALA, carbon source glycerol and substrate 7-ethoxycoumarin to be used. By combining the best conditions found in each study of 5 mM ALA, 20 gL⁻¹ glycerol and 1 mM 7-ethoxycoumarin P450SU1 and P450SU2 were actively expressed at a yield of 134 nmolg⁻¹ and 293 nmolg⁻¹ producing 4.02 ± 0.19 mgL⁻¹ and 6.50 ± 0.10 mgL⁻¹ respectively of 7-hydroxycoumarin. This represented 7-ethoxycoumarin conversions of 2.1 % and 3.4 % from P450SU1 and P450SU2, respectively. These results corresponded to a 5-fold improvement in enzymatic expression and a 5-fold and 1.5-fold increase in product levels from P450SU1 and P450SU2, respectively.

The automated platform was demonstrated to be an effective tool to quickly test a range of process parameters. It can be used in two formats as an initial screen for end point bioconversion performance or to gain informative data on growth, whole cell bioconversion and active P450 yield depending on the users requirements. Information on these important steps is crucially important early during process design in order to determine the best culture, expression and bioconversion conditions for P450 biocatalysts. The ability to improve a process at the microscale has been achieved with two oxidative systems, however, if this data is to be effectively exploited the same results need to be reproduced at larger scales of operation. Due to the geometrical differences between microwells and stirred bioreactors the final objective of the thesis is to demonstrate predictive scale-up of the data collected at the microscale. Chapter 6 presents the lab/pilot scale studies conducted in this work.

6 Establishing the Scalability of Oxidative Biocatalytic Microscale Processes[†]

6.1 Introduction

Automated microscale approaches have been applied for the quantitative data collection and rapid bioprocess evaluation of two whole cell oxidative biocatalysts. Knowledge gained at the microscale can be used to effectively inform steps in bioprocess development. However, in order to build confidence in the data collected, there needs to be a suitable scale-up methodology demonstrating comparable results at larger scales of operation. Cell growth, maintenance and metabolite production are reliant on oxygen as a crucial substrate in many bacterial processes. One approach proved to be effective for scale-up of aerobic microbial culture is the use of a matched gas liquid mass transfer coefficient (K_{La}) approach (Ferreira et al., 2005; Micheletti et al., 2006; Islam et al., 2008; Kensy et al., 2009; Marques et al., 2009; Marques et al., 2010; Marques et al., 2012). During aerobic culture oxygen needs to be transported from the gas bubble to the medium containing cells. The solubility of oxygen in water is approximately 0.272 mmolL^{-1} at $25 \text{ }^\circ\text{C}$ and 101 kPa air pressure thus solubility may represent a transport bottleneck (Doran, 2003). The rate at which oxygen is transported OTR ($\text{mmolL}^{-1}\text{h}^{-1}$) will depend on K_{La} (h^{-1}) and a driving force $C_L^* - C_L$, where C_L (mmolL^{-1}) is the dissolved oxygen concentration in the bulk liquid and C_L^* (mmolL^{-1}) is the liquid phase concentration which is in equilibrium with the gas phase (Bailey and Ollis, 1986). This relationship is described by Equation 6.1:

$$OTR = K_L a (C_L^* - C_L) \quad (\text{Eq. 6.1})$$

In the case of K_{La} this is affected by a number of factors including culture vessel design (number of impellers and baffles), culture operating conditions

[†] Some of the results presented in this chapter are included in Baboo et al (2012), 'An automated microscale platform for evaluation and optimization of oxidative bioconversion processes', *Biotechnology Progress*, 28, 392-405, DOI: 10.1002/btpr.1500.

(temperature and volume), culture growth and physical fluid properties such as viscosity and media electrolytes. It can therefore be a challenge to keep a constant K_La especially in the case of growing cultures where Vashitz et al. (1989) found K_La to increase with oxygen uptake by the microorganism. It may therefore be appropriate to consider a biological enhancement factor termed E which takes into account mass transfer enhancement due to oxygen uptake by the microorganism. In order to establish an appropriate scale-up criteria K_La needs to be determined experimentally or calculated using available correlations. In this study K_La was determined experimentally as described in section 2.6.1.2. A number of experimental approaches are available for example it is possible to use growing cells to follow the depletion of oxygen (direct methods) or use cell free based methodologies (indirect methods).

One of the methods using growing cells is the oxygen-balance method or gas phase analysis and it can be conducted during normal operation whilst culturing (Bailey and Ollis, 1986). It involves measuring the oxygen content in the gas streams from the fermenter inlet and outlet. Using steady state mass balance analysis and from very accurate measurements of partial pressure, temperature and flow rate K_La values can be determined. It is quite a reliable method if compared to others, however it is very dependant on the accurate measurement of gas composition and considerable errors can be introduced in the absence of sensitive equipment available for these measurements.

A common method involves analysing the dynamic change in dissolved oxygen concentrations during batch cell culture to measure K_La . Bandyopadhyay et al. (1966) describes a method which involves an initial de-oxygenation of the culture by switching the gas supply off so that the rate at which the dissolved oxygen concentration decreases is equivalent to the oxygen consumption of actively respiring cells. The oxygen supply is then turned back on and continuously monitored until a steady oxygen concentration is reached. Measurements are carried out using an oxygen electrode where, in the case of high probe response times, an appropriate correction has been applied. Similarly, the dynamic pressure method uses pressure to change the interfacial oxygen concentration (Linek et al., 1989). Dynamic measurements are inappropriate for

viscous cultures as large residence times of bubbles affect the accuracy of measurement (Heijnen et al., 1980). Additionally, very low oxygen concentrations make measurements difficult and for this reason modifications to the method have been proposed by Gomez et al. (2006) using pure oxygen.

Indirect measurements of K_{La} can be carried out in the presence of metal catalysts, responsible for catalysing the reaction of sodium sulfite in the presence of dissolved oxygen to produce sulfate. In this method K_{La} is determined from the rate of sulfite consumption. It is relatively easy to carry out and the method has been used previously (Thibault et al., 1990; Yasukawa et al., 1991; Hermann et al., 2003; Kensy et al., 2009), however it was found to overestimate the K_{La} as differences in physicochemical properties to culture broths cause changes in the hydrodynamics of the solution (Garcia-Ochoa and Gomez, 2009). A few alternative procedures involving chemical reactions exist. For example, Ortiz-Ochoa et al. (2005) used catechol-2,3-dioxygenase bio-oxidation of catechol yielding 2-hydroxymuconic semialdehyde to measure K_{La} in 4 mL cuvettes, Warnecke and Hubmann (1989) used hydrazine oxidation, while Duetz et al. (2004) used a horseradish peroxidase and glucose oxidase coupled enzyme reaction. These enzymatic alternatives do have the advantage of being applicable to small-scales thus reducing assay times, however present difficulties when applied at large-scale and as this methods do not take place in actual culture broths may also result in overestimated K_{La} measurements.

One final method based on the dynamic approach without the requirement for cells is known as dynamic gassing out. In this method nitrogen is initially gassed into the vessel and once the solution has been fully de-oxygenated, the media is re-oxygenated under typical culture aeration techniques (agitation and airflow). Taking into account the probe response time and the rate of re-oxygenation, the K_{La} can be measured accurately. While the most accurate K_{La} measurement would be achieved using the cell population of interest, this presents experimental challenges including inoculum preparation, contamination prevention and requirement for cell culture control during measurement, thus making the use of actively growing cells inconvenient. Considering the issues reported with chemical approaches the gassing out approach was selected in this

work due to its simplicity and relative accuracy. In addition recent development of miniature probes (John et al., 2003) allows the same approach to be used at the microscale. Its application to K_{La} measurements leading to the successful scale-up from microwell plate format to stirred bioreactors has also been previously demonstrated (Ferreira-Torres et al., 2005; Islam et al., 2008).

The use of a miniature oxygen probe incorporated into a microwell plate for K_{La} measurements via the dynamic gassing out approach has been reported by Doig et al. (2005). Using this methodology Ferreira-Torres et al. (2005) measured K_{La} in both microwell and bioreactor configurations and successfully scaled up microscale growth and bioconversion using *E. coli* TOP10 [pQR239] expressing CHMO to a 2 L stirred bioreactor. It was found that operating under non-oxygen limited conditions was crucial in enabling predictive scale-up. Moreover, Funke et al. (2009) has stated that oxygen unlimited cultivations are necessary to prevent the selection of suboptimal strains, media and culture condition. Islam et al. (2008) applied scale-up on the basis of matched K_{La} to the culture of *E. coli* BL21 (DE3) expressing firefly luciferase where microwell cell growth, protein expression and substrate utilization were accurately reproduced at 7.5 L and 75 L stirred bioreactor scale. The provision of adequate mixing and gas liquid distribution were found to be very important, as studies conducted at a relatively low value of K_{La} did not present reproducible performance between scales. In this work it is hypothesized that a matched K_{La} approach can reliably reproduce microscale growth and bioconversion kinetics of the oxidative biocatalysts CHMO expressed in *E. coli* TOP10 [pQR210] and cytochrome P450SU1 and P450SU2 expressed in *E. coli* [pQR367] and *E. coli* [pQR368], respectively, at stirred tank bioreactor scale. A discussion on alternative scale-up strategies and their applicability to microscale will conclude this chapter.

6.2 Results and Discussion

6.2.1 Scale Translation at Matched K_{La} – Application to CHMO

It was first of interest to assess if the matched K_{La} approach would reproduce data collected at the microscale in a 75 L stirred tank bioreactor. In Chapter 3 the similarity of the strains *E. coli* TOP10 [pQR239] and *E. coli* TOP10 [pQR210] was confirmed. Initial K_{La} measurements at varying agitation rates and fill volumes were conducted previously in a modified 96-DSW plate equipped with a fibre optic oxygen sensor using LB-glycerol medium (Ferreira-Torres, 2008). A K_{La} of 115 h^{-1} was measured previously at a shaker speed of 1000 rpm and fill volume of 500 μL . Whilst in prior work the K_{La} -matched approach was applied to the bioconversion stage, it was of interest to extend the study it to the whole process sequence using *E. coli* TOP10 [pQR210]. Islam (2007) obtained a correlation between K_{La} and agitation rate (N) in the 75 L stirred tank bioreactor shown in Equation 6.2 from a series of gassing-out K_{La} measurements studies. This correlation was obtained from experiments conducted at a working volume of 45 L of TB medium with 0.2 mL^{-1} PPG, at room temperature and an airflow of 1 vvm.

$$K_{La} = 0.505N - 78.7 \quad (\text{Eq. 6.2})$$

Using this correlation a K_{La} of 115 h^{-1} can be achieved in the 75 L stirred tank bioreactor if operated at an agitation rate of 384 rpm. Table 6.1 contains the operating conditions selected for the present study at microwell and 75 L scale using a matched K_{La} approach where K_{La} was obtained from previous measurements (Islam, 2007 and Ferreira-Torres, 2008). To ensure both processes were operated under identical conditions no pH control was used and microscale cultures were inoculated with a sample taken from the inoculated 75 L bioreactor as described in section 2.4.1.2. This would eliminate any differences arising from inoculum preparation, media sterilisation or the use of antifoam agents. In this way both processes would begin under identical conditions and optical densities. Samples were taken periodically during

microscale and pilot plant processes to monitor the growth and bioconversion progress and results are shown in Figure 6.1 A and B respectively.

Table 6.1 Comparison of microwell and bioreactor parameters.

Parameter	96-DSW Microwell Plate	75 L Stirred Bioreactor
Agitation Rate	1000 rpm Throw: 3 mm	384 rpm
Vessel Total Volume	2 mL	75 L
Working Volume	500 μ L	45 L
$K_L a$	115 h ⁻¹	115 h ⁻¹
Airflow	n/a	1 vvm
Temperature	37 °C	37 °C

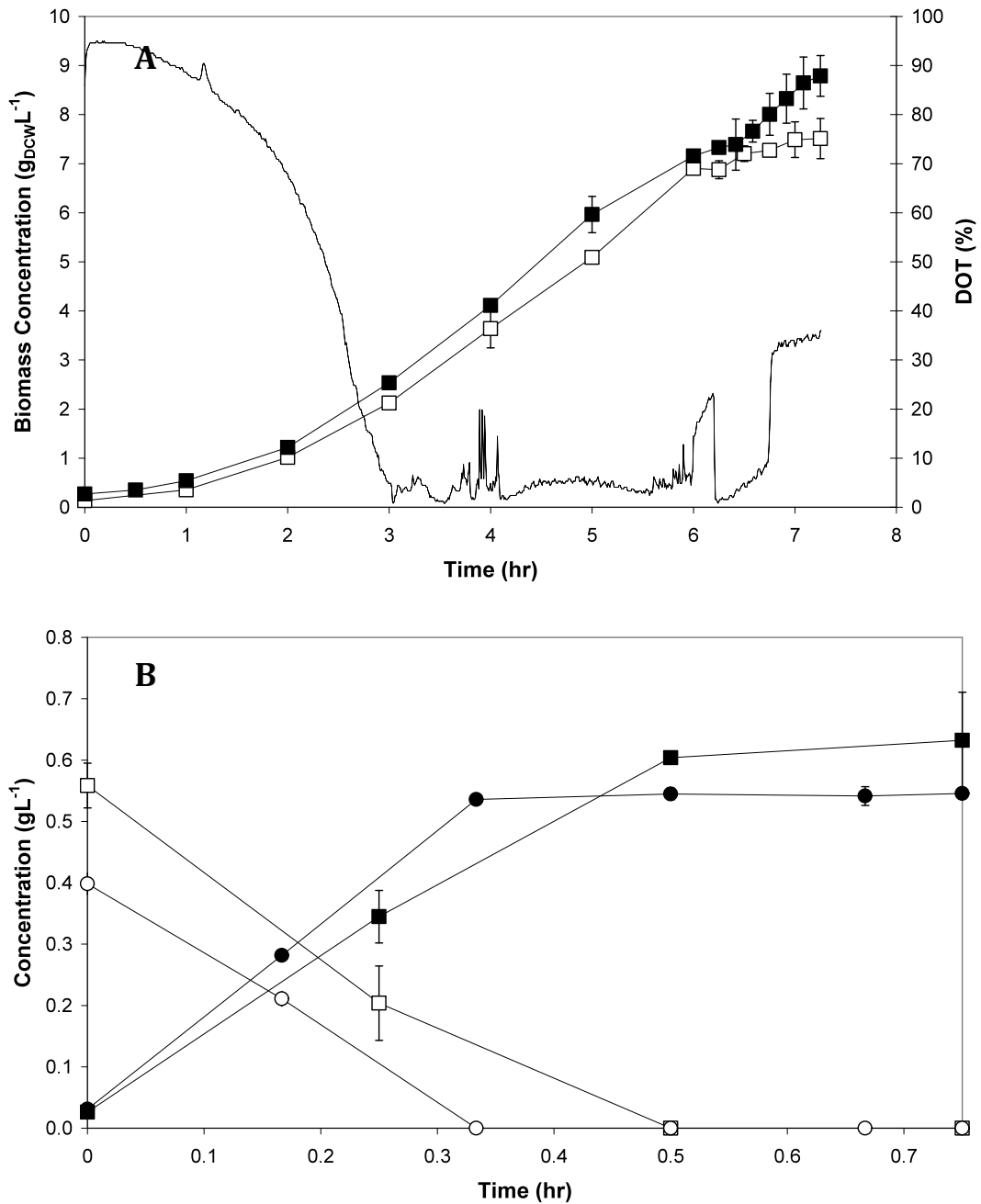


Figure 6.1 (A) Growth kinetics at a matched K_{La} of 115 h^{-1} for *E. coli* TOP10 [pQR210] in a 75 L bioreactor (working volume 45 L) (■) and 96-DSW plate with a 500 μL fill volume (□) and corresponding 75 L DOT profile (----). Error bars indicate the standard deviation of triplicate optical density readings for the 75 L process and the range of measured values about the mean for the microwell process. **(B)** Bioconversion kinetics of CHMO with 0.5 g L^{-1} bicyclo[3.2.0]hept-2-en-6-one (unfilled symbols) to lactone product (filled symbols) at a matched K_{La} of 115 h^{-1} in a 75 L bioreactor (●) and 96-DSW plate (■). Error bars indicate the range of measured values about the mean.

During the seven-hour culture cells grew in a similar fashion at specific growth rates of 0.89 h^{-1} and 0.77 h^{-1} up to final biomass concentrations of $8.8 \text{ g}_{\text{DCW}}\text{L}^{-1}$ and $7.5 \text{ g}_{\text{DCW}}\text{L}^{-1}$ for microwell and 75 L processes respectively. There is a gradual reduction in the 75 L DOT profile shown in Figure 6.1 A which precedes a rapid decline after 2 hours of culture where the fastest oxygen uptake rate is observed during exponential growth. The DOT profile obtained in this study compares well to that achieved by Ferreira-Torres, (2008) in a 2 L stirred bioreactor where the DOT achieves maximum values at 4, 6 and 7 hours. The presence of such peaks could be attributed to a depletion of primary carbon sources (Turner et al., 1994; Neubauer et al., 1995), to the addition of the bioconversion substrate which has been reported to be harmful to the cell (Shitu et al., 2009) and to the onset of cellular death, respectively. In terms of the 1 hour bioconversion similar substrate consumption and product formation profiles are observed in Figure 6.1 B. Full conversion was achieved in less than 30 minutes and a space time yield of $1.8 \text{ gL}^{-1}\text{h}^{-1}$ was calculated for the 75 L reactor. From initial rates of product formation specific activities of $21 \text{ U}_{\text{g}_{\text{DCW}}}^{-1}$ and $23 \text{ U}_{\text{g}_{\text{DCW}}}^{-1}$ were calculated for the microwell and 75 L processes respectively. A lower than expected 75 L initial substrate concentration is shown in Figure 6.1 B even though the same concentration was added to both cultures. High aeration rates in bioreactors can contribute to increased evaporation of volatile substrates and may be an explanation for the results obtained in this work (Zambianchi et al., 2004). The 10 % higher specific activity achieved at the 75 L scale is a result of the lower than expected initial substrate concentration added to the reactor. A summary of the comparable data obtained at both scales is shown in Table 6.2. This study has established the use of matched $K_{\text{L}}a$ approaches to reproduce microscale growth and bioconversion kinetics, hence in section 6.2.2 its application to the optimised process described in Chapter 4 will be presented.

Table 6.2 Summary of growth and bioconversion kinetics achieved at a matched K_{La} of 115 h^{-1} .

Growth			
Scale	$\mu \text{ (h}^{-1}\text{)}$	$X \text{ Final (g}_{DCW}\text{.L}^{-1}\text{)}$	
96-DSW (500 μL)	0.89	7.5	
75 L Bioreactor (45 L)	0.77	8.8	
Bioconversion			
Scale	Initial Lactone* Formation rate ($\mu\text{molL}^{-1}\text{min}^{-1}$)	Specific Activity (Ug^{-1})	Yield (%)
96-DSW (500 μL)	155	21	120
75 L Bioreactor (45 L)	203	23	106

* Produced from bicyclo[3.2.0]hept-2-en-6-one.

6.2.2 Scale Translation at Matched K_{La} – Optimised Production of CHMO

6.2.2.1 K_{La} Measurement Using Dynamic Gassing Out

K_{La} values ranging from $100 - 300 \text{ h}^{-1}$ in standard stirred-tank bioreactors of volumes between $30 - 50000 \text{ L}$ were reported by Trilli (1986). Previous studies have established that microwell plates are characterised by K_{La} values in the lower range of those achieved using stirred bioreactors as shown in Table 6.3. Therefore it should be possible to achieve conditions in both configurations where the K_{La} is matched. Proof of concept was demonstrated in section 6.2.1, however the matched K_{La} was based on previous correlations and was not experimentally measured.

Table 6.3 Range of K_La values achievable in microwell formats compared to stirred bioreactors.

Microwell Format	Microwell K_La range (h^{-1})	Bioreactor	Bioreactor K_La range	Measurement Method
Ferreira-Torres, (2008)				
96-DSW plate	16 – 186 ^{*†}	2 L	40 – 168 [*]	Dynamic gassing out
Islam, (2007)				
48-Rectangular flat base wells	0.7 - 88.9 [*]	7.5 L	9.7 - 272.1 [*]	Dynamic gassing out
24-Square round base wells	1.8 - 187.6 [*]	75 L	48.4 - 384.9 [*]	Dynamic gassing out
24-Square pyramidal base wells	2.1 – 241 [*]			Dynamic gassing out
Duetz et al., (2000)				
96-DSW plate	Maximum: 188 [†]	n/a	n/a	Oxygen-limited growth of <i>P.putida</i>
Funke et al., (2009)				
48-Well plate with square rounded edges	> 600 ^{*†}	n/a	n/a	Sulfite oxidation

* Achieved at varying shaker speeds.

† Achieved at varying fill volumes.

An adapted microwell plate and incorporated optical fibre were used in this work for K_La measurements. The system was designed as previously described by Ferreira-Torres (2008) and Islam (2007), and gassing out studies were conducted as described in section 2.6.11.1 using culture medium with 0.2 mL⁻¹ PPG in order to replicate at the microscale the same conditions experienced by cells at large-scale. PPG is typically added to stirred bioreactors as a antifoam agent. Antifoam has been found to decrease the K_La at low concentrations and increase

it at high concentrations thus it was important to add it to the medium during microscale studies (Kawase and Moo-Young, 1990; Morão et al., 1999). The ultimate aim was to determine the K_{La} at the optimised microwell operating conditions as determined from the results presented in Chapter 4. However, it was first of interest to determine if the predicted trends described in section 4.2 concerning the effect of microwell fill volume on K_{La} could also be observed from the experimental measurements.

From DOT measurements at varying fill volumes the K_{La} was calculated as described in section 2.6.11.1. Figure 6.2 shows K_{La} to increase in a linear fashion with decreasing fill volume as observed in a similar study carried out by Ferreira-Torres (2008). This effect has been reported in other works for a number of microwell plate geometries (Kensy et al., 2005; Funke et al., 2009). John et al. (2003), reported K_{La} values being inversely proportional to fill volume in round well formats. In Chapter 4 the same trend was predicted using the correlation found by Doig et al. (2005) for the prediction of K_{La} values in microwell plate format. The authors attributed the reason for this finding to the fact that a decrease in fill volume increases the specific interfacial area for oxygen transfer, thus resulting in an improvement in growth. Unexpectedly, the predicted values were significantly larger than those determined experimentally. Zhang et al. (2008) used the same methodology described in this work to measure K_{La} values in 96-DSW plates and reported their predicted values to be higher than their measured values. This discrepancy between predicted and measured values was explained by Zhang et al. (2008) to be due to a combination of factors ie the high sensitivity of the probe to the shaking movement, probe location and well mixing time, all of which are likely to have an impact on measured K_{La} values when using the dynamic approach (Doig et al., 2005; Zhang et al., 2008). For these reasons the experimentally determined values were deemed to be a more accurate representation of the system K_{La} values than the predicted ones as they were obtained using the medium, the bioreactor geometry and agitation system used in actual experiments.

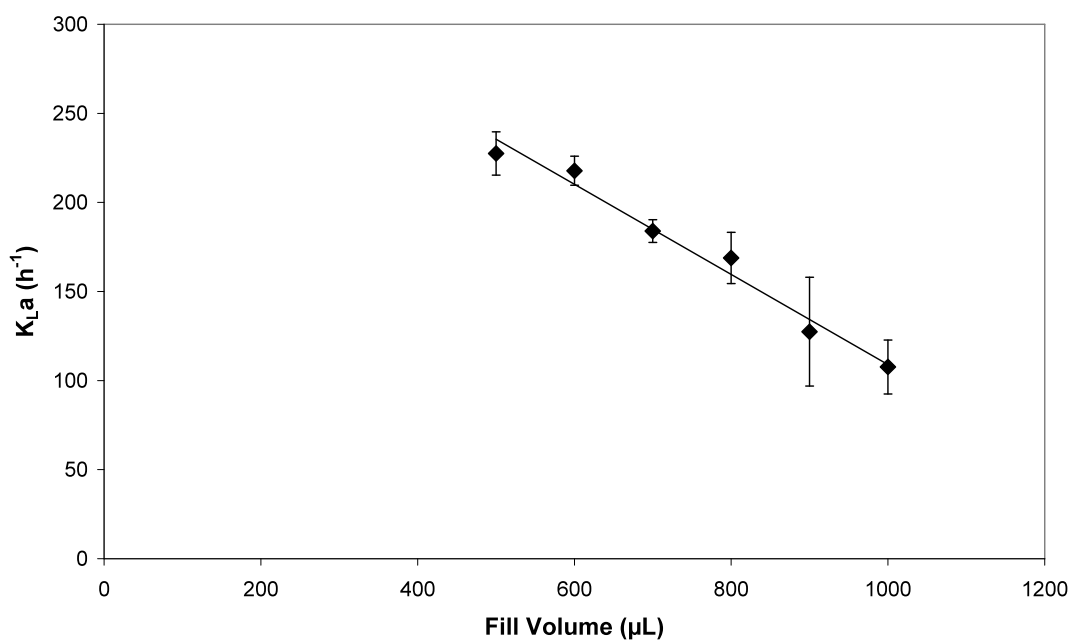


Figure 6.2 Relationship between 96-DSW plate fill volume and $K_{L}a$. Values were measured using the gassing out approach in an adapted 96-DSW as described in section 2.6.11.1. These experiments were conducted at 37 °C, in LB glycerol medium with 0.2 mL⁻¹ PPG and at 1000 rpm. Errors bars indicate the standard deviation of triplicate measurements.

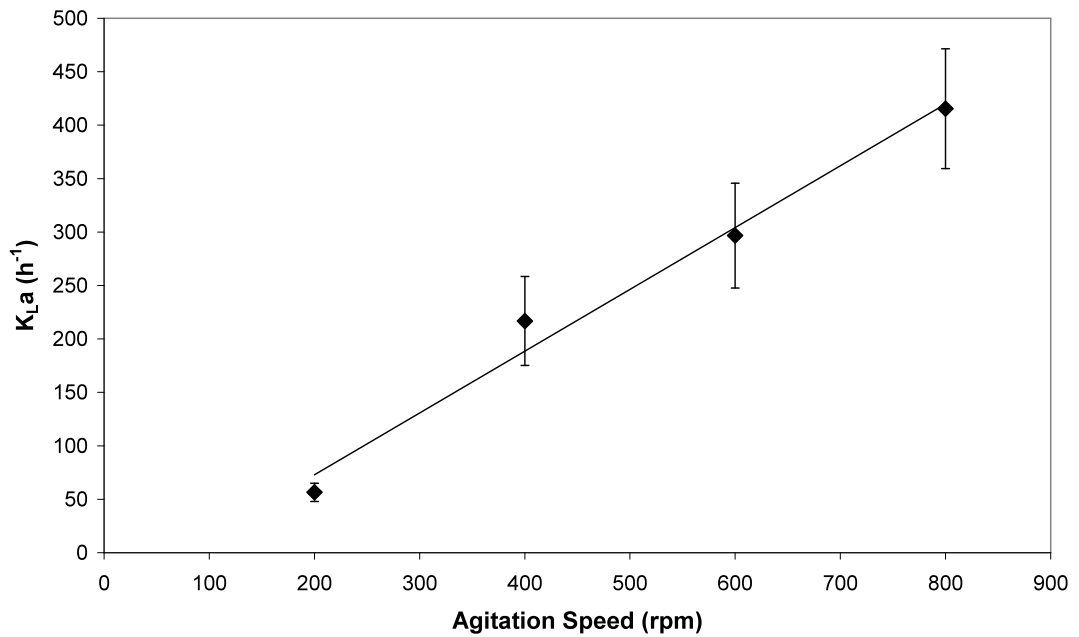


Figure 6.3 Relationship between 75 L stirred bioreactor agitation speed and K_{La} . Values were measured using the gassing out approach as described in section 2.6.11.3. These experiments were conducted at 37 °C, in LB glycerol medium with 0.2 mL⁻¹ PPG, at a working volume of 45 L and an aeration rate of 1 vvm. Errors bars indicate the standard deviation of triplicate measurements.

In Chapter 4 the optimised microscale process was operated at 37 °C, 1000 rpm and 500 µL and a K_{La} of 228 h⁻¹ was measured at these conditions. Dynamic gassing out was then carried out in a 75 L stirred tank bioreactor using LB-glycerol medium with 0.2 mL⁻¹ PPG to determine the range of K_{La} values achievable at this scale as described in section 2.6.11.3. Figure 6.3 shows how the K_{La} varies with agitation speed.

The K_{La} was found to increase with increasing agitation rate from 57 h⁻¹ up to 415 h⁻¹ at the conditions tested, and the values measured at the microscale fall within this range. This linear relationship has been reported previously in a range of bioreactors (Ni et al., 1995; Islam, 2007) and miniature bioreactors (Gill et al., 2008). Finn, (1954) explains that agitation improves K_{La} by three different mechanisms including increasing the interfacial area by creating small gas bubbles, circulating the liquid into swift eddies thus delaying the escape of gas bubbles, and thirdly creating turbulent shear which reduces the liquid film thickness. Equation 6.3 relates agitation speed (N) to K_{La} and the coefficient in the equation was found by linear interpolation of the data presented in Figure 6.3. Using Equation 6.3 an agitation rate of 467 rpm was calculated to achieve a K_{La} of 228 h⁻¹ in the 75 L bioreactor to enable scale-up of optimised microscale kinetics.

$$K_{La} = 0.58N - 42.8 \quad (\text{Eq. 6.3})$$

The relation achieved by Islam (2007) shown in Equation 6.2 is similar to the one obtained in this work. The difference is thought to be due to the media used for K_{La} measurement in the two studies, as TB medium was used by Islam (2007) and LB-glycerol was used in this work. The ion concentration in the medium has a significant influence on bubble size because it has been found to decrease bubble size by preventing bubble coalescence (Craig et al., 1993), thus increasing the specific gas-liquid interfacial area and therefore K_{La} (Ferreira-Torres, 2008). LB-glycerol has a higher salt concentration than TB and this may explain the higher K_{La} values obtained in this study than those achieved by Islam (2007). Furthermore, Islam (2007) also took measurements at room temperature

whereas studies done in this work were conducted at 37 °C which would also cause an increase in K_{La} .

6.2.2.2 Scale Comparison at Matched K_{La}

The optimised process described in Chapter 4 was scaled up to 75 L stirred bioreactor scale by operating at conditions to achieve a matched K_{La} of 228 h^{-1} . A summary of the operating conditions at both scales is shown in Table 6.4. The 75 L was initially inoculated and the first sample used to inoculate the microwell process which was run in parallel as described in section 2.4.1.2. The growth was run for a total of 3 hours as found to be the optimum time frame for production of active CHMO, cultivations exceeding three hours were found in Chapter 4 to cause a significant decline in biocatalyst activity. A 1-hour bioconversion was then conducted at a substrate concentration of 0.5 gL^{-1} as this concentration was found to be below substrate inhibitory limits. The growth kinetic data in Figure 6.4 A from microscale and pilot scale runs follow very similar profiles where cells grew at specific rates of 0.86 h^{-1} and 0.82 h^{-1} up to final biomass concentrations of 4.92 $\text{g}_{\text{DCW}}\text{L}^{-1}$ and 4.34 $\text{g}_{\text{DCW}}\text{L}^{-1}$, respectively. The DOT profile of the 75 L bioreactor was found to decrease rapidly after 1 hour of growth and decreases to zero at around 3 hours. In the initial scale-up study described in section 6.2.1 the same profile was obtained, however, in that case the growth lasted for a total of 6 hours of which 4 were conducted under oxygen limited conditions possibly reducing the effectiveness of the bioconversion. In this case this is not considered to be an issue because the bioconversion only lasted for 1 hour and complete conversion of substrate to product was achieved in 20 minutes as shown in Figure 6.4 B. The calculated CHMO specific activities for microscale and pilot scale processes were 53 $\text{U}_{\text{g}_{\text{DCW}}}^{-1}$ and 49 $\text{U}_{\text{g}_{\text{DCW}}}^{-1}$ respectively. The results of this study are summarised in Table 6.5. Bioconversion completion was achieved in an approximately similar time scale to the experiment described in section 6.2.1 at the same substrate concentration. In terms of the whole process time this was reduced by a total of 3 hours.

Table 6.4 Comparison of microwell and bioreactor parameters.

Parameter	96-DSW Microwell	75 L Stirred Bioreactor
Agitation Rate	1000 rpm Throw: 3 mm	467 rpm
Vessel Total Volume	2 mL	75 L
Working Volume	500 μ L	45 L
$K_L a$	228 h ⁻¹	228 h ⁻¹
Airflow	n/a	1 vvm
Temperature	37 °C	37 °C

From the automated process conducted prior to the scale-up study as described in Chapter 4 cells were reported to grow at a slower specific rate, reached a lower final biomass concentration and there were also slight differences in the bioconversion. These were due to differences in media sterilisation, antifoam addition and to a change in bioconversion temperature (30 °C was used previously, 37 °C was used for the present study). Islam (2007) reported that differences in the temperature-time profiles achieved during standard autoclave sterilisation cycles and in-situ sterilisation within the 75 L bioreactor caused differences in the nutrient level in the medium, resulting in differences in performance between microscale and pilot scale processes. This is why in the present study the microwell was inoculated with a sample taken from the 75 L bioreactor.

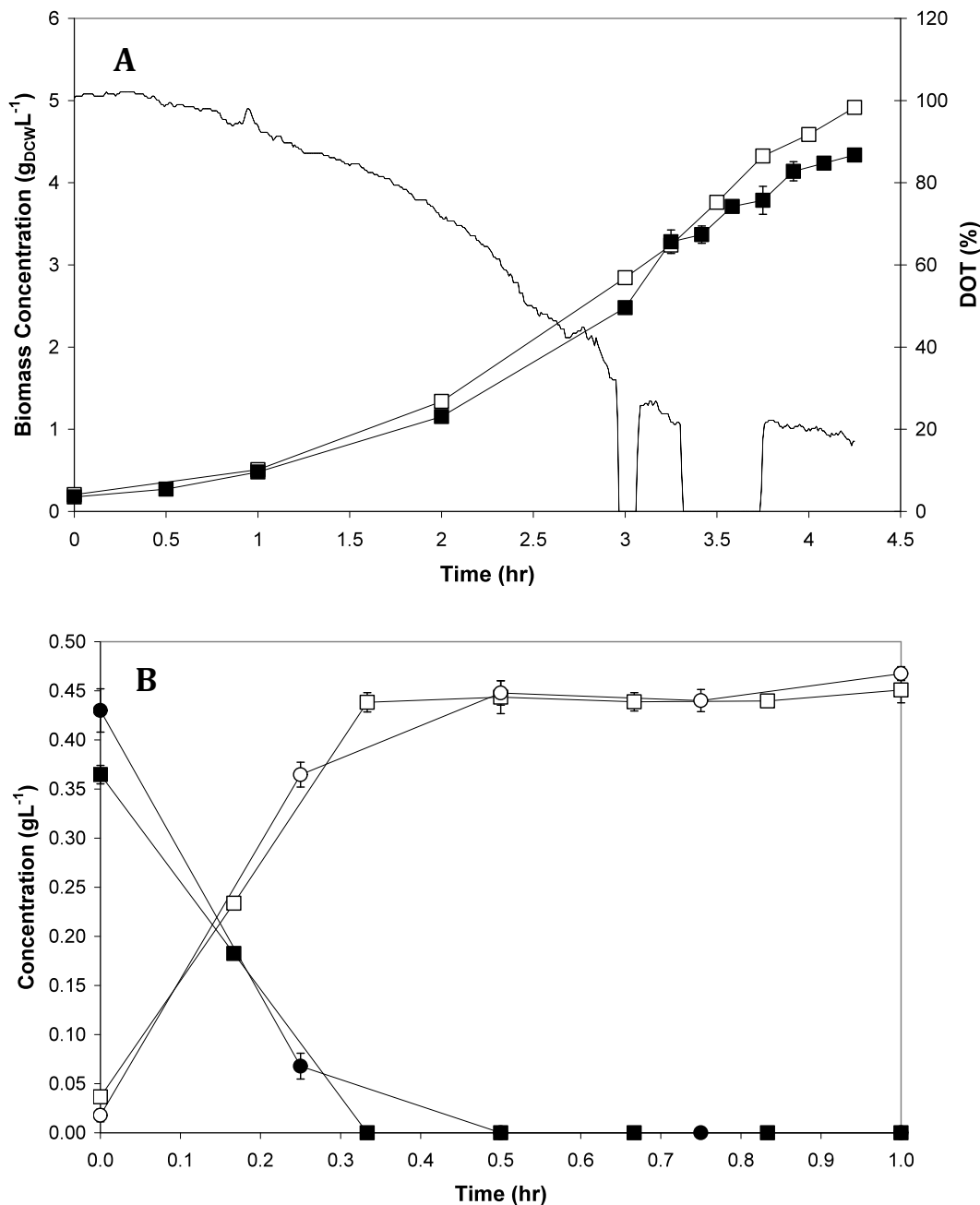


Figure 6.4 (A) Growth kinetics of *E. coli* TOP10 [pQR210] at a matched K_{La} of 228 h^{-1} in a 75 L bioreactor (working volume 45 L) (■) and 96-DSW plate with a 500 μL fill volume (□) and corresponding 75 L DOT profile (----). Error bars indicate the standard deviation of triplicate optical density readings for the 75 L process and microwell process. **(B)** Bioconversion kinetics of *E. coli* TOP10 [pQR210] biocatalyst with 0.5 g L^{-1} bicyclo[3.2.0]hept-2-en-6-one (unfilled symbols) to lactone product (filled symbols) at a matched K_{La} of 228 h^{-1} in a 75 L bioreactor (■) and 96-DSW plate (●). Error bars indicate the standard deviation of triplicate GC samples.

Table 6.5 Summary of growth and bioconversion kinetics achieved at a matched K_{La} of 228 h^{-1} .

Growth			
Scale	$\mu \text{ (h}^{-1}\text{)}$	$X \text{ Final (g}_{DCW}\text{.L}^{-1}\text{)}$	
96-DSW (500 μL)	0.86	4.92	
75 L Bioreactor (45 L)	0.82	4.34	
Bioconversion			
Scale	Initial Lactone* Formation rate ($\mu\text{molL}^{-1}\text{min}^{-1}$)	Specific Activity (Ug^{-1})	Yield (%)
96-DSW (500 μL)	174	53	94
75 L Bioreactor (45 L)	161	49	90

* Produced from bicyclo[3.2.0]hept-2-en-6-one.

6.2.3 Scale Translation at Matched K_{La} – Application to Cytochrome P450SU1 and P450SU2

6.2.3.1 K_{La} Measurement Using Dynamic Gassing Out

In Chapter 5 a microscale approach for the production of cytochrome P450s was developed using specified operating conditions. It was of interest to scale-up the cytochrome P450 kinetics on the basis of matched K_{La} as oxygen was again a crucial substrate in both growth and bioconversion and this approach proved to be successful with the CHMO enzyme. Dynamic gassing out experiments conducted at the microscale in the adapted 96-DSW plate using TB medium with 0.2 mL^{-1} PPG. Two distinct stages can be observed: a rapid growth phase and an expression phase during the production of cytochrome P450s. Each phase is conducted at a particular agitation rate and temperature, as described in Chapter 5, and both factors have an impact on K_{La} . The growth phase was conducted at a 1 mL fill volume, 1000 rpm and $37 \text{ }^\circ\text{C}$ and the expression phase at a 1 mL fill volume, 800 rpm and $25 \text{ }^\circ\text{C}$, the measured microscale K_{La} values for each

condition were 200 h^{-1} and 62 h^{-1} , respectively. Gassing out studies using TB medium with 0.2 mL L^{-1} PPG were aimed at achieving these $K_{L}a$ values in a 7.5 L stirred tank bioreactor. Studies were conducted at varying agitation speeds at $37 \text{ }^{\circ}\text{C}$ and $25 \text{ }^{\circ}\text{C}$ and the results are shown in Figure 6.5. A linear trend is observed for the relation between agitation rate and $K_{L}a$, as observed previously in the 75 L bioreactor, and is described by Equation 6.4 and 6.5 at $37 \text{ }^{\circ}\text{C}$ and $25 \text{ }^{\circ}\text{C}$, respectively.

$$K_{L}a = 0.471N - 159.17 \quad (\text{Eq. 6.4})$$

$$K_{L}a = 0.206N - 55.7 \quad (\text{Eq. 6.5})$$

An agitation speed of 200 rpm was tested, however, during gassing out studies it was found that the rate of re-oxygenation did not settle to a constant rate at $37 \text{ }^{\circ}\text{C}$ and was extremely slow at $25 \text{ }^{\circ}\text{C}$ making it difficult to accurately measure the $K_{L}a$ at this agitation rate. This is thought to be due to low turbulence levels resulting in a non-homogenous bioreactor mixing environment and poor gas-liquid dispersion. For this reason Equations 6.4 and 6.5 should only be used for $K_{L}a$ determination between agitation rates of 400 rpm and 800 rpm in this geometry. Figure 6.5 shows how reducing the temperature reduces the $K_{L}a$, in agreement with results reported previously (Finn, 1954; Aiba et al., 1984; Hichri et al., 1992) where changes in liquid viscosity and solute gas mass diffusivity in the liquid were found to be responsible for this effect (Hichri et al., 1992). However, as the agitation rate decreases, the effect of temperature has a reduced effect on $K_{L}a$ where at 400 rpm there is a 1.5-fold reduction in $K_{L}a$ between $37 \text{ }^{\circ}\text{C}$ and $25 \text{ }^{\circ}\text{C}$ compared to over a 2-fold reduction at 800 rpm. The gas-liquid dispersion becomes less effective as the agitation speed decreases and therefore the $K_{L}a$ is found to have a greater dependence on agitation compared to temperature at these conditions. Using Equations 6.4 and 6.5 agitation rates of 763 rpm at and 571 rpm were calculated to achieve a $K_{L}a$ of 200 h^{-1} at $37 \text{ }^{\circ}\text{C}$ and 62 h^{-1} at $25 \text{ }^{\circ}\text{C}$ in the 7.5 L stirred bioreactor to enable scale-up of cytochrome P450 kinetics.

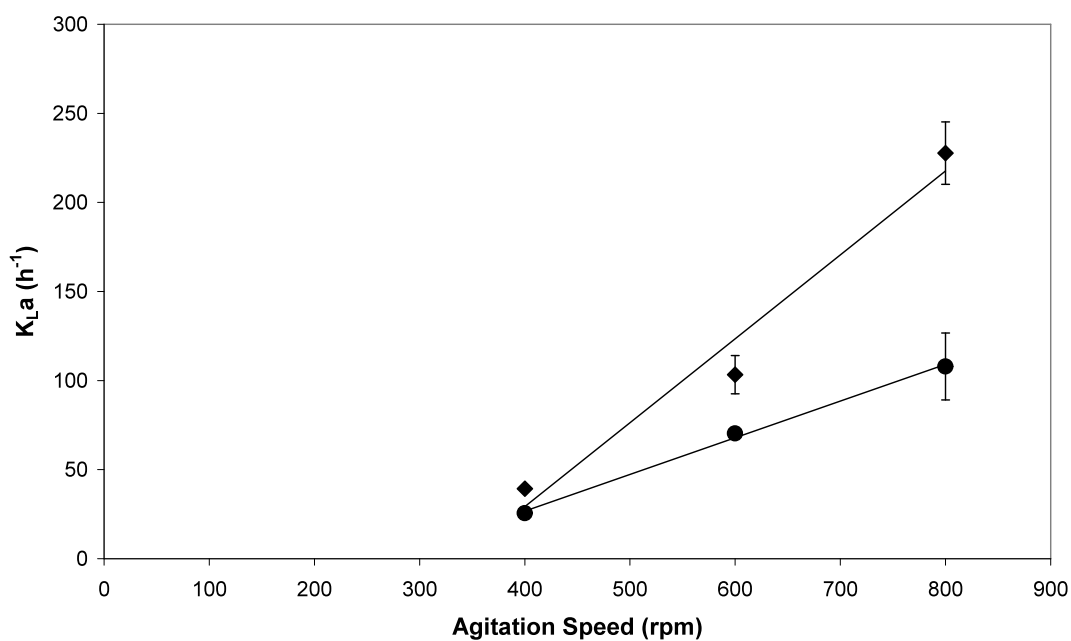


Figure 6.5 The effect of agitation speed and temperature (◆ 37 °C, ● 25 °C) on measured $K_{L}a$ values in a 7.5 L stirred bioreactor. Values were measured using the gassing out approach as described in section 2.6.11.2. These experiments were conducted in TB medium with 0.2 mL^{-1} PPG, at a working volume of 5 L and an aeration rate of 1 vvm. Errors bars indicate the standard deviation of triplicate measurements.

6.2.3.2 Scale Comparison at Matched K_{La}

Two 7.5 L scale processes were conducted for the 5000-fold scale translation of *E. coli* [pQR367] expressing P450SU1 and *E. coli* [pQR368] expressing P450SU2 as described in section 2.4.2.1. Stirred tank bioreactors were first inoculated with 1 % v/v overnight prepared culture. Once the cultures were well-mixed a sample was taken and used to inoculate the microscale process which was run in parallel. Both strains were grown at 37 °C at a matched K_{La} of 200 h⁻¹ in both stirred tank and microwell plates until a OD of 0.6 - 0.8 was reached. The temperature was then dropped to 25 °C and the agitation adjusted to achieve a matched K_{La} of 62 h⁻¹ for the remainder of the culture. Culture conditions at both configurations during the entirety of the process are shown in Table 6.6.

Table 6.6 Comparison of microwell and bioreactor parameters.

Parameter	96-DSW Microwell Plate	7.5 L Stirred Bioreactor
Growth Phase (Until OD reached ~ 0.6 - 0.8)		
Agitation Rate	1000 rpm Throw: 3 mm	763 rpm
Vessel Total Volume	2 mL	7.5 L
Working Volume	1 mL	5 L
K_{La}	200 h ⁻¹	200 h ⁻¹
Airflow	n/a	1 vvm
Temperature	37 °C	37 °C
Expression Phase		
Agitation Rate	800 rpm Throw: 3 mm	571
K_{La}	62 h ⁻¹	62 h ⁻¹
Temperature	25 °C	25 °C

In Chapter 5, 5 mM ALA and 20 gL⁻¹ glycerol were found to promote both the active yield of cytochrome P450 and bioconversion and thus were added to both cultures and incubated for 20 minutes. Once the temperature had reached 25 °C enzymatic expression was induced with 1 mM IPTG and after a further 10 minutes of incubation 1 mM 7-ethoxycoumarin added to begin bioconversion. Cultures were left for a total of 30 hours and samples taken periodically to monitor cellular growth and bioconversion. The growth profiles and bioconversion kinetics at both scales are shown in Figures 6.6 A and B along with the respective DOT profiles from 7.5 L cultures. CO assay analysis was not conducted in this study as 7-ethoxycoumarin was added to all cultures. When bound, substrates have been found to cause spectral shifts and cause conformational changes which can affect CO binding (McLean et al., 1996) and interfere with the CO difference spectrum. This has not been investigated with P450SU1 and P450SU2, however, previous works have conducted CO assay experiments using substrate-free samples (Hussain and Ward, 2003) and, as shown in section 2.6.9.2, no P450 peak could be obtained in the presence of substrate in this work.

Both strains grew similarly for the first 3 hours in both the 7.5 L stirred tank bioreactor and the 96-DSW plate as no nutritional or oxygen limitation occurred during this stage. Specific growth rates of *E. coli* [pQR367] and *E. coli* [pQR368] were 1.46 h⁻¹ and 1.43 h⁻¹ for the 7.5 L bioreactor and 1.28 h⁻¹ and 1.20 h⁻¹ for the 96-DSW plate, respectively. Once the temperature was dropped and the agitation reduced to promote expression, there was a significant change in growth rate between the two formats. Cells in the bioreactor grew faster than those in the 96-DSW, final biomass concentrations of 13.39 g_{DCW}L⁻¹ and 13.65 g_{DCW}L⁻¹ were achieved for *E. coli* [pQR367] and *E. coli* [pQR368] in the 7.5 L bioreactor while 7.48 g_{DCW}L⁻¹ and 8.50 g_{DCW}L⁻¹ were obtained at the microscale. This is quite different to what was obtained for *E. coli* expressing CHMO where matched K_La approaches resulted in the effective reproduction of growth kinetics at the pilot plant scale.

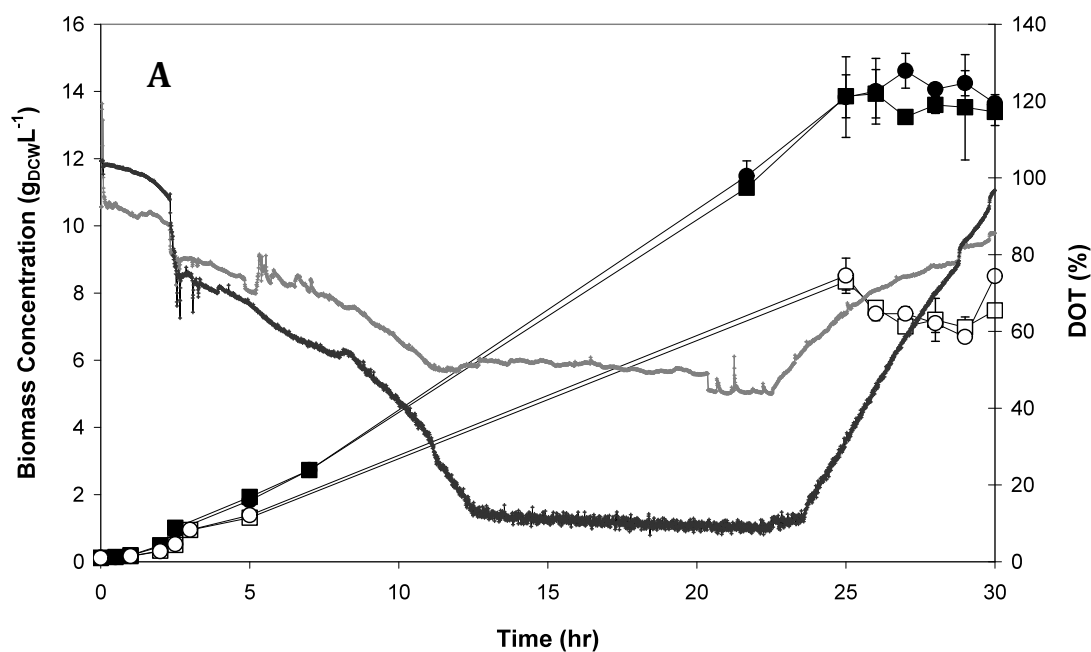


Figure 6.6 (A) Growth kinetics of *E. coli* [pQR367] (■) and *E. coli* [pQR368] (●) at a matched K_{La} of 200 h^{-1} in a 7.5 L bioreactor (working volume 5 L) and 96-DSW plate with a 1 mL fill volume (open symbols) for the first 3 hours of culture and then a matched K_{La} of 62 h^{-1} for the remaining culture time and corresponding 7.5 L DOT profile for *E. coli* [pQR367] (light grey line) and *E. coli* [pQR368] (dark grey line) cultures. Error bars indicate the standard deviation of triplicate optical density readings for the 7.5 L process and the range of measured values about the mean for the microwell process.

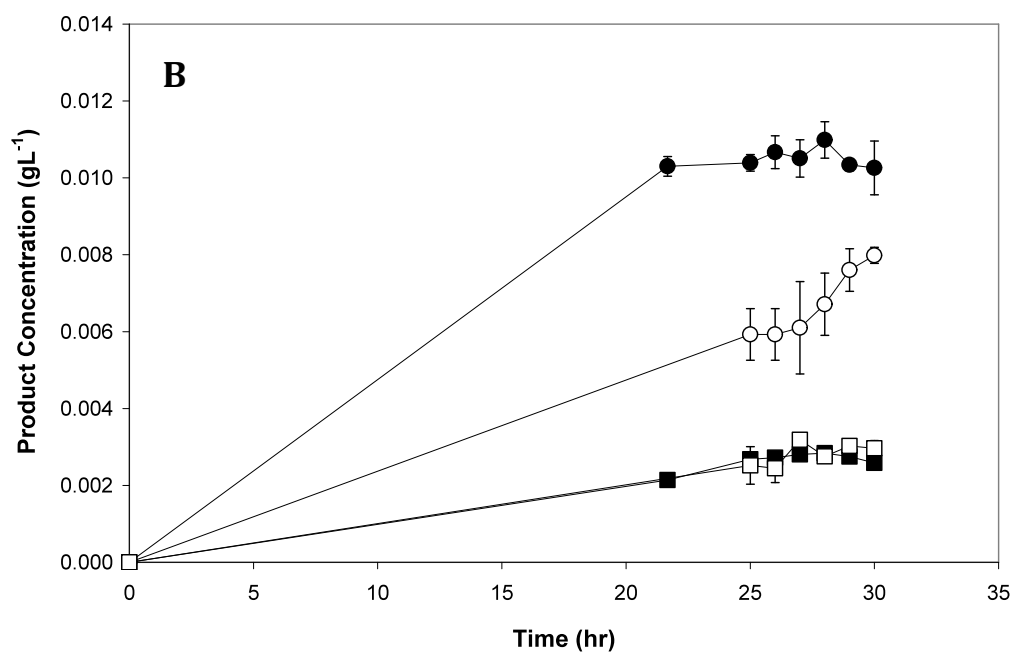


Figure 6.6 (B) 7-hydroxycoumarin production from P450SU1 (■) and P450SU2 (●) at a matched K_{La} of 62 h^{-1} in a 7.5 L bioreactor (closed symbol) and 96-DSW plate (open symbol). Error bars indicate the standard deviation of triplicate 7.5 L HPLC samples and the range of measured values about the mean for 96-DSW plate HPLC samples.

Comparing the DOT profiles of *E. coli* [pQR367] and *E. coli* [pQR368] from the 7.5 L bioreactors, oxygen was utilised quite differently even though similar biomass concentrations were reached. Both strains readily consumed oxygen for the first 10 to 12 hours of culture after which DOT remained approximately constant up until the 23rd hour when the DOT started to rise potentially due to the onset of cellular death. However, *E. coli* [pQR367] only depleted the oxygen to a point where the lowest DOT measured was 44 % whereas in the case of *E. coli* [pQR368] DOT fell to 7 %. Oxygen utilisation includes cell maintenance, growth and oxidation of substrates to products. The growth and cell maintenance of both strains is the same as shown by the growth profiles (Bailey and Ollis, 1986). This difference in oxygen utilisation could be associated with protein expression and product formation as P450SU1 was expressed at a lower level and produced less product than P450SU2 and hence probably had a lower oxygen requirement. Moreover, this result may suggest that in the case of *E. coli* [pQR367] oxygen control may be required. Previously, Zhang et al. (2010) found a 2-fold improvement in P450SMO production when the DO was maintained at a level below 10 % compared to no DO control. In the current study the increased DO levels during the expression phase of *E. coli* [pQR367] could have resulted in oxidative damage and be a contributory factor to lower expression levels compared to P450SU2.

Interestingly, even though there was a difference in growth, very similar product formation profiles were achieved from *E. coli* [pQR367] for the 7.5 L bioreactor and the microwell process. Final 7-hydroxycoumarin concentrations were 2.59 mgL⁻¹ and 2.97 mgL⁻¹, respectively. However, in the case of *E. coli* [pQR368] higher product concentrations were observed from the 7.5 L bioreactor which produced a final 7-hydroxycoumarin concentration of 10.26 mgL⁻¹ compared to 7.98 mgL⁻¹ at the microscale. A summary of this study is shown in Table 6.7. The results obtained in this work at the microscale are similar to those obtained from the automated experiments.

Table 6.7 Summary of growth and bioconversion kinetics achieved at a matched K_{La} .

Scale	Growth		Bioconversion	
	μ (h^{-1})	X Final ($g_{DCW}\cdot L^{-1}$)	Final Product Concentration (mgL^{-1})	Yield (%)
<i>E. coli</i> [pQR367] Expressing P450SU1				
96-DSW (1 mL)	1.28	7.48	2.97	1.9
7.5 L Bioreactor (5 L)	1.46	13.39	2.59	1.6
<i>E. coli</i> [pQR368] Expressing P450SU2				
96-DSW (1 mL)	1.20	8.50	7.98	5.0
7.5 L Bioreactor (5 L)	1.43	13.65	10.26	6.4

Islam (2007) reported that similar kinetic data at the microscale and 7.5 L scale could only be obtained at high K_{La} values of $247 h^{-1}$ whereas when a low K_{La} of $55 h^{-1}$ was tested very different results were obtained. This was attributed to poor gas-liquid distribution observed in the 7.5 L bioreactor at the low K_{La} value. The K_{La} values used in this work are of the same magnitude to those reported by Islam (2007). It is noteworthy that the growth phase was conducted at the high K_{La} ($200 h^{-1}$) and the expression phase conducted at the low K_{La} ($62 h^{-1}$) and, as reported by Islam (2007), operation at a low K_{La} could explain the lack of reproducibility observed in the present study across the scales. However, this does not fully explain the improved stirred bioreactor growth kinetics compared to the microscale. It is possible that a factor associated solely with the microscale process is causing the observed behaviour.

Marques et al. (2009) scaled up whole cell growth and bioconversion processes from a 24-well microtitre plate to a 5 L stirred bioreactor using a matched K_{La} approach. The authors reported successful scale-up based on the shape of the growth and bioconversion profiles, however, found that the results from the 5 L were consistently higher than those achieved at the microscale. Marques et al.

(2009) attributed the reason for this finding to differences in intrinsic hydrodynamic conditions at the different scales.

The shaking diameter has been found to be critical in influencing the oxygen transfer rates in microwells where as the shaking diameter increases so to does the rate of oxygen transfer (Duetz et al., 2000; Hermann et al., 2003; Duetz and Witholt, 2004; Kensy et al., 2005; Funke et al., 2009). Therefore when working at low shaking diameters a higher critical shaking frequency is required to achieve the maximum oxygen transfer rate (Fernandes and Cabral, 2006). In the present work high shaking frequencies of 1000 rpm were actually found to considerably reduce product formation and showed no benefit on growth. Thus increasing the shaking diameter could contribute to improve the oxygen transfer rate whilst operating at a shaking frequency less detrimental to bioconversion. Marques et al. (2007) found that when a high shaking diameter (25 mm) was used the agitation rate had a strong influence on product formation. It was explained that at low shaking diameters the flow pattern developed was unable to fully disperse cell clusters which were found deposited at the well bottom. Similarly, the same behaviour was noticed during initial microscale development studies as discussed in Chapter 5, however this was not observed during the matched K_La study. This is probably due to low axial velocity characteristics present inside the well at the tested shaking diameters, which are responsible for poor substrate dispersion and limited substrate uptake (Marques et al., 2007). Furthermore, the hydrodynamics of microwell systems can be controlled by the shaking diameter and in particular, low shaking diameters have been associated with out-of-phase mixing (Büchs et al., 2001; Duetz and Witholt, 2004) where the liquid does not circulate in phase with the orbital motion of the shaker. Choice of shaking diameter may be a likely explanation for the lack of reproducibility observed across the scales for the cytochrome P450s. In particular, the improved growth rates, biomass concentration and product yield reached in the stirred tank reactor highlight a better oxygen and substrate supply compared to the microscale process. Alternative methods to improve oxygen transfer, such as varying the fill volume, were tested in this work but proved ineffective as discussed in Chapter 5, thus it is uncertain whether a change in operating conditions could improve mass transfer rates.

Based on the previous discussion it is quite challenging to point out a likely reason for the behaviour observed. The growth of *E. coli* [pQR367] was considerably higher at the 7.5 L scale compared to the microscale, indicating that bioconversion was independent of growth as observed in a number of previous studies as discussed in Chapter 5. The rate-limiting step in biotransformation can be due to the poor substrate solubility hindering mass transport rates of substrates/products to and from cells (Manosroi et al., 2008) and this is a reasonable explanation for the results observed in this work.

E. coli [pQR367] expressing P450SU1 and *E. coli* [pQR368] expressing P450SU2 were grown at the 7.5 L scale and both successfully metabolised 7-ethoxycoumarin to 7-hydroxycoumarin. However, growth and bioconversion kinetics did not mimic those achieved at the microscale when a matched K_{La} approach was used. An overview of alternative scale-up methodologies will be discussed in section 6.2.4.

6.2.4 Alternative Scale-Up Strategies

6.2.4.1 The Dynamic Measurement of K_{La}

The dynamic measurement of K_{La} has already been discussed and was tested for the scale-up of two oxidative systems. However, it is worth noting that the approach used in this work did not take into consideration the cells oxygen uptake rate. It is recommended that accurate oxygen transfer rate measurements are carried out in the bioreactor, nutrient broth and the cell population of interest (Bailey and Ollis, 1986). A number of studies have found that the oxygen transfer rate is enhanced when oxygen is consumed during microbial growth (Calik et al., 1997; Calik et al., 2004). Vashitz et al. (1989) reported an increase in the oxygen liquid transfer coefficient as the oxygen uptake rate of *Xanthomonas campestris* cultures increased. Moreover, K_{La} values obtained using inoculated culture were found to be higher than those using sterile medium (Djelal et al., 2006). To consider this effect a biological enhancement factor termed E has been suggested. This factor encompasses the enhancement of

transport due to oxygen uptake and includes the resistances caused by the presence of cells, surfactants or stagnant liquid films and their interaction with gas bubbles and the bulk liquid film. Thus depending on biomass and media composition K_La can be described by Equation 6.6 (Garcia-Ochoa and Gomez, 2009).

$$K_La = E * k_La \quad (\text{Eq. 6.6})$$

Typically E is close to 1 when the biochemical rate (rate of oxygen consumption due to cellular activity) is not much higher than the mass transfer rate, consequently when the k_La is very high the influence of oxygen uptake rate is insignificant and the enhancement low. However, in cultures with a high oxygen uptake rate E will be greater than one, thus increasing the overall K_La . This typically becomes more significant with increases in biomass concentration. The oxygen uptake rate therefore should be considered when measuring K_La as oxygen consumption is both organism and growth condition specific and can enable a more accurate and realistic prediction of K_La values during culture.

6.2.4.2 Volumetric Power Consumption

The volumetric power consumption (P/V) is the energy input within a given time period required to generate fluid motion within a vessel. Heat and mass transfer, mixing and circulation times are all influenced by the volumetric power consumption. Volumetric power consumption is traditionally used for the effective scale-up of bioreactor configurations using well-known correlations and dimensionless analysis but, while estimations of power consumption have been achieved in shaken geometries (Buchs et al., 2001), no widely applicable method is currently available for well plate format. This is because there is no measurement device sensitive enough to perform accurate torque measurements at the microscale. Furthermore, as torque measurements need to be measured inside the liquid most devices are too large to fit inside the well and can be intrusive to the flow pattern. The presence of surface tension, a crucial parameter in microwell hydrodynamics, is also not accounted for when using a

matched (P/V) approach (Hermann et al., 2003; Maier and Buchs, 2001). However, Zhang et al. (2008) has used computational fluid dynamics (CFD) to estimate power consumption in 24 – well and 96 – well microtitre plates. It was found that power consumption estimations were in the range of those required for bacterial cultivation in large-scale stirred bioreactors. Following on from this work Barret et al. (2010) reproduced growth kinetics and antibody titer of murine hybridoma cells in 24-well plates to 250 mL shake flasks using matched energy dissipation rates based on CFD predictions. (P/V) has also been tested to scale-up mammalian culture at the microscale to 5 L stirred bioreactor scale and while similarities were observed there were still distinct differences between the scales in terms of growth rate and antibody production kinetics (Micheletti et al., 2006). Therefore, (P/V) may or may not be ideal as a scale-up parameter from microwell to stirred configurations. It is important to conduct a more accurate evaluation of experimental velocity and mixing characteristics in shaken bioreactors to be able to compare the hydrodynamics of the two configurations and therefore define appropriate scale-up parameters.

6.3 Concluding Remarks

In Chapters 3 to 5 two fully automated microscale processes were developed for the quantitative analysis of CHMO and novel cytochrome P450 expressing systems. A range of process parameters, culture conditions and alternative reactions were tested enabling optimised process conditions to be defined for CHMO and cytochrome P450 bioconversion improvement. Nevertheless, this data can only be deemed useful in early stage bioprocess design and development if comparable data can be reproduced in typical stirred tank reactors, the configuration of choice for large-scale production. This chapter thus focused on using established scale-up methodologies to reproduce the best conditions achieved from the various microscale studies in laboratory and pilot plant scale fermenters.

Scale-up based on a matched $K_L a$ approach has previously proved to be suitable for the reproduction of microscale kinetics on growth, protein expression and

bioconversion for a number of microorganisms in stirred systems. Based on previous findings a preliminary scale-up study using this approach was designed with *E. coli* TOP10 [pQR210] expressing CHMO. Using pre-determined $K_{L,a}$ measurements from 96-DSW plates and a 75 L stirred bioreactor, growth and bioconversion kinetics were found to be similar at both scales. An adapted 96-DSW plate with an incorporated fibre optic sensor was manufactured and used to enable the dynamic measurement of $K_{L,a}$ at the microscale in a similar manner to a 75 L bioreactor. $K_{L,a}$ was found to vary linearly with microscale fill volume and stirred bioreactor agitation speed. By identifying conditions which would enable both processes to be operated at a matched $K_{L,a}$, a parallel study was run which produced comparable results for the growth and bioconversion steps. This study also highlighted the advantage of operating under non-oxygen limited conditions thus enabling reproducible growth from aerobic cultures.

Oxygen is required for both the growth of cytochrome P450 strains and the O-dealkylation of 7-ethoxycoumarin, thus the matched $K_{L,a}$ approach was applied for the scale-up of the improved process identified from automated microscale studies in Chapter 5. During the production of cytochrome P450SU1 and P450SU2 growth and expression phases took place at different agitation speeds and temperatures both of which have been found to have an impact on $K_{L,a}$. $K_{L,a}$ measurements carried out at different operating conditions allowed a matched $K_{L,a}$ approach to be adopted to compare the microwell and 7.5 L stirred bioreactor processes. Both strains grew and successfully metabolised 7-ethoxycoumarin to 7-hydroxycoumarin. Strains were found to grow faster in the stirred bioreactor where a significant increase in biomass concentration was observed once the expression was initiated. While operation was conducted under non-oxygen limitations, as previously discussed in Chapter 5, comparison of the results found in this work with previous ones suggest that the use of a small shaking diameter may have been responsible for the lack of scalability in this case. In particular the turbulence levels present in the well may have not been sufficient for effective dispersion of oxygen and substrate. It was also important to assess the alternative scale-up strategies in order to determine whether different approaches could be successfully applied to scale translation from microwell to stirred bioreactor configuration. In this study the impact of

the oxygen consumption by microorganisms was not taken into account in the K_{La} determination, however it is advisable to conduct such measurements in the presence of media and cells to enable accurate assessment of the variation of K_{La} during culture.

Scale translation of microscale operations is necessary if they are to be considered a reliable tool for bioprocess development. Accordingly, the cost and time benefit can only be accepted if the data collected is accurate and predicts trends and relationships achievable in larger scale configurations. Using established methodologies successful scale-up was demonstrated under non-oxygen limited conditions but in the case of more complex systems requiring specific expression conditions accurate measurement of K_{La} variations during culture are crucial and should consider the biological enhancement promoted by metabolic activity.

7 Conclusions and Future Work

7.1 Concluding Remarks

A major challenge of bringing biologics to market is the establishment of robust manufacturing processes. In particular, the industrial exploitation of oxidative biocatalytic approaches has been limited by the slow implementation time due to the number of process variables requiring characterisation and optimisation. The development of miniaturised systems which can effectively mimic the large-scale processes is a potential solution to reducing the costs and accelerating process development. Moreover, linking multiple unit operations by means of automated processing to gain a better understanding of process interactions is a novel concept and has only be investigated to a limited extent. For this reason this thesis tested the hypothesis that high-throughput automated microscale approaches could be used for the development and investigation of novel oxidative biocatalytic processes.

The initial objective was to develop a generic microscale automated platform for bioprocess investigation. The well-established recombinant CHMO expressing strain *E. coli* TOP10 [pQR210] was used as a model system as the focus of this research was on oxidative biocatalysis. The Tecan automated robotic platform was used to achieve process automation, where three distinct steps in the production and use of CHMO were demonstrated at the microscale and linked to enable the investigation of process interactions. Unit operations including growth, bioconversion and liquid-liquid extraction along with relevant analytic techniques were performed using 96-DSW plates. Each step was found to enable the rapid and reproducible collection of quantitative kinetic data over multiple runs. In particular up to six variables could be screened per run and up to 96 samples processed for GC analysis. Key achievements included a demonstration of robustness, increased throughput and accuracy of data collection comparable to manual alternatives. Furthermore, as time-consuming cell culture and maintenance steps were automated, ‘walk away operation’ was achieved where

the majority of the process time could be utilised for data analysis, further experimentation and analytical operations.

Once the generic microscale platform was in place it was of interest to demonstrate its use for whole bioprocess evaluation and optimisation. Considering the progress that had already been made with similar CHMO expressing systems oxygen transfer rate, biomass concentration and amino acid source were chosen to identify the effect on CHMO specific activity. Each was shown to have an impact on both growth and bioconversion activities. Furthermore, effects of varying media composition described in this thesis have not been previously reported and the data collected thus contributes to improve current knowledge of factors which can influence CHMO activity. The ability to assess the combined effect of changing variables on multiple steps enabled conditions maximizing CHMO specific activity and bioconversion effectiveness to be identified. This study was followed by an investigation into alternative CHMO reactions including an assessment of substrate inhibitory effects and screening of Baeyer-Villiger substrates previously untested with *E. coli* TOP10 [pQR210]. Substrate specificity and product selectivity were effectively demonstrated where two new substrates were successfully metabolised to the respective products. With a view to develop an optimised process sequence and to improve the bioconversion of the new substrates, the best condition obtained from each study was selected. Using the optimised process, an almost 2-fold decrease in processing time and 5-fold increase in CHMO specific activity were achieved. These conditions were also found to confirm substrate mass transfer limitation to be the reason for the lack of conversion with unproductive substrates.

From the literature review it was found that novel cytochrome P450 systems show great promise and would significantly benefit from high-throughput microscale approaches for rapid evaluation. The automated approach had already been demonstrated for robustness and application to biocatalytic process evaluation and improvement. It thus was applied to the novel self-sufficient cytochrome P450 systems expressed from *E. coli* [pQR367] and *E. coli* [pQR368]. The automated approach was adapted and a linked sequence of

growth, induction, expression, bioconversion and liquid-liquid extraction was established for the investigation of these systems. This approach was initially used to screen fourteen factors for bioconversion improvement and from this study the best three were selected and assessed in detail for their influence on growth, expression and bioconversion phases. In particular, the automated approach successfully identified limitations in haem prosthetic group formation, NAD(P)H regeneration and substrate inhibitory limits. Previous to this work there have been limited reports on the positive impact of glycerol supplementation and inhibitory effects of 7-ethoxycoumarin thus these findings contribute new data to the field of cytochrome P450 biocatalysis. When the best conditions from these studies were combined, a 5-fold improvement in enzymatic expression of both systems was achieved as well as a 5-fold and 1.5-fold increase in product formation from P450SU1 and P450SU2 bioconversions, respectively. This therefore confirmed high-throughput automated microscale approaches could be applied for the creation and rapid evaluation and optimisation of novel biocatalytic processes.

Finally, in order for data collected using microscale automated approaches to be accepted as a tool for early stage bioprocess design and development, the data needs to be reproduced in typical stirred tank reactors. To examine the potential for predictive scale-up, the optimised CHMO process was scaled to 75 L stirred bioreactor scale and both cytochrome P450 improved processes were scaled to 7.5 L stirred bioreactor scale. A matched K_{La} approach was chosen as reported previously to be successful for aerobic systems. This scale-up methodology proved successful for the CHMO based process where near identical results to the microscale were reproduced at the pilot plant scale. The approach was not successful, however, for the two novel cytochrome P450 systems. While similar growth profiles and product formation trends were observed, the final biomass concentrations for both strains and also product titre from P450SU2 catalysed bioconversion were significantly higher in laboratory scale bioreactors than at the microscale. A number of reasons for these results were discussed in Chapter 6 including the small shaking diameter used in microscale operations potentially preventing effective mass and oxygen dispersion. Published works have demonstrated that K_{La} estimation can be significantly effected by the biological

enhancement resulting from cellular metabolism and oxygen uptake (Calik et al., 1997; Calik et al., 2004). This was not considered in these studies where K_{La} measurements were carried out using cell free medium. K_{La} should therefore be determined in the presence of both cells and medium to enable accurate assessment of the variation of K_{La} as the biomass increases during culture. This may be critical for the scale translation of complex systems such as the cytochrome P450s.

7.2 Future Work

The outcome of this thesis has been the development of a generic fully automated microscale approach for the whole bioprocess evaluation of oxidative biocatalytic processes. The next step would be to apply the microscale platform to a range of challenging strains and bioconversion substrates which have yet to be fully studied. In particular, novel systems were shown to be rapidly evaluated in this work, making the technology an important tool during initial characterisation and developmental studies.

The short-term future work stemming from the findings of this project would be to establish the reason for the lack of scalable data achieved with the cytochrome P450 systems. This could involve initially testing a different shaking platform to enable a range of shaking diameters to be assessed. Visually monitoring the fluid flow and mixing of the current system by means of a high-speed camera would also be worthwhile. Grant et al. (2012) used this method and visually identified poor bioconversion performance to be due to poor mixing in microwell formats. In the case of the present work a transparent glass mimic could be designed for such investigations. In addition, K_{La} measurements could be carried out during cell cultivations as described by Bandyopadhyay et al. (1996) in order to check if biological enhancement is causing a significant change to the K_{La} measured in cell free medium. The demonstration of scalable kinetics for cytochrome P450 systems is of crucial importance, while the data collected in the present work is still useful predictive scale-up would strengthen the results for early stage bioprocess design and development.

Building on the work done in this thesis there are a number of studies which could be done to improve the implemented sequences further. The control of evaporation was found to be an issue during developmental experiments. An appropriate microwell closure system which prevents evaporation but is not detrimental to oxygen transfer capacity could be developed. In particular, being able to automate the opening and closure or using non-destructive lid piercing options to enable additions and sampling would be an advantage. Such a system would considerably benefit those cultures requiring extended culture or bioconversion times and sustain higher cell densities.

Incorporating control and monitoring of factors such as DO and pH at the microscale would contribute to better process understanding. Development of smaller, more accurate and reliable sensor technology would be crucial to enable variations in optimum culture conditions to be readily controlled.

The incorporation of Design of Experiments (DoE) for the selection of appropriate experiments could also improve the overall approach. While this was not an objective of the present thesis, in the case of novel systems the number of process variables to be initially tested can be significantly reduced by carrying out a DoE study.

Substrate inhibition was highlighted in the present work and is typically a limitation of many oxidative bioconversions. Substrate feeding regimes as well as the use of resins for product removal have been reported (Hilker et al., 2008). Incorporating such methods into the current automated approach would lead to more productive processes. In particular, using plates with incorporated resins for substrate addition and product removal represent an interesting future study.

One additional improvement related to achieving better bioconversion processes would be the trial of two-liquid phase systems. Some of the substrates used in this work were poorly water-soluble. It has been found that using a system comprised of both aqueous and organic phases can aid bioconversion, especially when those substrates are toxic or inhibitory and in addition can simplify downstream processing operations. This approach has been found effective at

the microscale (Marques et al., 2009; Grant et al., 2012) and may be worth incorporating for those substrates found to be unproductive in the present work.

In order to take the present work further, incorporation of more microscale unit operations into the current automated sequence would be an advantage. All the steps in the production and use of the biocatalyst were automated, including the effective extraction into organic solvent, however, small-scale purification may also be appropriate. For example, in the large-scale process, steps such as silica gel chromatography and crystallization may be required to achieve a final purified product. The impact of production steps on final purification steps could be modeled at small-scale to determine product processing capacity. Moreover, analytic techniques such as GC, HPLC and the CO assay used to quantify active cytochrome P450 are currently the rate-limiting step where each sample has to be processed individually. Chhatre and Titchener-Hooker (2009) state that assay run times ideally need to be similar to, if not shorter than, the actual experiment to prevent analysis becoming the process bottleneck. In this way incorporating high-throughput analytics capable of working with small volume samples could reduce the turnaround time prior to the start of process development experimentation.

8 References

- Abril, O., Ryerson, C.C., Walsh, C., and Whitesides, G.M. (1989). Enzymatic Baeyer-Villiger type oxidations of ketones catalyzed by cyclohexanone oxygenase. *Bioorganic Chemistry* 17, 41–52.
- Aiba, S., Koizumi, J., Shi Ru, J., and Mukhopadhyay, S.N. (1984). The effect of temperature on K_{1a} in thermophilic cultivation of *Bacillus stearothermophilus*. *Biotechnology and Bioengineering* 26, 1136–1138.
- Alphand, V., Carrea, G., Wohlgemuth, R., Furstoss, R., and Woodley, J.M. (2003). Towards large-scale synthetic applications of Baeyer-Villiger monooxygenases. *Trends in Biotechnology* 21, 318–323.
- Andersen, J.F., Tatsuta, K., Gunji, H., Ishiyama, T., and Hutchinson, C.R. (1993). Substrate specificity of 6-deoxyerythronolide B hydroxylase, a bacterial cytochrome P450 of erythromycin A biosynthesis. *Biochemistry* 32, 1905–1913.
- Arinç, E., Schenkman, J.B., and Hodgson, E. (1999). *Molecular and Applied Aspects of Oxidative Drug Metabolizing Enzymes* (Springer).
- Baboo, J.Z., Galman, J.L., Lye, G.J., Ward, J.M., Hailes, H.C., and Micheletti, M. (2012). An automated microscale platform for evaluation and optimization of oxidative bioconversion processes, *Biotechnology Progress*, 28, 392–405.
- Baeyer A, Villiger V (1899), *Ber. Dtsch. Chem. Ges.* 32:3625
- Bailey, J., and Ollis, D. (1986). *Biochemical Engineering Fundamentals* (McGraw-Hill Education).
- Baldwin, C.V.F., and Woodley, J.M. (2006). On oxygen limitation in a whole cell biocatalytic Baeyer–Villiger oxidation process. *Biotechnology and Bioengineering* 95, 362–369.

Bareither, R., and Pollard, D. (2011). A review of advanced small-scale parallel bioreactor technology for accelerated process development: Current state and future need. *Biotechnology Progress* 27, 2–14.

Barrett, T.A., Wu, A., Zhang, H., Levy, M.S., and Lye, G.J. (2010). Microwell engineering characterization for mammalian cell culture process development. *Biotechnology and Bioengineering* 105, 260–275.

Bandyopadhyay, B., Humphrey, A.E., and Taguchi, H. (1967). Dynamic measurement of the volumetric oxygen transfer coefficient in fermentation systems. *Biotechnology and Bioengineering* 9, 533–544.

Barrett, T.A., Wu, A., Zhang, H., Levy, M.S., and Lye, G.J. (2010). Microwell engineering characterization for mammalian cell culture process development. *Biotechnology and Bioengineering* 105, 260–275.

Berezina, N., Kozma, E., Furstoss, R., and Alphand, V. (2007). Asymmetric Baeyer-Villiger Biooxidation of alpha-Substituted Cyanocyclohexanones: Influence of the Substituent Length on Regio- and Enantioselectivity. *Advanced Synthesis & Catalysis* 349, 2049–2053.

Betts, J.I., Doig, S.D., and Baganz, F. (2006). Characterization and Application of a Miniature 10 mL Stirred Tank Bioreactor, Showing Scale-Down Equivalence with a Conventional 7 L Reactor. *Biotechnology Progress* 22, 681–688.

Betts, J., and Baganz, F. (2006). Miniature bioreactors: current practices and future opportunities. *Microbial Cell Factories* 5, 21.

Bernhardt, R. (2006). Cytochromes P450 as versatile biocatalysts. *Journal of Biotechnology* 124, 128–145.

Bhambure, R., Kumar, K., and Rathore, A.. (2011). High-throughput process development for biopharmaceutical drug substances. *Trends in Biotechnology* 29, 127–135.

Bills, G.F., Platas, G., Fillola, A., Jiménez, M.R., Collado, J., Vicente, F., Martín, J., González, A., Bur-Zimmermann, J., Tormo, J.R., et al. (2008). Enhancement of antibiotic and secondary metabolite detection from filamentous fungi by growth on nutritional arrays. *Journal of Applied Microbiology* 104, 1644–1658.

Blaser, H.U., and Federsel, H.J. (2011). *Asymmetric Catalysis on Industrial Scale: Challenges, Approaches and Solutions* (John Wiley & Sons).

Bolwell, G.P., Bozak, K., and Zimmerlin, A. (1994). Plant cytochrome p450. *Phytochemistry* 37, 1491–1506.

Büchs, J. (2001). Introduction to advantages and problems of shaken cultures. *Biochemical Engineering Journal* 7, 91–98.

Büchs, J., Lotter, S., and Milbradt, C. (2001). Out-of-phase operating conditions, a hitherto unknown phenomenon in shaking bioreactors. *Biochemical Engineering Journal* 7, 135–141.

Çalik, G., Vural, H., and Özdamar, T.H. (1997). Bioprocess parameters and oxygen transfer effects in the growth of *Pseudomonas dacunhae* for L-alanine production. *Chemical Engineering Journal* 65, 109–116.

Çalik, P., Yilgör, P., Ayhan, P., and Demir, A.S. (2004). Oxygen transfer effects on recombinant benzaldehyde lyase production. *Chemical Engineering Science* 59, 5075–5083.

Carnell, A.J., Roberts, S.M., Sik, V., and Willetts, A.J. (1991). Microbial oxidation of 7endo-methylbicyclo[3.2.0]hept-2-en-6-one, 7,7-dimethylbicyclo[3.2.0]hept-2-en-6-one and 2exo-bromo-3endo-hydroxy-7,7-

dimethylbicyclo[3.2.0]heptan-6-one using *Acinetobacter* NCIMB 9871. *Journal of the Chemical Society, Perkin Transactions 1* 2385.

Celik, A., Flitsch, S.L., and Turner, N.J. (2005 a). Efficient terpene hydroxylation catalysts based upon P450 enzymes derived from Actinomycetes. *Organic Biomolecular Chemistry* 3, 2930–2934.

Celik, A., Speight, R.E., and Turner, N.J. (2005 b). Identification of broad specificity P450CAM variants by primary screening against indole as substrate. *Chem. Commun.* 43, 3652–3654.

Černuchová, P., and Mihovilovic, M.D. (2007). Microbial Baeyer–Villiger oxidation of terpenones by recombinant whole-cell biocatalysts—formation of enantiocomplementary regioisomeric lactones. *Org. Biomol. Chem.* 5, 1715–1719.

Chandler, M., and Zydney, A. (2004). High-throughput screening for membrane process development. *Journal of Membrane Science* 237, 181–188.

Chhatre, S., and Titchener-Hooker, N.J. (2009). Review: Microscale methods for high-throughput chromatography development in the pharmaceutical industry. *Journal of Chemical Technology and Biotechnology* 84, 927–940.

Cheesman, M., Kneller, M., Kelly, E., Thompson, S., Yeung, C., Eaton, D., and Rettie, A. (2001). Purification and characterization of hexahistidine-tagged cyclohexanone monooxygenase expressed in *saccharomyces cerevisiae* and *escherichia coli*. *Protein Expression and Purification* 21, 81–86.

Chen, G., Kayser, M.M., Mihovilovic, M.D., Mrstik, M.E., Martinez, C.A., and Stewart, J.D. (1999). Asymmetric oxidations at sulfur catalyzed by engineered strains that overexpress cyclohexanone monooxygenase. *New Journal of Chemistry* 23, 827–832.

Chen, W., Peter, R.M., Mcardle, S., Thummel, K.E., Sigle, R.O., and Nelson, S.D. (1996). Baculovirus Expression and Purification of Human and Rat Cytochrome P450 2E1. *Archives of Biochemistry and Biophysics* 335, 123–130.

Chen, A., Chitta, R., Chang, D., and Amanullah, A. (2009). Twenty-four well plate miniature bioreactor system as a scale-down model for cell culture process development. *Biotechnology and Bioengineering* 102, 148–160.

Chen, Y.C., Peoples, O.P., and Walsh, C.T. (1988). *Acinetobacter* Cyclohexanone Monooxygenase: Gene Cloning and Sequence Determination. *J. Bacteriol.* 170, 781–789.

Choi, S.-J., Kim, M., Kim, S.-I., and Jeon, J.-K. (2003). Microplate assay measurement of cytochrome p450-carbon monoxide complexes. *J. Biochem. Mol. Biol.* 36, 332–335.

Coffman, J.L., Kramarczyk, J.F., and Kelley, B.D. (2008). High-throughput screening of chromatographic separations: I. Method development and column modeling. *Biotechnology and Bioengineering* 100, 605–618.

Craig, V., Ninham, B., and Pashley, R. (1993). The effect of electrolytes on bubble coalescence in water. *Journal of Physical Chemistry* 97, 10192–10197.

Crige R (1948), *Justus Liebigs Ann. Chem.* 560:127

Degtyarenko, K.N., and Archakov, A.I. (1993). Molecular evolution of P450 superfamily and P450-containing monooxygenase systems. *FEBS Letters* 332, 1–8.

Delcarte, J., Fauconnier, M.L., Jacques, P., Matsui, K., Thonart, P., and Marlier, M. (2003). Optimisation of expression and immobilized metal ion affinity chromatographic purification of recombinant (His)₆-tagged cytochrome P450 hydroperoxide lyase in *Escherichia coli*. *Journal Of Chromatography B Analytical Technologies In The Biomedical And Life Sciences* 786, 229–236.

Deshpande, R., Wittmann, C., and Heinzle, E. Microplates with integrated oxygen sensing for medium optimization in animal cell culture. *Cytotechnology* 46, 1–8.

Djelal, H., Larher, F., Martin, G., and Amrane, A. (2006). Effect of the dissolved oxygen on the bioproduction of glycerol and ethanol by *Hansenula anomala* growing under salt stress conditions. *Journal of Biotechnology* 125, 95–103.

Doig, S.D., O'Sullivan, L.M., Patel, S., Ward, J.M., and Woodley, J.M. (2001). Large-scale production of cyclohexanone monooxygenase from *Escherichia coli* TOP10 pQR239. *Enzyme and Microbial Technology* 28, 265–274.

Doig, S.D., Pickering, S.C.R., Lye, G.J., and Woodley, J.M. (2002). The use of microscale processing technologies for quantification of biocatalytic Baeyer-Villiger oxidation kinetics. *Biotechnology and Bioengineering* 80, 42–49.

Doig, S.D., Simpson, H., Alphand, V., Furstoss, R., and Woodley, J.M. (2003). Characterization of a recombinant *Escherichia coli* TOP10 [pQR239] whole-cell biocatalyst for stereoselective Baeyer-Villiger oxidations. *Enzyme and Microbial Technology* 32, 347–355.

Doig, S.D., Pickering, S.C.R., Lye, G.J., and Baganz, F. (2005). Modelling surface aeration rates in shaken microtitre plates using dimensionless groups. *Chemical Engineering Science* 60, 2741–2750.

Donoghue, N.A., Norris, D.B., and Trudgill, P.W. (1976). The Purification and Properties of Cyclohexanone Oxygenase from *Nocardia globerula* CL1 and *Acinetobacter* NCIB 9871. *European Journal of Biochemistry* 63, 175–192.

Donoghue, N.A., and Trudgill, P.W. (1975). The Metabolism of Cyclohexanol by *Acinetobacter* NCIB 9871. *European Journal of Biochemistry* 60, 1–7.

Doo, E.-H., Lee, W.-H., Seo, H.-S., Seo, J.-H., and Park, J.-B. (2009). Productivity of cyclohexanone oxidation of the recombinant *Corynebacterium*

glutamicum expressing *chnB* of *Acinetobacter calcoaceticus*. *Journal of Biotechnology* 142, 164–169.

Doran, P.M. (1995). *Bioprocess engineering principles* (Academic Press).

Dörnenburg, H. (2010). Cyclotide synthesis and supply: From plant to bioprocess. *Peptide Science* 94, 602–610.

Duetz, W.A., Ruedi, L., Hermann, R., O'Connor, K., Buchs, J., and Witholt, B. (2000). Methods for Intense Aeration, Growth, Storage, and Replication of Bacterial Strains in Microtiter Plates. *Appl. Environ. Microbiol.* 66, 2641–2646.

Duetz, W.A., and Witholt, B. (2001). Effectiveness of orbital shaking for the aeration of suspended bacterial cultures in square-deepwell microtiter plates. *Biochemical Engineering Journal* 7, 113–115.

Duetz, W.A., Beilen, J.B.V., and Witholt, B. (2001). Using proteins in their natural environment: potential and limitations of microbial whole-cell hydroxylations in applied biocatalysis. *Current Opinion in Biotechnology* 12, 419–425.

Duetz, W.A., and Witholt, B. (2004). Oxygen transfer by orbital shaking of square vessels and deepwell microtiter plates of various dimensions. *Biochemical Engineering Journal* 17, 181–185.

Duetz, W.A. (2007). Microtiter plates as mini-bioreactors: miniaturization of fermentation methods. *Trends in Microbiology* 15, 469–475.

Elmahdi, I., Baganz, F., Dixon, K., Harrop, T., Sugden, D., and Lye, G.J. (2003). pH control in microwell fermentations of *S. erythraea* CA340: influence on biomass growth kinetics and erythromycin biosynthesis. *Biochemical Engineering Journal* 16, 299–310.

Fernandes, P., and Cabral, J.M.S. (2006). Microlitre/millilitre shaken bioreactors in fermentative and biotransformation processes – a review. *Biocatalysis and Biotransformation* 24, 237–252.

Fernandes, P. (2010). Miniaturization in Biocatalysis. *International Journal of Molecular Sciences* 11, 858–879.

Ferreira-Torres, C., Micheletti, M., and Lye, G. (2005). Microscale process evaluation of recombinant biocatalyst libraries: application to Baeyer–Villiger monooxygenase catalysed lactone synthesis. *Bioprocess and Biosystems Engineering* 28, 83–93.

Ferreira-Torres C (2008), Microscale process characterisation of oxidative conversions. PhD Thesis, University of London.

Finn, R. K. (1954). Agitation-aeration in the laboratory and in industry. *Microbiology and Molecular Biology Reviews* 18, 254–274.

Finnerty, W.R. (1992). The Biology and Genetics of the Genus *Rhodococcus*. *Annual Review of Microbiology* 46, 193–218.

Fisher, C.W., Caudle, D.L., Martin-Wixtrom, C., Quattrochi, L.C., Tukey, R.H., Waterman, M.R., and Estabrook, R.W. (1992). High-level expression of functional human cytochrome P450 1A2 in *Escherichia coli*. *Faseb J.* 6, 759–764.

Freyer, S.A., König, M., and Künkel, A. (2004). Validating shaking flasks as representative screening systems. *Biochemical Engineering Journal* 17, 169–173.

Fukui, Y., Tanaka, Y., Kusumi, T., Iwashita, T., and Nomoto, K. (2003). A rationale for the shift in colour towards blue in transgenic carnation flowers expressing the flavonoid 3',5'-hydroxylase gene. *Phytochemistry* 63, 15–23.

Fulco, A.J. (1991). P450BM-3 and other Inducible Bacterial P450 Cytochromes: Biochemistry and Regulation. *Annual Review of Pharmacology and Toxicology* 31, 177–203.

Funke, M., Diederichs, S., Kensy, F., Müller, C., and Büchs, J. (2009). The baffled microtiter plate: Increased oxygen transfer and improved online monitoring in small-scale fermentations. *Biotechnology and Bioengineering* 103, 1118–1128.

Garcia-Ochoa, F., and Gomez, E. (2009). Bioreactor scale-up and oxygen transfer rate in microbial processes: An overview. *Biotechnology Advances* 27, 153–176.

Garfinkel, D. (1958). Studies on pig liver microsomes. I. Enzymic and pigment composition of different microsomal fractions. *Archives of Biochemistry and Biophysics* 77, 493–509.

Gatfield, I. (1997). Biotechnological production of flavour-active lactones. In *Biotechnology of Aroma Compounds*. (Springer Berlin / Heidelberg).

Geitner, K., Kirschner, A., Rehdorf, J., Schmidt, M., Mihovilovic, M.D., and Bornscheuer, U.T. (2007). Enantioselective kinetic resolution of 3-phenyl-2-ketones using Baeyer–Villiger monooxygenases. *Tetrahedron: Asymmetry* 18, 892–895.

Gill, N.K., Appleton, M., Baganz, F., and Lye, G.J. (2008). Design and characterisation of a miniature stirred bioreactor system for parallel microbial fermentations. *Biochemical Engineering Journal* 39, 164–176.

Gillam, E.M., Guo, Z., Martin, M.V., Jenkins, C.M., and Guengerich, F.P. (1995). Expression of cytochrome P450 2D6 in *Escherichia coli*, purification, and spectral and catalytic characterization. *Arch. Biochem. Biophys.* 319, 540–550.

Girard, P., Jordan, M., Tsao, M., and Wurm, F.M. (2001). Small-scale bioreactor system for process development and optimization. *Biochemical Engineering Journal* 7, 117–119.

Gomez, E., Santos, V.E., Alcon, A., and Garcia-Ochoa, F. (2006). Oxygen transport rate on *Rhodococcus erythropolis* cultures: Effect on growth and BDS capability. *Chemical Engineering Science* 61, 4595–4604.

Grant, C., Pinto, da S.D., Catarina, A., Lui, H., Woodley, J.M., and Baganz, F. (2012). Tools for characterizing the whole-cell bio-oxidation of alkanes at microscale, Tools for characterizing the whole-cell bio-oxidation of alkanes at microscale. *Biotechnology and Bioengineering*.

Gu, M.B., Dhurjati, P.S., Dyk, V., K, T., and LaRossa, R.A. (1996). A Miniature Bioreactor for Sensing Toxicity Using Recombinant Bioluminescent *Escherichia coli* Cells. *Biotechnology Progress* 12, 393–397.

Guarna, M.M., Lesnicki, G.J., Tam, B.M., Robinson, J., Radziminski, C.Z., Hasenwinkle, D., Boraston, A., Jervis, E., MacGillivray, R.T.A., Turner, R.F.B., et al. (1997). On-line monitoring and control of methanol concentration in shake flask cultures of *Pichia pastoris*. *Biotechnology and Bioengineering* 56, 279–286.

Guengerich, F.P. (1995). Cytochrome P450 proteins and potential utilization in biodegradation. *Environ. Health Perspect.* 103 Suppl 5, 25–28.

Gustafsson, M.C.U., Roitel, O., Marshall, K.R., Noble, M.A., Chapman, S.K., Pessegueiro, A., Fulco, A.J., Cheesman, M.R., von Wachenfeldt, C., and Munro, A.W. (2004). Expression, Purification, and Characterization of *Bacillus subtilis* Cytochromes P450 CYP102A2 and CYP102A3: Flavocytochrome Homologues of P450 BM3 from *Bacillus megaterium*. *Biochemistry* 43, 5474–5487.

Hammonds, T.R., Maxwell, A., and Jenkins, J.R. (1998). Use of a Rapid Throughput In Vivo Screen To Investigate Inhibitors of Eukaryotic Topoisomerase II Enzymes. *Antimicrob. Agents Chemother.* *42*, 889–894.

Hannemann, F., Bichet, A., Ewen, K.M., and Bernhardt, R. (2007). Cytochrome P450 systems—biological variations of electron transport chains. *Biochimica Et Biophysica Acta (BBA) - General Subjects* *1770*, 330–344.

Harikrishna, M., Mohan, H.R., Dubey, P.K., and Subbaraju, G.V. (2009). Synthesis of 2-Normisoprostol, Methyl 6-(3-Hydroxy-2-((E)-4-hydroxy-4-methyloct-1-enyl)-5-oxocyclopentyl)hexanoate. *Synthetic Communications* *39*, 2763–2775.

Harms, P., Kostov, Y., French, J.A., Soliman, M., Anjanappa, M., Ram, A., and Rao, G. (2006). Design and performance of a 24-station high-throughput microbioreactor. *Biotechnology and Bioengineering* *93*, 6–13.

Hasegawa, Y., Hamano, K., Obata, H., and Tokuyama, T. (1982). Microbial degradation of cycloheptanone. *Agricultural and Biological Chemistry* *46*, 1139.

Hasler, J.A., Estabrook, R., Murray, M., Pikuleva, I., Waterman, M., Capdevila, J., Holla, V., Helvig, C., Falck, J.R., Farrell, G., et al. (1999). Human cytochromes P450. *Molecular Aspects of Medicine* *20*, 1–137.

Healy, F.G., Krasnoff, S.B., Wach, M., Gibson, D.M., and Loria, R. (2002). Involvement of a Cytochrome P450 Monooxygenase in Thaxtomin A Biosynthesis by *Streptomyces acidiscabies*. *Journal of Bacteriology* *184*, 2019–2029.

Heijnen, J.J., Riet, K.V., and Wolthuis, A.J. (1980). Influence of very small bubbles on the dynamic K_La measurement in viscous gas–liquid systems. *Biotechnology and Bioengineering* *22*, 1945–1956.

Hermann, R., Lehmann, M., and Buchs, J. (2003). Characterization of gas-liquid mass transfer phenomena in microtiter plates. *Biotechnology and Bioengineering* 81, 178–186.

Hibbert, E.G., Baganz, F., Hailes, H.C., Ward, J.M., Lye, G.J., Woodley, J.M., and Dalby, P.A. (2005). Directed evolution of biocatalytic processes. *Biomolecular Engineering* 22, 11–19.

Hichri, H., Accary, A., Puaux, J.P., and Andrieu, J. (1992). Gas-liquid mass-transfer coefficients in a slurry batch reactor equipped with a self-gas-inducing agitator. *Ind. Eng. Chem. Res.* 31, 1864–1867.

Hilker, I., Roland Wohlgemuth, Veronique Alphan, and Roland Furstoss (2005). Microbial transformations 59: First kilogram scale asymmetric microbial Baeyer-Villiger oxidation with optimized productivity using a resin-based in situ SFPR strategy. *Biotechnology and Bioengineering* 92, 702–710.

Hilker, I., Gutierrez, M.C., Furstoss, R., Ward, J., Wohlgemuth, R., and Alphan, V. (2008). Preparative scale Baeyer-Villiger biooxidation at high concentration using recombinant *Escherichia coli* and in situ substrate feeding and product removal process. *Nature Protocols* 3, 546–554.

Hill, G.A. (2006). Measurement of Overall Volumetric Mass Transfer Coefficients for Carbon Dioxide in a Well-Mixed Reactor Using a pH Probe. *Ind. Eng. Chem. Res.* 45, 5796–5800.

Holton, T.A., Brugliera, F., Lester, D.R., Tanaka, Y., Hyland, C.D., Menting, J.G.T., Lu, C.-Y., Farcy, E., Stevenson, T.W., and Cornish, E.C. (1993). Cloning and expression of cytochrome P450 genes controlling flower colour. , Published Online: 18 November 1993; | Doi:10.1038/366276a0 366, 276–279.

Holz, C., Hesse, O., Bolotina, N., Stahl, U., and Lang, C. (2002). A micro-scale process for high-throughput expression of cDNAs in the yeast *Saccharomyces cerevisiae*. *Protein Expression and Purification* 25, 372–378.

Huber, R., Ritter, D., Hering, T., Hillmer, A.-K., Kensy, F., Müller, C., Wang, L., and Büchs, J. (2009). Robo-Lector – a novel platform for automated high-throughput cultivations in microtiter plates with high information content. *Microbial Cell Factories* 8, 42.

Hussain, H.A., and Ward, J.M. (2003 a). Ferredoxin reductase enhances heterologously expressed cytochrome CYP105D1 in *Escherichia coli* and *Streptomyces lividans*. *Enzyme and Microbial Technology* 32, 790–800.

Hussain, H.A., and Ward, J.M. (2003 b). Enhanced Heterologous Expression of Two *Streptomyces griseolus* Cytochrome P450s and *Streptomyces coelicolor* Ferredoxin Reductase as Potentially Efficient Hydroxylation Catalysts. *Appl. Environ. Microbiol.* 69, 373–382.

Imai Y., and Sayo, R. (1967). Studies on the Substrate Interactions with P-450 in Drug Hydroxylation by Liver Microsomes. *J Biochem* 62, 239–249.

Imai, T., Globerman, H., Gertner, J.M., Kagawa, N., and Waterman, M.R. (1993). Expression and purification of functional human 17 alpha-hydroxylase/17,20-lyase (P450c17) in *Escherichia coli*. Use of this system for study of a novel form of combined 17 alpha-hydroxylase/17,20-lyase deficiency. *J. Biol. Chem.* 268, 19681–19689.

Inui, H., Kodama, T., Ohkawa, Y., and Ohkawa, H. (2000). Herbicide Metabolism and Cross-Tolerance in Transgenic Potato Plants Co-Expressing Human CYP1A1, CYP2B6, and CYP2C19. *Pesticide Biochemistry and Physiology* 66, 116–129.

Isett, K., George, H., Herber, W., and Amanullah, A. (2007). Twenty-four-well plate miniature bioreactor high-throughput system: Assessment for microbial cultivations. *Biotechnology and Bioengineering* 98, 1017–1028.

Islam, R.S., Tisi, D., Levy, M.S., and Lye, G.J. (2008). Scale-Up of *Escherichia coli* Growth and Recombinant Protein Expression Conditions From Microwell to

Laboratory and Pilot Scale Based on Matched K_{La} . *Biotechnology and Bioengineering* 99, 1128–1139.

Islam, R.S (2007), Novel engineering tools to aid drug discovery processes. PhD Thesis, University of London.

Iwaki, H., Hasegawa, Y., Teraoka, M., Tokuyama, T., Bergeron, H., and Lau, P.C.K. (1999). Identification of a Transcriptional Activator (ChnR) and a 6-Oxohexanoate Dehydrogenase (ChnE) in the Cyclohexanol Catabolic Pathway in *Acinetobacter Sp.* Strain NCIMB 9871 and Localization of the Genes That Encode Them. *Appl. Environ. Microbiol.* 65, 5158–5162.

Iwaki, H., Hasegawa, Y., Wang, S., Kayser, M.M., and Lau, P.C.K. (2002). Cloning and Characterization of a Gene Cluster Involved in Cyclopentanol Metabolism in *Comamonas Sp.* Strain NCIMB 9872 and Biotransformations Effected by *Escherichia Coli*-Expressed Cyclopentanone 1,2-Monooxygenase. *Appl. Environ. Microbiol.* 68, 5671–5684.

Jackson, N.B., Liddell, J.M., and Lye, G.J. (2006). An automated microscale technique for the quantitative and parallel analysis of microfiltration operations. *Journal of Membrane Science* 276, 31–41.

Jansson, I., Stoilov, I., Sarfarazi, M., and Schenkman, J.B. (2000). Enhanced expression of CYP1B1 in *Escherichia coli*. *Toxicology* 144, 211–219.

Jennewein, S., Park, H., DeJong, J.M., Long, R.M., Bollon, A.P., and Croteau, R.B. (2005). Coexpression in yeast of *Taxus* cytochrome P450 reductase with cytochrome P450 oxygenases involved in Taxol biosynthesis. *Biotechnol. Bioeng.* 89, 588–598.

Jensen, V.J., and Rugh, S. (1987). Industrial-scale production and application of immobilized glucose isomerase. Part C: Immobilized Enzymes and Cells 136, 356–370.

John, G.T., Klimant, I., Wittmann, C., and Heinzle, E. (2003). Integrated optical sensing of dissolved oxygen in microtiter plates: A novel tool for microbial cultivation. *Biotechnology and Bioengineering* 81, 829–836.

John, G.T., and Heinzle, E. (2001). Quantitative screening method for hydrolases in microplates using pH indicators: Determination of kinetic parameters by dynamic pH monitoring. *Biotechnology and Bioengineering* 72, 620–627.

Kagawa, N., and Cao, Q. (2001). Osmotic Stress Induced by Carbohydrates Enhances Expression of Foreign Proteins in *Escherichia coli*. *Archives of Biochemistry and Biophysics* 393, 290–296.

Kamerbeek, N.M., Moonen, M.J.H., Ven, V.D., M, J.G., Berkel, V., H, W.J., Fraaije, M.W., and Janssen, D.B. (2001). 4-Hydroxyacetophenone monooxygenase from *Pseudomonas fluorescens* ACB, *European Journal of Biochemistry* 268, 2547–2557.

Kamerbeek, N.M., Janssen, D.B., Van Berkel, W. J.H., and Fraaije, M.W. (2003). Baeyer-Villiger Monooxygenases, an Emerging Family of Flavin-Dependent Biocatalysts. *Advanced Synthesis & Catalysis* 345, 667–678.

Katagiri, M., Ganguli, B.N., and Gunsalus, I.C. (1968). A Soluble Cytochrome P-450 Functional in Methylene Hydroxylation. *J. Biol. Chem.* 243, 3543–3546.

Kawase, Y., and Moo-Young, M. (1990). The effect of antifoam agents on mass transfer in bioreactors. *Bioprocess and Biosystems Engineering* 4, 169–173.

Kellner, D.G., Maves, S.A., and Sligar, S.G. (1997). Engineering cytochrome P450s for bioremediation. *Curr. Opin. Biotechnol.* 8, 274–278.

Kensy, F., Zimmermann, H.F., Knabben, I., Anderlei, T., Trauthwein, H., Dingerdissen, U., and Buchs, J. (2005). Oxygen transfer phenomena in 48-well microtiter plates: Determination by optical monitoring of sulfite oxidation and

verification by real-time measurement during microbial growth. *Biotechnology and Bioengineering* 89, 698–708.

Kensy, F., Engelbrecht, C., and Buchs, J. (2009). Scale-up from microtiter plate to laboratory fermenter: evaluation by online monitoring techniques of growth and protein expression in *Escherichia coli* and *Hansenula polymorpha* fermentations. *Microbial Cell Factories* 8, 1–15.

Kermis, H.R., Kostov, Y., Harms, P., and Rao, G. (2002). Dual Excitation Ratiometric Fluorescent pH Sensor for Noninvasive Bioprocess Monitoring: Development and Application. *Biotechnology Progress* 18, 1047–1053.

Kieslich, K. (1991). Biotransformations of industrial use. *Acta Biotechnologica* 11, 559–570.

Kim, Y.-M., Jung, S.-H., Chung, Y.-H., Yu, C.-B., and Rhee, I.-K. (2008). Cloning and characterization of a cyclohexanone monooxygenase gene from *Arthrobacter sp.* L661. *Biotechnology and Bioprocess Engineering* 13, 40–47.

Klingenberg, M. (1958). Pigments of rat liver microsomes. *Archives of Biochemistry and Biophysics* 75, 376–386.

Knorr, B., Schlieker, H., Hohmann, H.-P., and Weuster-Botz, D. (2007). Scale-down and parallel operation of the riboflavin production process with *Bacillus subtilis*. *Biochemical Engineering Journal* 33, 263–274.

Kostichka, K., Thomas, S.M., Gibson, K.J., Nagarajan, V., and Cheng, Q. (2001). Cloning and Characterization of a Gene Cluster for Cyclododecanone Oxidation in *Rhodococcus ruber* SC1. *J. Bacteriol.* 183, 6478–6486.

Kostov, Y., Harms, P., Randers-Eichhorn, L., and Rao, G. (2001). Low-cost microbioreactor for high-throughput bioprocessing. *Biotechnology and Bioengineering* 72, 346–352.

Kubota, M., Nodate, M., Yasumoto-Hirose, M., Uchiyama, T., Kagami, O., Shizuri, Y., and Misawa, N. (2005). Isolation and functional analysis of cytochrome P450 CYP153A genes from various environments. *Biosci. Biotechnol. Biochem.* *69*, 2421–2430.

Kumar, S., Wittmann, C., and Heinzle, E. (2004). Minibioreactors. *Biotechnol Lett* *26*, 1–10.

La Du, B.N., Gaudette, L., Trousof, N., and Brodie, B.B. (1955). Enzymatic Dealkylation of Aminopyrine (pyramidon) and Other Alkylamines. *Journal of Biological Chemistry* *214*, 741–752.

Lamping, S.R., Zhang, H., Allen, B., and Shamlou, P.A. (2003). Design of a prototype miniature bioreactor for high-throughput automated bioprocessing. *Chemical Engineering Science* *58*, 747–758.

Lander KS (2003), *In situ* product recovery from a Baeyer-Villiger monooxygenase catalysed bioconversion. PhD Thesis, University of London.

Leak, D.J., Sheldon, R.A., Woodley, J.M., and Adlercreutz, P. (2009). Biocatalysts for selective introduction of oxygen. *Biocatalysis and Biotransformation* *27*, 1–26.

Levitt, M.S., Newton, R.F., Roberts, S.M., and Willetts, A.J. (1990). Preparation of optically active 6'-fluorocarbocyclic nucleosides utilising an enantiospecific enzyme-catalysed Baeyer–Villiger type oxidation. *J. Chem. Soc., Chem. Commun.* 619–620.

Linek, V., Beneš, P., and Vacek, V. (1989). Dynamic pressure method for *K_{La}* measurement in large-scale bioreactors. *Biotechnology and Bioengineering* *33*, 1406–1412.

Linek, V., Kordac, M., Fujasová, M., and Moucha, T. (2004). Gas-liquid mass transfer coefficient in stirred tanks interpreted through models of idealized eddy

structure of turbulence in the bubble vicinity. *Chemical Engineering and Processing* 43, 1511–1517.

Liu, L., Schmid, R.D., and Urlacher, V.B. (2006). Cloning, expression, and characterization of a self-sufficient cytochrome P450 monooxygenase from *Rhodococcus ruber* DSM 44319. *Applied Microbiology and Biotechnology* 72, 876–882.

Liu, L., Schmid, R.D., and Urlacher, V.B. (2010). Engineering cytochrome P450 monooxygenase CYP 116B3 for high dealkylation activity. *Biotechnol. Lett.* 32, 841–845.

Losen, M., Frölich, B., Pohl, M., and Büchs, J. (2004). Effect of Oxygen Limitation and Medium Composition on *Escherichia coli* Fermentation in Shake Flask Cultures. *Biotechnology Progress* 20, 1062–1068.

Lu, H., Ma, J., Liu, N., and Wang, S. (2010). Effects of heme precursors on CYP1A2 and POR expression in the baculovirus/*Spodoptera frugiperda* system. *Journal of Biomedical Research* 24, 242–249.

Lu, Y., and Mei, L. (2007). Co-expression of P450 BM3 and glucose dehydrogenase by recombinant *Escherichia coli* and its application in an NADPH-dependent indigo production system. *J. Ind. Microbiol. Biotechnol.* 34, 247–253.

Lye, G.J., Dalby, P.A., and Woodley, J.M. (2002). Better Biocatalytic Processes Faster: New Tools for the Implementation of Biocatalysis in Organic Synthesis. 37, 1198–1209.

Lye, G.J., Ayazi-Shamlou, P., Baganz, F., Dalby, P.A., and Woodley, J.M. (2003). Accelerated design of bioconversion processes using automated microscale processing techniques. *Trends in Biotechnology* 21, 29–37.

Maier, U., and Büchs, J. (2001). Characterisation of the gas–liquid mass transfer in shaking bioreactors. *Biochemical Engineering Journal* 7, 99–106.

Manosroi, A., Saowakhon, S., and Manosroi, J. (2008). Enhancement of androstadienedione production from progesterone by biotransformation using the hydroxypropyl- β -cyclodextrin complexation technique. *The Journal of Steroid Biochemistry and Molecular Biology* 108, 132–136.

Marques, M.P., de Carvalho, C.C., Claudino, M.J., Cabral, J.M., and Fernandes, P. (2007). On the feasibility of the microscale approach for a multistep biotransformation: sitosterol side chain cleavage. *Journal of Chemical Technology and Biotechnology* 82, 856–863.

Marques, M.P.C., Magalhães, S., Cabral, J.M.S., and Fernandes, P. (2009). Characterization of 24-well microtiter plate reactors for a complex multistep bioconversion: From sitosterol to androstenedione. *Journal of Biotechnology* 141, 174–180.

Marques, M.P.C., de Carvalho, C.C.C., Cabral, J.M.S., and Fernandes, P. (2010). Scaling-up of complex whole-cell bioconversions in conventional and non-conventional media. *Biotechnology and Bioengineering* 106, 619–626.

Marques, M.P.C., Walshe, K., Doyle, S., Fernandes, P., and de Carvalho, C.C.C.R. (2012). Anchoring high-throughput screening methods to scale-up bioproduction of siderophores. *Process Biochemistry* 47, 416–421.

Matosevic, S., Micheletti, M., Woodley, J., Lye, G., and Baganz, F. (2008). Quantification of kinetics for enzyme-catalysed reactions: implications for diffusional limitations at the 10 ml scale. *Biotechnology Letters* 30, 995–1000.

Matsumura, I., and Ellington, A.D. (2001). In vitro Evolution of Beta-glucuronidase into a Beta-galactosidase Proceeds Through Non-specific Intermediates. *Journal of Molecular Biology* 305, 331–339.

Mazza, C.B., Rege, K., Breneman, C.M., Sukumar, N., Dordick, J.S., and Cramer, S.M. (2002). High-throughput screening and quantitative structure-efficacy relationship models of potential displacer molecules for ion-exchange systems. *Biotechnology and Bioengineering* 80, 60–72.

McLean, M.A., Yeom, H., and Sligar, S.G. (1996). Carbon monoxide binding to cytochrome P450BM-3: Evidence for a substrate-dependent conformational change. *Biochimie* 78, 700–705.

Micheletti, M., Barrett, T., Doig, S.D., Baganz, F., Levy, M.S., Woodley, J.M., and Lye, G.J. (2006). Fluid mixing in shaken bioreactors: Implications for scale-up predictions from microlitre-scale microbial and mammalian cell cultures. *Chemical Engineering Science* 61, 2939–2949.

Micheletti, M., and Lye, G.J. (2006). Microscale bioprocess optimisation. *Current Opinion in Biotechnology* 17, 611–618.

Mihovilovic, M.D., Müller, B., Kayser, M.M., Stewart, J.D., Fröhlich, J., Stanetty, P., and Spreitzer, H. (2001). Baeyer-Villiger oxidations of representative heterocyclic ketones by whole cells of engineered *Escherichia coli* expressing cyclohexanone monooxygenase. *Journal of Molecular Catalysis B: Enzymatic* 11, 349–353.

Mihovilovic, M.D., Kapitán, P., and Kapitánová, P. (2008). Regiodivergent Baeyer–Villiger Oxidation of Fused Ketones by Recombinant Whole-Cell Biocatalysts. *ChemSusChem* 1, 143–148.

Mirjalili, N., Zormpaidis, V., Leadlay, P.F., and Ison, A.P. (1999). The Effect of Rapeseed Oil Uptake on the Production of Erythromycin and Triketide Lactone by *Saccharopolyspora erythraea*. *Biotechnology Progress* 15, 911–918.

Morão, A., Maia, C.I., Fonseca, M.M.R., Vasconcelos, J.M.T., and Alves, S.S. (1999). Effect of antifoam addition on gas-liquid mass transfer in stirred fermenters. *Bioprocess Engineering* 20, 165.

Morii, S., Sawamoto, S., Yamauchi, Y., Miyamoto, M., Iwami, M., and Itagaki, E. (1999). Steroid Monooxygenase of *Rhodococcus Rhodochrous*: Sequencing of the Genomic DNA, and Hyperexpression, Purification, and Characterization of the Recombinant Enzyme. *J Biochem* 126, 624–631.

Mouri, T., Michizoe, J., Ichinose, H., Kamiya, N., and Goto, M. (2006). A recombinant *Escherichia coli* whole cell biocatalyst harboring a cytochrome P450cam monooxygenase system coupled with enzymatic cofactor regeneration. *Applied Microbiology and Biotechnology* 72, 514–520.

Mozhaev, V.V., and Martinek, K. (1982). Inactivation and reactivation of proteins (enzymes). *Enzyme and Microbial Technology* 4, 299–309.

Nagasawa, T., and Yamada, H. (1990). Application of nitrile converting enzymes for the production of useful compounds. 62, 141–1444.

Nakayama, N., Takemae, A., and Shoun, H. (1996). Cytochrome P450foxy, a Catalytically Self-Sufficient Fatty Acid Hydroxylase of the *Fungus Fusarium Oxysporum*. *J Biochem* 119, 435–440.

Narhi, L., and Fulco, A. (1986). Characterization of a catalytically self-sufficient 119,000-dalton cytochrome P-450 monooxygenase induced by barbiturates in *Bacillus megaterium*. *J. Biol. Chem.* 261, 7160–7169.

Nealon, A.J., O’Kennedy, R.D., Titchener-Hooker, N.J., and Lye, G.J. (2006). Quantification and prediction of jet macro-mixing times in static microwell plates. *Chemical Engineering Science* 61, 4860–4870.

Nealon, A.J., Willson, K.E., Pickering, S.C.R., Clayton, T.M., O’Kennedy, R.D., Titchener-Hooker, N.J., and Lye, G.J. (2005). Use of Operating Windows in the Assessment of Integrated Robotic Systems for the Measurement of Bioprocess Kinetics. *Biotechnology Progress* 21, 283–291.

Nebert, D.W., and Nelson, D.R. (1991). P450 gene nomenclature based on evolution. In *Cytochrome P450*, (Academic Press), pp. 3–11.

Neubauer, P., Häggström, L., and Enfors, S. O (1995). Influence of substrate oscillations on acetate formation and growth yield in *Escherichia coli* glucose limited fed-batch cultivations. *Biotechnology and Bioengineering* 47, 139–146.

Newton, R., and Roberts, S. (1980). Steric control in prostaglandin synthesis involving bicyclic and tricyclic intermediates. *Tetrahedron* 36, 2163–2196.

Ni, X., Gao, S., Cumming, R.H., and Pritchard, D.W. (1995). A comparative study of mass transfer in yeast for a batch pulsed baffled bioreactor and a stirred tank fermenter. *Chemical Engineering Science* 50, 2127–2136.

Niraula, N.P., Kanth, B.K., Sohng, J.K., and Oh, T.J. (2011). Hydrogen peroxide-mediated dealkylation of 7-ethoxycoumarin by cytochrome P450 (CYP107AJ1) from *Streptomyces peucetius* ATCC27952. *Enzyme Microb. Technol.* 48, 181–186.

O’Keefe, D.P., Gibson, K.J., Emptage, M.H., Lenstra, R., Romesser, J.A., Litle, P.J., and Omer, C.A. (1991). Ferredoxins from two sulfonylurea herbicide monooxygenase systems in *Streptomyces griseolus*. *Biochemistry* 30, 447–455.

Olsen K. (2000). A quantitative study of factors governing automatic pipetting performance. *American Laboratory* 32, 49–51.

Omura, T., and Sato, R. (1964). The Carbon Monoxide-binding Pigment of Liver Microsomes. *Journal of Biological Chemistry* 239, 2370–2378.

Ordidge, G.C., Mannall, G., Liddell, J., Dalby, P.A., Micheletti, M., and Mannall, G. (2012). A generic hierarchical screening method for the analysis of microscale refolds using an automated robotic platform. *Biotechnology Progress* 28, 435–444.

Ordidge, G.C (2012), Rapid microscale evaluation of the impact of fermentation conditions on inclusion body formation. PhD Thesis, University College London.

Ortiz-Ochoa, K., Doig, S.D., Ward, J.M., and Baganz, F. (2005). A novel method for the measurement of oxygen mass transfer rates in small-scale vessels. *Biochemical Engineering Journal* 25, 63–68.

Ottolina, G., de Gonzalo, G., Carrea, G., and Danieli, B. (2005). Enzymatic Baeyer–Villiger Oxidation of Bicyclic Diketones. *Advanced Synthesis & Catalysis* 347, 1035–1040.

Parikh, A., Gillam, E., and Guengerich, P. (1997). Drug metabolism by *Escherichia coli* expressing human cytochrome P450. *Nature Biotechnology* 15, 784–788.

Persidis, A. (1998). High-throughput screening. *Nature Biotechnology* 16, 488–489.

Peterson, D.H., Murray, H.C., Eppstein, S.H., Reineke, L.M., Weintraub, A., Meister, P.D., and Leigh, H.M. (1952). Microbiological Transformations of Steroids.1 I. Introduction of Oxygen at Carbon-11 of Progesterone. *J. Am. Chem. Soc.* 74, 5933–5936.

Phillips, I.R., and Shephard, E.A. (2006). *Cytochrome P450 protocols* (Humana Press).

Picataggio, S., Rohrer, T., Deanda, K., Lanning, D., Reynolds, R., Mielenz, J., and Eirich, L.D. (1992). Metabolic engineering of *Candida tropicalis* for the production of long-chain dicarboxylic acids. *Biotechnology (N.Y.)* 10, 894–898.

Punt, P.J., van Biezen, N., Conesa, A., Albers, A., Mangnus, J., and van den Hondel, C. (2002). Filamentous fungi as cell factories for heterologous protein production. *Trends in Biotechnology* 20, 200–206.

Puskeiler, R., Kaufmann, K., and Weuster-Botz, D. (2005). Development, parallelization, and automation of a gas-inducing milliliter-scale bioreactor for high-throughput bioprocess design (HTBD). *Biotechnology and Bioengineering* 89, 512–523.

Rachinskiy, K., Schultze, H., Boy, M., Bornscheuer, U., and Büchs, J. (2009). “Enzyme Test Bench,” a high-throughput enzyme characterization technique including the long-term stability. *Biotechnology and Bioengineering* 103, 305–322.

Raillard, S., Krebber, A., Chen, Y., Ness, J.E., Bermudez, E., Trinidad, R., Fullem, R., Davis, C., Welch, M., Seffernick, J., et al. (2001). Novel enzyme activities and functional plasticity revealed by recombining highly homologous enzymes. *Chemistry & Biology* 8, 891–898.

Ramachandra, M., Seetharam, R., Emptage, M.H., and Sariaslani, F.S. (1991). Purification and Characterization of a Soybean Flour-Inducible Ferredoxin Reductase of *Streptomyces Griseus*. *J. Bacteriol.* 173, 7106–7112.

Rayat, A.C.M.E., Micheletti, M., Lye, G.J., (2010). Evaluation of cell disruption effects on primary recovery of antibody fragments using microscale bioprocessing techniques, *Biotechnology Progress*, 26, 1312–1321.

Rege, K., Ladiwala, A., Tugcu, N., Breneman, C.M., and Cramer, S.M. (2004). Parallel screening of selective and high-affinity displacers for proteins in ion-exchange systems. *Journal of Chromatography* 1033, 19–28.

Rege, K., Pepsin, M., Falcon, B., Steele, L., and Heng, M. (2006). High-throughput process development for recombinant protein purification. *Biotechnology and Bioengineering* 93, 618–630.

Richardson, T.H., Jung, F., Griffin, K.J., Wester, M., Raucy, J.L., Kemper, B., Bornheim, L.M., Hassett, C., Omiecinski, C.J., and Johnson, E.F. (1995). A

universal approach to the expression of human and rabbit cytochrome P450s of the 2C subfamily in *Escherichia coli*. *Arch. Biochem. Biophys.* *323*, 87–96.

Roberts, G.A., Grogan, G., Greter, A., Flitsch, S.L., and Turner, N.J. (2002). Identification of a New Class of Cytochrome P450 from a *Rhodococcus sp.* *J. Bacteriol.* *184*, 3898–3908.

Roberts, S.M., and Wan, P.W.H. (1998). Enzyme-catalysed Baeyer–Villiger oxidations. *Journal of Molecular Catalysis B: Enzymatic* *4*, 111–136.

Rozman, D., Pertot, E., Belič, I., and Komel, R. (1985). Soybean peptones as nutrients in the fermentative production of clavine ergot alkaloids with *Claviceps fusiformis*. *Biotechnology Letters* *7*, 563–566.

Samorski, M., Müller Newen, G., and Büchs, J. (2005). Quasi-continuous combined scattered light and fluorescence measurements: A novel measurement technique for shaken microtiter plates. *Biotechnology and Bioengineering* *92*, 61–68.

Schein, C.H. (1989). Production of Soluble Recombinant Proteins in Bacteria. *Nat Biotech* *7*, 1141–1149.

Schmid, A., Dordick, J.S., Hauer, B., Kiener, A., Wubbolts, M., and Witholt, B. (2001). Industrial biocatalysis today and tomorrow. *Nature* *409*, 258–268.

Schulze, B., and Wubbolts, M.G. (1999). Biocatalysis for industrial production of fine chemicals. *Current Opinion in Biotechnology* *10*, 609–615.

Secundo, F., Carrea, G., Dallavalle, S., and Franzosi, G. (1993). Asymmetric oxidation of sulfides by cyclohexanone monooxygenase. *Tetrahedron: Asymmetry* *4*, 1981–1982.

Serizawa, N., and Matsuoka, T. (1991). A two component-type cytochrome P-450 monooxygenase system in a prokaryote that catalyzes hydroxylation of ML-

236B to pravastatin, a tissue-selective inhibitor of 3-hydroxy-3-methylglutaryl coenzyme A reductase. *Biochimica Et Biophysica Acta (BBA) - Lipids and Lipid Metabolism* 1084, 35–40.

Sevrioukova, I.F., Li, H., and Poulos, T.L. (2004). Crystal Structure of Putidaredoxin Reductase from *Pseudomonas putida*, the Final Structural Component of the Cytochrome P450cam Monooxygenase. *Journal of Molecular Biology* 336, 889–902.

Shiloach, J., and Fass, R. (2005). Growing *E. coli* to high cell density - a historical perspective on method development. *Biotechnol. Adv.* 23, 345–357.

Shimada, T., Wunsch, R.M., Hanna, I.H., Sutter, T.R., Guengerich, F.P., and Gillam, E.M. (1998). Recombinant human cytochrome P450 1B1 expression in *Escherichia coli*. *Arch. Biochem. Biophys.* 357, 111–120.

Shin, J.-A., Kwon, Y.D., Kwon, O.-H., Lee, H.S., and Kim, P. (2007). 5-aminolevulinic acid biosynthesis in *Escherichia coli* coexpressing NADP-dependent malic enzyme and 5-aminolevulinate synthase. *J. Microbiol. Biotechnol.* 17, 1579–1584.

Shipston, N.F., Lenn, M.J., and Knowles, C.J. (1992). Enantioselective whole cell and isolated enzyme catalysed Baeyer-Villiger oxidation of bicyclo[3.2.0]hept-2-en-6-one. *Journal of Microbiological Methods* 15, 41–52.

Shitu, J.O., Chartrain, M., and Woodley, J.M. (2009). Evaluating the impact of substrate and product concentration on a whole-cell biocatalyst during a Baeyer-Villiger reaction. *Biocatalysis and Biotransformation* 27, 107–117.

Skjelbred, B., Edvardsen, B., and Andersen, T. (2012). A high-throughput method for measuring growth and loss rates in microalgal cultures. *Journal of Applied Phycology*.

Sivropoulou, A., Kokkini, S., Lanaras, T., and Arsenakis, M. (1995). Antimicrobial activity of mint essential oils. *J. Agric. Food Chem.* *43*, 2384–2388.

Sonnleitner, B. (1997). Bioprocess automation and bioprocess design. *Journal of Biotechnology* *52*, 175–179.

Sonomoto, K., Hoq, M.M., Tanaka, A., and Fukui, S. (1983). 11β -Hydroxylation of Cortisolone (Reichstein Compound S) to Hydrocortisone by *Curvularia lunata* Entrapped in Photo-Cross-Linked Resin Gels. *Appl Environ Microbiol* *45*, 436–443.

Speight, R.E., Hancock, F.E., Winkel, C., Bevinakatti, H.S., Sarkar, M., Flitsch, S.L., and Turner, N.J. (2004). Rapid identification of cytochrome P450cam variants by in vivo screening of active site libraries. *Tetrahedron* *15*, 2829–2831.

Sriniva, R., and Panda, T. Enhancing the feasibility of many biotechnological processes through enzyme deactivation studies. *Bioprocess Engineering* *21*, 363–369.

Stahl, S., R, Greasham, olph, and Chartrain, M. (2000). Implementation of a rapid microbial screening procedure for biotransformation activities. *Journal of Bioscience and Bioengineering* *89*, 367–371.

Stassi, D.L., Kakavas, S.J., Reynolds, K.A., Gunawardana, G., Swanson, S., Zeidner, D., Jackson, M., Liu, H., Buko, A., and Katz, L. (1998). Ethyl-Substituted Erythromycin Derivatives Produced by Directed Metabolic Engineering. *Pnas* *95*, 7305–7309.

Stewart, J.D., Reed, K.W., and Kayser, M.M. (1996). “Designer yeast”: a new reagent for enantioselective Baeyer-Villiger oxidations. *Journal of the Chemical Society. Perkin Transactions 1* *8*, 755–757.

Stewart, J.D., Reed, K.W., Martinez, C.A., Zhu, J., Chen, G., and Kayser, M.M. (1998). Recombinant Baker's Yeast as a Whole-Cell Catalyst for Asymmetric Baeyer–Villiger Oxidations. *J. Am. Chem. Soc.* *120*, 3541–3548.

Strukul, G. (1998). Transition Metal Catalysis in the Baeyer-Villiger Oxidation of Ketones. *Angewandte Chemie International Edition* *37*, 1198–1209.

Sundberg, S.A. (2000). High-throughput and ultra-high-throughput screening: solution- and cell-based approaches. *Current Opinion in Biotechnology* *11*, 47–53.

Szczebara, F., Chandelier, C., Villeret, C., Masurel, A., Bourot, S., Duport, C., Blanchard, S., Groisillier, A., Testet, E., Costaglioli, P., et al. Total biosynthesis of hydrocortisone from a simple carbon source in yeast. *Nature Biotechnology* *21*, 143–149.

Szita, N., Boccazzi, P., Zhang, Z., Boyle, P., Sinskey, A.J., and Jensen, K.F. (2005). Development of a multiplexed microbioreactor system for high-throughput bioprocessing. *Lab on a Chip* *5*, 819.

Taylor, M., Lamb, D.C., Cannell, R., Dawson, M., and Kelly, S.L. (1999). Cytochrome P450105D1 (CYP105D1) from *Streptomyces griseus*: Heterologous Expression, Activity, and Activation Effects of Multiple Xenobiotics. *Biochemical and Biophysical Research Communications* *263*, 838–842.

Thibault, J., Leduy, A., and Denis, A. (1990). Chemical enhancement in the determination of K_La by the sulfite oxidation method. *The Canadian Journal of Chemical Engineering* *68*, 324–326.

Tjernberg, A., Markova, N., Griffiths, W.J., and Hallén, D. (2006). DMSO-related effects in protein characterization. *J Biomol Screen* *11*, 131–137.

- Tolosa, L., Kostov, Y., Harms, P., and Rao, G. (2002). Noninvasive measurement of dissolved oxygen in shake flasks. *Biotechnology and Bioengineering* 80, 594–597.
- Tramper, J. (1996). Chemical versus biochemical conversion: When and how to use biocatalysts. *Biotechnology and Bioengineering* 52, 290–295.
- Tressl, R., Apetz, M., Arietta, R. and Gruewald, K.G. (1978). Formation of lactones and terpenoids by microorganisms. In *Flavour of Food and Beverages*. London Academic Press Inc.
- Tribe, L.A., Briens, C.L., and Margaritis, A. (1995). Determination of the volumetric mass transfer coefficient ($k_L a$) using the dynamic “gas out–gas in” method: Analysis of errors caused by dissolved oxygen probes. *Biotechnology and Bioengineering* 46, 388–392.
- Trilli, A. (1986). Scale-up of fermentations. *Manual of industrial microbiology and biotechnology*. American Society for Microbiology.
- Trower, M.K., Buckland, R.M., and Griffin, M. (1989). Characterization of an FMN-containing cyclohexanone monooxygenase from a cyclohexane grown *Xanthobacter sp.* *European Journal of Biochemistry* 181, 199–206.
- Trudgill, P.W. (1990). Cyclohexanone 1,2-monooxygenase from *Acinetobacter* NCIMB 9871. *Hydrocarbons and Methylophony* 188, 70–77.
- Turner, C., Gregory, M.E., and Thornhill, N.F. (1994). Closed-loop control of fed-batch cultures of recombinant *Escherichia coli* using on-line HPLC. *Biotechnology and Bioengineering* 44, 819–829.
- Ueng, Y.F., Kuwabara, T., Chun, Y.J., and Guengerich, F.P. (1997). Cooperativity in oxidations catalyzed by cytochrome P450 3A4. *Biochemistry* 36, 370–381.

Uno, T., Okamoto, S., Masuda, S., Imaishi, H., Nakamura, M., Kanamaru, K., Yamagata, H., El-Kady, M.A.H., Kaminishi, Y., and Itakura, T. (2008). Bioconversion by functional P450 1A9 and P450 1C1 of *Anguilla japonica*. *Comparative Biochemistry and Physiology Toxicology Pharmacology CBP* 147, 278–285.

Urlacher, V.B., and Eiben, S. (2006). Cytochrome P450 monooxygenases: perspectives for synthetic application. *Trends Biotechnol.* 24, 324–330.

Urlacher, V.B., and Girhard, M. (2012). Cytochrome P450 monooxygenases: an update on perspectives for synthetic application. *Trends in Biotechnology* 30, 26–36.

Warman, A.J., Roitel, O., Neeli, R., Girvan, H., Seward, H., Murray, S., McLean, K., Joyce, M., Toogood, H., Holt, R., et al. (2005). Flavocytochrome P450 BM3: an update on structure and mechanism of a biotechnologically important enzyme. *Biochemical Society Transactions* 33, 747–753.

Warnecke, H.J., and Hubmann, P. (1989). Volumetric mass transfer coefficients of gas liquid jet loop reactors by oxidation of hydrazine. *Chemical engineering communications* 78, 131–138.

Weis, R., Luiten, R., Skranc, W., Schwab, H., Wubbolts, M., and Glieder, A. (2004). Reliable high-throughput screening with *Pichia pastoris* by limiting yeast cell death phenomena. *FEMS Yeast Research* 5, 179–189.

Welch, C.J., Shaimi, M., Biba, M., Chilenski, J.R., Szumigala Jr, R.H., Ulf Dolling, Mathre, D.J., and Reider, P.J. (2002). Microplate evaluation of process adsorbents. *Journal of Separation Science* 25, 847–850.

Werck-Reichhart, D., and Feyereisen, R. (2000). Cytochromes P450: a success story. *Genome Biology* 1, reviews3003.1–reviews3003.9.

Weuster-Botz, D., Puskeiler, R., Kusterer, A., Kaufmann, K., John, G., and Arnold, M. Methods and milliliter scale devices for high-throughput bioprocess design. *Bioprocess Biosystem Engineering* 28, 109–119.

Williams, P.A., Cosme, J., Sridhar, V., Johnson, E.F., and McRee, D.E. (2000). Mammalian Microsomal Cytochrome P450 Monooxygenase: Structural Adaptations for Membrane Binding and Functional Diversity. *Molecular Cell* 5, 121–131.

Willetts, A. (1997). Structural studies and synthetic applications of Baeyer-Villiger monooxygenases. *Trends in Biotechnology* 15, 55–62.

Wittmann, C., Kim, H.M., John, G., and Heinzle, E. (2003). Characterization and application of an optical sensor for quantification of dissolved O₂ in shake flasks. 25, 377–380.

Woodard, S.I., and Dailey, H.A. (1995). Regulation of heme biosynthesis in *Escherichia coli*. *Arch. Biochem. Biophys.* 316, 110–115.

Weuster-Botz, D., Altenbach-Rehm, J., and Arnold, M. (2001). Parallel substrate feeding and pH-control in shaking-flasks. *Biochemical Engineering Journal* 7, 163–170.

Wüst, M., and Croteau, R.B. (2002). Hydroxylation of specifically deuterated limonene enantiomers by cytochrome p450 limonene-6-hydroxylase reveals the mechanism of multiple product formation. *Biochemistry* 41, 1820–1827.

Vail, R.B., Homann, M.J., Hanna, I., and Zaks, A. (2005). Preparative synthesis of drug metabolites using human cytochrome P450s 3A4, 2C9 and 1A2 with NADPH-P450 reductase expressed in *Escherichia coli*. *J. Ind. Microbiol. Biotechnol.* 32, 67–74.

van Beilen, J.B., Duetz, W.A., Schmid, A., and Witholt, B. (2003). Practical issues in the application of oxygenases. *Trends in Biotechnology* 21, 170–177.

Vandezande, P., Gevers, L.E.M., Paul, J.S., Vankelecom, I.F.J., and Jacobs, P.A. (2005). High-throughput screening for rapid development of membranes and membrane processes. *Journal of Membrane Science* 250, 305–310.

Van't Riet, K. (1979). Review of Measuring Methods and Results in Nonviscous Gas-Liquid Mass Transfer in Stirred Vessels. *Ind. Eng. Chem. Proc. Des. Dev.* 18, 357–364.

Vashitz, O., Sheintuch, M., and Ulitzur, S. (1989). Mass transfer studies using cloned-luminous strain of *Xanthomonas campestris*. *Biotechnology and Bioengineering* 34, 671–680.

Vasina, J.A., and Baneyx, F. (1996). Recombinant protein expression at low temperatures under the transcriptional control of the major *Escherichia coli* cold shock promoter cspA. *Appl Environ Microbiol* 62, 1444–1447.

Yamaji, H., Tagai, S.-I., and Fukuda, H. (1999). Optimal production of recombinant protein by the baculovirus-insect cell system in shake-flask culture with medium replacement. *Journal of Bioscience and Bioengineering* 87, 636–641.

Yamazaki, H., Tanaka, M., and Shimada, T. (1999). Highly sensitive high-performance liquid chromatographic assay for coumarin 7-hydroxylation and 7-ethoxycoumarin O-deethylation by human liver cytochrome P450 enzymes. *J. Chromatogr. B Biomed. Sci. Appl.* 721, 13–19.

Yasukawa, M., Onodera, M., Yamagiwa, K., and Ohkawa, A. (1991). Gas holdup, power consumption, and oxygen absorption coefficient in a stirred-tank fermentor under foam control. *Biotechnology and Bioengineering* 38, 629–636.

Zambianchi, F., Pasta, P., Carrea, G., Colonna, S., Gaggero, N., and Woodley, J.M. (2002). Use of isolated cyclohexanone monooxygenase from recombinant *Escherichia coli* as a biocatalyst for Baeyer–Villiger and sulfide oxidations. *Biotechnology and Bioengineering* 78, 489–496.

Zambianchi, F., Raimondi, S., Pasta, P., Carrea, G., Gaggero, N., and Woodley, J.M. (2004). Comparison of cyclohexanone monooxygenase as an isolated enzyme and whole cell biocatalyst for the enantioselective oxidation of 1,3-dithiane. *Journal of Molecular Catalysis B: Enzymatic* *31*, 165–171.

Zhang, H., Lamping, S.R., Pickering, S.C.R., Lye, G.J., and Shamlou, P.A. (2008). Engineering characterisation of a single well from 24-well and 96-well microtitre plates. *Biochemical Engineering Journal* *40*, 138–149.

Zimmermann, H.F., John, G.T., Trauthwein, H., Dingerdissen, U., and Huthmacher, K. (2003). Rapid evaluation of oxygen and water permeation through microplate sealing tapes. *Biotechnol. Prog.* *19*, 1061–1063.

9 Appendices

9.1 Appendix A – Calibration Curves

A.1 Dry Cell Weight Calibration Curves

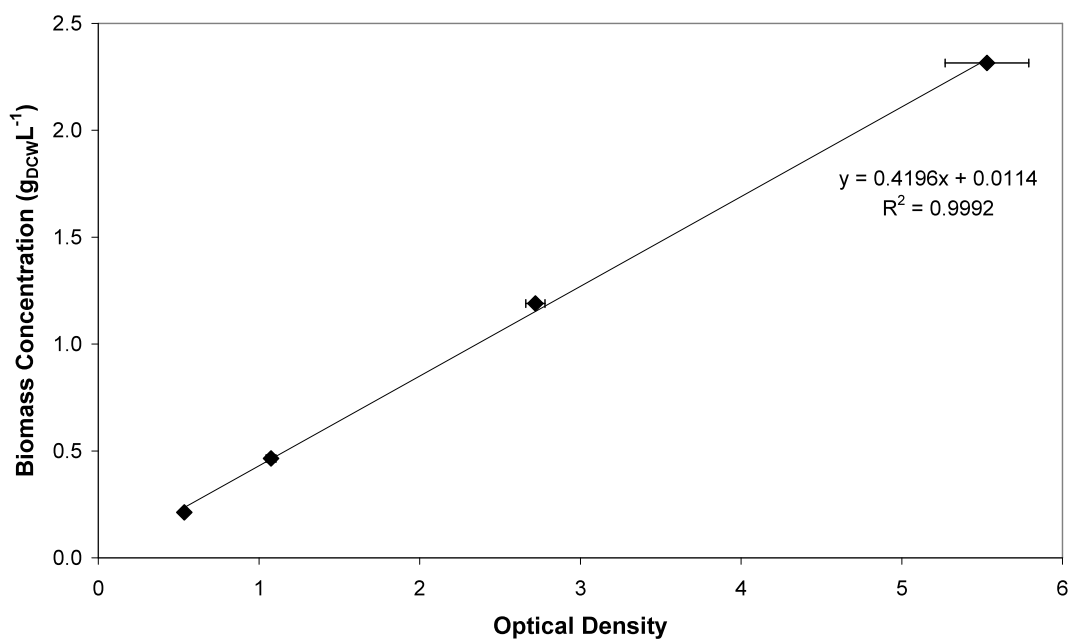


Figure A.1 Dry cell weight calibration curve for *E. coli* TOP10 [pQR210] cells. Error bars indicate the range about the mean of duplicate optical density readings (x) and duplicate biomass concentration measurements (y). Measurements were conducted as described in section 2.6.1 and 2.6.2.

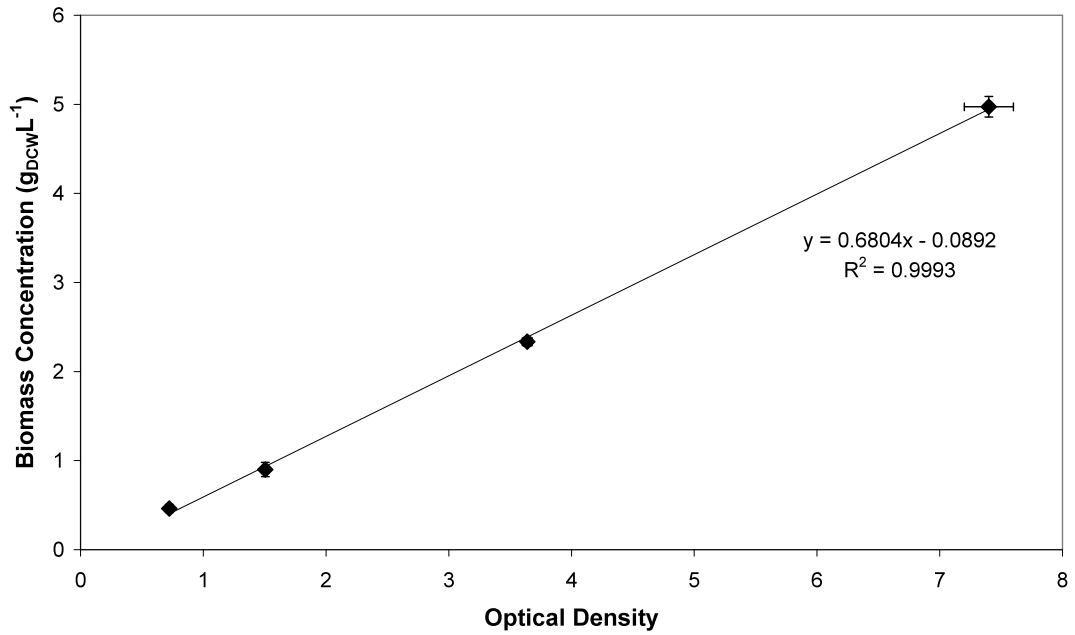


Figure A.2 Dry cell weight calibration curve for *E. coli* [pQR367] cells. Error bars indicate the range about the mean of duplicate optical density readings (x) and duplicate biomass concentration measurements (y). Measurements were conducted as described in section 2.6.1 and 2.6.2.

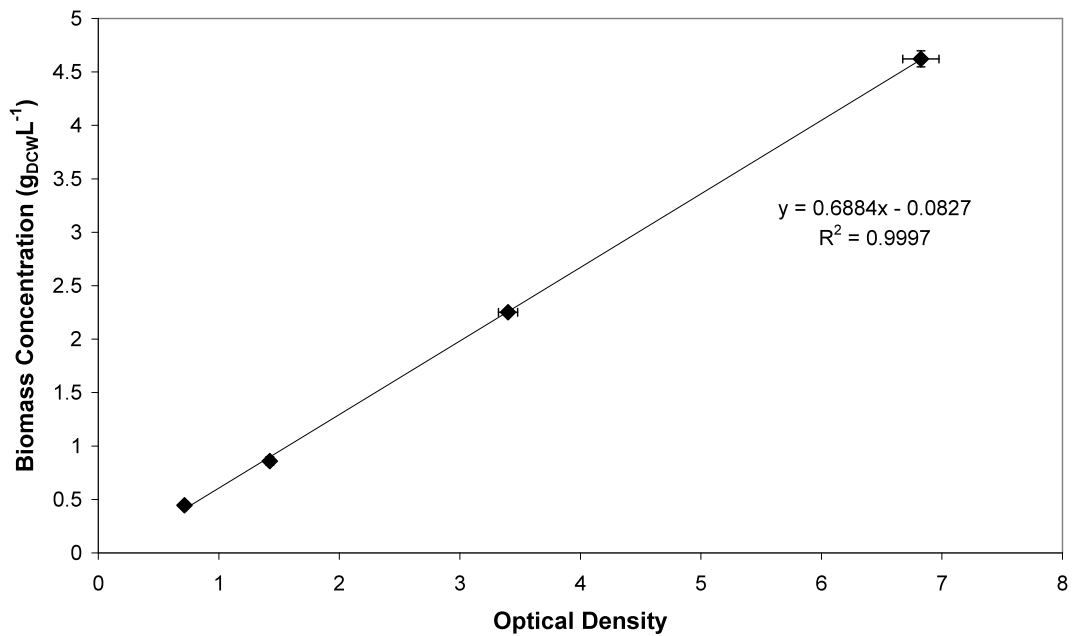


Figure A.3 Dry cell weight calibration curve for *E. coli* [pQR368] cells. Error bars indicate the range about the mean of duplicate optical density readings (x) and duplicate biomass concentration measurements (y). Measurements were conducted as described in section 2.6.1 and 2.6.2.

A.2 Gas Chromatography Calibration Curves

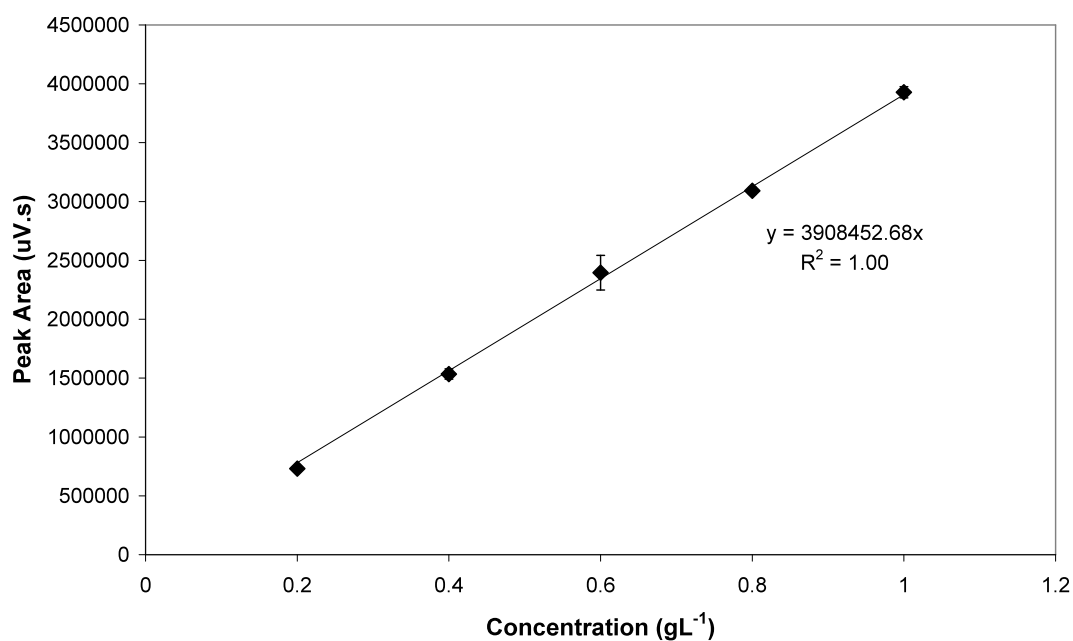


Figure A.4 Bicyclo[3.2.0]hept-2-en-6-one calibration curve. Error bars indicate the standard deviation of triplicate stock preparations in ethyl acetate. Experiments were conducted as described in section 2.6.4.2.

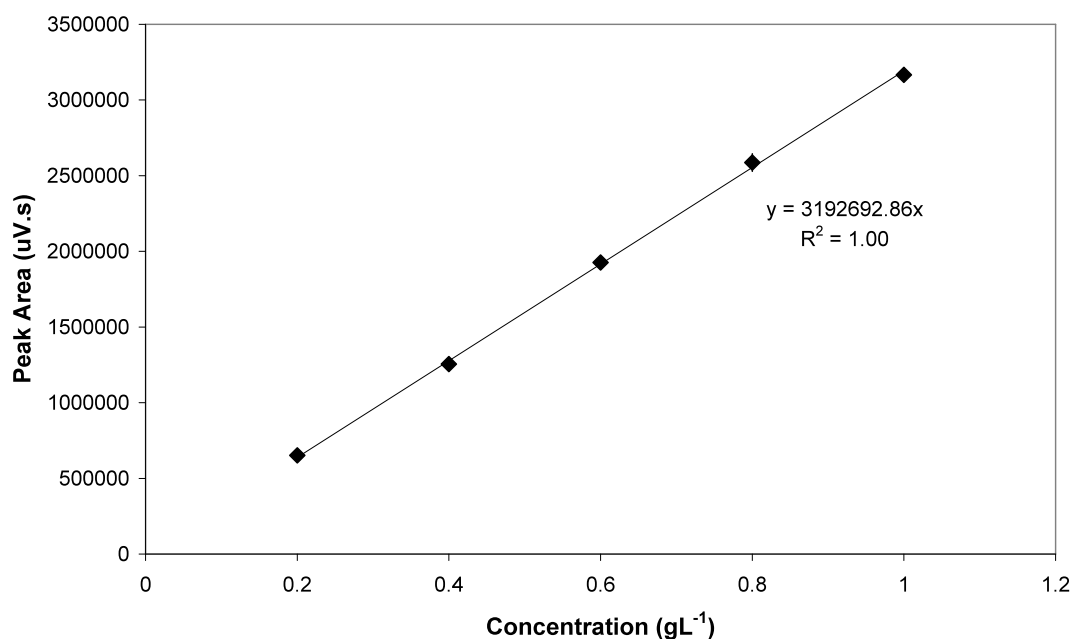


Figure A.5 (1*S*,5*R*)-2-oxabicyclo[3.3.0]oct-6-en-3-one calibration curve. Error bars indicate the standard deviation of triplicate stock preparations in ethyl acetate. Experiments were conducted as described in section 2.6.4.2.

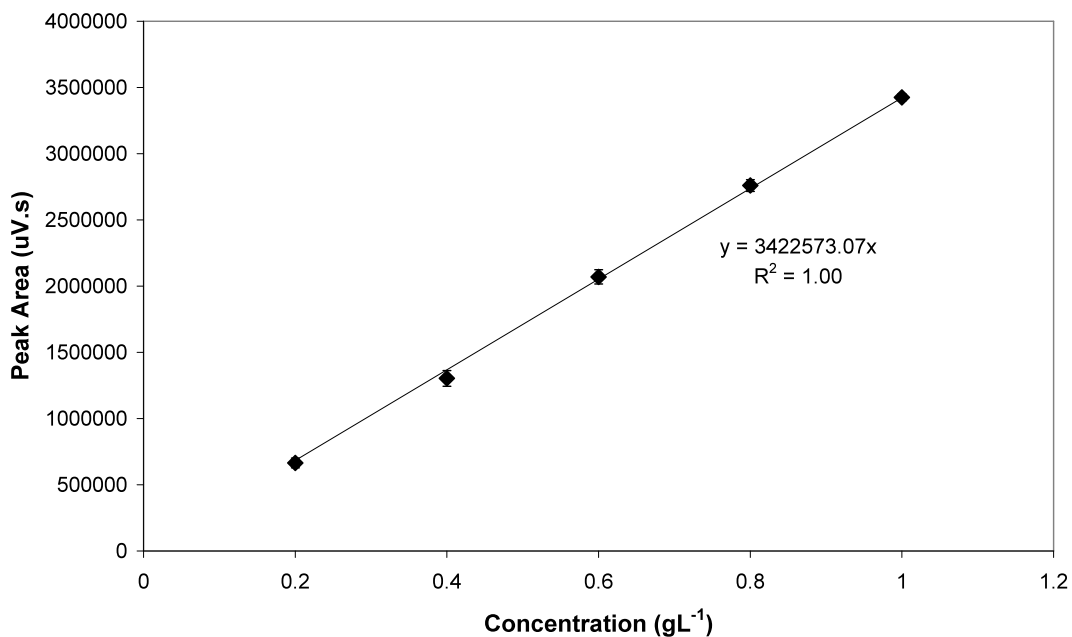


Figure A.6 Cyclohexanone calibration curve. Error bars indicate the standard deviation of triplicate stock preparations in ethyl acetate. Experiments were conducted as described in section 2.6.4.2.

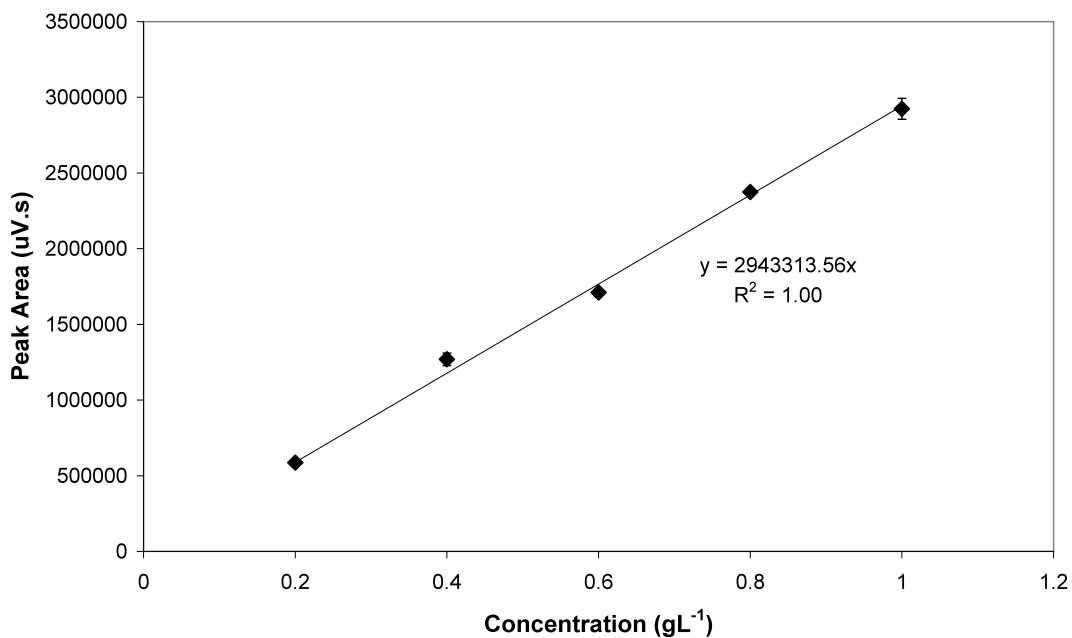


Figure A.7 ϵ -caprolactone calibration curve. Error bars indicate the standard deviation of triplicate stock preparations in ethyl acetate. Experiments were conducted as described in section 2.6.4.2.

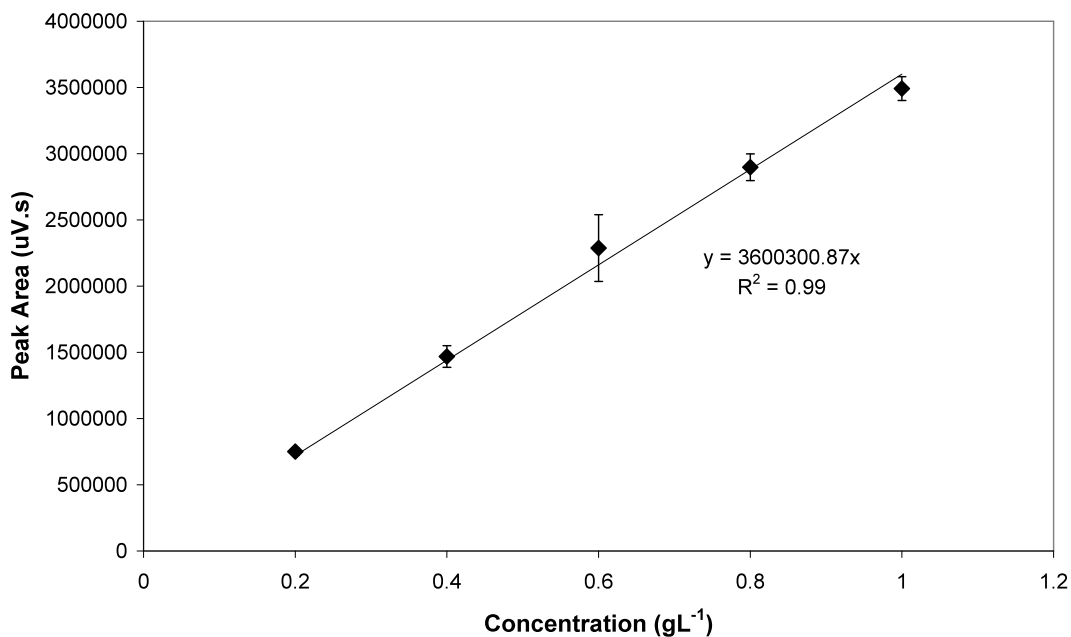


Figure A.8 Norcamphor calibration curve. Error bars indicate the standard deviation of triplicate stock preparations in ethyl acetate. Experiments were conducted as described in section 2.6.4.2.

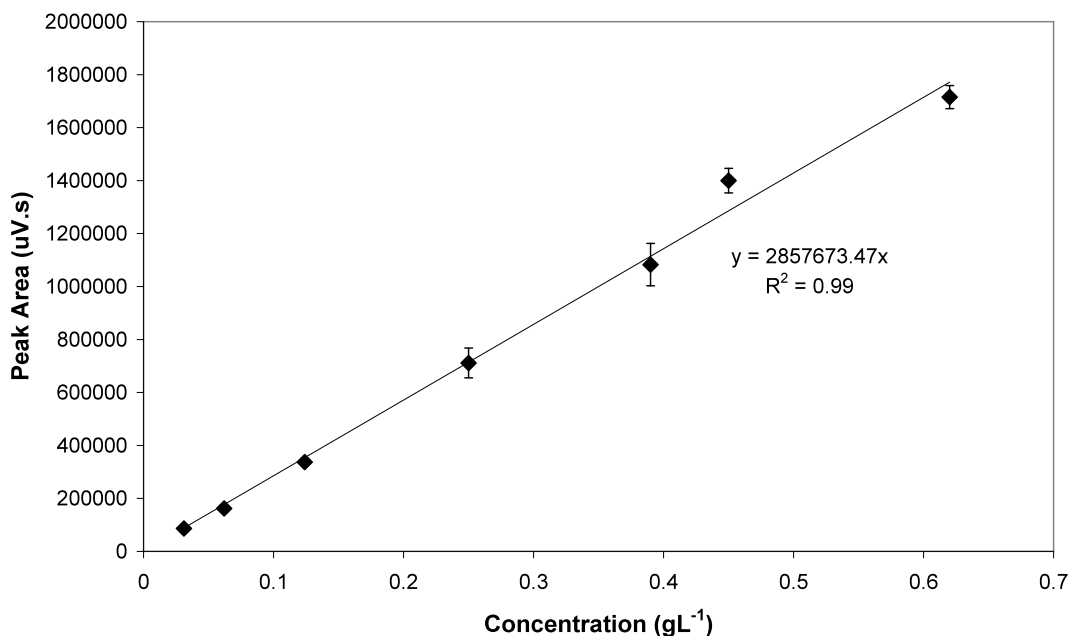


Figure A.9 2-oxabicyclo[3.2.1]octan-3-one calibration curve. Error bars indicate the standard deviation of triplicate stock preparations in ethyl acetate. Experiments were conducted as described in section 2.6.4.2.

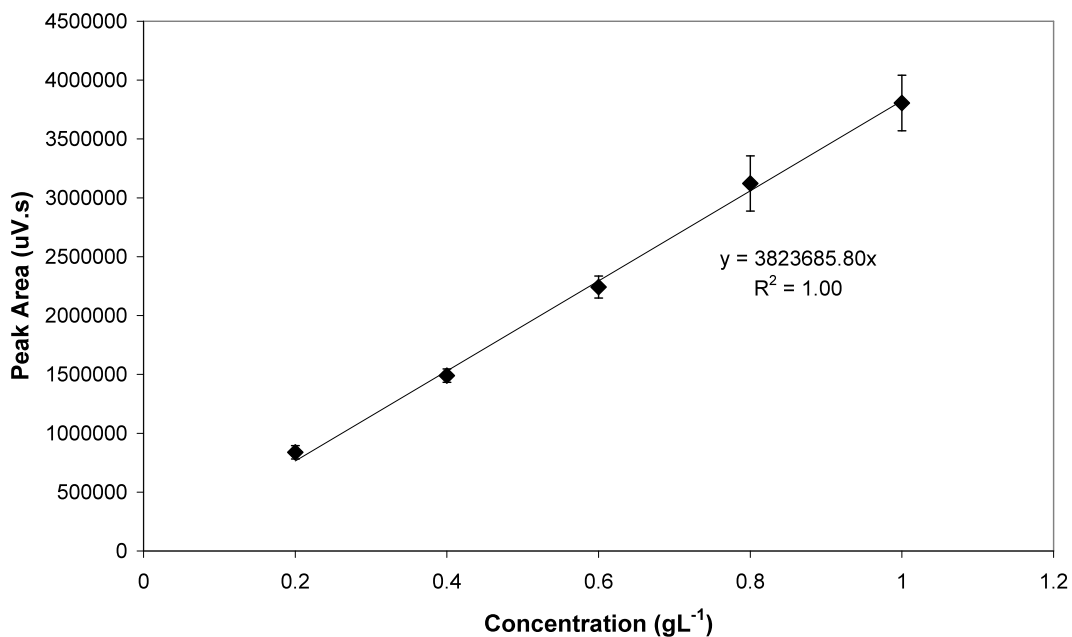


Figure A.10 Cycloheptanone calibration curve. Error bars indicate the standard deviation of triplicate stock preparations in ethyl acetate. Experiments were conducted as described in section 2.6.4.2.

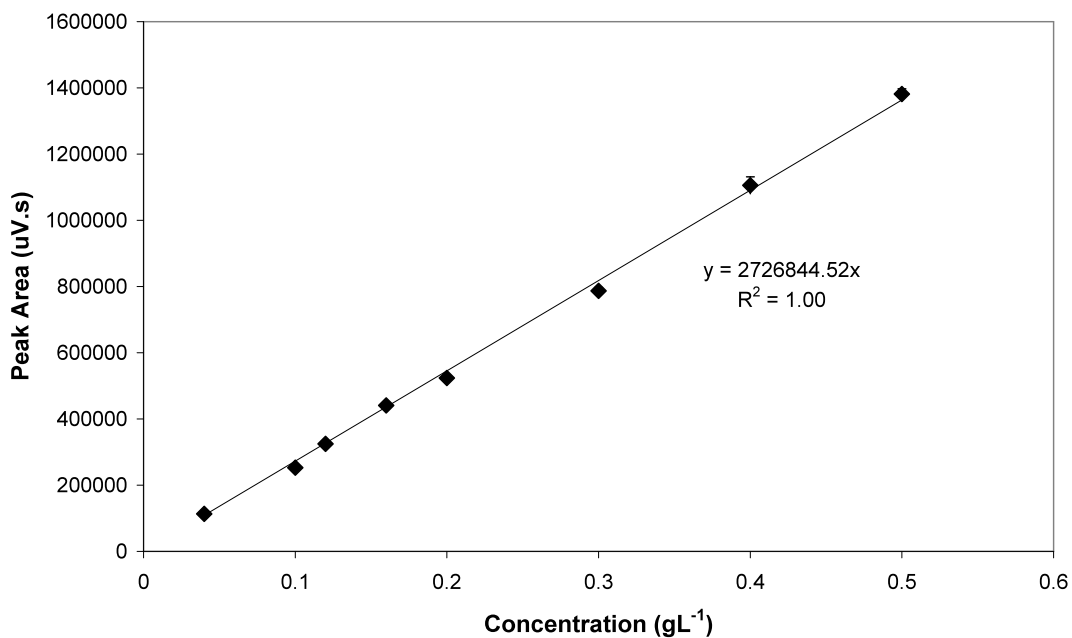


Figure A.11 Oxocan-2-one calibration curve. Error bars indicate the standard deviation of triplicate stock preparations in ethyl acetate. Experiments were conducted as described in section 2.6.4.2.

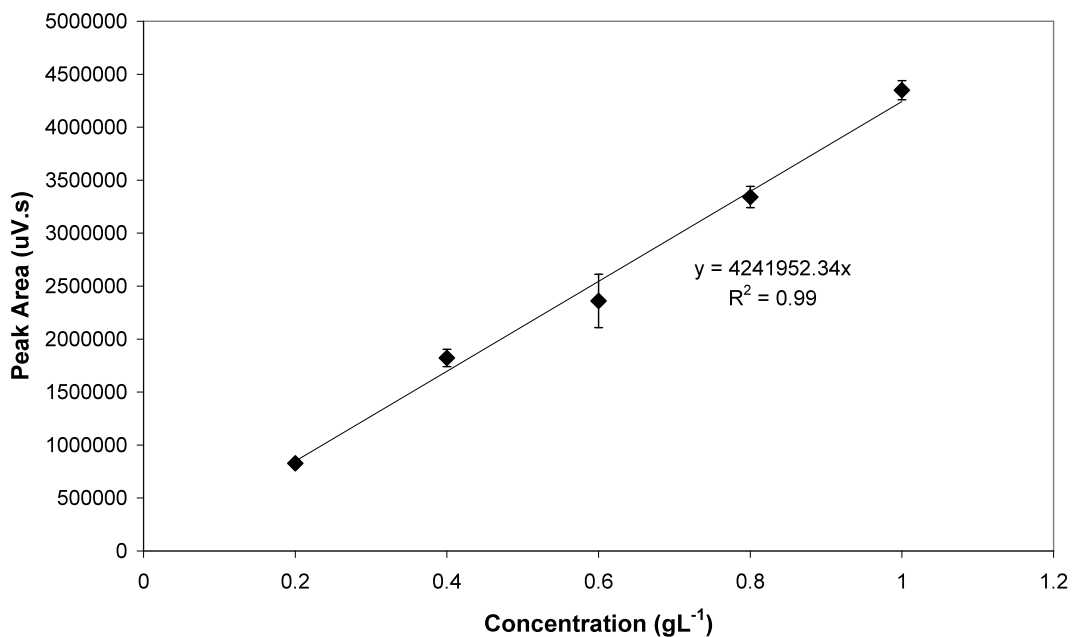


Figure A.12 (1R)-(-)-fenchone calibration curve. Error bars indicate the standard deviation of triplicate stock preparations in ethyl acetate. Experiments were conducted as described in section 2.6.4.2.

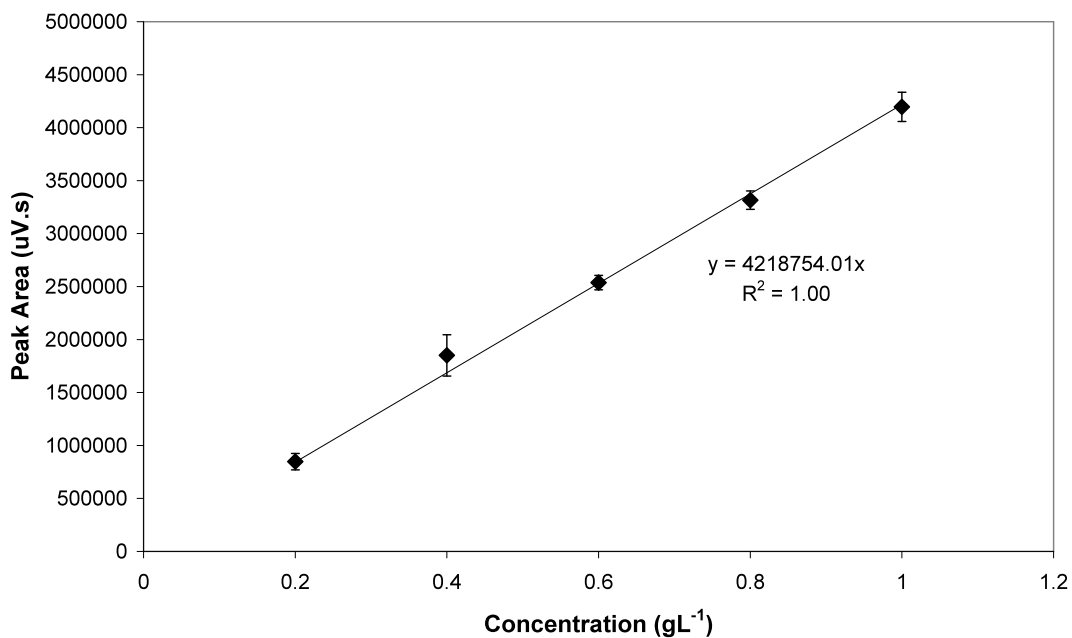


Figure A.13 (+)-(3R,6SR)-Dihydrocarvone calibration curve. Error bars indicate the standard deviation of triplicate stock preparations in ethyl acetate. Experiments were conducted as described in section 2.6.4.2.

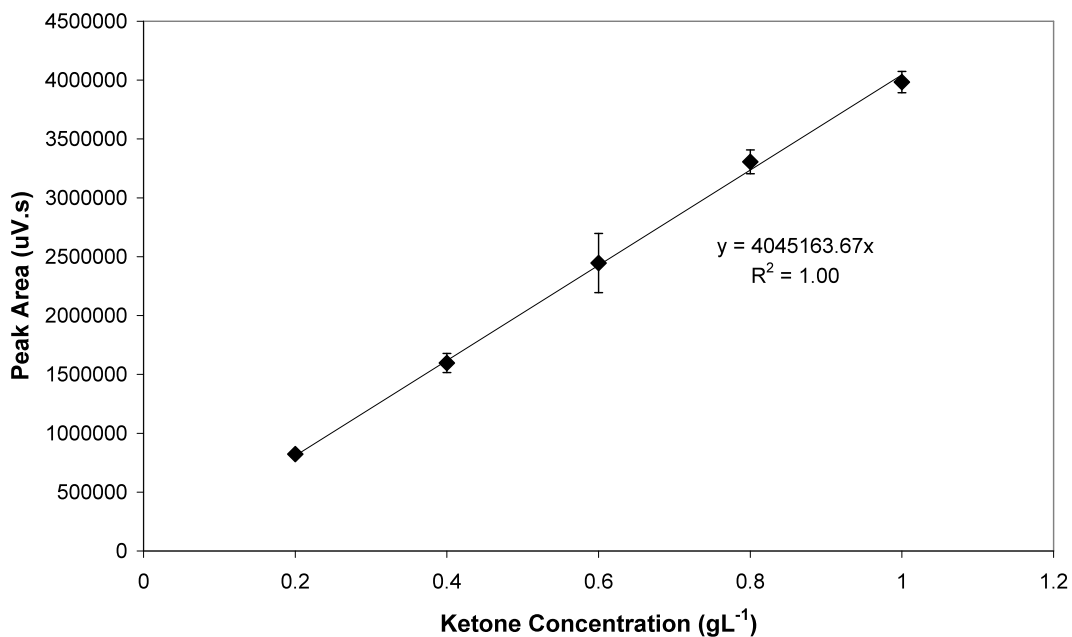


Figure A.14 Cyclooctanone calibration curve. Error bars indicate the standard deviation of triplicate stock preparations in ethyl acetate. Experiments were conducted as described in section 2.6.4.2.

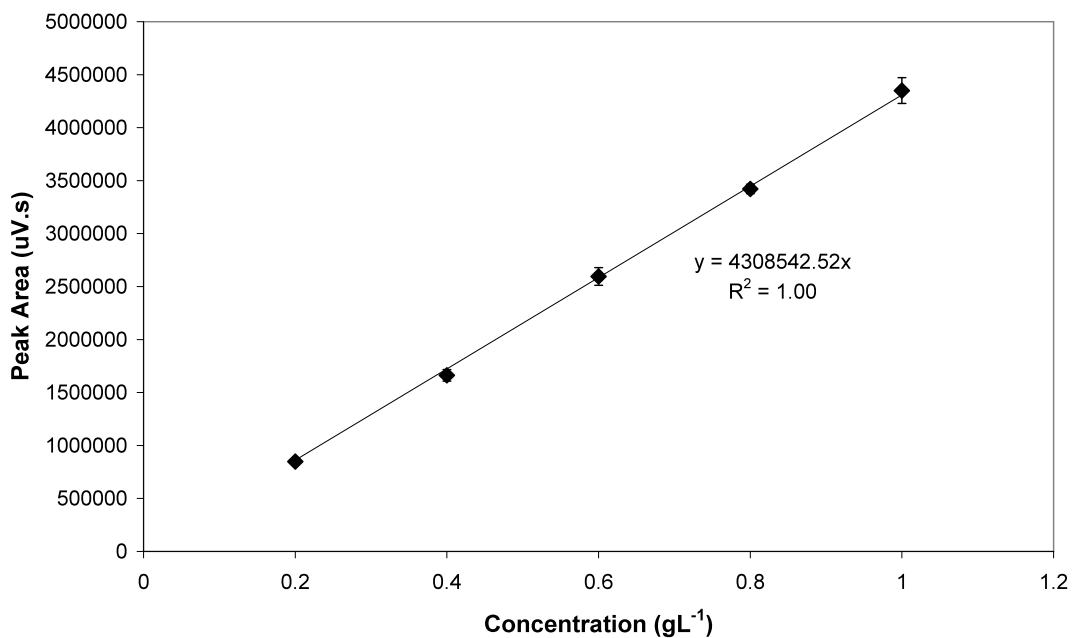


Figure A.15 (1R)-(+)-camphor calibration curve. Error bars indicate the standard deviation of triplicate stock preparations in ethyl acetate. Experiments were conducted as described in section 2.6.4.2.

A.3 HPLC Calibration Curves

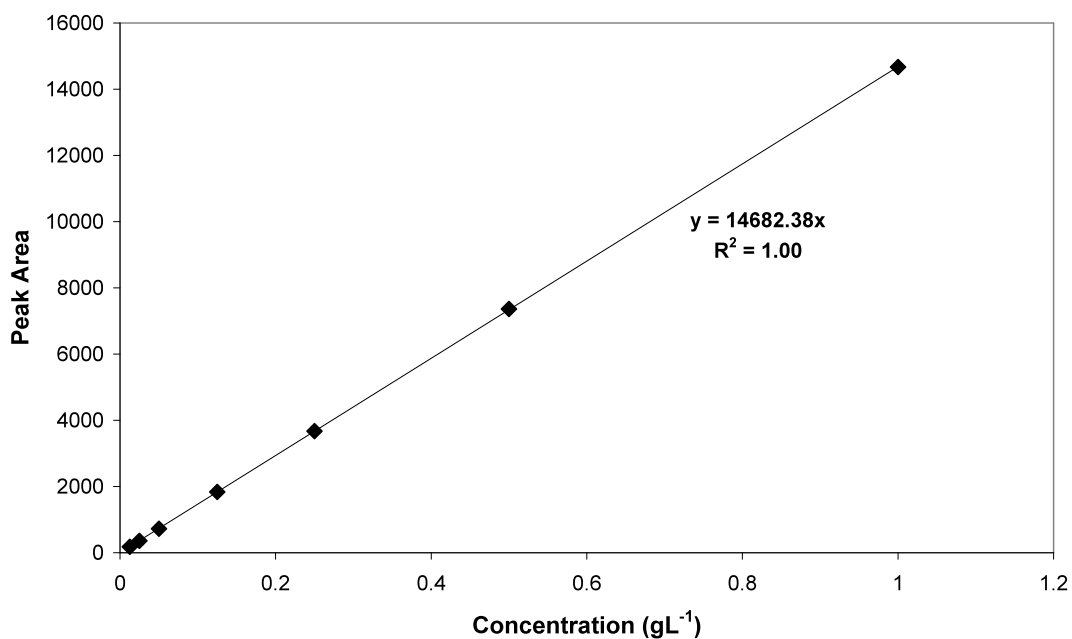


Figure A.16 7-ethoxycoumarin calibration curve. Error bars indicate the standard deviation of triplicate stock preparations in acetonitrile. Experiments were conducted as described in section 2.6.5.2.

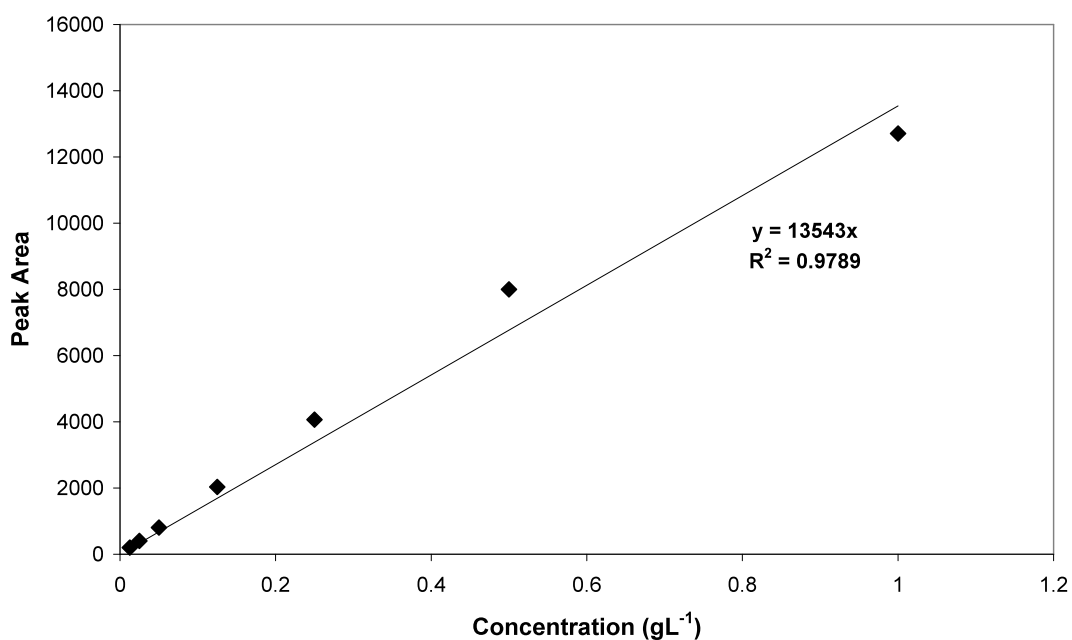


Figure A.17 7-hydroxycoumarin calibration curve. Error bars indicate the standard deviation of triplicate stock preparations in acetonitrile. Experiments were conducted as described in section 2.6.5.2.

9.2 Appendix B – Sample Chromatograms

B.1 Gas Chromatography Chromatograms

B.1.1 Standards

Experiments conducted as described in section 2.6.4.2.

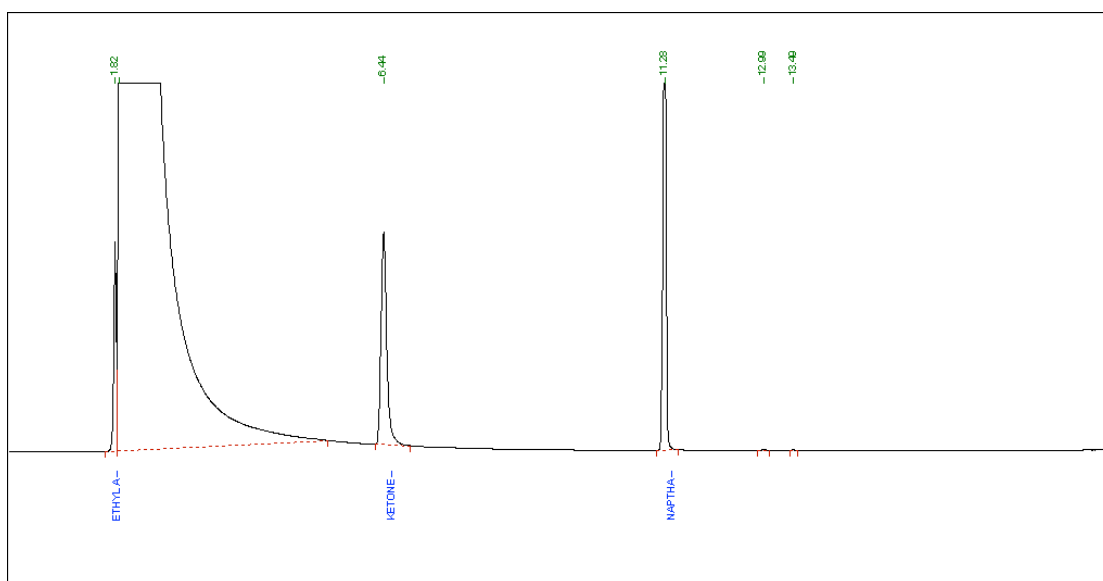


Figure B.1 Chromatogram of 1 gL^{-1} bicyclo[3.2.0]hept-2-en-6-one (retention time: 6.44 min) dissolved in ethyl acetate. Peak present at 11 minutes corresponds to naphthalene which was used as an internal standard and added to all samples.

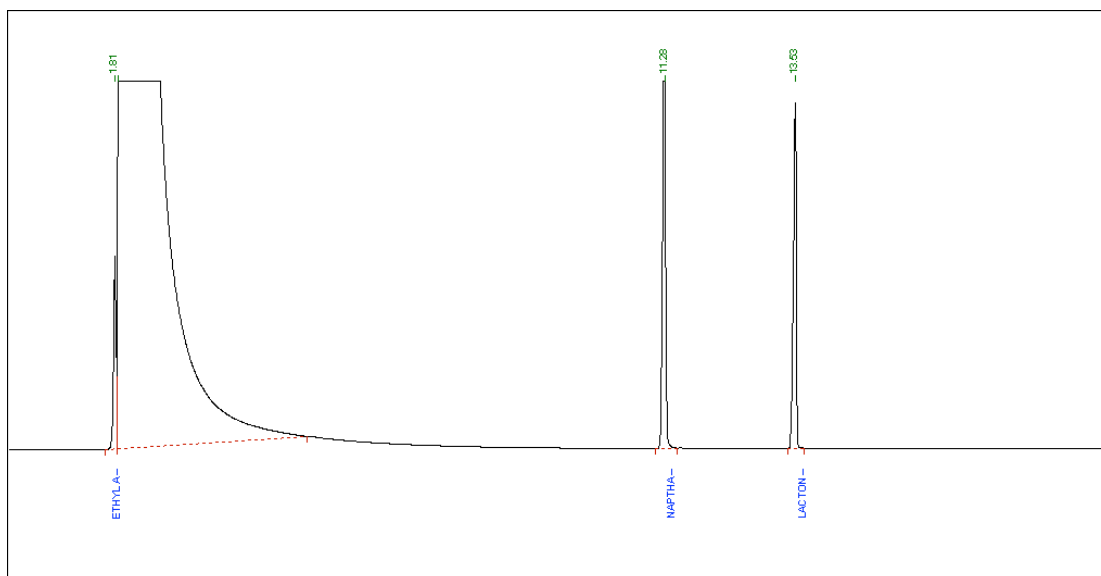


Figure B.2 Chromatogram of 1 gL⁻¹ (1*S*,5*R*)-2-oxabicyclo[3.3.0]oct-6-en-3-one (retention time: 13.53 min) dissolved in ethyl acetate. Peak present at 11 minutes corresponds to naphthalene which was used as an internal standard and added to all samples.

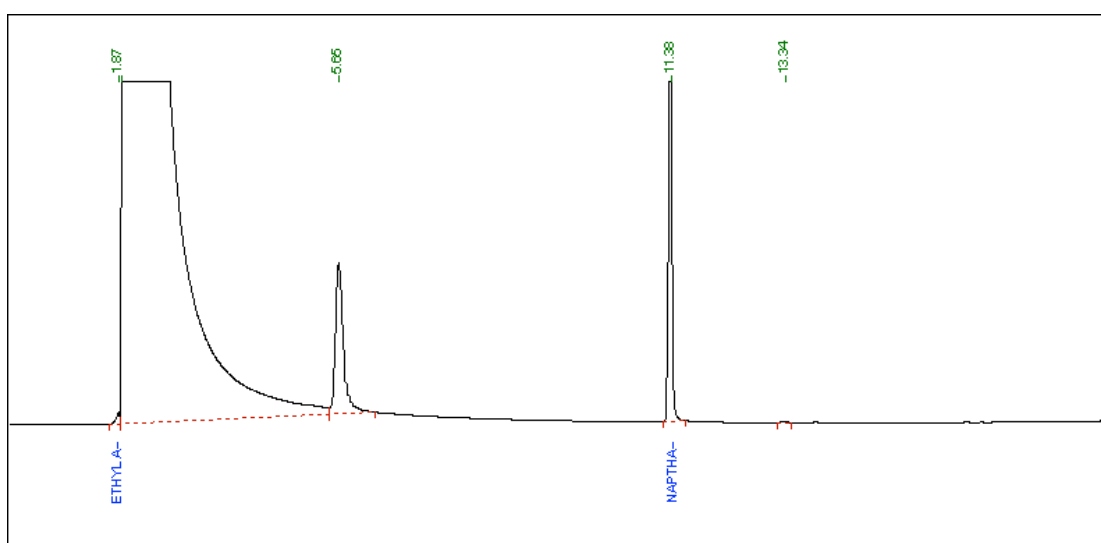


Figure B.3 Chromatogram of 1 gL⁻¹ cyclohexanone (retention time: 5.65 min) dissolved in ethyl acetate. Peak present at 11 minutes corresponds to naphthalene which was used as an internal standard and added to all samples.

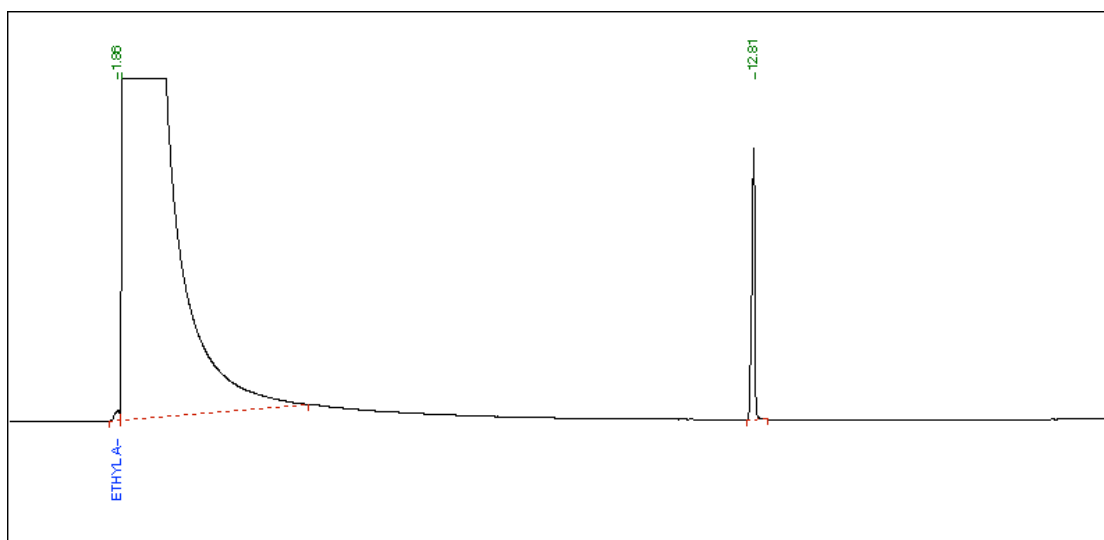


Figure B.4 Chromatogram of 1 gL⁻¹ ε-caprolactone (retention time: 12.81 min) dissolved in ethyl acetate.

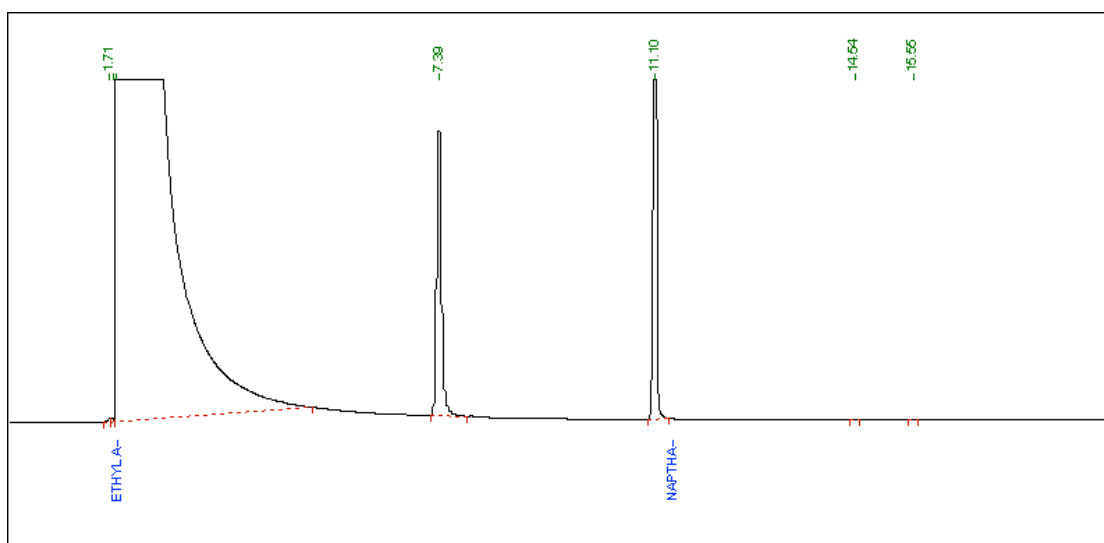


Figure B.5 Chromatogram of 1 gL⁻¹ norcamphor (retention time: 7.39 min) dissolved in ethyl acetate. Peak present at 11 minutes corresponds to naphthalene which was used as an internal standard and added to all samples.

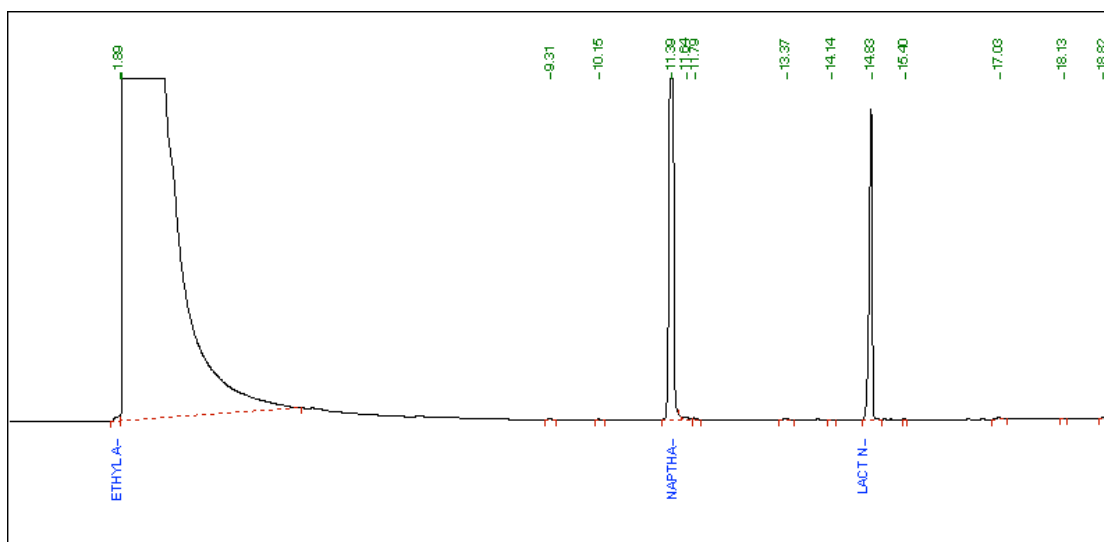


Figure B.6 Chromatogram of 1 gL^{-1} 2-oxabicyclo[3.2.1]octan-3-one (retention time: 14.83 min) dissolved in ethyl acetate. Peak present at 11 minutes corresponds to naphthalene which was used as an internal standard and added to all samples.

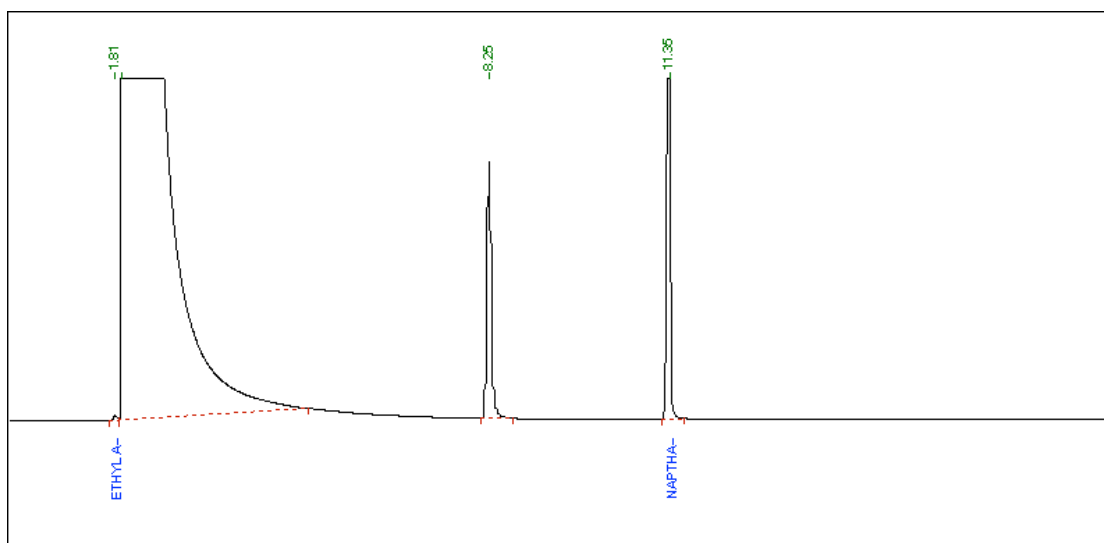


Figure B.7 Chromatogram of 1 gL^{-1} cycloheptanone (retention time: 8.25 min) dissolved in ethyl acetate. Peak present at 11 minutes corresponds to naphthalene which was used as an internal standard and added to all samples.

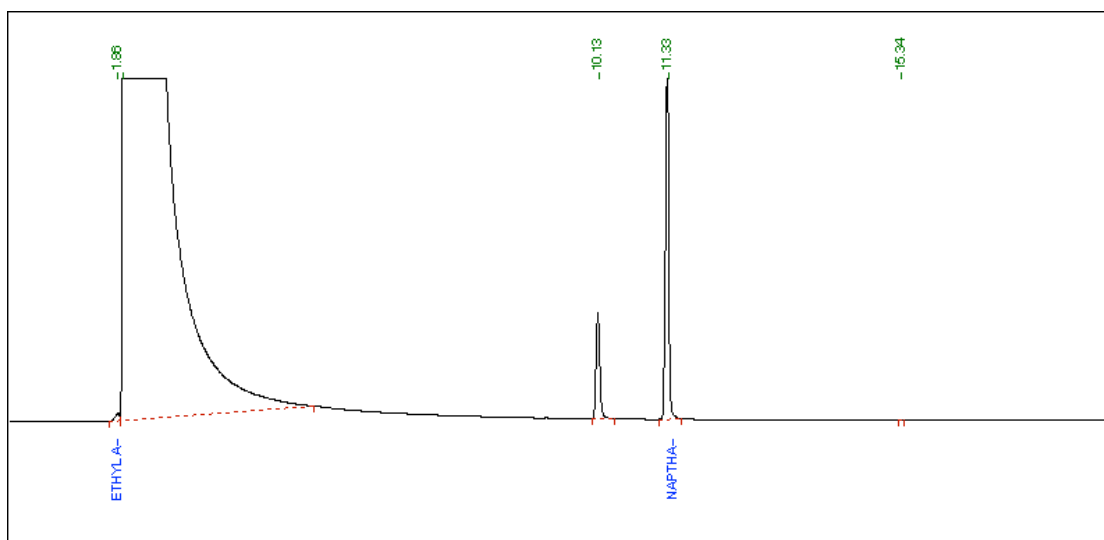


Figure B.8 Chromatogram of 0.5 gL^{-1} oxocan-2-one (retention time: 10.13 min) dissolved in ethyl acetate. Peak present at 11 minutes corresponds to naphthalene which was used as an internal standard and added to all samples.

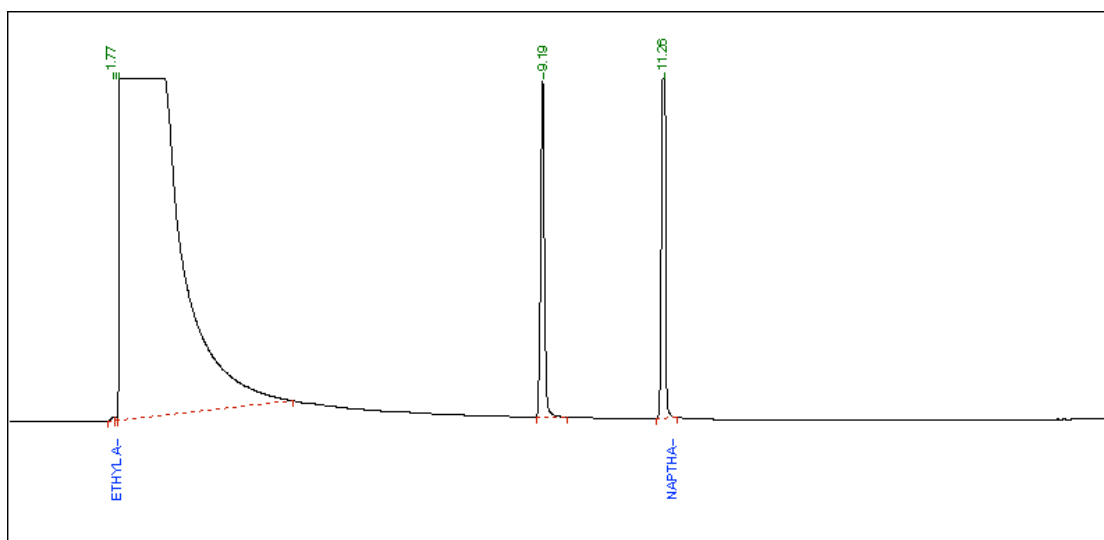


Figure B.9 Chromatogram of 1 gL^{-1} (1R)-(-)-fenchone (retention time: 9.19 min) dissolved in ethyl acetate. Peak present at 11 minutes corresponds to naphthalene which was used as an internal standard and added to all samples.

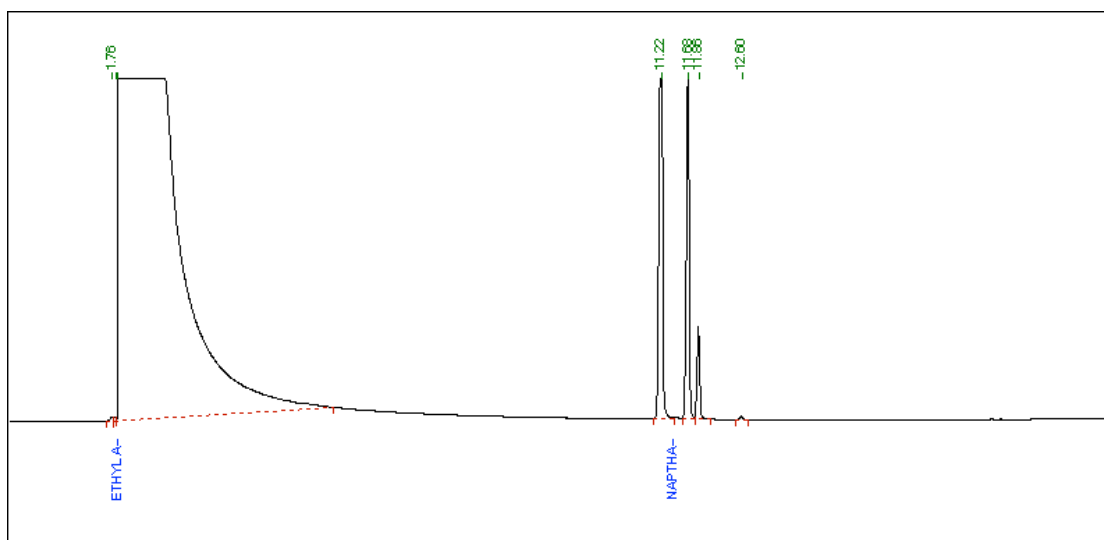


Figure B.10 Chromatogram of 1 gL^{-1} (+)-(3R,6SR)-dihydrocarvone (isomer 1 retention time: 11.68 min, isomer 2 retention time: 11.86 min) dissolved in ethyl acetate. Peak present at 11 minutes corresponds to naphthalene which was used as an internal standard and added to all samples.

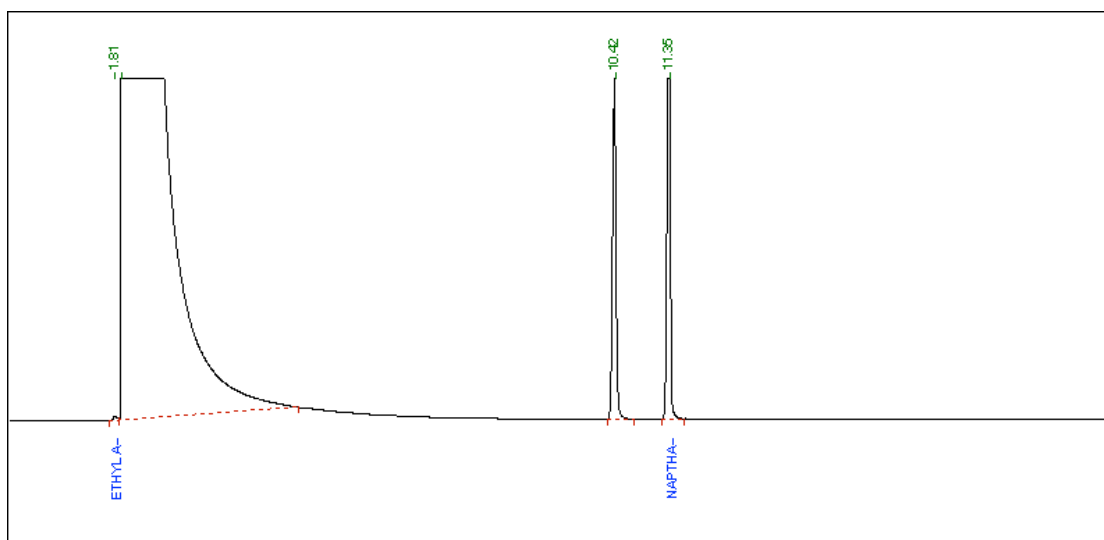


Figure B.11 Chromatogram of 1 gL^{-1} cyclooctanone (retention time: 10.42 min) dissolved in ethyl acetate. Peak present at 11 minutes corresponds to naphthalene which was used as an internal standard and added to all samples.

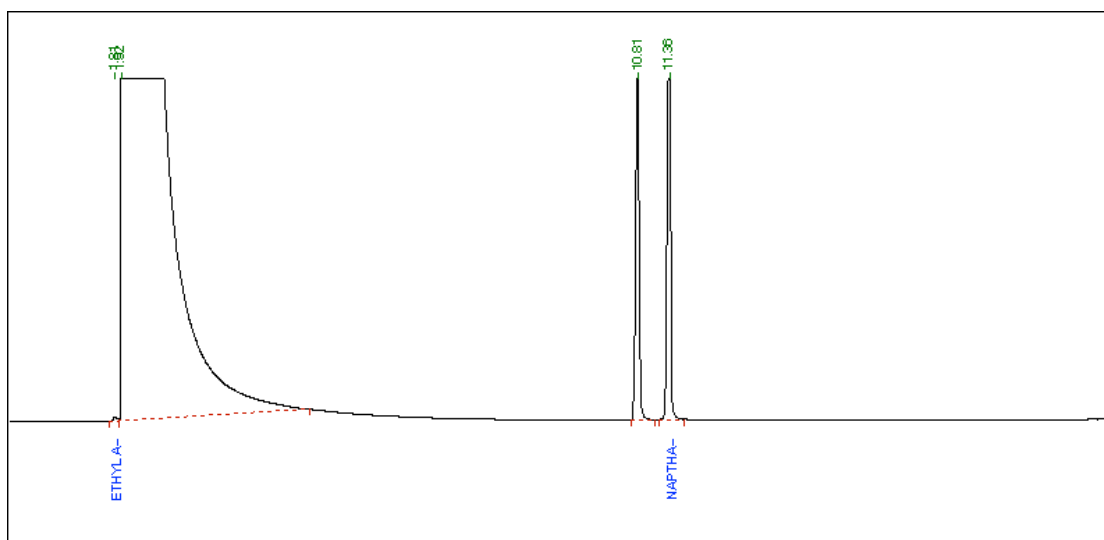


Figure B.12 Chromatogram of 1 gL^{-1} camphor (retention time: 10.81 min) dissolved in ethyl acetate. Peak present at 11 minutes corresponds to naphthalene which was used as an internal standard and added to all samples.

B.1.2 Bioconversions

Experiments conducted as described in section 2.3.1.2 and analysed by GC as described in section 2.6.4.2.

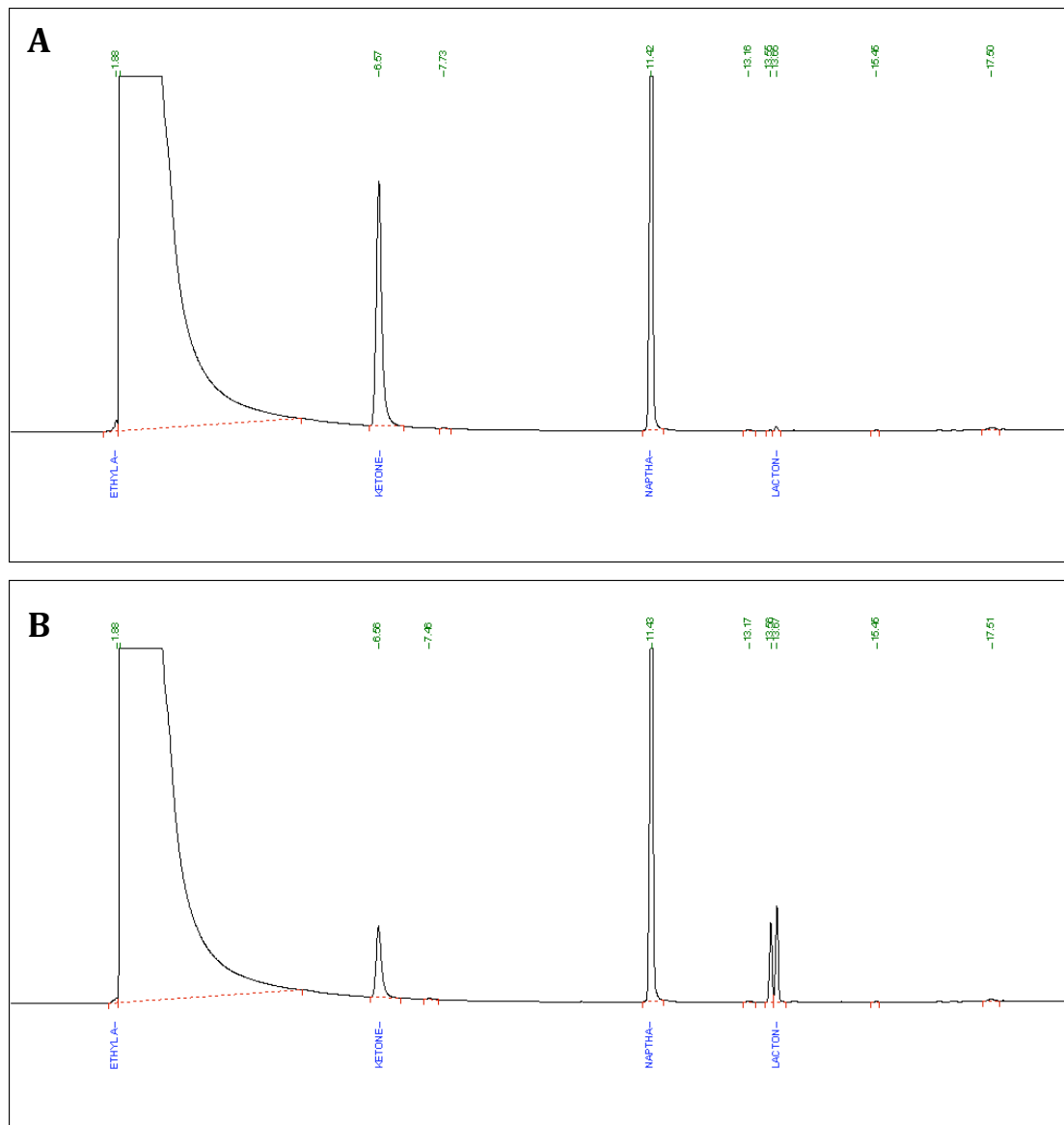


Figure B.13 Chromatograms displaying the *E. coli* TOP10 [pQR210] bioconversion of 1 gL⁻¹ bicyclo[3.2.0]hept-2-en-6-one (retention time: 6.57 min) to (-)-(1*S*,5*R*)-2-oxabicyclo[3.3.0]oct-6-en-3-one and (-)-(1*R*,5*S*)-3-oxabicyclo[3.3.0]oct-6-en-2-one (retention times: 13.56 min and 13.67 min) at (A) 0 minutes and (B) 60 minutes. Peak present at 11 minutes corresponds to naphthalene which was used as an internal standard and added to all samples. Results are from microwell based bioconversions.

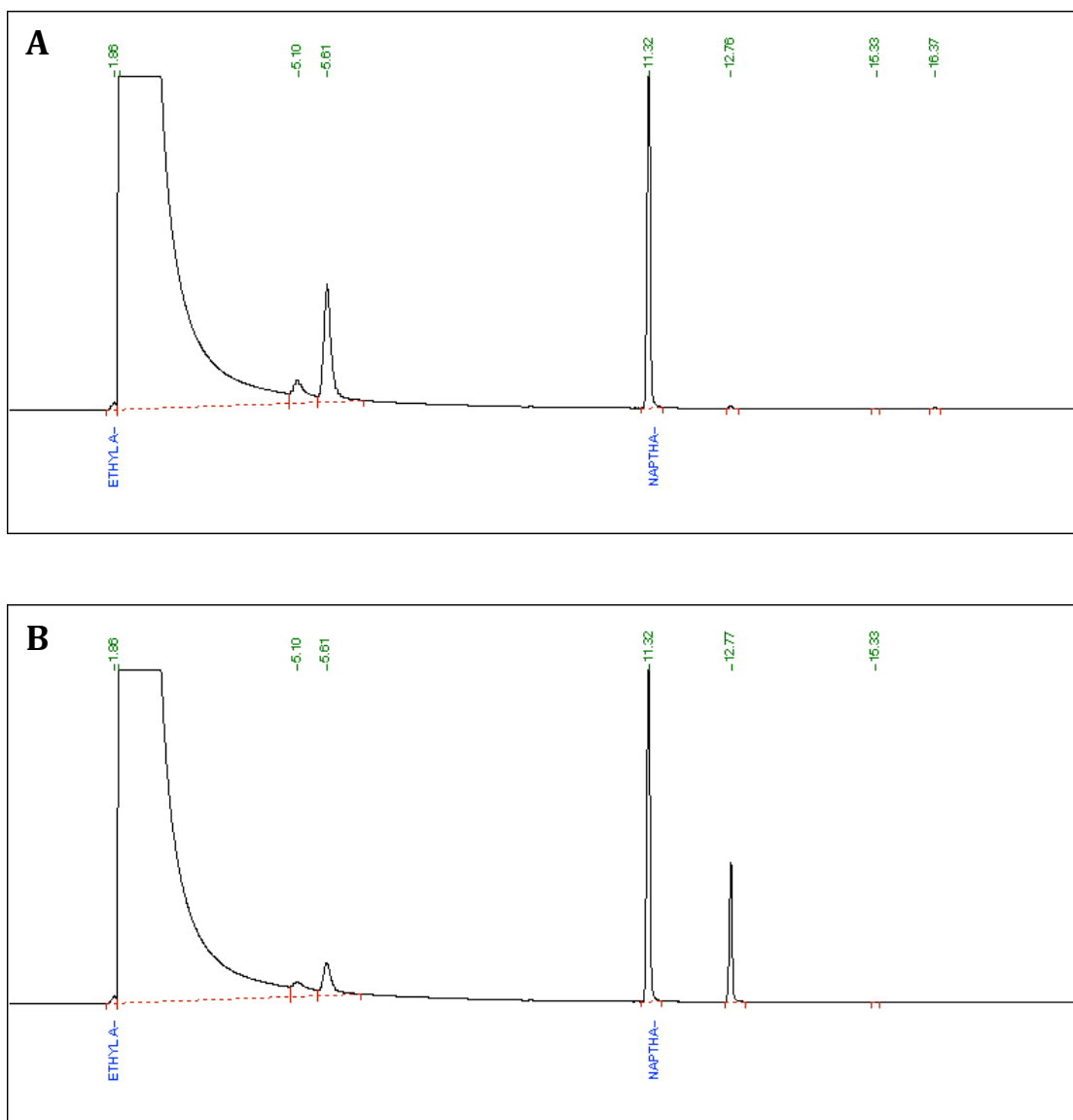


Figure B.14 Chromatograms displaying the *E. coli* TOP10 [pQR210] bioconversion of 1 gL⁻¹ cyclohexanone (retention time: 5.10 min) to ε-caprolactone (retention time: 12.77 min) at (A) 0 minutes and (B) 60 minutes. Peak present at 11 minutes corresponds to naphthalene which was used as an internal standard and added to all samples. Results are from microwell based bioconversions.

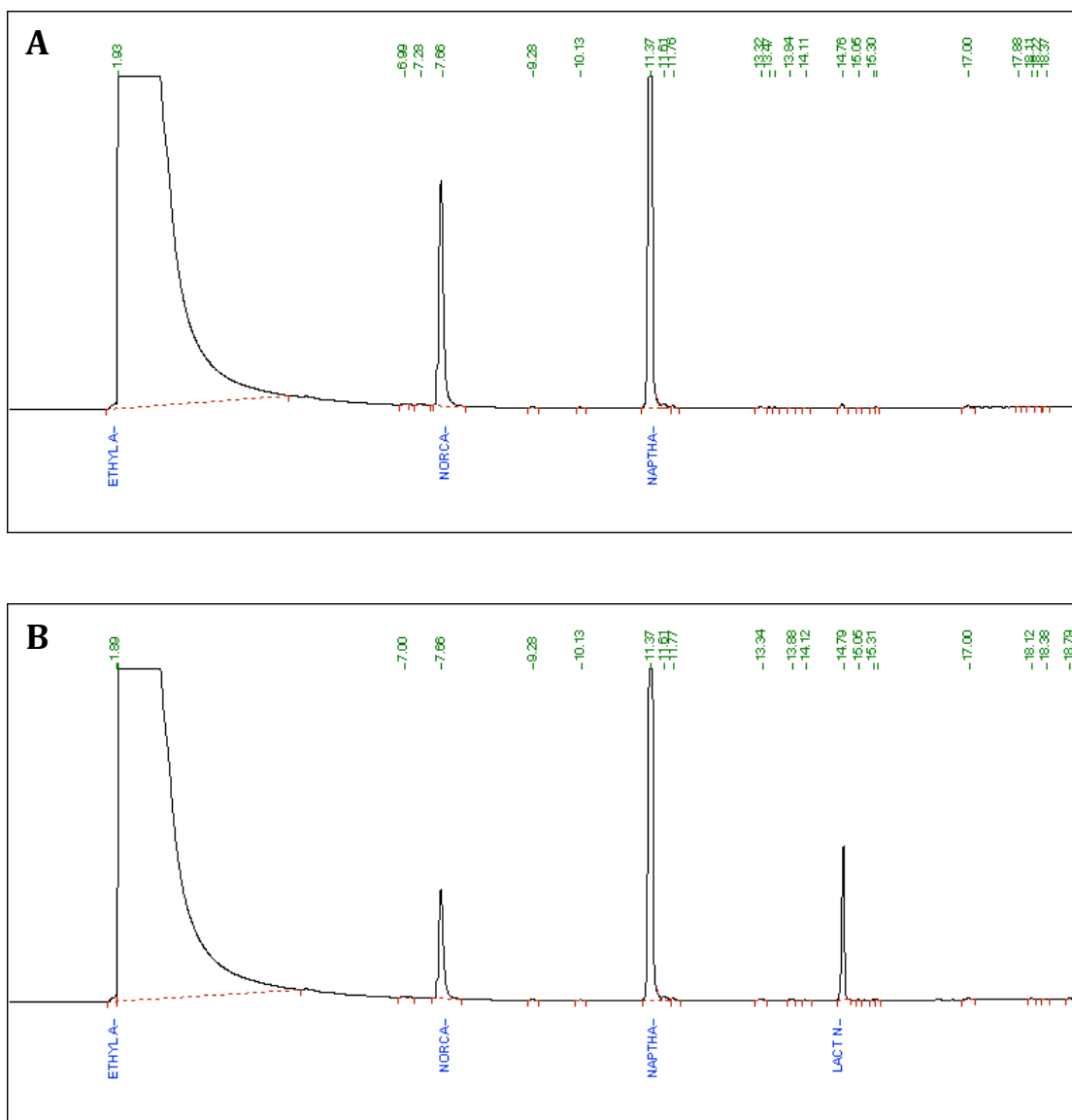


Figure B.15 Chromatograms displaying the *E. coli* TOP10 [pQR210] bioconversion of 1 gL⁻¹ norcamphor (retention time: 7.66 min) to 2-oxabicyclo[3.2.1]octan-3-one (retention time: 14.79 min) at **(A)** 0 minutes and **(B)** 60 minutes. Peak present at 11 minutes corresponds to naphthalene which was used as an internal standard and added to all samples. Results are from microwell based bioconversions.

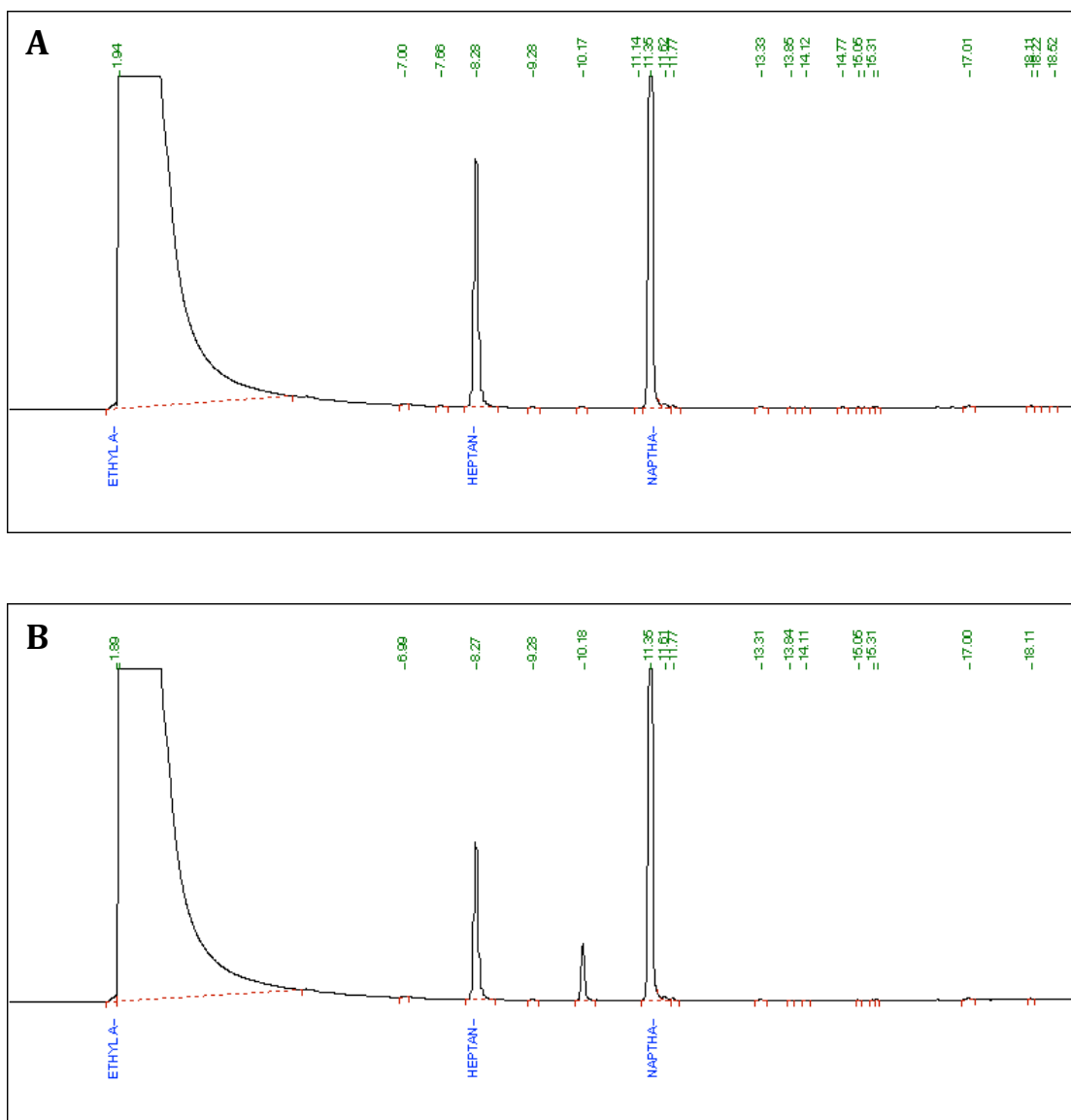


Figure B.16 Chromatograms displaying the *E. coli* TOP10 [pQR210] bioconversion of 1 gL⁻¹ cycloheptanone (retention time: 8.28 min) to oxocan-2-one (retention time: 10.18 min) at **(A)** 0 minutes and **(B)** 60 minutes. Peak present at 11 minutes corresponds to naphthalene which was used as an internal standard and added to all samples. Results are from microwell based bioconversions.

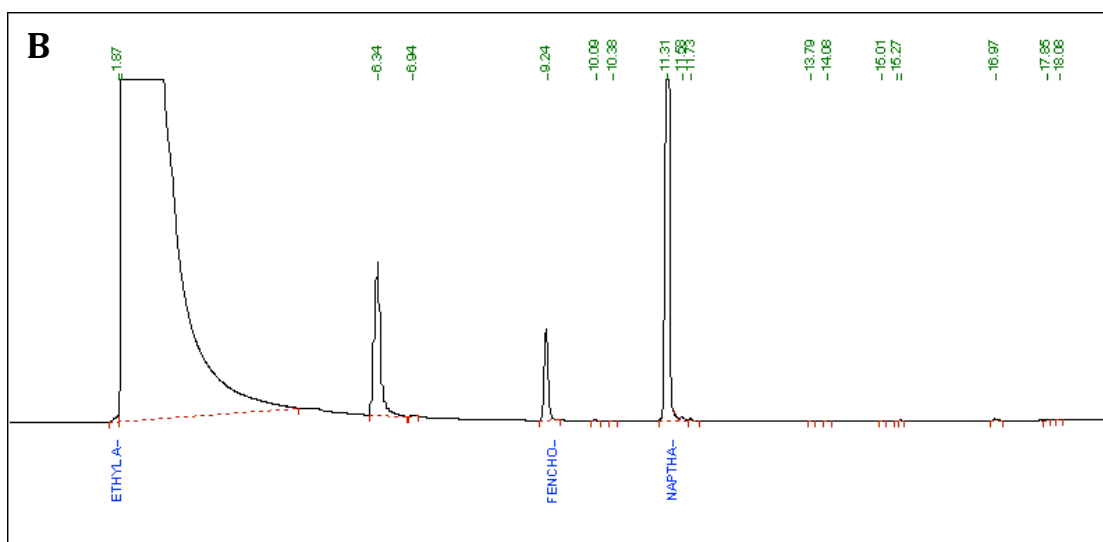
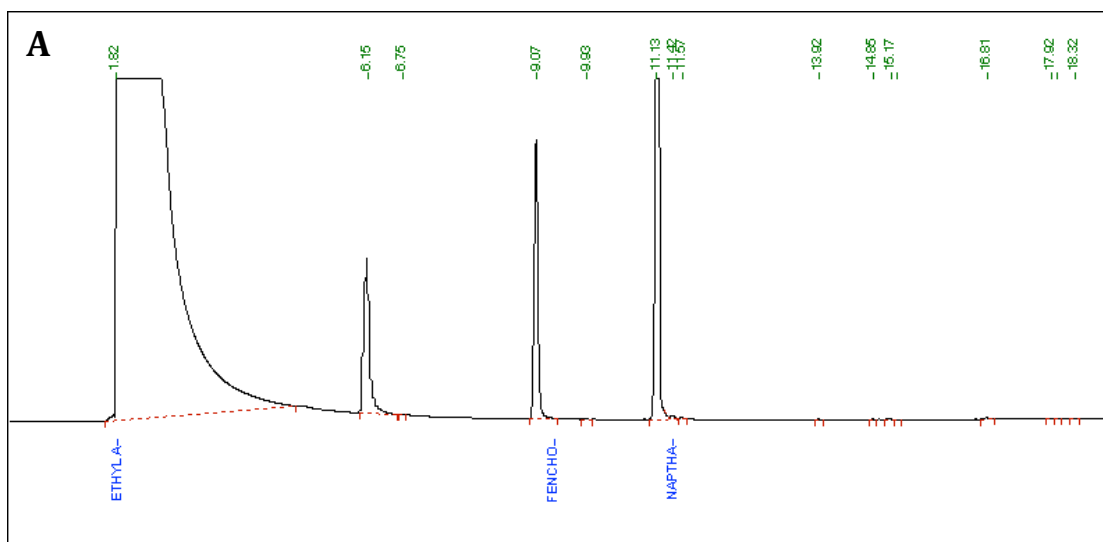


Figure B.17 Chromatograms displaying the *E. coli* TOP10 [pQR210] bioconversion of 1 gL^{-1} (1R)-(-)-fenchone (retention time: 9.24 min) at **(A)** 0 minutes and **(B)** 60 minutes. Peak present at 6.34 minutes corresponds to DMSO used to solubilise substrate. Peak present at 11 minutes corresponds to naphthalene which was used as an internal standard and added to all samples. Results are from microwell based bioconversions.

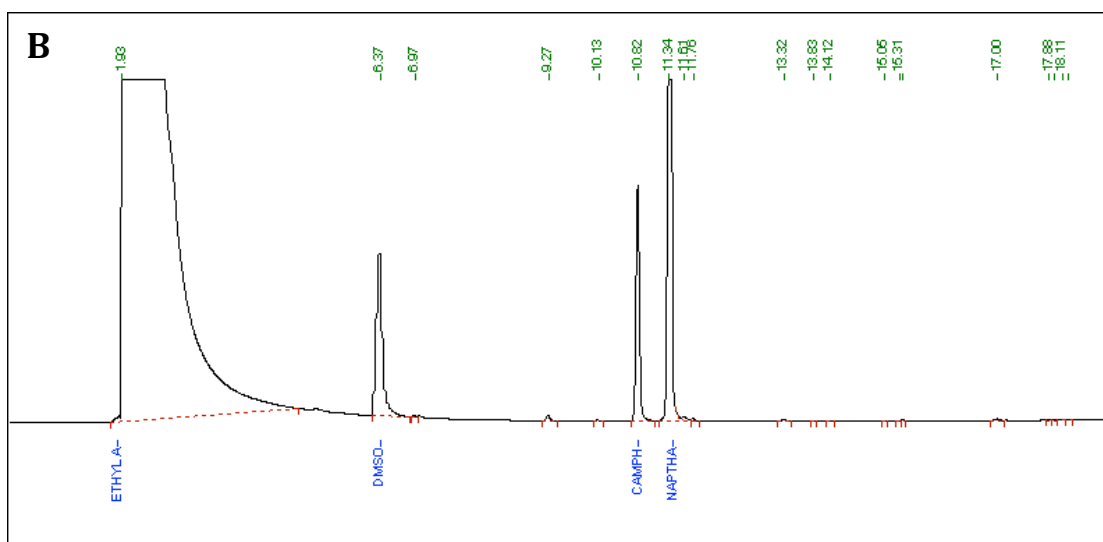
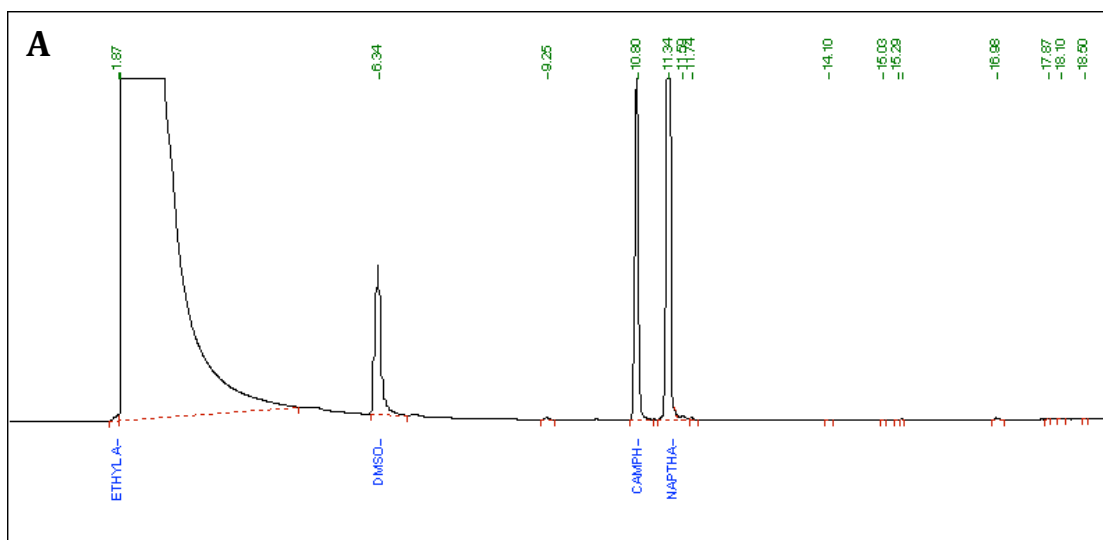


Figure B.18 Chromatograms displaying the *E. coli* TOP10 [pQR210] bioconversion of 1 gL⁻¹ camphor (retention time: 10.82 min) at **(A)** 0 minutes and **(B)** 60 minutes. Peak present at 6.37 minutes corresponds to DMSO used to solubilise substrate. Peak present at 11 minutes corresponds to naphthalene which was used as an internal standard and added to all samples. Results are from microwell based bioconversions.

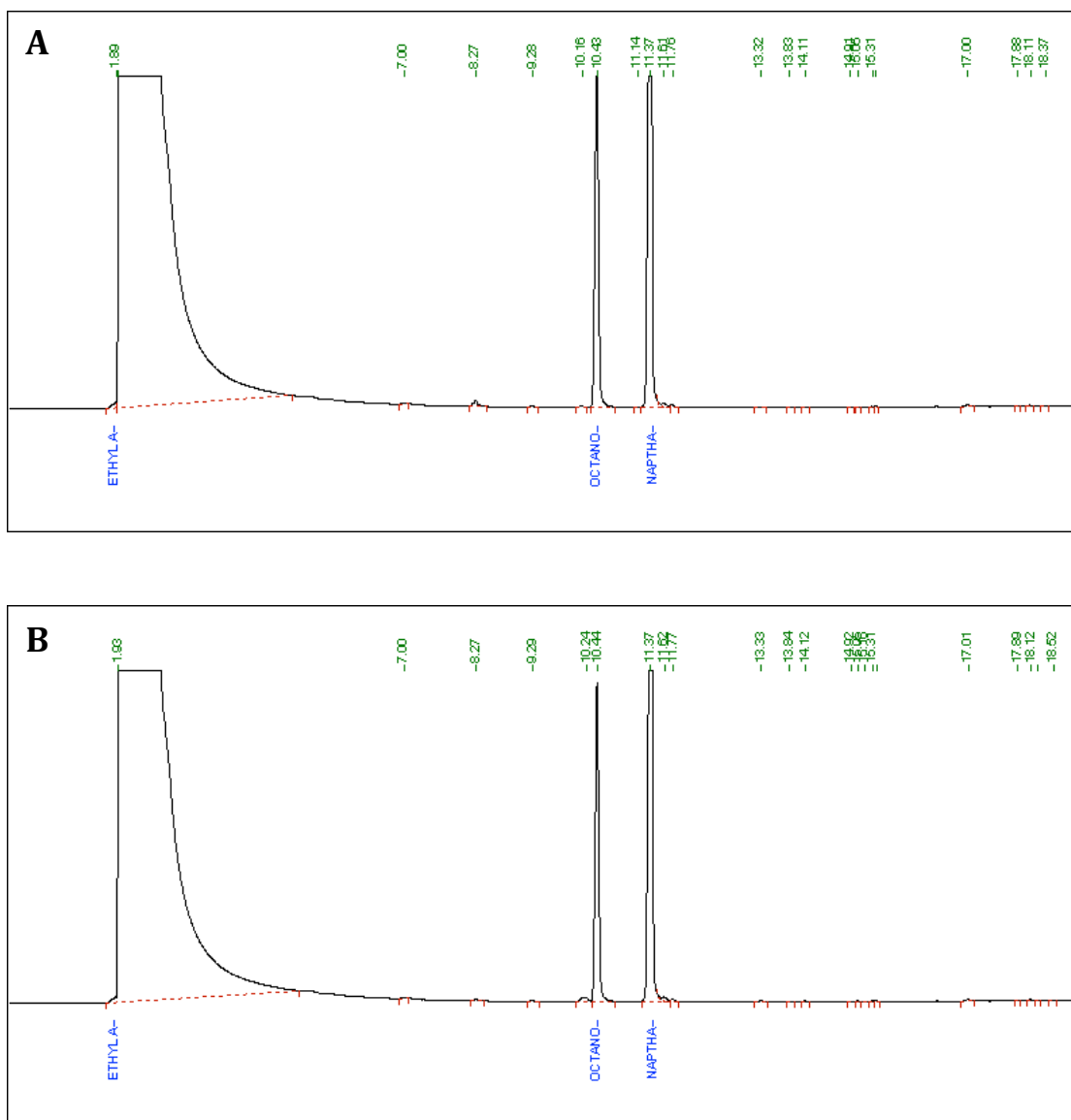


Figure B.19 Chromatograms displaying the *E. coli* TOP10 [pQR210] bioconversion of 1 gL⁻¹ cyclooctanone (retention time: 10.44 min) at **(A)** 0 minutes and **(B)** 60 minutes. Peak present at 11 minutes corresponds to naphthalene which was used as an internal standard and added to all samples. Results are from microwell based bioconversions.

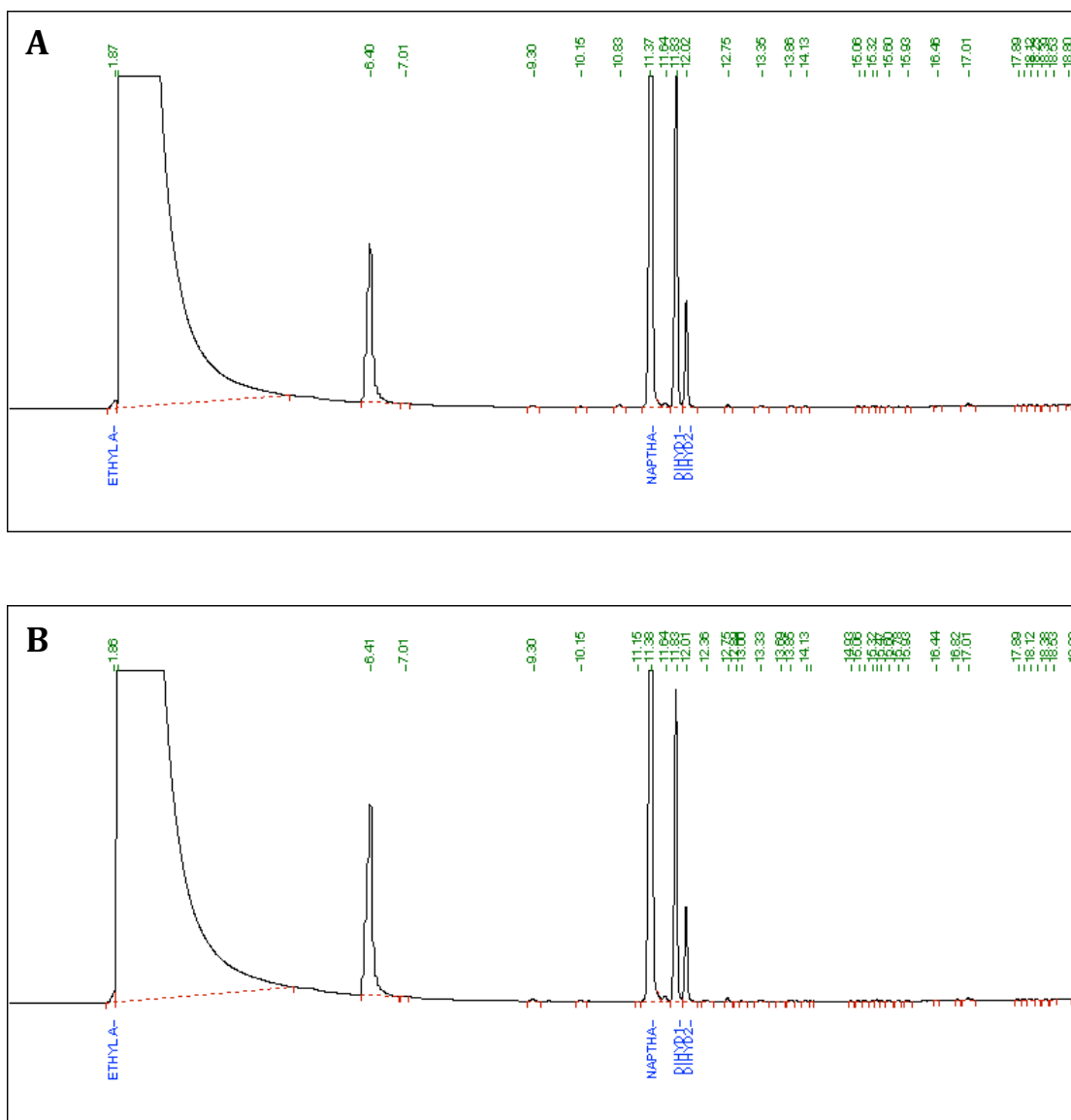


Figure B.20 Chromatograms displaying the *E. coli* TOP10 [pQR210] bioconversion of 1 gL^{-1} (+)-(3*R*,6*SR*)-dihydrocarvone (isomer 1 retention time: 11.83 min, isomer 2 retention time: 12.02 min) at **(A)** 0 minutes and **(B)** 60 minutes. Peak present at 6.40 minutes corresponds to DMSO used to solubilise substrate. Peak present at 11 minutes corresponds to naphthalene which was used as an internal standard and added to all samples. Results are from microwell based bioconversions.

B.2 HPLC Chromatograms

B.2.1 Standards

Experiments conducted as described in section 2.6.5.2.

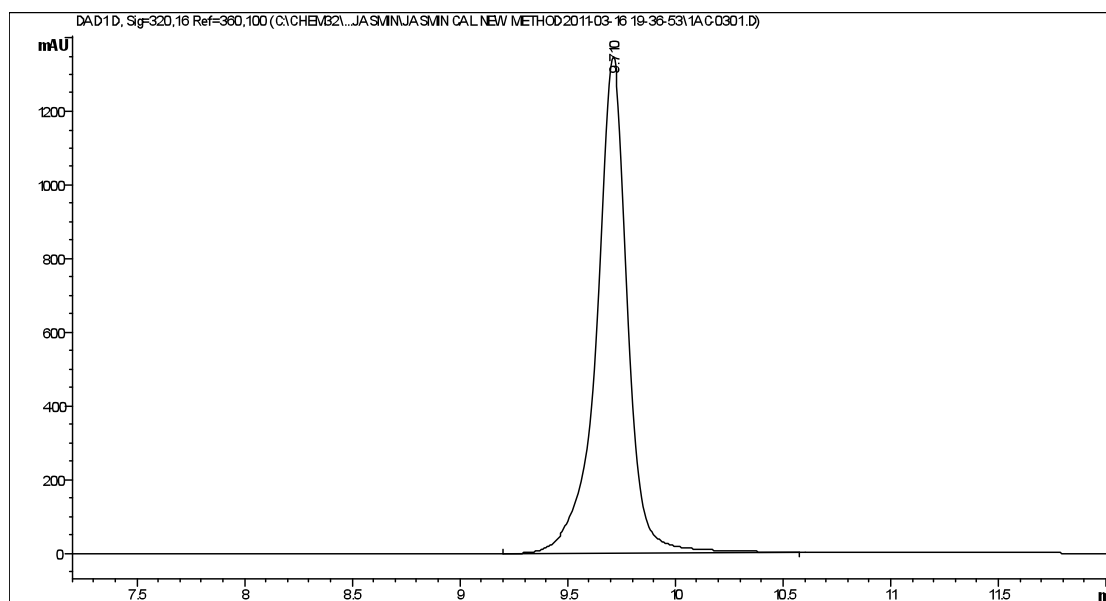


Figure B.21 Chromatogram of 1 gL^{-1} 7-ethoxycoumarin (retention time: 9.7 min) dissolved in acetonitrile.

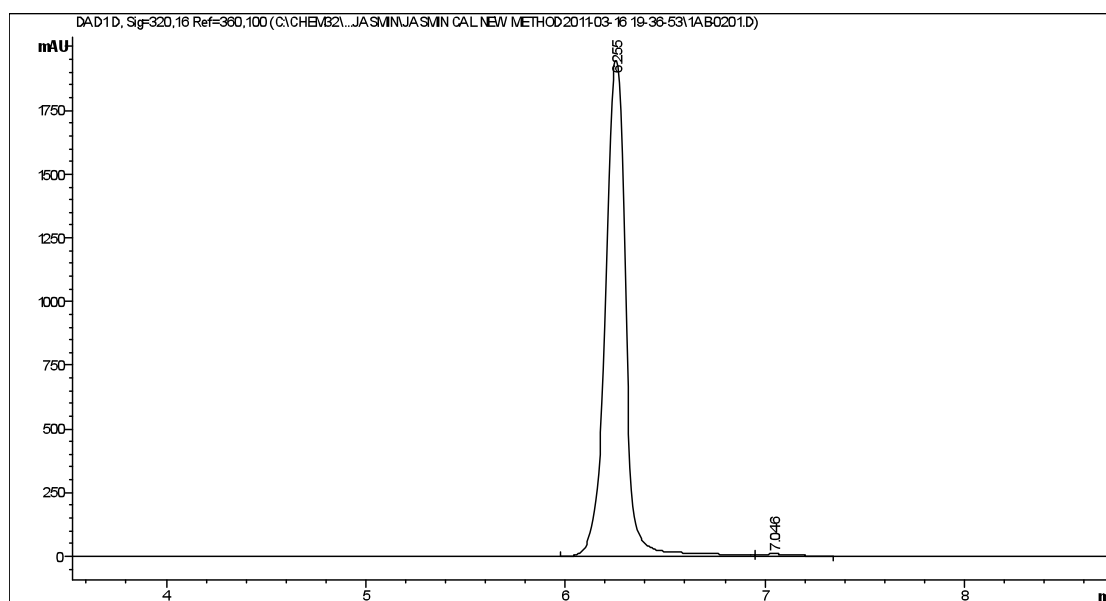


Figure B.22 Chromatogram of 1 gL^{-1} 7-hydroxycoumarin (retention time: 6.26 min) dissolved in acetonitrile.

B.2.2 Bioconversions

Experiments conducted as described in section 2.2.2.5 and analysed by HPLC as described in section 2.6.5.

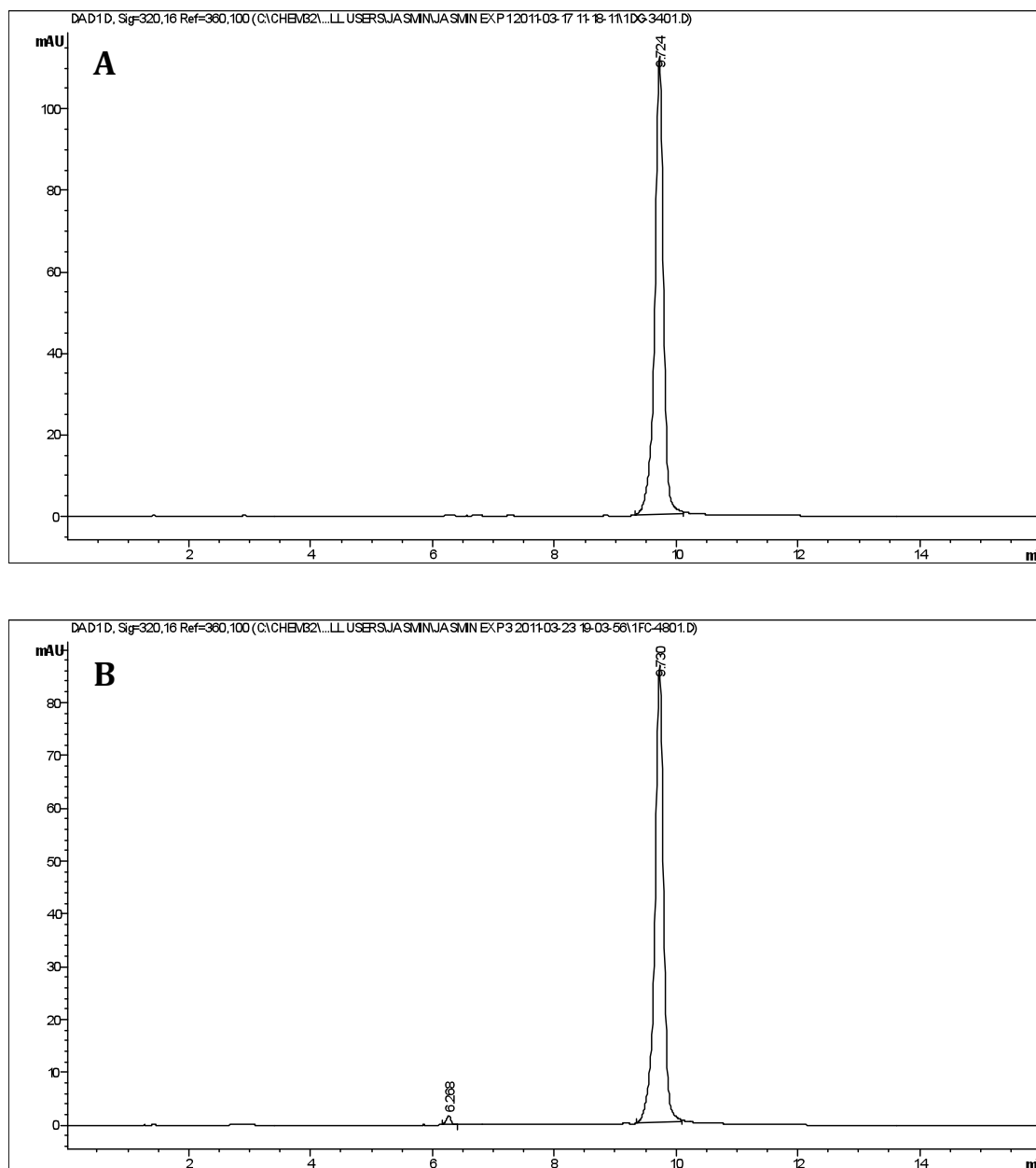


Figure B.23 Chromatograms displaying *E. coli* [pQR367] bioconversion of 1 mM 7-ethoxycoumarin (retention time: 9.73 min) to 7-hydroxycoumarin (retention time: 6.26 min) at (A) 0 minutes and (B) 30 hours of bioconversion. Results are from induced shake flask based bioconversions.

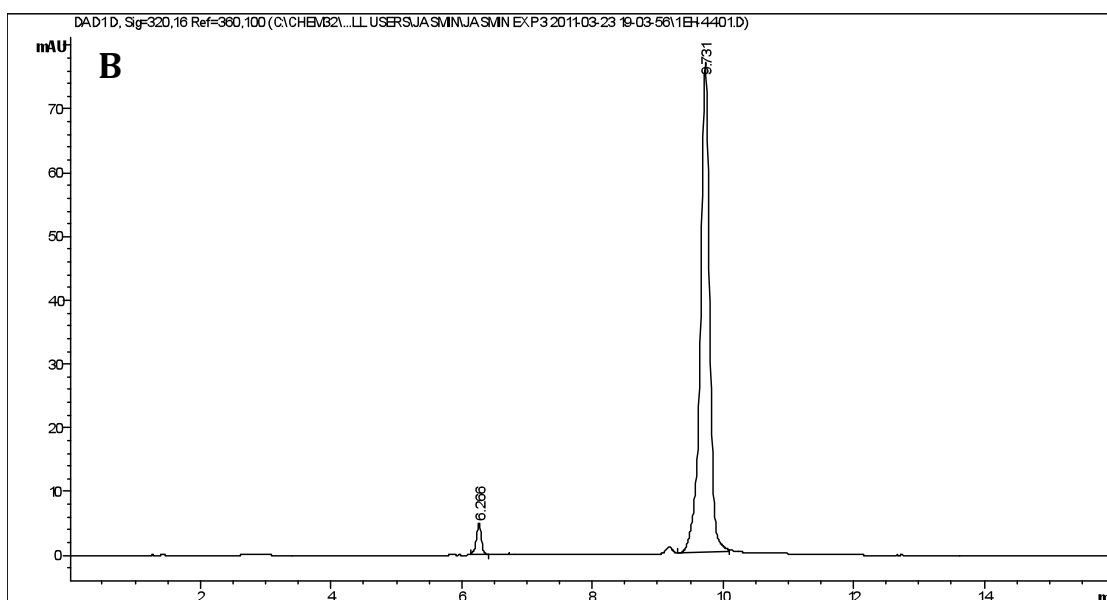
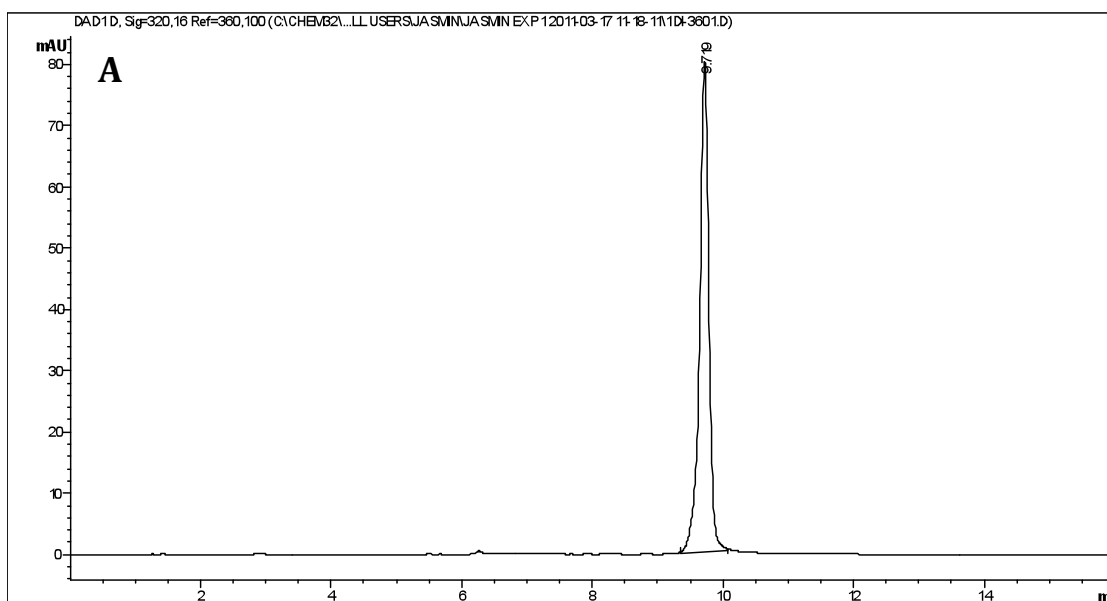


Figure B.24 Chromatograms displaying *E. coli* [pQR368] bioconversion of 1 mM 7-ethoxycoumarin (retention time: 9.73 min) to 7-hydroxycoumarin (retention time: 6.26 min) at **(A)** 0 minutes and **(B)** 30 hours of bioconversion. Results are from induced shake flask based bioconversions.

9.3 Appendix C – Assays

C.1 NADPH Assay – Sample Calculation

The activity of the sample was expressed in Units (U) where one unit is equivalent to the number of μmoles of NADPH consumed per minute. The concentration of NADPH in the microwell was calculated using the Beer Lambert Law shown in Equation C1.

$$A_{340nm} = \epsilon cl \quad (\text{Eq. C1})$$

A_{340nm} = Absorbance at 340 nm

ϵ = Extinction coefficient ($\text{mL}\mu\text{mol}^{-1}\text{cm}^{-1}$), for NADPH $\epsilon = 6.22$

c = NADPH concentration (μmolmL^{-1})

l = Light path length (cm)

The sample and background activity in units can therefore be obtained using Equation C2.

$$Units = \frac{\Delta A_{340nm}}{l\epsilon\Delta t} \quad (\text{Eq. C2})$$

In Figure C.1 the initial linear rate of absorbance change after substrate addition is $0.0427 \Delta A_{340}\text{min}^{-1}$ and the background rate is $0.0131 \Delta A_{340}\text{min}^{-1}$. Subtraction of the background rate from the initial linear rate gives $0.0296 \Delta A_{340}\text{min}^{-1}$. Using equation C2 a $\epsilon = 6.22 \text{ mL}\mu\text{mol}^{-1}\text{cm}^{-1}$ and a path length of 0.55 cm in a microplate well the number of units in the sample is 8.66 UL^{-1} . Taking into account the dilution of 3.3 and the biomass concentration is 1.3 gL^{-1} the sample has a CHMO activity of 21.98 Ug^{-1} .

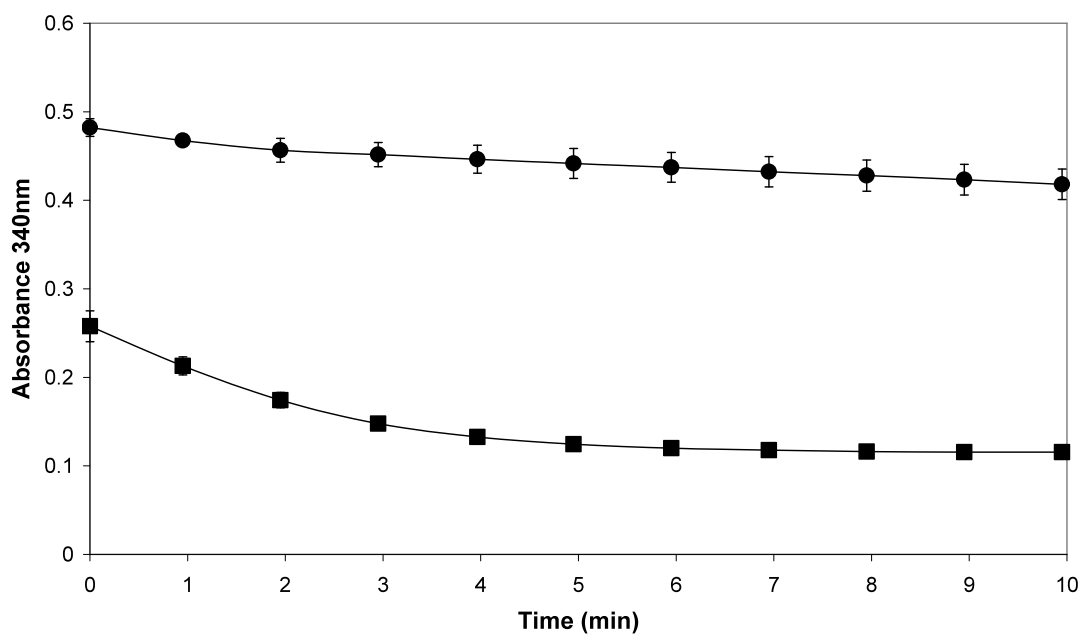


Figure C.1 The background absorbance change with time and the absorbance change with time after addition of the cyclohexanone substrate for a typical spectrophotometric assay for CHMO activity. Assay performed as described in section 2.6.8.

C.2 CO Assay Development

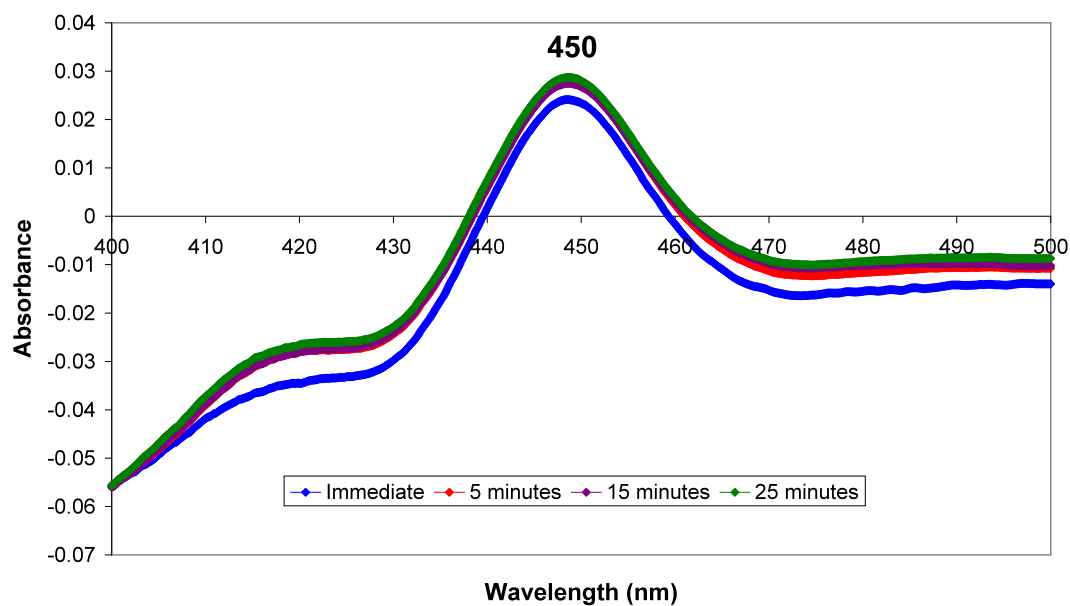


Figure C.2 CO difference spectrums showing the effect of sample incubation time with carbon monoxide prior to wavelength scan.

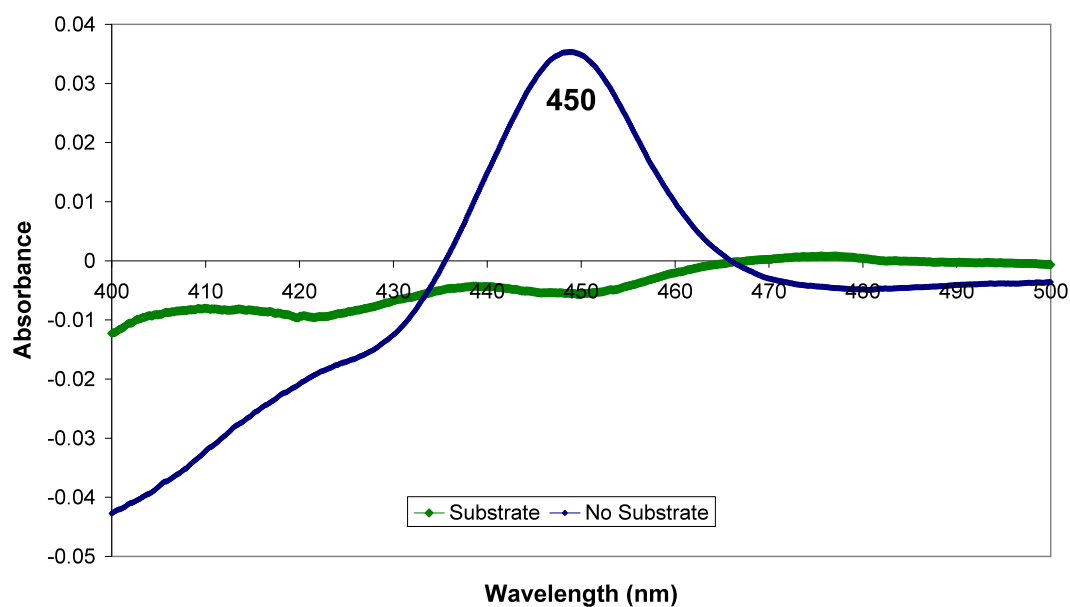


Figure C.3 The effect of substrate addition on CO difference spectrum.

C.3 CO Assay - Sample Calculation

A sample prepared as described in section 2.6.9.1 and reduced with 25 mM sodium hydrosulphite is first scanned on a UV-Vis spectrophotometer between 400 and 500 nm giving the green spectrum in Figure C.4. CO is then bubbled through the sample and the sample scanned between 400 and 500 nm giving the dark blue spectrum in Figure C.4.

Subtraction of the reduced spectrum from that complexed with CO produces the spectrum in Figure C.5.

Using the values from the CO difference spectrum in Figure C.5 the active P450 content can be calculated using Equation C3:

$$P450Content(nmolg^{-1}) = \left[\frac{(A_{\lambda 450nm} - A_{\lambda 490nm}) \div (\epsilon_{cytP450})}{TProtein_{conc}} \right] * 1000 \quad (\text{Eq. C3})$$

$\epsilon_{cytP450}$ = Extinction Coefficient $0.091 \mu M^{-1}cm^{-1}$

$TProtein_{conc}$ = Total Protein Concentration = $1.6 gL^{-1}$

$$P450Content = \left[\frac{(0.056 - 0) \div (0.091)}{1.6} \right] * 1000 = 389nmolg^{-1}$$

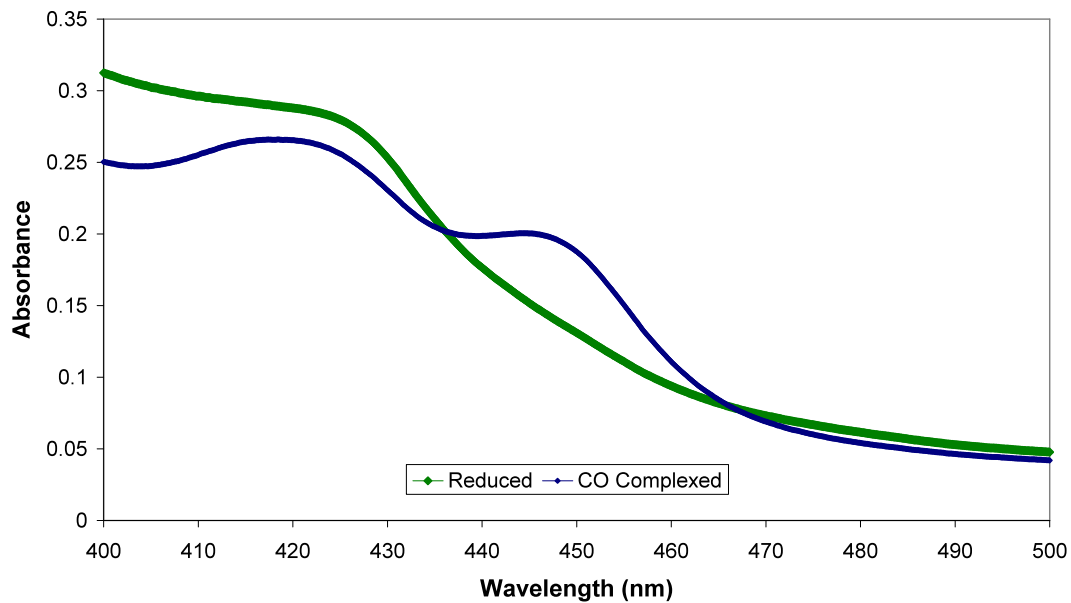


Figure C.4 Spectrums of sample reduced with sodium hydrosulphite and the same sample which has been bubbled with CO.

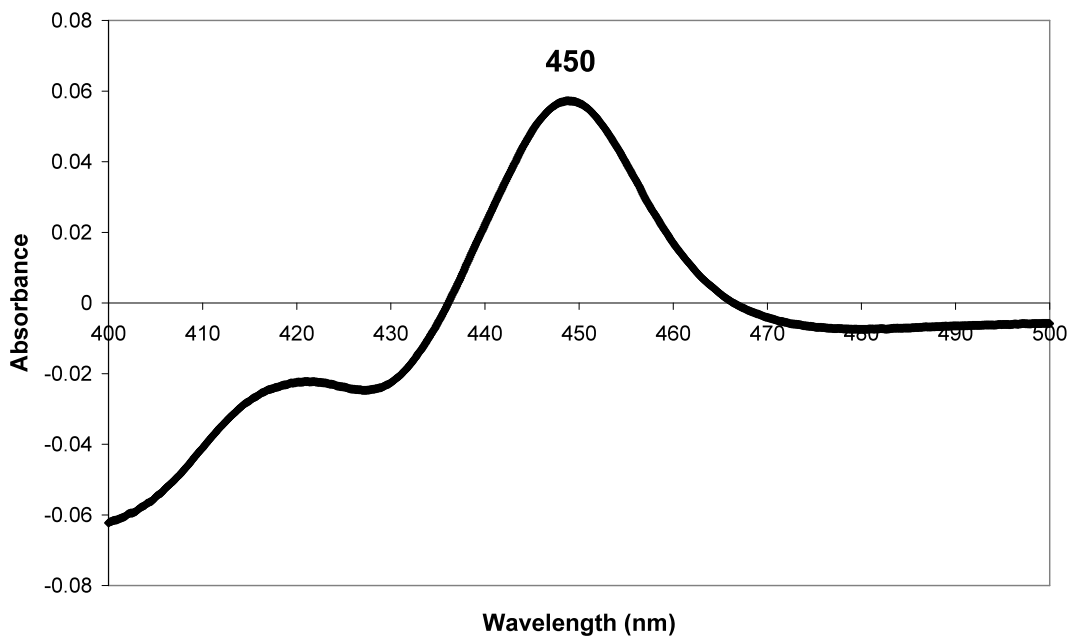


Figure C.5 CO difference spectrum.

9.4 Appendix D – NMR, MS and IR Data

D.1 2-Oxa-bicyclo[3.2.1]octan-3-one Data

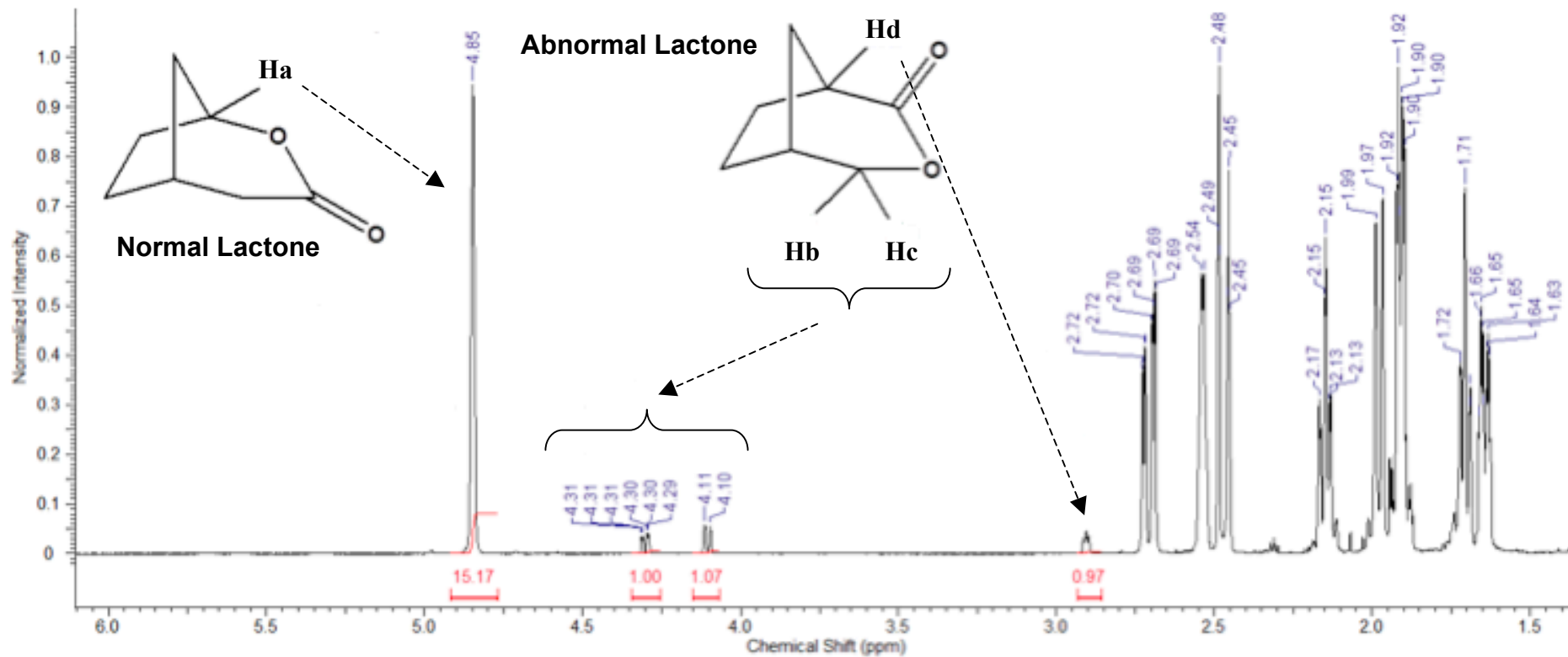


Figure D.1 Representative Proton NMR of purified norcamphor products 2-oxabicyclo[3.2.1]octan-3-one and 3-oxabicyclo[3.2.1]octan-2-one.

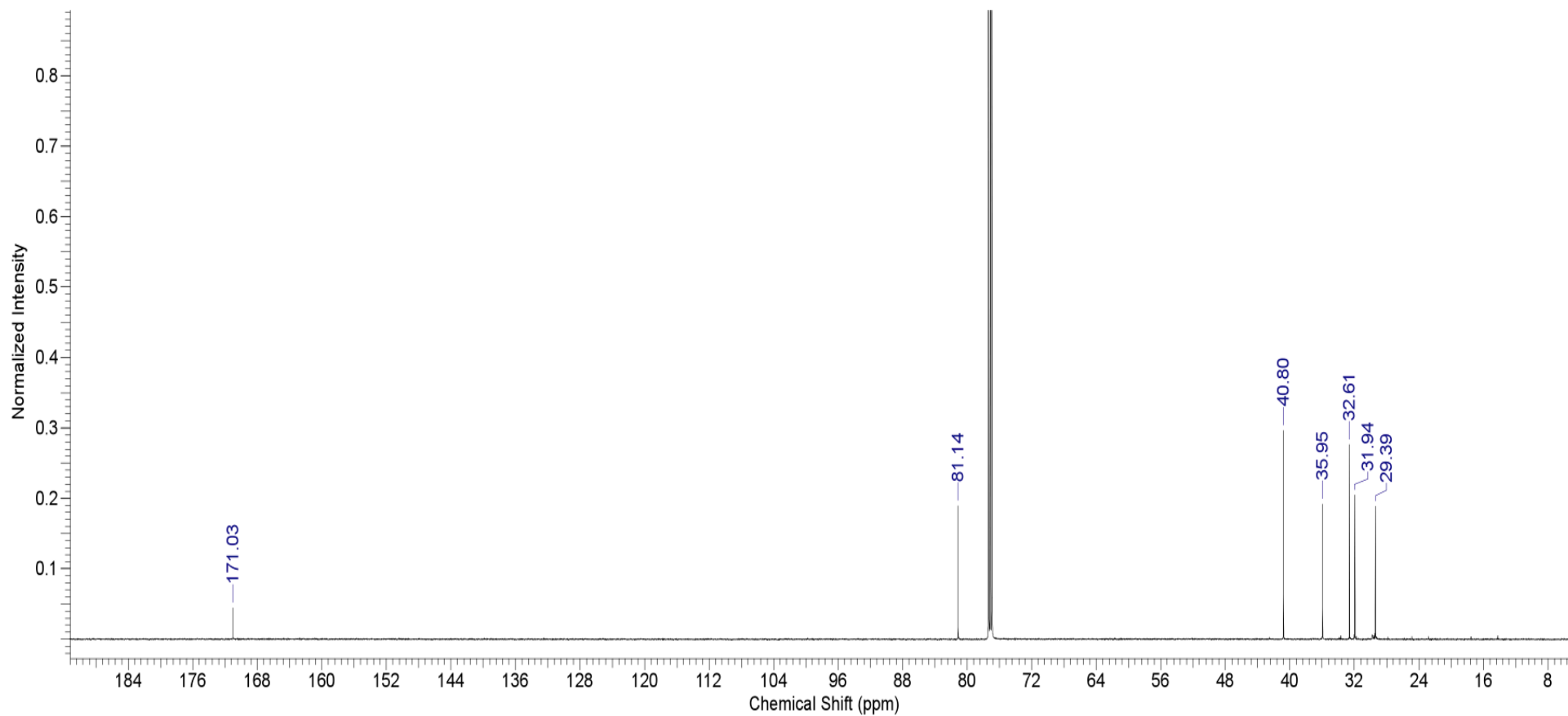


Figure D.2 Representative C-13 NMR of purified norcamphor product 2-oxabicyclo[3.2.1]octan-3-one.

12-aug-2010_100812145811 #65 RT: 5.69 AV: 1 NL: 7.64E7
T: + c EI Full ms [79.50-800.50]

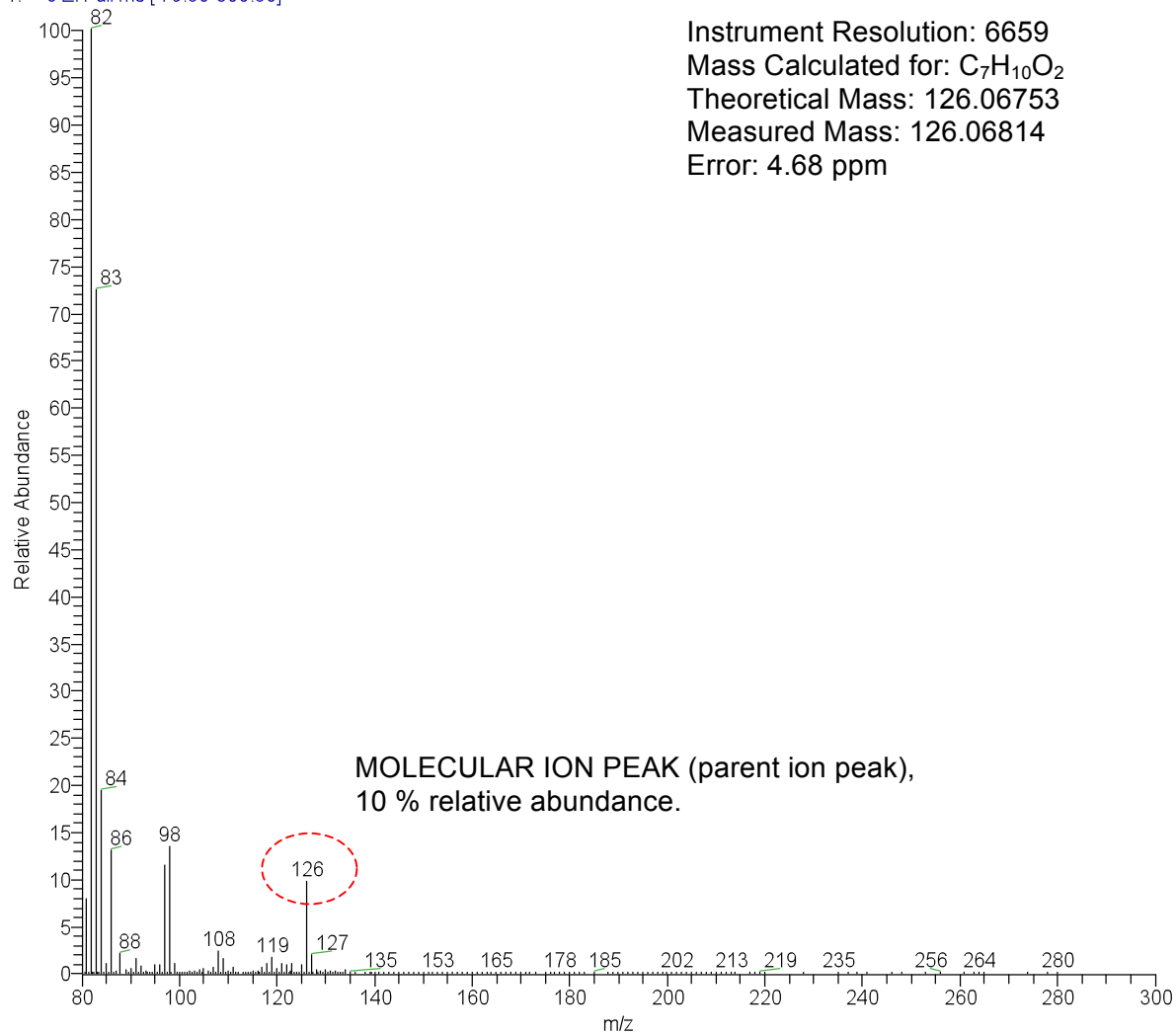


Figure D.3 Representative mass spectrum of purified norcamphor product 2-oxabicyclo[3.2.1]octan-3-one.

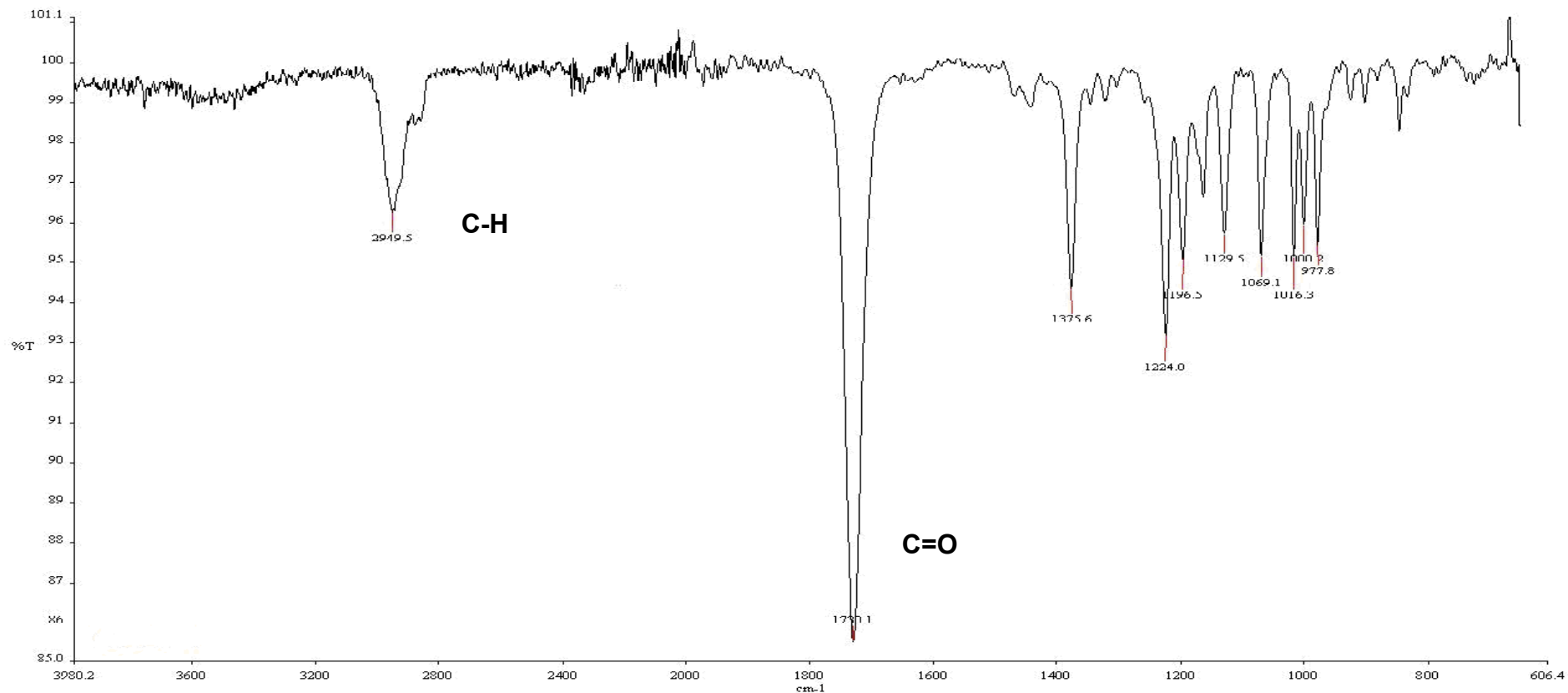


Figure D.4 Representative infra red spectrum of purified norcamphor product 2-oxabicyclo[3.2.1]octan-3-one. Trough at 1730.1 cm^{-1} indicates a carbonyl group (C=O) and a trough at 2949.5 cm^{-1} indicates a C-H group.

D.2 Oxocan-2-one Data

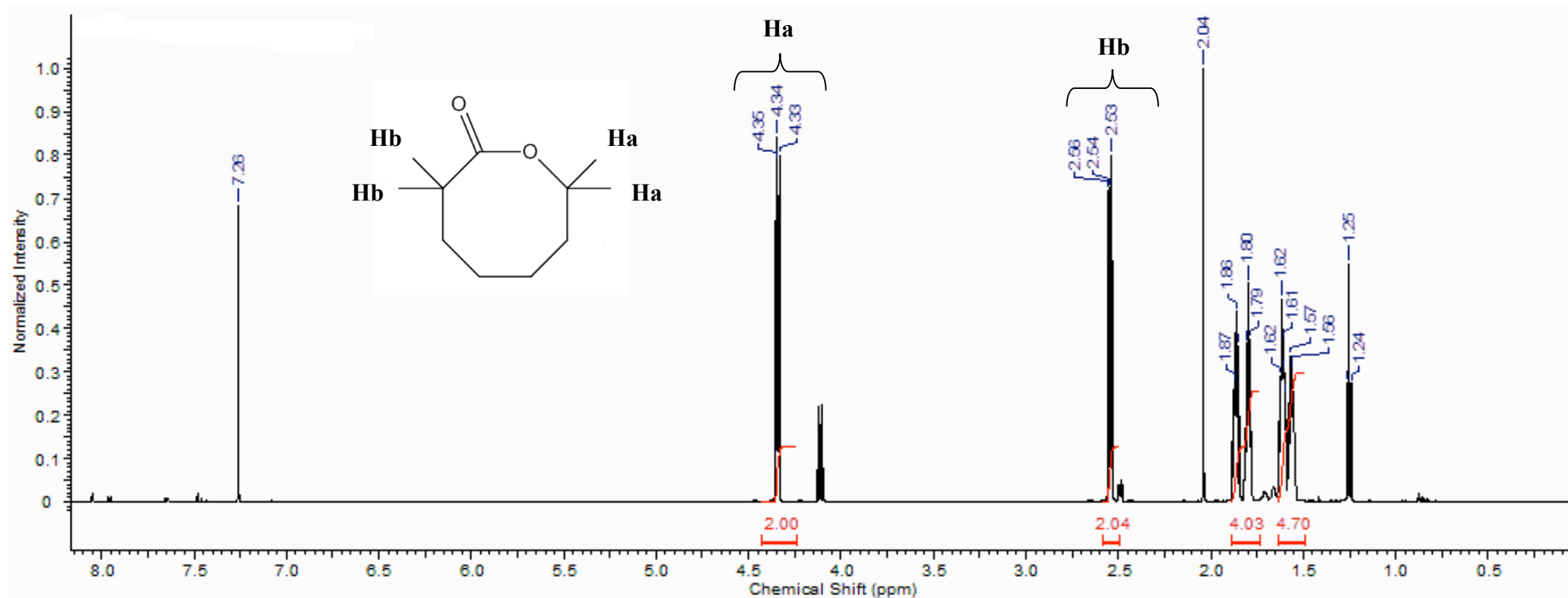


Figure D.5 Representative Proton NMR of chemically synthesised oxocan-2-one from cycloheptanone.

26-aug-2010 #302 RT: 31.33 AV: 1 SB: 79 21.89-29.98 NL: 1.27E7
T: + c Cl Full ms [49.50-800.50]

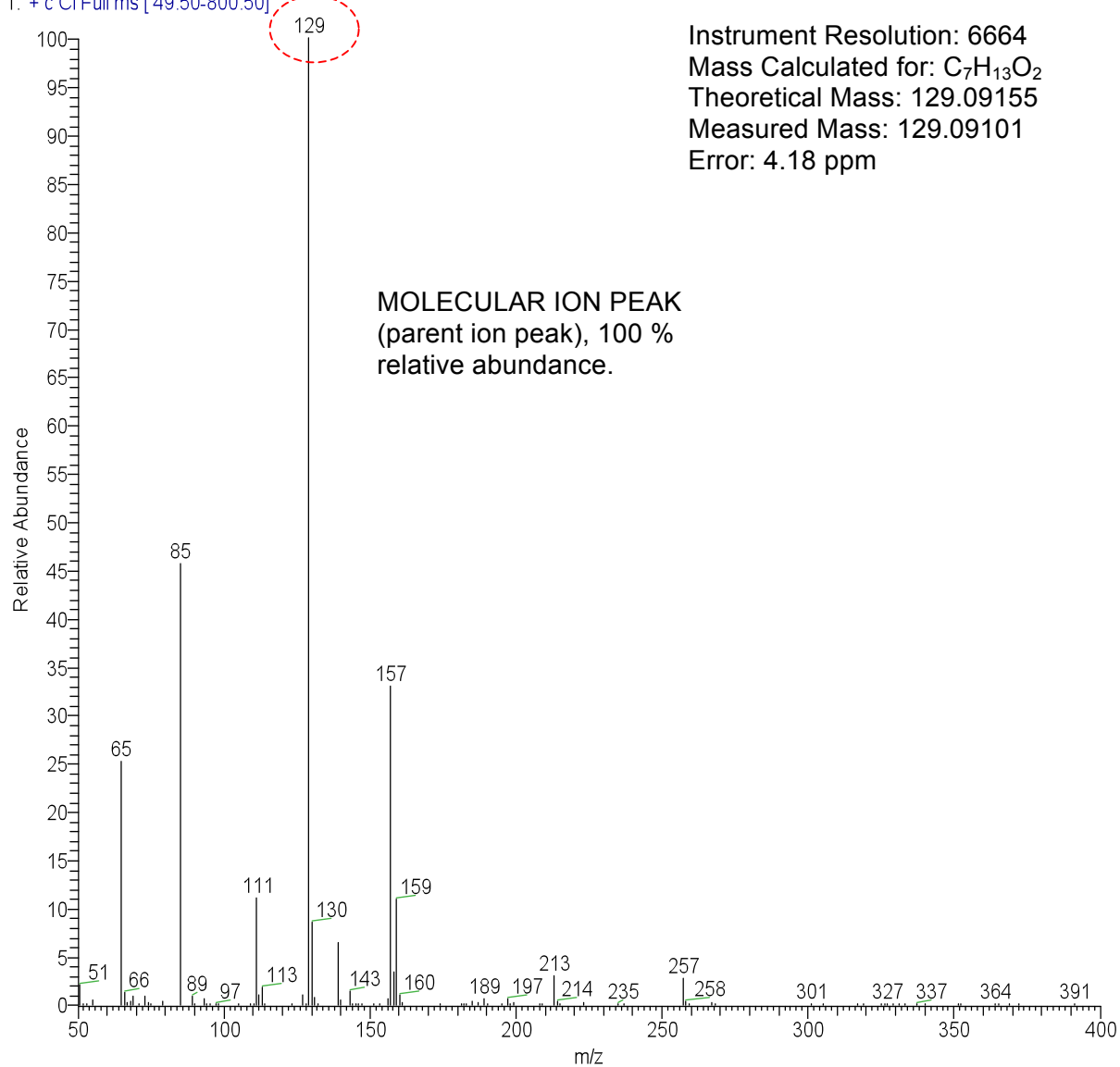


Figure D.6 Representative mass spectrum of chemically synthesised oxocan-2-one from cycloheptanone.

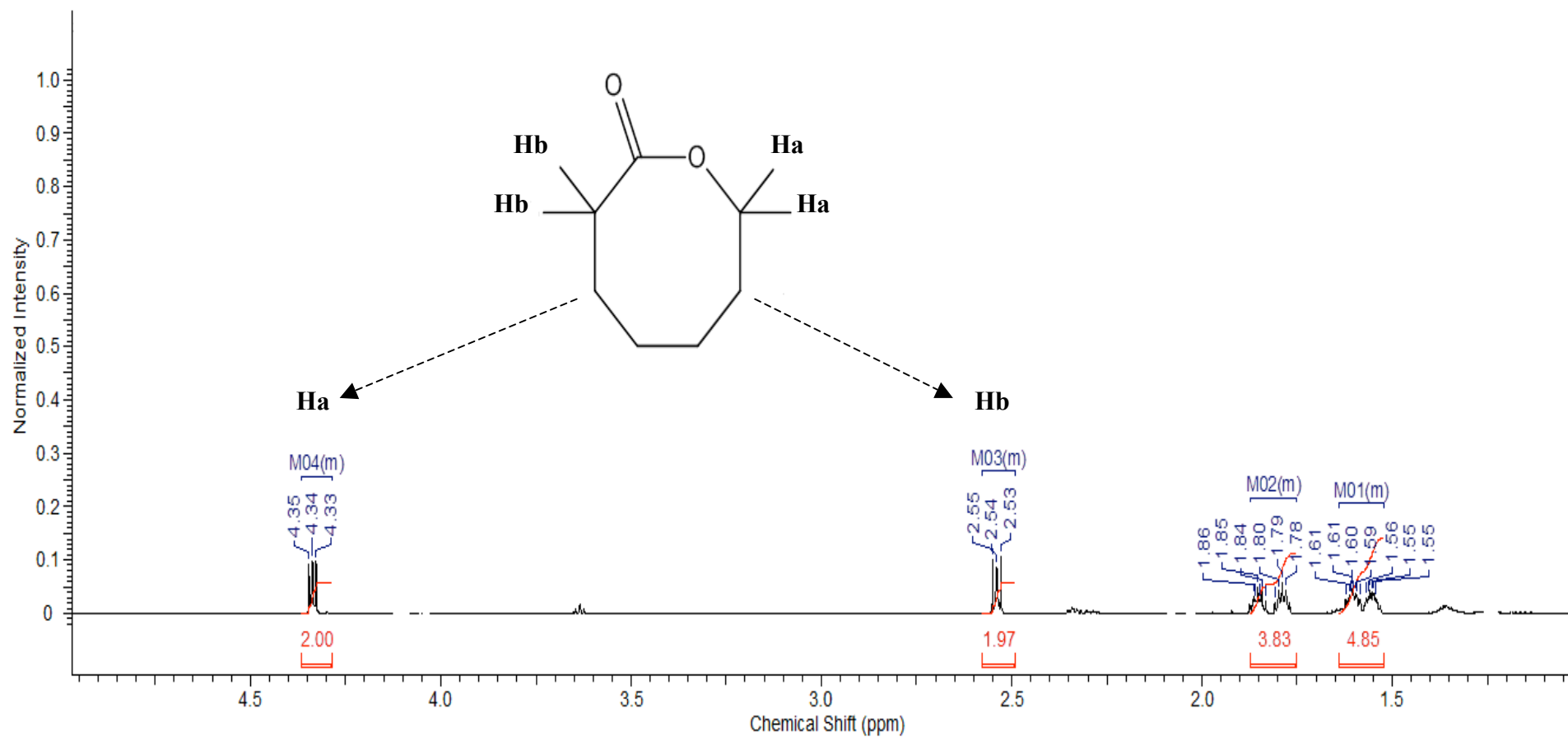


Figure D.7 Representative Proton NMR of purified oxocan-2-one from CHMO catalysed cycloheptanone.

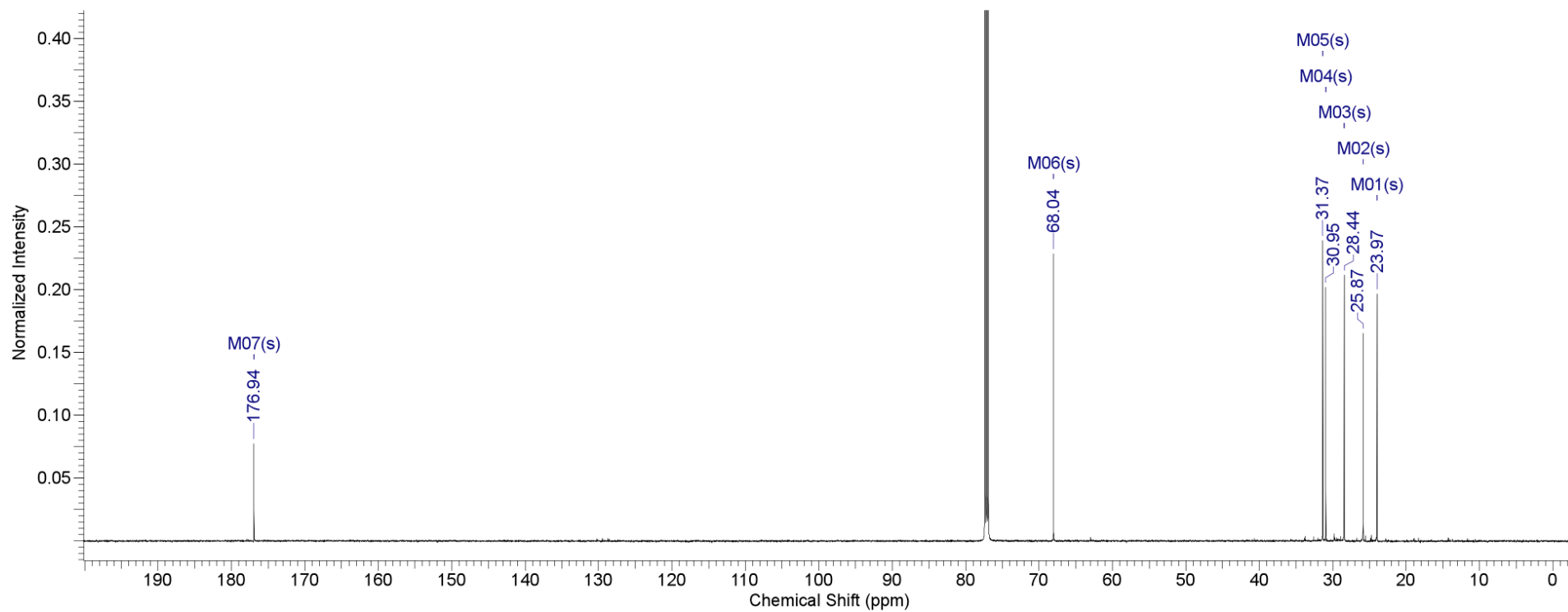


Figure D.8 Representative C-13 NMR of purified oxocan-2-one from CHMO catalysed cycloheptanone.

21-sep-2010_100921101649 #121 RT: 12.63 AV: 1 SB: 3 13.05-13.25 NL: 1.56E6
T: + c Cl Full ms [49.50-800.50]

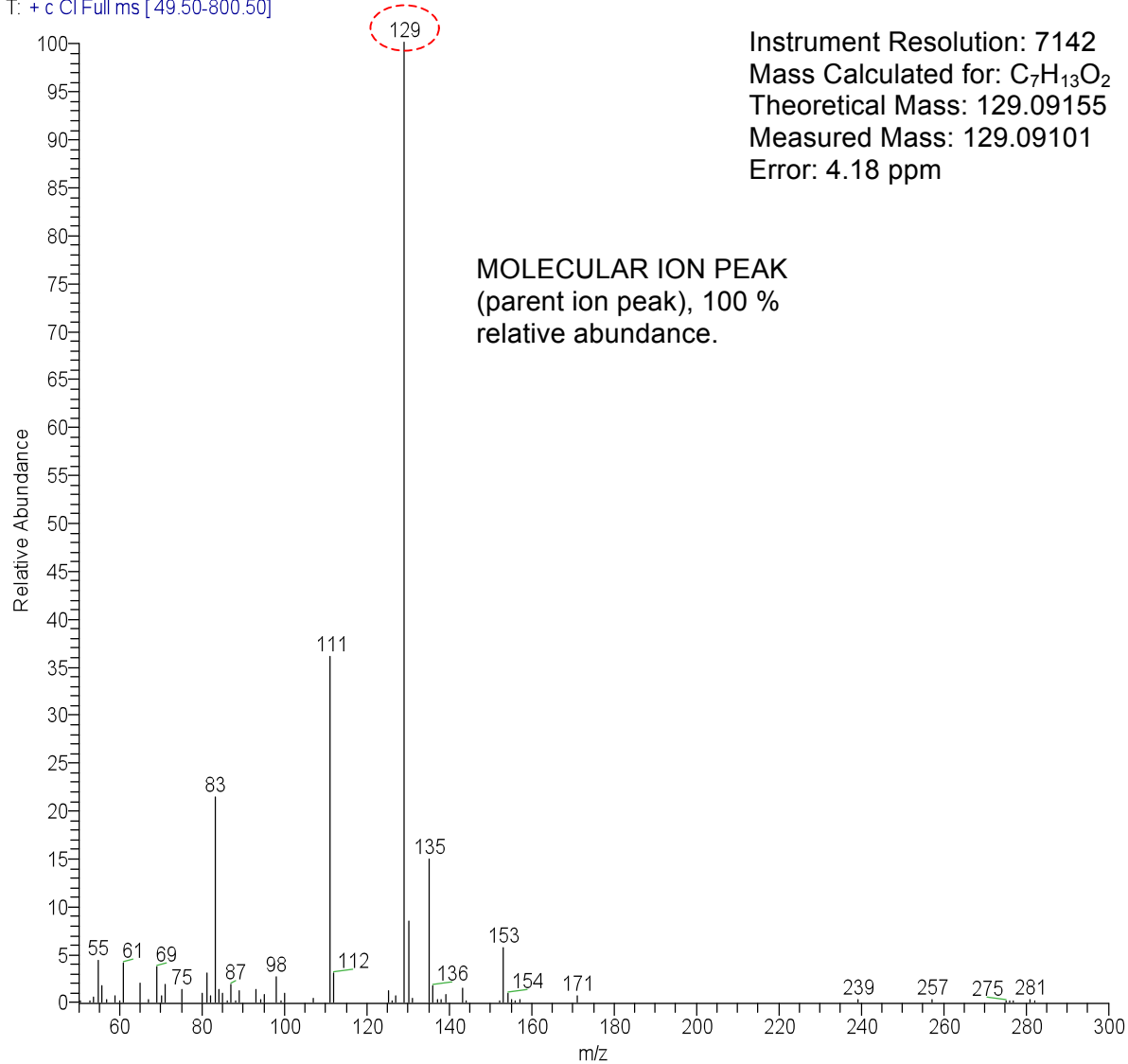


Figure D.9 Representative mass spectrum of purified oxocan-2-one from CHMO catalysed cycloheptanone.

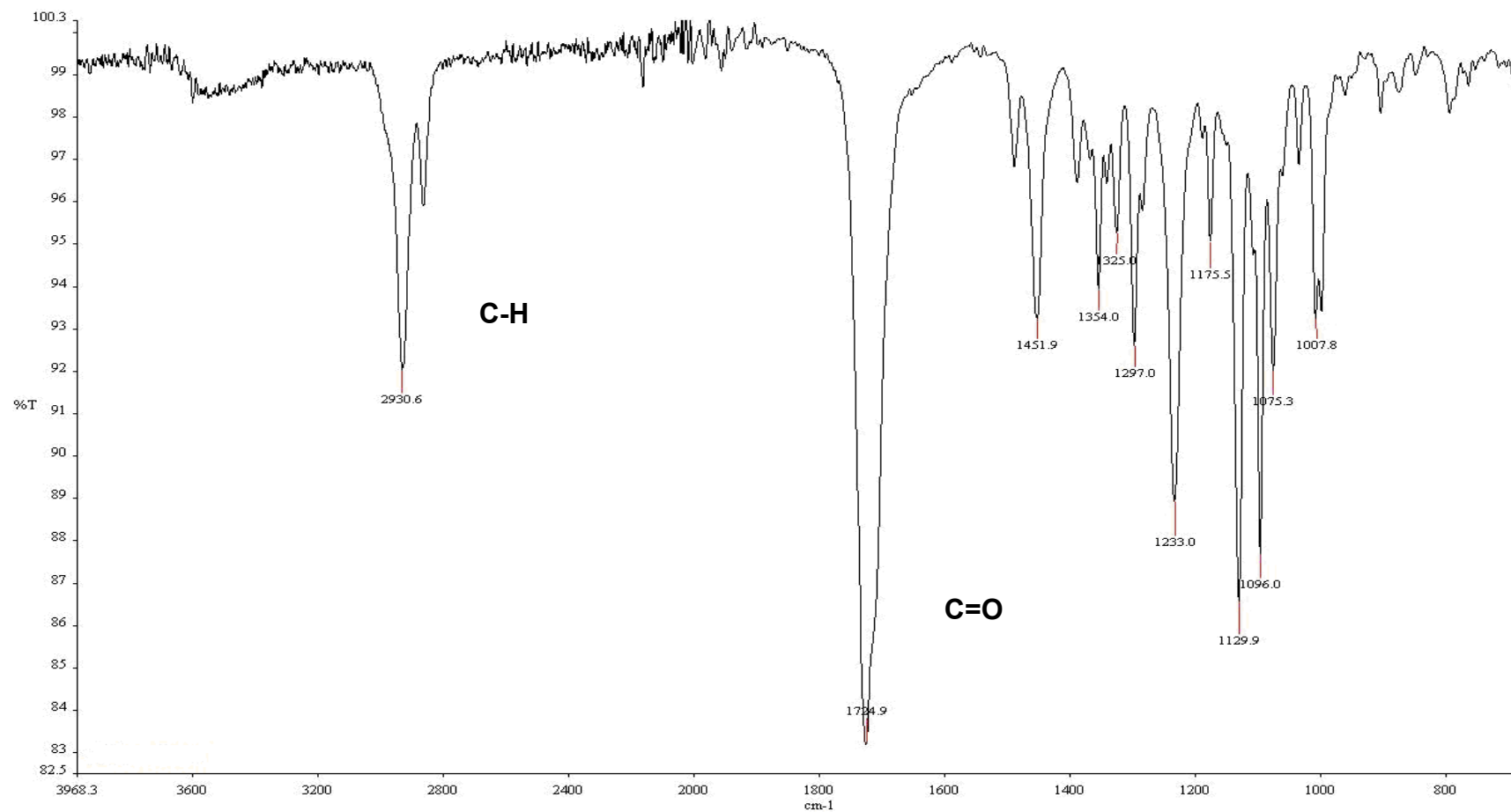


Figure D.10 Representative infra red spectrum of purified oxocan-2-one from CHMO catalysed cycloheptanone. Trough at 1724.9 cm^{-1} indicates a carbonyl group (C=O) and a trough at 2930.6 cm^{-1} indicates a C-H group.